UNIVERSITY OF CAPE TOWN
IYUNIVESITHI YASEKAPA • UNIVERSITEIT VAN KAAPSTAD

The influence of concrete mix composition and environmental exposure on long-term chloride ingress in concrete

By

Rukshani Heiyantuduwa Beushausen

Thesis Presented for the Degree of
DOCTOR OF PHILOSOPHY
in the Department of Civil Engineering
Faculty of Engineering and the Built Environment
UNIVERSITY OF CAPE TOWN

September 2022

Supervisor: Professor Mark Alexander

Declaration

I, Rukshani Heiyantuduwa Beushausen, hereby declare that this Thesis is my own, unaided work. All the work in this document, apart from that which is properly acknowledged, is my own. It is being submitted for the degree of DOCTOR OF PHILOSOPHY at the University of Cape Town. It has not been submitted before for any degree or examination in any other University.

Signed by candidate

_____

Rukshani Heiyantuduwa Beushausen, September 2022

Abstract

The parameters influencing long-term chloride ingress in concrete structures exposed to different environmental conditions in South Africa were investigated, aiming at improving service life prediction models for reinforced concrete structures situated in marine exposure classes. Time-dependent chloride ingress was measured over a period of roughly 4 years with respect to the influences of binder type, w/b ratio and environmental conditions, exposing samples to submerged, tidal, splash/spray and airborne chloride exposure in the Atlantic Ocean in Cape Town and the Indian Ocean in Durban. As a comparison, chloride ingress was measured under laboratory-controlled conditions. The data was analysed to identify the parameters used in the modelling of long-term chloride ingress into concrete using Fick's laws of diffusion. The time-dependency of apparent diffusion coefficients and chloride surface concentrations was identified and used in the long-term service life prediction with respect to the various experimental parameters. Based on the model predictions, the combined influences of binder type, w/b ratio, exposure condition and cover depth on the expected service life duration of RC structures in South African marine environments were investigated quantitively.

Executive summary

Worldwide, chloride-induced reinforcement corrosion is one of the main challenges for design and maintenance of marine concrete infrastructure, which has resulted in numerous prediction models for chloride ingress and associated service life design models. Uncertainties, however still exist with regard to the various parameters that influence long-term chloride ingress in real concrete structures exposed to different environmental conditions. The aim of this research is therefore to determine service life prediction and performance-based design of reinforced concrete structures in typical South African marine environments, taking into consideration local environmental conditions and cementitious binder types. The influences of binder type, w/b ratio and environmental exposure conditions on time-dependent chloride ingress and related material parameters were investigated based on experimental work on concrete specimens exposed to both controlled laboratory and real site conditions.

Concrete specimens were produced with the binder types commonly used in the Western Cape and Kwazulu Natal Provinces in South Africa, and subjected to marine conditions in the respective locations, i.e., the Atlantic Ocean in Cape Town and the Indian Ocean in Durban. At each of these locations, samples were exposed to the four marine zones commonly used to design concrete structures for durability, namely submerged, tidal, splash/spray and airborne exposure zones. In addition, specimens produced from all concrete mixes were exposed to chloride ingress by immersion in a chloride solution in a controlled laboratory environment. Binder types included plain Portland cement (PC) with blends of fly ash (FA), ground granulated blastfurnace slag (BS), ground granulated Corex slag (CS), Supperpozz ash (SP) and silica fume (SF). Two water/binder ratios were used, 0.40 and 0.60.

The influence of ambient temperatures on chloride ingress was clearly observed when comparing test results obtained on the same concrete mixes exposed in Durban and Cape Town, especially in the exposure zones related to regular wetting and drying cycles, i.e., splash/spray and tidal zones. Samples exposed to the Indian Ocean consistently showing significantly higher chloride concentrations compared to samples exposed to the Atlantic Ocean. On each of these two sites, the specific exposure zone had a marked influence on the chloride surface concentrations, the highest chloride surface concentration (C_s) values were found in the splash/spray zone, followed by the tidal, submerged and airborne zones. In contrast, the apparent diffusion coefficients were found to relate mainly to the characteristics of the various concrete mixes, especially with regards to binder type, and to a much lesser extent on the exposure conditions. As expected, concrete made with plain Portland cement was found to have substantially higher apparent diffusion coefficient (D_a) values, compared to concrete made with blended cements. Concrete containing blast furnace slag was found to have the lowest diffusion coefficient, followed by concretes containing fly ash and Corex slag.

Time-dependent chloride ingress was measured for a period of roughly 4 years and the chloride profiles obtained were interpreted using regression analysis based on Fick's laws of diffusion to determine time-dependent values for D_a and C_S. The time-dependency of D_a and C_s was determined through the quantification of the "m" and "n" values. The m-value was found to be a basic material property related to the binder type but independent of w/b ratio or exposure conditions. For PC concrete, an average m-value of 0.3 was measured, indicating a relatively small change in D_a over time, compared to blended binder types, which had m-values between 0.6 (SF) and 0.8 (BS, CS, FA, SP). In contrast, the n-value was found to be independent of the

binder type or any other experimental variables. Most n-values ranged between 0.4 and 0.6, with an average value of around 0.5.

For the modelling of long-term chloride ingress, the same cut-off point in time was defined for both m- and n-values, i.e. the same age at which the two parameters are taken to no longer undergo further change. Based on the predicted long-term chloride ingress, which was extrapolated from the measurements taken over the 4-year period, two different scenarios were modelled for all concrete mixes, i.e. cut-off dates of 10 and 20 years. For these two cut-off points, chloride profiles for an age of 50 years were predicted. The model outputs were compared to long-term chloride ingress data from actual concrete structures along the west coast of Southern Africa. It was then concluded that cut-off dates of 10 years and 20 years are reasonably realistic for concrete made with plain Portland cement and concrete containing blended cements, respectively.

With relation to the various experimental parameters used in this research, the predicted long-term chloride profiles were then used to model the expected service life of reinforced concrete structures, where the service life duration was defined as the time needed to reach a chloride threshold value of 0.4% by mass of binder at the depth of the steel reinforcement. Based on the model predictions, the combined influences of binder type, w/b ratio, exposure condition and cover depth on the expected service life duration of RC structures in South African marine environments were investigated quantitively.

Compared to concrete with a w/b of 0.40, a w/b of 0.60 resulted in predicted D_a values that were about 70% higher (on average, across all samples tested). In this comparison, the binder type had no apparent influence on how much “better” a concrete with lower water/binder ratio performed, indicating that the influence of the w/b ratio is independent of the binder type. For blended cement concrete, the w/b ratio has a marked influence on chloride surface concentrations. In this research, chloride surface concentrations for concrete containing fly ash and slag were consistently about 20-30% higher in concrete with a w/b of 0.60, compared to concrete with a w/b ratio of 0.40. The combined influence of the w/b on diffusion coefficients and surface concentrations is apparent when the predicted long-term chloride ingress is considered. For all concretes tested in this research, a decrease in w/b ratio from 0.60 to 0.40 resulted in an average increase in service life duration of 80%.

Samples exposed to the Indian Ocean in Durban had consistently higher diffusion coefficients, higher chloride surface concentrations, and shorter predicted service life durations (about 40% when the same concrete mix was considered (containing FA)), compared to samples exposed to the Atlantic Ocean in Cape Town, which can be assigned to the influence of ambient air and ocean temperatures on the rate of chloride ingress.

The predicted service life durations for PC concrete were very low, confirming that plain PC concrete is not suitable for marine exposure conditions. Concrete containing FA, BS and CS generally perform comparably with regards to the predicted long-term chloride ingress, indicating that all 3 binder types (at the investigated cement replacement ratios) are suitable for marine concrete structures. Overall, concrete made with SP and SF performed better than PC concrete but significantly worse than concrete with slag or fly ash.

The cover depth also has a significant influence on the predicted service life duration, irrespective of binder type, w/b ratio or exposure condition. Changing the cover from 50 to 40 mm or 50 to 30 mm resulted in a reduction in the predicted service life of about 35% and 63% respectively.

Based on the comparison of test results obtained on samples exposed to the laboratory and samples exposed to site conditions, it was confirmed that laboratory-based research can be used to establish chloride diffusion coefficients, chloride surface concentration, and n- and m-values, which are characteristic of those expected for concrete exposed to submerged conditions on site. This is considered relevant for predicting long-term chloride ingress in real structures using a performance-based design approach.

Acknowledgements

My supervisor Professor Mark G. Alexander for his much-appreciated guidance, academic mentorship, continuous support, and patience over the lengthy duration of this project.

The laboratory and workshop staff at the Department of Civil Engineering, University of Cape Town for their invaluable technical assistance. Especially Leonard Adams for his dedication to grinding through countless concrete core specimens to produce thousands of powder samples for chloride titration.

My husband Hans Beushausen for his invaluable advice, insightful comments, and encouragement, for supporting me throughout this experience, and for pushing me to finally finish this thesis.

Janosh, Sanjay and Raya, my beautiful children, without whom I would not have taken so long to complete this project.

My parents, my mother Ajantha Perera and my late father Nimal Perera, and my sister Shashika Heiyantuduwa for their continued encouragement and support over the years.

Table of contents

List of symbols

C is the concentration of chloride ions

C_i is the initial chloride content of the cementitious mixture prior exposure to the chloride environment, mass %

C_0 is the surface chloride content at time t=0

$C_c(n)$ is the calculated chloride concentration in the middle of the n^{th} concrete layer (% by mass), where n is the number of concrete layers sampled

$C_m(n)$ is the measured chloride concentration in the n^{th} layer (% by mass), where n is the number of concrete layers sampled

C_s is the equilibrium chloride content on the concrete surface

$C_S(t)$ is the average surface chloride content at any time t

$C_{S, 2y}$ is the surface chloride content at 2 years

$C_{S, 20y}$ is the surface chloride content at 20 years

C_x is the chloride concentration at depth x measured normal to the section at time t expressed by% weight of binder

D is the apparent or effective diffusion coefficient (m^2/s)

D_a is the apparent diffusion coefficient (m^2/s).

$D_{a, 35d}$ is the apparent diffusion coefficient (m^2/s) at 35 days

$D_{a, 1y}$ is the apparent diffusion coefficient (m^2/s) at 1 year

$D_{a, 20y}$ is the apparent diffusion coefficient (m^2/s) at 20 years

D_R is the diffusion coefficient at time t_R

D_{ref} is a reference diffusion coefficient at some specified time t_{ref} D(t) is the average diffusion coefficient representing the observed chloride profile at any time t

erfc is the error function, a mathematical construct found in math tables or as a function in common computer spread sheets

m is a ‘time-reduction index’, quantifying the time related dependence of the diffusivity.

n is the empirical material coefficient relating to the increase in C_S with time t

t is the time of exposure (s)

t_E the time of exposure to chlorides

t_i time at the first exposure to chlorides

t_R the reference time

1. Introduction

1.1 Background

Degradation of reinforced concrete structures is one of the greatest challenges facing the structural engineering industry at the moment. The deterioration of concrete differs from one region to another depending on factors such as environment, materials, design method and construction. In many countries, money spent on repair and maintenance of existing reinforced concrete structures exceeds that spent on new construction. In South Africa, the rehabilitation of existing infrastructure is beginning to consume a considerable amount of the GDP. A large part of these expenses can be related to problems of lack of durability of the structure, thus stressing the need to design for the duration of the service life of a structure, and the improvement of current design specifications for concrete structures has become increasingly important.

Traditional methods for durability design are usually based on deem-to-satisfy rules, where sufficient durability of a concrete structure is assumed with prescriptive requirements. Such requirements include the use of specified water/binder ratios, execution during construction/site practice, minimum cover to reinforcement, and minimum cement content. With the deem-to-satisfy methods, it is expected that the concrete structure will achieve a long but not specified service life. In contrast to the traditional prescriptive design methods, performance-based durability design for concrete structures is based on modelling deterioration mechanisms under the prevailing environmental conditions and using actual concrete properties, i.e. resistance against deterioration obtained from experimental investigations, as input parameters in the model. Such deterioration models are typically based on characterization of the environmental exposure conditions and relate the durability of the concrete structure to the aggressiveness of the environment. Consequently, adequate characterization of environmental exposure conditions is of very high importance in performance-based approaches for concrete durability.

In most countries including South Africa, the upgrading of durability requirements in current concrete codes lags behind the technical and scientific developments. Code specifications for concrete durability are still mostly based on the traditional requirements for concrete composition, construction procedures and curing conditions, the application of which have shown on occasions to yield insufficient and unsatisfactory results. By proper utilization of existing knowledge from recent research on new procedures for durability design, improved construction quality and life cycle management, it should be possible to produce new concrete structures with a more controlled durability and longer service life (Gjørv, 2002).

In recent years an extensive amount of research work has been carried out to better understand and control several of the most important deteriorating mechanisms such as alkali aggregate reactions, freezing and thawing, and corrosion of embedded steel. Particular attention has been paid to the corrosion of reinforcing steel, which represents the greatest threat to the durability of reinforced concrete structures. The engineer now faces the challenge of utilizing and transforming this existing knowledge into good and appropriate engineering practice (Gjørv, 2002).

The main concrete durability-related problem encountered in South Africa is reinforcement corrosion resulting from chloride ingress in marine environments. In order to combat the

problem, a performance-based approach was developed for design and quality control of concrete structures. This approach is linked to the modelling of time-dependent chloride ingress into concrete and makes use of standard marine exposure conditions found in codes and standards. Chloride ingress is typically modelled using Fick's laws of diffusion, which allow to predict the time-dependent increase in chloride concentrations in the concrete cover zone. In the model, the chloride ingress is largely dependent on environmental exposure conditions, which influence the chloride surface concentrations in the concrete, and the concrete's resistance against chloride ingress, which is assumed to be directly related to its chloride diffusion coefficient. In performance-based design, chloride diffusion coefficients can be experimentally obtained or predicted using accepted test methods such as the bulk diffusion test ASTM C1556-04 (2004) or the South African Chloride Conductivity Index (CCI) test (Streicher and Alexander, 1995).

Existing performance-based approaches used in South Africa for concrete durability prediction are based on standard exposure conditions, which may not accurately reflect actual exposure conditions experienced on site. In addition, existing knowledge on chloride ingress into concrete is largely based on outdated data and does not take into account the influence of modern cementitious binder types on chloride ingress. There is therefore a need to update local data on chloride ingress into concrete and relate the associated performance to the prevailing South African exposure conditions. Such updated data can then be used in the development of a more reliable and accurate service life prediction model for concrete structures in local marine exposure conditions.

This research is aimed at providing engineers with information that helps them to understand the impact their decisions have on the durability performance and service life of a concrete structure subjected to marine exposure, and to guide them in the use of performance-based criteria in the specification of parameters for the evaluation of concrete durability. Work done as part of this research includes the information derived from four years of natural site exposure of the test concrete's and results obtained from a detailed laboratory programme.

1.2 Problem statement

The South African performance-based methods for concrete durability design and quality control have progressed to a state where they are applied in the design of actual concrete structures. However, the approaches used are based on outdated assumptions for both actions, i.e. environmental exposure conditions, and resistance, i.e. concrete diffusion characteristics, which renders the modelling of time-dependent chloride ingress into concrete questionable.

Standard exposure conditions (which in Codes of Practice are typically loosely divided into mild, severe and extreme exposure) do not necessarily account for the prevailing marine exposure conditions experienced in South Africa. In the currently used design models, no difference is made between environmental exposure conditions experienced on the different South Africa coastlines, which are exposed to the Atlantic Ocean on the west coast and Indian Ocean on the south and east coasts. These two oceans have very different characteristics, e.g. temperature and salinity, that may influence chloride ingress into concrete. Further, the classification of environmental exposure needs further refinement to better take into account direct and indirect exposure to sea water.

Existing prediction models for chloride ingress into concrete are largely based on outdated experimental data and do not sufficiently take account of modern cementitious binder types used in South Africa, such as the range of common cements (i.e. “CEM”) as well as additives such as Blastfurnace Slag, Corex Slag, Fly Ash and Silica Fume. Currently, a proper characterization of the chloride ingress resistance of concrete made with these binder types is lacking, which limits the applicability of current service life prediction models.

The prediction of time-dependent chloride ingress into concrete is reliant on the time development of model input parameters, notably chloride surface concentrations and diffusion coefficients. The literature contains conflicting information on these parameters, which is related to a general lack of experimental data obtained under real exposure conditions. With existing knowledge, the translation of experimentally based service life prediction models into practical applications is therefore difficult.

1.3 Research objectives

The main objectives of this research work are to develop a chloride ingress model for the durability prediction of concrete structures in actual South African marine environments and to understand how the model parameters influence durability analysis. It is important to quantify appropriate input values for the prediction of time to corrosion initiation, using the Fick’s law type models and to relate these to practical laboratory tests that can characterise the expected durability of a particular concrete mix.

Consequently, one of the key objectives of the research was to quantify the time-dependent surface concentration C_s, the apparent chloride diffusion coefficient D_a, and any associated time and temporal dependence in the diffusion coefficients, for each of the concrete types and environmental conditions investigated. These are the critical input values for predicting time to corrosion initiation using a Fick’s Law type model.

Another objective of this work is the identification of diffusion parameters for Fick’s Model that are fundamentally sound and appropriate for South African environmental conditions and to research the range of different available materials in South Africa. This durability research programme is to provide specific data on the chloride ingress of concretes made with South African cement and aggregates that incorporate locally available materials.

1.4 Research questions

The above-mentioned research aims translated into a range of specific research questions, which can be summarized as follows:

- What are reasonable or realistic values for time-dependent chloride surface concentrations and chloride diffusion coefficients (D), which should be used for service life prediction of concrete structures exposed to various South African marine exposure conditions?
- How can the time-dependencies in chloride surface concentrations and diffusion coefficients be appropriately incorporated in service life prediction models?

- How can the influences of concrete mix characteristics (binder type, w/b ratio) and environmental exposure conditions be quantified in terms of their influence on long-term chloride ingress?
- How can laboratory-based experimental research be used in prediction of chloride ingress into concrete structures in-situ?

1.5 Structure of thesis

This thesis is divided into six Chapters, together with an appendix and list of references. The first Chapter forms an introduction to the topic and looks at research objectives and aims. The next Chapter is a literature review on the durability of reinforced concrete structures in the marine environment. The interaction of environment and material is investigated and chloride deterioration mechanisms are discussed. Chloride penetration is detailed, as this is the main cause of corrosion of reinforced concrete structures located in marine environments. Relevant current models for degradation and service life prediction of concrete due to corrosion are also discussed.

In chapter three, experimental procedures, techniques and methodology of this study are discussed. It describes the exposure site testing and the derivation of appropriate input data for Fick's Law based service life prediction models from the collected data.

Chapter four presents the experimental results of this study and discusses and evaluates the results. It discusses existing relationships and correlations between the test results that indicate the applicability of the tests in determining the durability and service life performance of marine concretes. It will also examine early age laboratory tests that may be suitable to act as simple durability indices i.e. methods of characterising the expected in service durability performance of a particular concrete mix design.

In chapter five, several proposals for a Service Life Model are presented, where chloride induced corrosion of reinforced concrete structures is the mechanism modelled. Appropriate cut-off points for the time-dependency of D_a and C_s. are analysed and presented. These results and conclusions will serve as the basis for the application of the proposed model, in an attempt to evaluate the service-life of these structures.

Finally, in chapter six, the main findings and conclusions of this work are presented as well as recommendations for future developments.

Appendix A contains a summary of all chloride ingress data.

2.Literature review

2.1 Introduction

The deterioration of reinforced concrete structures built in aggressive environments is recognised as a major technical and financial problem that affects a multitude of infrastructure. Common deterioration mechanisms include reinforcement corrosion, sulphate attack, alkali-aggregate reaction, freeze-thaw cycling, creep and shrinkage, and temperature effects (Kropp and Hillsdorf, 1995). In addition to these environmental factors, overloading, poor design and detailing, and inadequate inspection and maintenance constitute the other main causes of deterioration and failure of concrete structures.

Chloride induced reinforcement corrosion is recognised as the main cause of deterioration and loss of durability of concrete structures (Kong and Hooton, 1999, Zhang and Lounis, 2006 and Vidal et al, 2007). It is estimated that one third to one half of the projected bridge rehabilitation costs in the U.S are related to bridge deck deterioration (Cady and Weyers, 1983). The major sources of chlorides are de-icing salts applied to roadways and bridges during winter and chlorides from the marine environment. For the purposes of this research the focus will be on corrosion induced due to the presence of chlorides in seawater.

This research also deals with the service-life of reinforced concrete structures in marine environments. Inadequate durability properties of concrete are by far the most common cause of premature degradation of concrete structures. Traditionally the codes of practice contain requirements to the design formulated directly in terms of the load carrying capacity of structures. Durability aspects have often been considered as being of secondary importance and hence durability-based requirements to the design have typically been given implicitly. Service-life design and prediction are currently an area of significant international research. This chapter will look at the service-life concept in association with concrete durability design, and will also look at existing models. These are discussed in detail with respect to the corrosion of reinforced concrete. Finally, a brief overview of current codes for concrete durability is presented.

2.2 Corrosion of reinforcing steel in concrete

2.2.1 Steel corrosion in general

Concrete has to be reinforced with embedded steel when used to resist tensile and flexural loading, and it is the potential for corrosion of this embedded steel that is a prime issue in structural deterioration.

Corrosion can be described as the destructive attack of a metal by an electrochemical process undergoing a number of oxidation and reduction reactions. It is a process by which a refined metal reverts back to its natural state by an oxidation reaction with the environment (e.g. oxygen and water).

In the corrosion process two electrochemical reactions take place simultaneously at different sites on the steel surface. The two reactions are known as ‘anodic’ and ‘cathodic’ reactions, and the areas on the surface of the corroding metal where the reactions occur are called the anode

and the cathode respectively. At the anode, metal atoms are ionised and pass into the solution around the metal as positively charged hydrated ions (anodic oxidation). Electrons are thereby left on the metal surface and therefore raise its electrical potential. The excess free electrons then flow through the metal to the cathodic region (lower potential area) of the metal where an electron acceptor such as dissolved oxygen (water and oxygen) is available to consume them to form hydroxyl ions (cathodic reduction). The flow of electrons occurs due to a potential difference that exists between the two electrodes, and as long as such a potential difference exists, electrons will flow from the anode to the cathode causing corrosion. The process continues by electro-migration of ions through the aqueous phase leading to the formation of corrosion products at the anode. If water and oxygen are not available at the cathodic sites, the corrosion process will be terminated (Bentur, Diamond and Berke, 1997).

The reactions taking place at the anode and cathode on a steel member are shown below:

Anodic reaction $2Fe - 4 \text{ electrons} \rightarrow 2Fe^{2+}$ [2.1]

Metallic atoms at steel surface — Ions dissolved in solution

Cathodic reaction $O_2 + 2H_2O + 4 \text{ electrons} \rightarrow 4OH^-$ [2.2]

Dissolved oxygen molecules — Ions dissolved in solution

2.2.2 Corrosion of steel in concrete

Corrosion of steel in concrete is a process similar to that described above. A characteristic feature of the corrosion of steel in concrete is the development of macro and micro cells that is the coexistence of passive and corroding areas on the rebar forming a galvanic element with the corroding area as the anode and the passive surface as the cathode. A corrosion current is therefore driven by a difference in potential between the anodic and cathodic areas that may exist on the same length of reinforcement. The potential difference occurs due to local differences in the environment surrounding the reinforcement or due to differences in the surface condition of the steel reinforcement (Broomfield, 1997). Concrete pore water functions as an aqueous medium, i.e. a complex electrolyte. Therefore, a reinforcement corrosion cell is formed as shown in Figure 2.1.

Concrete is alkaline in nature, that is, it contains microscopic pores with high concentrations of soluble calcium, sodium and potassium hydroxides (Broomfield, 1996). The alkalinity of concrete in pH terms is roughly between 12 and 13. Therefore, when steel is embedded in concrete it is in contact with highly alkaline pore solutions which form a tight and stable passivating film of ferric oxide around the steel surface protecting it against corrosion. This passive layer prevents corrosion by stopping the dissolution of Fe^{2+} ions into the surrounding pore solution, thereby preventing the flow of electrons from the anode to the cathode.

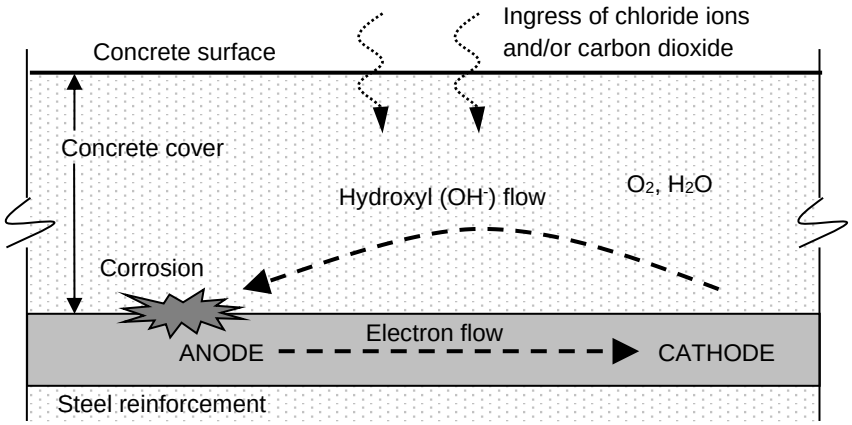

Figure 2.1: Mechanism of corrosion of steel in concrete

Most chloride attack on concrete reinforcement occurs due to the movement of chlorides into the concrete from the marine environment. The passive layer around the steel is not immediately affected when it comes into contact with chloride ions. This ferric oxide layer is able to withstand the presence of chloride ions to a certain extent. It has been suggested that there is a threshold concentration of chloride ions that must be exceeded before depassivation can take place.

The depassivation of the steel due to chloride attack occurs when the chloride ion attacks the passive layer, without there being an overall drop in pH. On reaching the iron substrate, the chloride ion acts as a catalyst for the oxidation of the iron by taking an active part in the reduction process thereby increasing the rate of breakdown of the passive layer of oxide and allowing the corrosion process to proceed.

The chloride ion combines with the iron to form the complex $FeCl_2$ and then draws this unstable ion into the solution where it reacts with the available hydroxyl ions to form $Fe(OH)_2$. This in turn releases the chloride ions back into the solution and consumes hydroxyl ions locally, as seen in the reactions below (Broomfield, 1996):

Primary Anodic Reaction: $Fe \rightarrow Fe^{2+} + 2e^-$ [2.3]

$Fe^{2+} + 2Cl^- \rightarrow FeCl_2$ [2.4]

Secondary Anodic Reaction: $FeCl_2 + 2H_2O \rightarrow 2Fe(OH)_2 + 2Cl^- + 2H^+$ [2.5]

The electrons released in the oxidation reaction then flow through the steel to the cathode surface. This process results in a concentration of chloride ions and a reduction of the pH at the points of corrosion initiation, probably accounting for the process of pitting corrosion. The lower pH also contributes to the continual breakdown of the passive oxide film, leading to corrosion.

Once depassivation is achieved corrosion may take place. The chemical reactions are the same regardless of the depassivating medium. The steel corrodes and dissolves in the pore water and gives up electrons at the anode. The electrons created at the anode must be consumed somewhere else on the surface of the steel to preserve electrical neutrality. Therefore in the presence of water and oxygen the electrons are consumed to produce hydroxyl ions at the cathode.

These anodic and cathodic reactions are the first steps in the corrosion process. If only the iron was to dissolve in the pore water without any further oxidation, cracking and spalling of the concrete would not occur. Several more stages must occur for formation of rust or expansive corrosion products, which affect the surrounding concrete. In subsequent stages ferrous hydroxide becomes ferric hydroxide and then hydrated ferric oxide or rust. This is expressed in the following equations (Broomfield, 1996):

$$Fe^{2+} + 2OH^{-} \rightarrow Fe(OH)_2 \quad [2.6]$$

Ferrous hydroxide

$$4Fe(OH)_2 + O_2 + 2H_2O \rightarrow 4Fe(OH)_3 \quad [2.7]$$

Ferric hydroxide

$$2Fe(OH) \rightarrow Fe_2O_3.H_2O + 2H_2O \quad [2.8]$$

Hydrated ferric oxide (rust)

The expansion associated with rust is due to the hydrated oxides, which can swell up to seven times the original steel volume. This in turn causes the cracking and spalling that are observed as the usual consequence of corrosion of steel in concrete, as well as the red/brown brittle, flaky rust on the bar and the rust stains seen at cracks in the concrete.

2.2.3 External factors affecting corrosion of steel in concrete

The primary reason for reinforcement corrosion is depassivation of the steel. However, a number of causes can provide the means by which this comes about. The factors affecting the corrosion of steel in concrete can be classified into external and internal factors. The former include mostly the environmental parameters outlined as follows.

- *Availability of oxygen and moisture at the level of the rebar:*
  Moisture fulfils the electrolytic requirement of the corrosion cell, and in the presence of oxygen increase the formation of OH^- ions thereby producing more $Fe(OH)_2$ (rust component). Oxygen also affects the progress of cathodic reactions, in the absence of sufficient amounts of oxygen, even in a situation of depassivation; corrosion will not progress due to cathodic polarisation.

- *Relative humidity and temperature:*
  Relative humidity is a moisture condition and is one of the parameters that governs hardening of concrete, especially close to the surface and consequently governs the permeability of gases, water and ions (Ferreira, 2004). Moisture also plays an important role in chemical reactions in concrete and in physical and chemical processes in various deterioration phenomena (Ferreira, 2004).Chlorides require moisture to penetrate the concrete, therefore, in the splash zone of marine structures, moisture plays a more active role when salts penetrate due to convection, moving with the water and depositing where and when the moisture evaporates (Ferreira, 2004).

  Temperature has been found to affect corrosion potentials, corrosion rates, concrete resistivity and transport processes in concrete. An increase in temperature has found to

generally increase the electrode reaction rates and decrease oxygen solubility, resulting in a reduction in the rate of corrosion (Mozer et al., 1965). However, corrosion rates are increased by high temperature and high humidity (Uhlig, 1983).

- *Carbonation and entry of acidic gaseous pollutants:*
  Carbonation is the process whereby the carbon dioxide gas from the atmosphere reacts with the calcium hydroxides in the concrete forming carbonic acid. Carbonation and other acidic gases, such as SO_2 and NO_2 reduce the pH of the concrete, resulting in the depassivation of the steel reinforcement and in turn reinforcement corrosion (Berkely and Pathmanaban, 1990).Where carbonation and chloride ingress occur simultaneously, apart from accelerating the depassivation, the pH lowering effect of carbonation causes some of the bound chlorides to be set free. This increases the chloride content of the pore solution which in effect accelerates chloride diffusion through concrete (Ballim et al, 2009, Arya and Xu, 1995).

- *Aggressive anions especially chloride ions:*
  The main cause of damage and early failure of reinforced concrete structures is as a result of corrosion of rebar due to chloride ions from de-icing salts or seawater. A chloride concentration above a certain threshold amount in the concrete cover results in the depassivation of the reinforcing steel. Chlorides in concrete are present as acid soluble chlorides, bound chlorides and free or water-soluble chlorides. It is generally recognised that only the free chlorides ions affect the corrosion process (Arya et al., 1987). It is reported that the resistivity decreases and the corrosion rate increases with an increase in the chloride content (Hope and Alan, 1987).

- *Stray currents:*
  Stray currents from various sources, e.g., building power supply systems, cathodic protection systems, locomotive power supply systems, etc. may cause electrolytic corrosion.

- *Bacterial action:*
  Bacteria decrease the amount of cover by disintegration of the cementitious materials (ASTM Special Technical publication, 1983). Anaerobic bacteria produce iron sulphides in an oxygen deficit condition e.g. concrete sewers, which enables the corrosion reaction to proceed even in the absence of oxygen (Berkely and Pathmanaban, 1990) and, aerobic bacteria aids in the formation of differential aeration cells, which can lead to corrosion.

2.2.4 Internal factors affecting the corrosion of steel in concrete

These include mainly concrete and steel quality parameters, as discussed below.

- *Cement composition:*
  The cement in the concrete provides protection to the reinforcing steel against corrosion by maintaining a high pH in the order of 12.5 to 13 as a result of $Ca(OH)_2$ and other alkaline materials which are produced during the process of hydration. The presence of cement also aids in the binding of a significant amount of total chlorides as a result of the chemical reaction between C_3A and C_4AF present in concrete, therefore an increase in the chloride threshold is observed with an increase in the C_3A content (Rasheeduzzafar, 1992). The use of blended cements e.g. micro silica-blended high C_3A cements are found to be somewhat

resistant to sulphate attack and chloride corrosion of reinforcement (Rasheeduzzafar et al., 1990).

The use of cement extenders such as Fly Ash, Silica Fume and Slag have shown to enhance concrete durability and resistance to chloride induced corrosion by increasing chloride binding (Lu et al, 2002, Tadayon et al., 2016), decreasing chloride permeability (Choi et al, 2006 and Thomas and Bamforth, 1999), increasing threshold chloride content (Manera et al, 2008) and improving the distribution of pore size and shape of the concrete matrix (Khan, 2010; Yang and Cho, 2003). Fly Ash blended cements were found to refine the concrete pore structure and hence reduce permeability (Saraswathy and Song, 2006). Saraswathy and Song (2007) also found that FA addition significantly improved resistance to chloride attack of reinforcement. The use of SF was found to significantly reduce permeability and improve resistance to chloride ingress (Song et al, 2010; Selvaraj et al, 2003). GGBS was found to considerably improve the pore structure of concrete, increase its chloride binding capacity (by forming more Friedel's salt), and reduce its chloride diffusivity (Luo et al, 2003; Cheng et al, 2005), thereby providing significant enhancement of resistance to chloride attack of reinforcement.

- *Impurities in aggregates:*
  Aggregates containing chlorides may cause serious corrosion problems, particularly those associated with seawater and those whose natural sites are in ground water containing a high concentration of chloride ions (ACI C201, 1991).

- *Impurities in mixing and curing water:*
  Mixing and curing water, either contaminated with sufficient amounts of chlorides or being highly acidified may prove to be detrimental as far as corrosion of rebar is concerned.

- *Admixtures:*
  The addition of calcium chloride as a common admixture for accelerating the hydration of cement is one of the most significant reasons for the presence of chlorides in reinforced concrete structures(ACI C201, 1991).

- *w/c ratio:*
  The w/c ratio, known to control principally the strength, durability and permeability of concrete, does not itself affect the rate of corrosion of the reinforcement. When reinforced concrete structures are exposed to aggressive environments it is the permeability of the concrete, which is a function of the w/c ratio, which affects the corrosion of the rebar. The depth of chloride penetration increases with an increase in the w/c ratio (Jaegermann, 1990). Similarly, carbonation depth has been found to increase linearly with an increase in the w/c ratio (Ho and Lewis, 1987). The oxygen diffusion coefficient has also been found to increase with an increase in the w/c ratio (Kobayashi and Suttoh, 1991). Low w/c ratios increase the impermeability of concrete, which in turn reduces the chloride penetration, carbonation penetration and oxygen diffusion in concrete. However, a low w/c ratio does not by itself assure concrete of low permeability. In addition to a low w/c ratio, the concrete must be well proportioned and well consolidated to produce a concrete of low permeability. In addition, adequate curing is required for achieving the required durability.

- *Aggregate size and grading:*
  The size of aggregate affects the consistency of concrete and therefore may have an effect on reinforcement corrosion. Aggregate grading is another important factor, which should be considered for high quality impermeable concrete. It has been observed that for a given w/c ratio, the coefficient of permeability of concrete increases considerably with increasing size of aggregate (US Bureau of Reclamation, 1975). The proportioning of coarse and fine aggregate is also important for the production of a workable and durable concrete. The aggregate proportioning for this purpose consists of fixing the optimum volume fraction of sand in the total aggregate content. The optimum proportioning for maximum workability has been reported to be corresponding to a specific surface area of the combined aggregates in the range of 70 to 75 cm^2/cm for concrete with a cement content in the range of 300 to 390 kg/m^3 (Maslehuddin, 1981). This enhanced workability as a result of optimum aggregate grading allows for a reduction in the w/c ratio resulting in increased durability of the concrete.

- *Construction practises:*
  Serious corrosion problems may occur if good construction practises are not followed. It is important that aggregate is washed for deleterious materials if any (Rasheeduzzafar, 1989), amounts of chlorides in all ingredients of concrete i.e. water, cement, aggregate, and admixtures must be controlled, designed and recommended w/c ratios, cement contents, cover thicknesses etc. must be enforced, the proper consolidation of freshly packed concrete and proper curing of concrete must be maintained.

- *Cover of reinforcing steel:*
  Cover depth has a significant effect on the corrosion of reinforcing steel due to the penetration of either chlorides or carbonation. Insufficient cover depth, resulting from inadequate specification or poor construction, is the main cause of premature deterioration of reinforced concrete structures.

- *Chemical composition and structure of the reinforcing steel:*
  The differences in the chemical composition and structure of reinforcing steel and the presence of stress in the reinforcement, either static or cyclic, create different potential at different locations on the surface of the reinforcement, causing the formation of differential corrosion cells, which eventually leads to corrosion (Mozer, 1965).

2.2.5 Effect of reinforcement corrosion on structural behaviour

The corrosion of reinforcing steel may have severe implications on the functionality of concrete structures and result in costly repairs. The effects of corrosion include poor aesthetics due to cracking and delamination, perforation of concrete containers and pipes, as well as structural problems such as increased deflections and loss of load bearing capacity. In terms of losing structural capacity, most problems with the corrosion of steel are not only due to the loss of steel cross-section but also the formation of the oxide, which leads to cracking and spalling of cover concrete (Ferreira, 2004).

This oxide (rust) produced as a result of corrosion of the reinforcement steel in concrete has two factors that predominate. Pore water in concrete is static and therefore there is no transport mechanism to move the oxide away from the steel surface, which results in all the oxides being

deposited at the metal/oxide interface (Ferreira, 2004). The second problem is that the oxide is very porous and has a volume 2 to 7 times that of steel (Neville, 1995).This increase in volume results in the development of tensile stresses within the cover concrete, which ultimately results in cracking and spalling of the cover concrete. Due to the loss of cover concrete there may be significant reductions in the load bearing capacity of the structure and the bond between concrete and steel. Therefore, the steel may become more accessible to the aggressive agents leading to further corrosion at an accelerated rate.

In addition, corrosion reduces the cross-sections of the steel and thereby the load carrying capacity of the structure. Pitting (i.e. localized) corrosion of the rebar is more dangerous than uniform corrosion because it progressively reduces the cross-sectional area of rebar to a point where the rebar can no longer withstand the applied load leading to failure of the structure.

2.3 Chloride penetration into concrete

2.3.1 Properties of concrete that affect the rate of chloride penetration

The rate of chloride ingress into concrete depends on the pore structure of the concrete, which is affected by factors including materials, construction practice and age. The penetrability of concrete is related to the pore structure of the cement matrix. This will be influenced by the w/c ratio of the concrete mix, the inclusion of various supplementary cementing materials and the degree of hydration of the concrete. The older the concrete, the greater the amount of hydration that has occurred and therefore the more developed the pore structure. This is especially true for concretes containing slower reacting binders such as Fly Ash that require a longer time to hydrate.

The rate of chloride penetration into concrete is also affected by the chloride binding capacity of the concrete. Concrete is not inert relative to the chlorides in the pore solution. A portion of the chloride ions reacts with the concrete matrix becoming either chemically or physically bound, and this binding reduces the rate of chloride diffusion. The chloride binding capacity is controlled by the cementing materials used in the concrete. The inclusion of supplementary cementing materials affects binding, though the exact influence is unclear (Byfors, 1986; Rasheeduzafar, et al., 1992; Sandberg and Larrson, 1993; Thomas, et al., 1995). The C_3A content of the cement also influences its binding capacity, with increased C_3A content leading to increased binding (Holden et al.,1992; Sandberg and Larrson, 1993; Thomas et al., 1995).The mechanisms and effects of chloride binding will be further explored in a later section.

2.3.2 Overview on transport properties of concrete

The ingress of chlorides is a major cause for reinforcement corrosion in concrete structures. Transport through concrete involves the movement of ions, liquids and gases from external sources into the concrete where chemical interactions may result in deterioration of the material. These agents are driven by gradients in physical and chemical properties including ionic concentration, hydraulic pressure and capillary potential.

The three main transport processes in concrete are absorption, permeation and diffusion, which can be briefly characterized as follows (Glanville and Neville,1997):

- Water absorption is the uptake of water resulting from capillary forces, characterized by a sorptivity coefficient. In environments where significant concrete drying is possible, water absorption may lead to rapid penetration of species dissolved in the water. For example, concrete in the tidal zone of an offshore structure, or bridge decks subjected to regular applications of de-icing salts, may suffer from rapid chloride ion ingress due to water absorption.
- Permeation of water due to the application of a hydrostatic head. This is characterized by a water permeability coefficient; this transport process has been researched more thoroughly than any other. However, it is rare for this to be the predominant transport process; exceptions include water-retaining structures and deeply submerged concrete.
- Water vapour diffusion is the diffusion of water as a vapour, characterized by a water vapour diffusivity coefficient. This is the process by which concrete dries and it controls the moisture distribution in a concrete element after a period of drying. In turn, moisture distribution influences properties such as water absorption during wet and dry cycles, electrical resistivity, gas permeability and gas diffusivity.
- Wick action is a combination of water absorption and water vapour diffusion, characterized by sorptivity and water vapour diffusivity coefficients respectively. Wick action is the transport of water from the wetted face of a concrete element to a drying face. Species dissolved in the water are transported to the zone of the element where drying occurs and may result in salt crystallization.
- Ion diffusion is the movement of ions as a result of a concentration gradient, characterized by an ion diffusion coefficient. Ion diffusion is only significant where the concrete is nearly or completely water saturated. Compared with most other transport processes, ion diffusion is very slow, but is often rapid enough to cause deterioration well within the design life of a concrete structure.

The transport of chloride ions in a concrete structure is a function of internal and external factors. In relation to the latter, the environmental conditions are very important, especially the concentration and duration of the solutions in contact with the concrete surface. These conditions are different in different exposure situations and generally, marine environmental exposure classes are grouped into submerged, tidal, splash, and atmospheric exposure, as illustrated in Figure 2.2.

In structures submerged in sea water, the concentration of chlorides is more or less constant with time and penetration is purely through diffusion, where chloride ions diffuse through the water saturated pore structure of the concrete in response to concentration gradients. At early ages, however, a negative pressure is produced as the hydration of cement takes place in the interior parts of the concrete (Gonzalez and Jalali, 2004). In the splash zone, salt water is absorbed into the concrete surface, and rain water washes the surface free from chlorides, removing some of the chlorides. Evaporation increases the concentration. Chlorides move inwards and outwards due to moisture flow and ion diffusion. Conditions are also different at different heights from the average sea level. Maximum chloride contents are found at a height where salt water is frequently supplied to the surface but where the surface intermittently dries out (Ferreira, 2004). At the sea water level the concrete is almost continuously submerged in water and therefore no additional salts can be absorbed. In the tidal zone the conditions are

somewhat similar to that of the splash zone, however, the time of wetness and the intermittent drying times are different. The concentration of chlorides at different depths is a time dependent function of the environmental conditions, the design of the structure and the material properties.

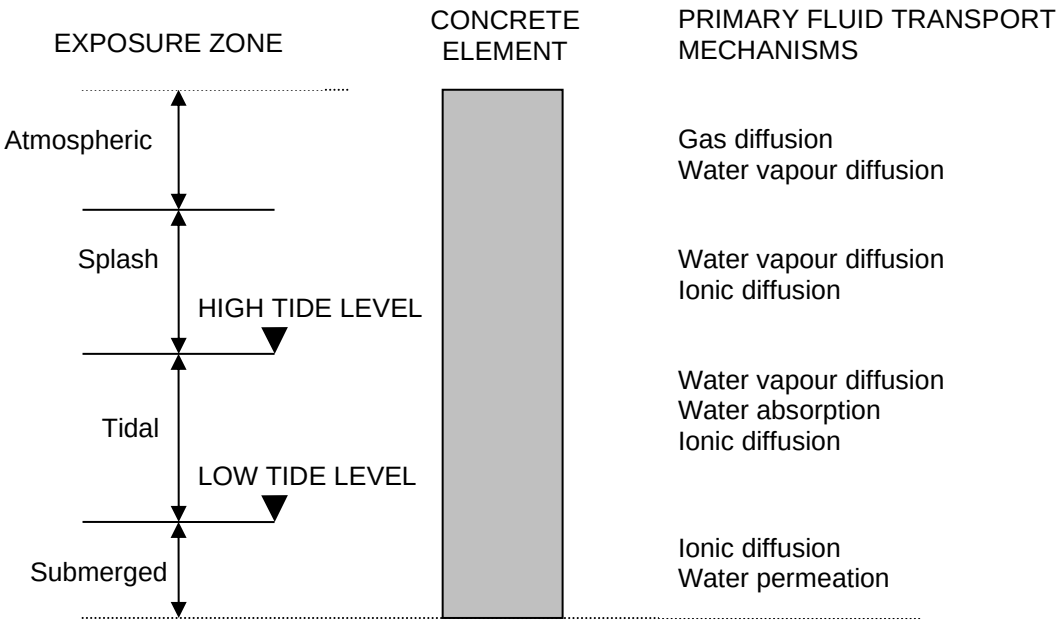

Figure 2.2: Dominant fluid transport mechanisms in marine concrete structures

Chloride ion diffusion as a result of sea spray and direct seawater wetting is the main mode of chloride contamination in South Africa and is the focus for this research. The diffusion process is described in more detail in the following sections.

2.4 Modelling chloride diffusion into concrete

Diffusion is the movement of a substance under a gradient of concentration. Or more strictly speaking molecules in a gas or a liquid will move from a high concentration to a low concentration in order to achieve system equilibrium. Diffusion in an ideal state follows Fick's Laws.

Chloride diffusion into concrete, like any other diffusion process, is controlled by Fick's First Law, which, in the one-dimensional situation is normally presented as below:

Fick's First Law – Steady state diffusion

$$J = -D \frac{dC}{dx} \quad [2.9]$$

Where J = Flux of chloride ions (g/m^2/s)

D = Apparent or effective diffusion coefficient (m^2/s)

C = Concentration of chloride ions (g/m^3)

x = Distance from 'upstream' face (m)

In a practical situation, this equation is only useful after steady-sate conditions have been reached, i.e. there is no change in chloride concentration with time. Equation 2.9 can however be used to derive the relevant equation for non-steady state conditions (where concentrations are changing), referred to as Fick's Second Law:

Fick's Second Law – Non steady state diffusion

$$\frac{\partial C_t}{\partial t} = D_a \frac{\partial^2 C_t}{\partial x^2} \quad [2.10]$$

Equation 2.10 includes the effect of changing chloride concentration with time (t).

Crank provides an analytical solution to Equation 2.10 for one-dimensional diffusion in a homogeneous, semi-infinite medium such as concrete (Equation 2.11) driven by a constant concentration gradient using the boundary condition $C_{(x=0,t>0)} = C_0$(the surface concentration is constant at C_0) and the infinite point condition $C_{(x=\infty,\ t>0)} = 0$ (far enough away from the surface, the concentration will always be 0).

$$C_t(x,t) = (C_s - C_i) erfc\left(\frac{x}{2\sqrt{D_a t}}\right) \quad [2.11]$$

Where erfc is the error function, a mathematical construct found in math tables or as a function in common computer spread sheets and C_s is the equilibrium chloride content on the concrete surface, C_i is the initial chloride content of the concrete before exposure to the chloride environment and D_a is the apparent diffusion coefficient (m^2/s).the calculation is simple and convenient and the values of parameters C_s and D_a can be easily estimated from experimental or filed data using regression analysis (J. Kim et al.,20016).

However, this model has limitations when applied to concrete (J. Crank, 1975, Saetta et al., 1993, Andrade et al., 1997). There are many factors that affect or interfere with the simple interpretation of diffusion data. Firstly, the chloride ions are not diffusing through a homogeneous solution; concrete is a porous matrix that has both solid and liquid components. The diffusion through the solid portion of the concrete matrix is negligible when compared to the rate of diffusion through the pore solution. The rate of diffusion is thus controlled not only by the diffusion coefficient through the pore solution but by the physical characteristics of the capillary pore structure. Values of C_s and D_a also vary significantly depending on the exposure environment, time and concrete composition. In recent years a number of modifications have

been put forward to allow for the time dependency of these parameters through aging factors, some of which are presented in Table 2.1. However, most of these are based on concrete specimens at relative short exposure periods and from concrete structures with varying concrete compositions and exposure conditions.

Table 2.1: Aging functions used in erfc solution (Kim et al., 2016)

Surface chloride concentration (C_s)	Apparent diffusion coefficient (D_a)	Reference
C_0 (constant)	$D_a(t) = \frac{D_R}{1-m}\left(\frac{t_R}{t}\right)^m$	Mangat et al. (1994)
C_0 (constant)	$D_a(t) = D_R\left(\frac{t_R}{t}\right)^m$	Maage et al. (1996)
C_0 (constant)	$D_a(t) = \frac{D_R}{(1-m)} {t_R}^m \left(\frac{t^{1-m} - {t_i}^{1-m}}{t - t_i}\right)$	Stanish et al. (2003)
$C_0(1-e^{-nt})$	$D_a(constant)$	Kassir et al. (2001)
$C_0 t$	$D_a(constant)$	Arney et al. (1998)
$C_0 t^n$	$D_a(t) = D_R\left(\frac{t_R}{t}\right)^m$	Costa et al. (1999)
$C_0\left(1-e^{-n(t-t_R)}\right)$	$D_a(t) = \frac{D_R}{(1-m)}\left[\left(\frac{t_R}{t}\right)^m - \frac{t_R}{t}\right]$	Maheswaran et al. (2004)
$C_0\sqrt{t}$	$D_a = \frac{D_R}{1-m}\left[\left(1+\frac{t_i}{t_E}\right)^{1-m} - \left(\frac{t_i}{t_E}\right)^{1-m}\right]\left(\frac{t_R}{t_E}\right)^m t_E$	Petcherdchoo et al. (2013)
$C_0[ln(\beta t+1)]+k$	$D_a(t) = \frac{D_R}{(1-m)}\left(\frac{t_R}{t}\right)^m$	Pack et al. (2010)

Note: C_0,m,n,k and β are regression values; t_R the reference time; D_R the diffusion coefficient at time t_R; $t_i$the time at the first exposure to chlorides; t_E the time of exposure to chlorides, and t is the age of the concrete.

A long-term field investigation on concrete samples exposed to marine environments in Norway indicated that both the surface chloride concentration and the apparent diffusion coefficient are time dependent and seem to reach a constant value after about 10-15 years (Skjolsvold et al., 2009, Markeset et al., 2011 and Markeset et al., 2017).

2.4.1 Chloride diffusion coefficients

Following Crank (1975), the diffusion coefficient is defined as the rate of transfer of the diffusing substance across a unit area of a section divided by the space gradient of concentration at the section.

$$D(cm^2/s) = \frac{F}{\partial c/\partial t} \qquad [2.12]$$

F being the flow in mol/cm^2 and $\delta c/\delta t$ the gradient of concentration

2.4.2 Measurement and experimental techniques

In order to determine surface chloride concentrations (C_0) and diffusion coefficient (D) values it is necessary to have a 'chloride profile' (explained in detail in a later section), i.e. experimental

data for C vs x at any time t, for concrete exposed to a chloride environment. In practice, such a profile is obtained by incrementally drilling into the concrete, perpendicular to the exposed surface or grinding off layers of concrete samples at required depth increments. The powdered concrete from each depth interval is collected and analysed for chloride content by potentiometric titration.

The values of C_0 and D are determined by fitting equation 2.11 to the chloride profile through non-linear regression using least squares, i.e. minimising the sum S given by the equation below:

$$S = \sum_{n=1}^{N} \Delta C^2(n) = \sum_{n=1}^{N} (C_m(n) - C_c(n))^2 \qquad [2.13]$$

Where N is the number of concrete layers sampled

$C_m(n)$ is the measured chloride concentration in the n^{th} layer (% by mass)

$C_c(n)$ is the calculated chloride concentration in the middle of the n^{th} concrete layer (% by mass).

Diffusion coefficients are expressed in SI units of m^2/s. Chloride concentrations are determined by mass percent of concrete or cement binder. The latter is more correct, the former more convenient, and the conversion between the two is simple where density and cement content of the concrete are known.

Figure 2.3 shows an example of a chloride profile from a concrete structure. The bars represent the measured chloride concentrations, and the curve is optimised using Fick's law given by Equation 2.11 after optimisation of the C_0 and D parameters.

The surface chloride concentration, C_0, therefore does not represent a physical measurement on the concrete, but rather the extrapolation of the idealised Fick's Law profile back to the y axis intercept (x=0). It can be visualised as the concentration determined in the analysis of an infinitely thin depth increment of concrete, sampled infinitely close to the exposed surface. The D value expresses the resistance of the concrete to penetration and controls the curvature, (more precisely the second derivative) of the concentration vs depth curve (Lee and Chisholm, 2005).

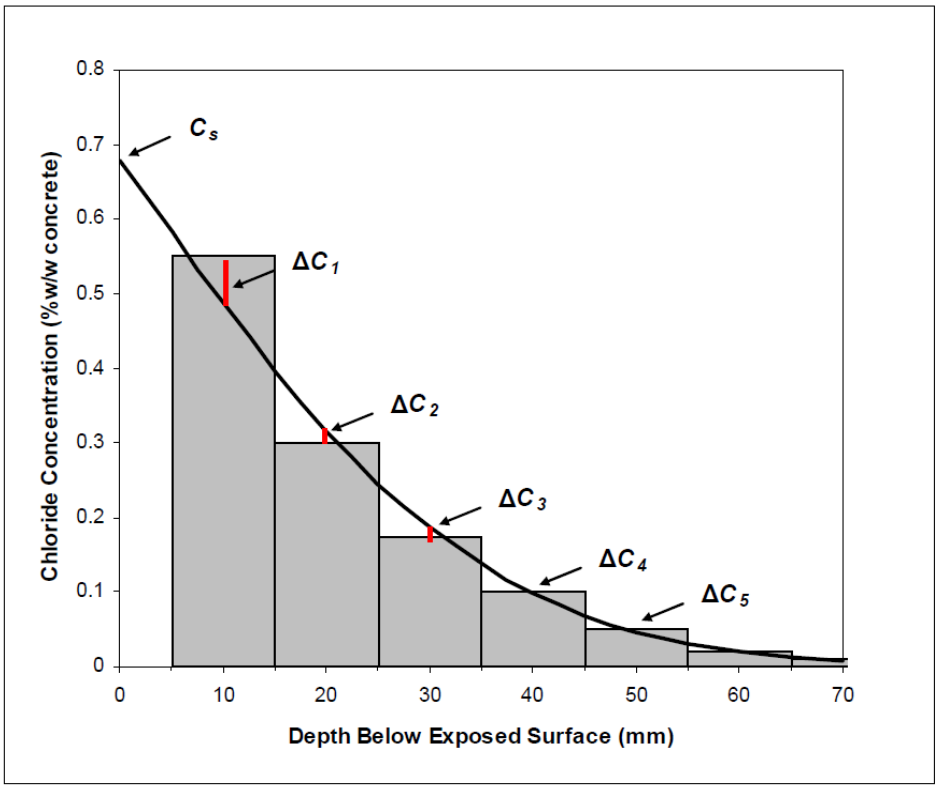

Figure 2.3: An example of a chloride profile from a concrete structure. The bars represent the measured chloride concentration and the curves shows modelling of chloride ingress using Fick's laws of diffusion (Lee and Chisholm, 2005)

This procedure can be used for both short-term laboratory-based testing to characterise the durability of new concrete and also to interpret and predict the performance of existing structures from site data. Crank's solution is applied to the analysis of concrete in two ways which, although superficially similar, are quite distinct in meaning and need to be carefully distinguished.

The first application is to determine the 'apparent diffusion coefficient', D_a. This attempts to measure the intrinsic diffusivity of concrete as correctly as possible via a bulk immersion test. One example of such a test is ASTM C1556-04 (described in detail in a later section), in which a completely saturated concrete specimen is immersed in a chloride solution for around 35 days. A diffusion coefficient is calculated from the chloride profile derived by applying the non-linear regression analysis described above, which yields best-fit values for D_a and C_0. The apparent diffusion coefficient is therefore the global diffusion coefficient involved in Fick's second law which takes chloride binding into account. It is used as input data in empirical models of chloride ingress (FIB Bulletin 34, 2006).

The second application is to use Equation 2.11 and the same curve fitting procedure to determine the 'effective diffusion coefficient', D_e of existing structures where a near- surface chloride ingress profile has already developed in the concrete through natural exposure. This provides a means of characterising the historical performance of a particular concrete or structure and can also be used for predicting future performance.The effective chloride diffusion coefficient is therefore the pure transport property involved in Fick's first law or in the Nernst-Planck equation.

D_e and D_a can both be used to predict corrosion initiation. Corrosion occurs when the concentration of chlorides at the depth of the steel reinforcement exceeds the critical threshold value required for depassivation of steel. This value is estimated to be between 0.4 and 1% of chlorides by mass of cement (Kropp and Hilsdorf, 1995). This age can be calculated simply by solving Equation 2.11 for t, using the appropriately derived values of D_e and D_a and C_0, with the smallest reinforcement cover depth representing x. Of critical importance to the accuracy of this technique, is the choice of appropriate C_0 and D values. It is with this problem that the research described in this study is mostly concerned.

D_e is different from D_a both because it reflects the influence of all the possible transport mechanisms acting on the concrete that have contributed to establishing the chloride profile, and also because it does not yield an instantaneous measure of the current resistance to chloride penetration. Instead, it reflects the 'time-averaged' performance of the concrete over the period between first exposure of the structure and the time when the chloride profile was determined.

2.4.3 Arguments against the chloride diffusion approach

It should be emphasised that the justification for adopting diffusion theory for the ingress of chloride ions into concrete is primarily convenience and empiricism: the mathematics of Crank's solution are straight forward and incorporate terms that are familiar to structural engineers (an imposed environmental load, C_0, and a resistance to that load, D), and it models the chloride profiles which are physically measured on a structure or specimen. It is however important to realise that except for the always submerged parts of marine structures, the pore system of concrete is rarely under complete saturation when exposed to chlorides and other transport mechanisms such as permeation, capillary absorption and wick action are also likely to be significant contributors to the movement of chloride ions in addition to pure ionic diffusion. Even a completely water-saturated concrete will violate the conditions necessary for the compliance with the assumptions of classical diffusion theory to some extent. For example, the hydrated cement matrix is not an inert material and will partially immobilise chloride-ions, primarily through the reaction of tri-calcium aluminate to form Friedel's salt ($3CaO.Al_2O_3.CaCl_2.10H_2O$) (Nagataki, 1995; Rapin et al, 2001; and Jensen et al, 2000). The extent of this chloride binding is known to be at the very least a complex function dependent on chloride concentration, the binder composition and the pore solution pH. For this reason, the value of D depends on the environmental chloride load, a clear violation of one of the main assumptions of classical diffusion.

It is has not been clearly established as to what extent neglecting these theoretical considerations might compromise the integrity of service life prediction. A number of researchers have developed multi-mechanistic transport models for partially-saturated concrete from first principles (Boddy et al., 1999). It is unfortunate that their meaningful application requires an extensive knowledge of a wide variety of material properties and site-specific conditions that are not usually available or familiar to structural engineers. Simply describing the spatial moisture distribution within a concrete structure sufficiently well to use such a model currently represents a formidable technical and economic barrier.

The importance of attempting to account for chloride binding also remains questionable. The removal of chloride ions from the pore solution of the cement matrix through binding reduces

the free chloride concentration and therefore the quantity of mobile chlorides at all depths within the concrete. Modelling of chloride binding isotherms, however, demonstrates that an increased chloride binding capacity also serves to maintain higher concentration gradients for extended periods in the near-surface concrete, thereby increasing the velocity and quantity of the chloride-ions entering the concrete through diffusion. Glass et al. (2000) presented experimental evidence that shows that the corrosion risk presented by bound chlorides at the steel-concrete interface may be very similar to that presented by free chlorides. This is contrary to a long-standing view that only the free chloride concentration is important and that the relative aggressiveness of a particular chloride-contaminated concrete is best expressed by the pore solution concentration of chloride and hydroxyl ions (Schiessl, 1998). This potential importance of the bound ions justifies the simple analysis of total chlorides per unit of mass, as described in earlier sections, rather than extraction and analysis of pore fluids. However this procedure does produce some non-intuitive consequences. For example, the boundary C_s value of concrete completely submerged in seawater is not equal to the chloride concentration of the brine but also depends, because of binding effects, on the chemistry of the cement, the concrete's total porosity and even surface finishing and curing.

However it can be argued that the simplicity and practicality of the empirical Fick's Law approach described appears to outweigh any theoretical disadvantage over a more complex multi-mechanistic treatment of chloride ion flow. It should however always be borne in mind that the necessary surface chloride concentrations and diffusion coefficients for input to these models are combined parameters, reflecting a variety of physical, chemical and environmental variables. They need to be collected and interpreted with great care, especially when trying correlate laboratory test results with field data.

2.4.4 Time dependent diffusion coefficients

One of the major steps in service life modelling of marine structures has been determining that chloride ingress decreases with time. Initially D was treated as a constant over time for any particular concrete type. However, extensive observations of marine structures in Japan led Takewaka and Mastumoto (1998) to propose a modified equation allowing for an apparent time related dependence of the diffusion coefficient. Laboratory testing (Maage *et al.* 1994; Mangat *et al.* 1994) and results from existing structures (Sandberg 1995) showed that the concrete's age dependency of the coefficient obeys a straight line in a double logarithmic co-ordination system. This meant that the resistance of concrete to chloride ions, as determined by chloride ingress profiles, is seen to improve with age according to a simple power function (Takewakaand Mastumoto, 1988):

$$D(t) = D_{ref} \cdot \left(\frac{t_{ref}}{t} \right)^{m} \qquad [2.14]$$

Where D(t) is the average diffusion coefficient representing the observed chloride profile at any time t and D_{ref} is a reference diffusion coefficient at some specified time t_{ref} (often chosen to be 28 days, D_{28}, simply for consistency with standard concrete tests), and m is a 'time-reduction index', quantifying the time related dependence of the diffusivity.

Both m and D_{28} (or any other convenient reference diffusion values) are mathematically fitted parameters which are derived by plotting experimental data for D vs t in a logarithmic coordinate system and m is the (negative) gradient of the resulting best-fit line. Equation 2.14 can simply be substituted into Crank's solution to Fick's Law to take into account time dependence, as shown below. The meaning of the terms remain as previously defined.

$$C(x,t) = C_0\left(1 - erf\left(\frac{x}{2\sqrt{D_{ref}\left(\frac{t_{ref}}{t}\right)^m.t}}\right)\right) \qquad [2.15]$$

The value of m is known to be influenced by the cement type and w/b (water to binder) ratio of the concrete under consideration. The literature (Maage et al., 2003 and Bamforth, 1999) indicates that concrete containing blast furnace slag, fly ash or silica fume can demonstrate substantial reductions in effective diffusivity with time which corresponds to m values of approximately between 0.6 to 0.8. Portland cement concretes by contrast show much smaller reductions in diffusivity with time; Bamforth indicates an m value of 0.25 while Takewaka's original figure was m=0.1.

Any time dependence to chloride ion diffusivity has the potential to impact enormously on the predicted service life for marine concrete. Figures 2.4, 2.5 and 2.6 demonstrate the effect of systematically varying m, C_s and D_{28} respectively on the time to corrosion initiation for reinforcement at various depths, calculated using Equation 2.11 (Lee and Chisholm, 2005). The figures are based on the usually accepted chloride threshold of 0.4% by mass of binder.

In Figures 2.4 – 2.6, the range of input parameters used encompasses the typical spectrum of values encountered in the literature. The 'reference concrete' chosen, has values of C_s=3.0% w/w on cement, D_{28}=100 mm^2/yr and m=0.1, intended to represent a high quality Portland cement concrete in a sea splash or tidal zone. Varying the time reduction index m for the effective diffusion coefficient is a much stronger control on the corrosion initiation time than either C_s, the environmental chloride load, or D_{28}, the initial resistance of the concrete to chloride penetration. Possessing accurate values for m for each concrete type therefore becomes a matter of critical importance. Modelling constant chloride ion diffusivity potentially underestimates durability. However, an overestimation in predicted service life is also possible if too large reduction indicies are assumed.

The decrease in D with time may be due to the refinement of the pore structure or a higher binding ratio in more mature concretes; however it can also be due to an increase in C_s values.

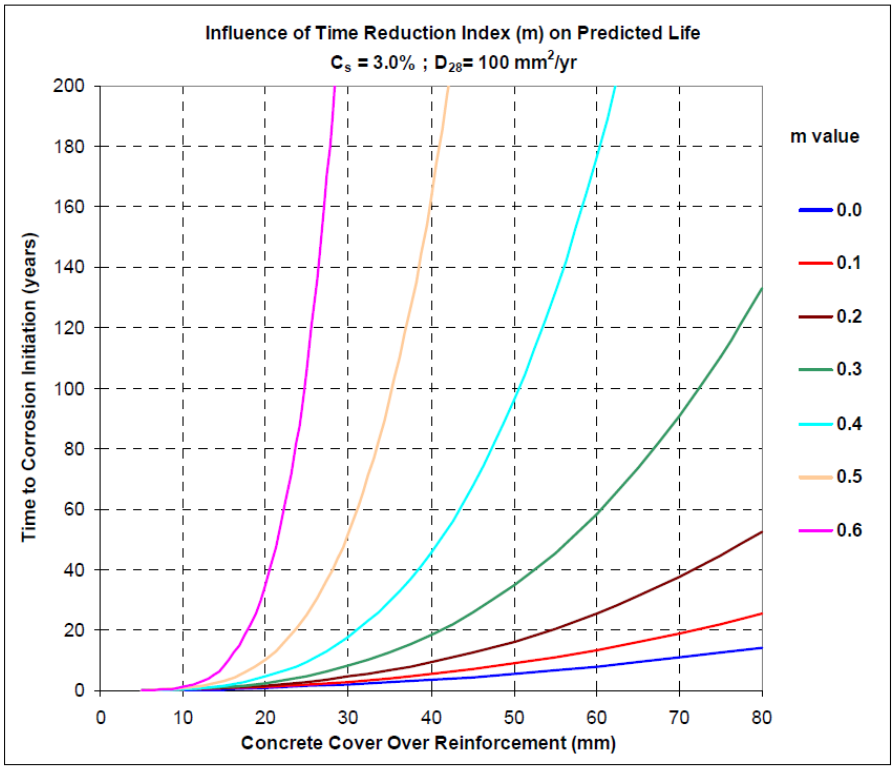

Figure 2.4: The effect of various values of the time-reduction index, m, on predicted service life (Lee and Chisholm, 2005)

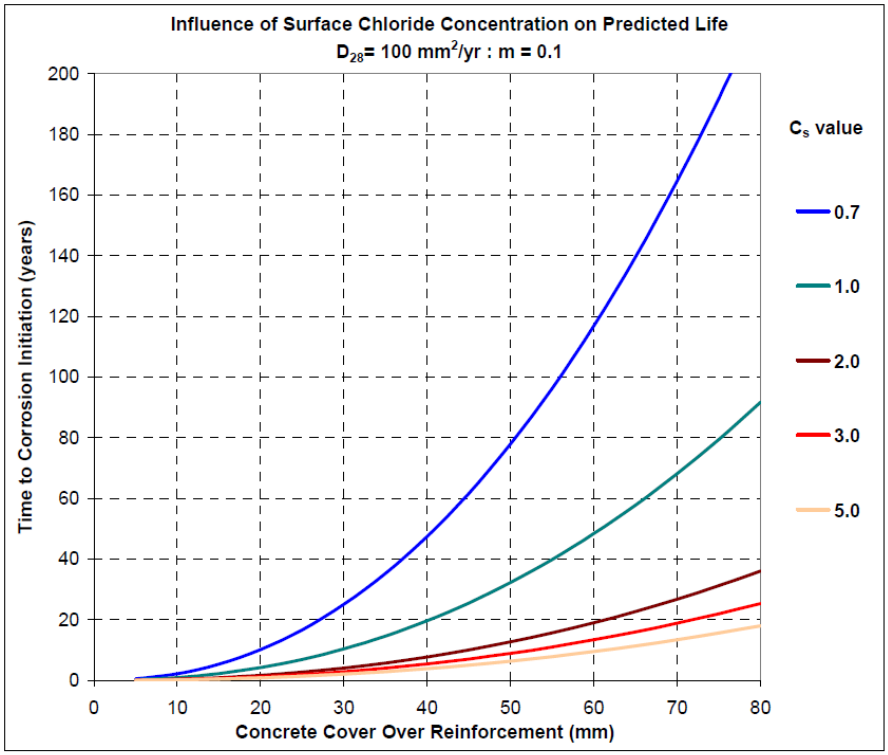

Figure 2.5: The effect of surface chloride concentration, C_S on predicted service life (Lee and Chisholm, 2005)

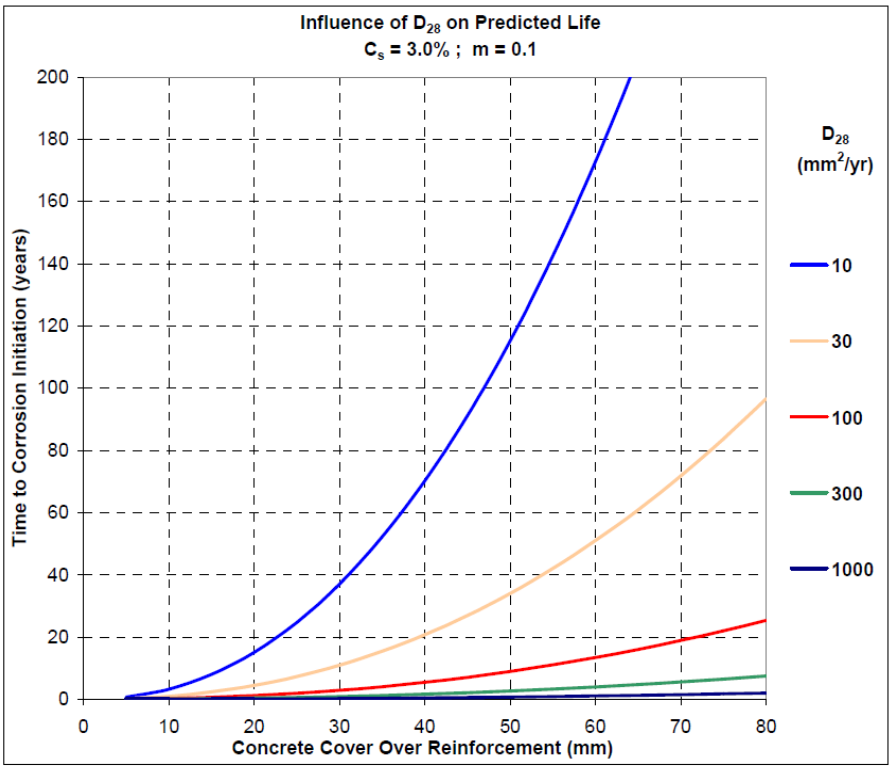

Figure 2.6: The effect of variable initial effective diffusion coefficients at 28 days, D_{28} on predicted service life (Lee and Chisholm, 2005)

2.4.5 Time reduction index (m)

The m-value is a constant and it was developed to account for the rate of reduction of diffusivity with time. It is dependent on variables such as the type of cementitious materials used and the mix proportions. Values for m for different concretes have yet to be well established, although some values have been published, shown in Table 2.2.

Table 2.2: Overview on time reduction index values reported in the literature (see Figure 2.7 for an explanation on the different m-values)

Binder	w/b	m-value			Reference
		$m_{effective}$	$m_{average}$	m_{total}	
OPC	0.40	0.57	0.68	0.87	Nokken et al., 2006
8% SF	0.40	0.61	0.72	0.94	
10% FA	0.35	0.77	0.91	1.28	
12% FA	0.40	0.77	0.91	1.28	
15% FA	0.33	0.41	0.48	0.59	
OPC				0.32	Stanish and Thomas, 2003
25% FA				0.66	
56% FA				0.79	
OPC	0.40		0.44		Mangat and Molloy, 1994
OPC	0.58		0.53		
25% FA	0.40		0.86		
25% FA	0.58		1.34		
60% BS	0.58		1.23		

Further research to properly quantify the time reduction index would help improving the accuracy of service life predictions. Estimates of when the critical chloride concentration is reached at the depth of the steel reinforcement would be more accurate if the changes in diffusion properties of a concrete with time were better taken into account. On site the time of exposure to chlorides is usually much greater than the age of the concrete prior to contact with salt solutions. Given that the change in diffusion with time is non-linear, the determination of the effective age during exposure to chlorides that correlates to the average/actual diffusion coefficient determined for that period is not straight forward (Nokken et al., 2006).

The time reduction index is often determined using Equation 2.14. The apparent diffusion coefficient values calculated using Equation 2.11 are plotted against time on a log-log scale and using linear regression analysis of the data a vale of m is determined. Typically, m values are calculated using maturity achieved at the end of the exposure period as the time basis (Mangat and Molloy, 1994; Bramforth, 1999; Tang and Nilsson, 1992). Determining the m value, however, presents problems. The diffusion coefficient for each exposure period in fact lies somewhere in between the instantaneous values one would find if the specimen were tested at the beginning of the the exposure period and at the end (Nokken et al., 2006).

Equation 2.11 which is often used to determine the diffusion coefficient remains constant with time and this is in fact not true. As concrete matures, hydration decreases the ability of ions to penetrate the concrete. As a result, during the exposure period, the diffusion coefficient is changing. As mentioned earlier, several published work used the calculated apparent diffusion coefficient and the time at the end of the exposure period to calculate m. Using Equation 2.11is therefore inaccurate and using the time dependient solution is more appropriate (Equation 2.15) (Nokken et al., 2006). The difficulty with this approach is that D_{ref} and m cannot be solved independently using one profile (Nokken et al., 2006).

Instead of determining m by linear regression of a log D vs. log time plot, Thomas and Bramforth used a multi-mechanistic finite-difference model developed at the University of Toronto (Boddy et al., 1999). In this model chloride diffusion profiles at 6 ages (ranging from 6 months to 8 years) were investigated. The input parameter used included the average surface concentration found for all ages of each concrete mix, an initial diffusion coefficient (28 days) and a m value was determined my minimizing the sum of the squares of the errors for all ages.

Nokken et al. (2006) calculated the m value using three different methods. These methods used different techniques to represent time, and therefore generated different m values. The time that was used as the basis to calculate m for each method for a specific exposure period is shown schematically in Figure 2.7 (Nokken et al., 2006). The apparent diffusion coefficient was calculated using Equation 2.11 for all the three methods. The first method, m_{total}, uses concrete maturity versus the calculated apparent diffusion coefficient. The second method, $m_{average}$ uses average age during the exposure period versus the calculated apparent diffusion coefficient (i.e., a specimen exposed for a 28 day period for 28 days after casting to 56 days after casting would yield an average age of 42 days). The third method uses the method of Stanish and Thomas (2003), which is discussed in detail in the following section.

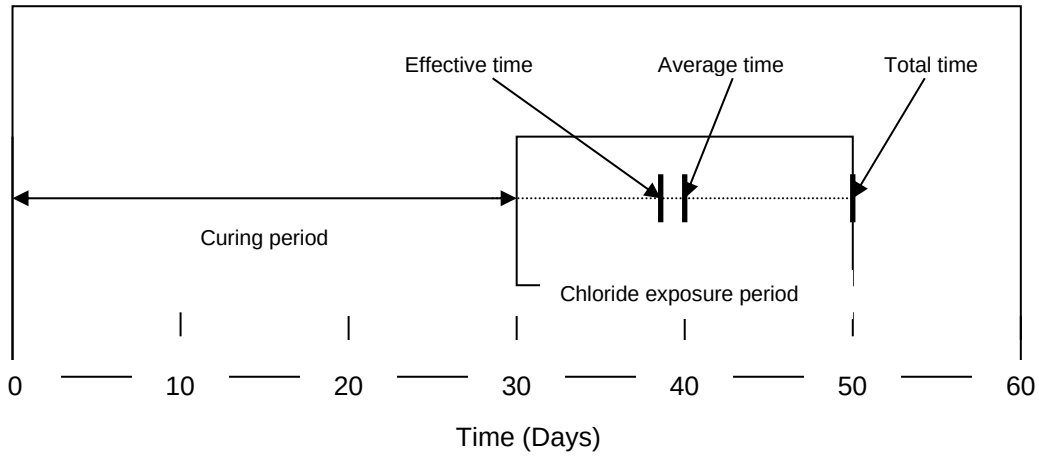

Figure 2.7: Example of time used for calculation of m (Nokken et al., 2006)

There is a considerable amount of variability in determining chloride diffusion coefficients as an indicator of the durability of concrete structures. In particular, the concrete diffusivity depends on the concrete pore structure and all the factors that determine it, such as: mix design parameters (w/c ratio, type and proportion of mineral admixtures and cement, compaction, curing etc.). The chloride diffusion coefficient is also a function of chloride exposure condition (submerged, tidal, splash/spray or atmospheric, etc.) and the length of exposure, partly due to hydration of slowly reacting cementitious constituents such as blast furnace slag or fly ash. More testing and research are warranted in order to understand existing knowledge gaps and shed light on the fundamental relationships (Shi et al., 2012).

2.4.6 Chloride surface concentration

Surface chloride concentration and chloride diffusion coefficients are two important parameters in the quantitative analysis and design for durability of reinforced concrete structures (Li et al., 2008). The error function solution of Fick's second law (Equation 2.11) assumes a constant surface chloride concentration (C_s), when it is used to calculate the apparent average chloride diffusion coefficient (D_a) in concrete during the exposure period. However, the surface chloride concentration in concrete often vary with time. In recent years, several C_s models have been developed to investigate the influence of age of concrete on C_s. Petcherdchoo (2013) proposed a square root model to describe the time dependent C_s. Arorap et al. (1997) adopted an exponential function to exhibit the time-dependent behaviour of C_s. More detailed information of time-dependent models for C_s are shown in Table 2.3.

Table 2.3: Time varying models of C_s (Zhao et al., 2020)

Surface chloride concentration, $C_S(t)$	Reference
C_0 (constant)	Mangat et al. (1994), Maage et al. (1996), Stanish et al. (2003)
$C_0 t$	Arney et al., 1998
$C_0 t^n$	Costa et al., 1999
$C_0(1 - e^{-nt})$	Arorap et al., 1997; Kassir et al., 2001
$C_0\left(1 - e^{-n(t-t_R)}\right)$	Maheswaran et al., 2004
$C_0[ln(\beta t + 1)] + k$	Pack et al., 2010
$C_0\sqrt{t}$	Petcherdchoo et al., 2013
$C_0\left(\frac{n.t}{(1+n).t}\right)$	Riding et al., 2013

Note: C_0,,n,k and β are regression values; t_R the reference time and t is the age of the concrete.

The chloride surface concentration has a significant effect on the apparent diffusion coefficient of concrete and therefore incorporating the time dependency of C_s is fundamental in the service life prediction of concrete structures.

2.4.7 Establishing the effective age of bulk diffusion test samples

Stanish and Thomas (2003) presented a method to account for the time-dependency of chloride diffusion coefficients in concrete. This method is discussed in detail in the following section as it will later be employed in the analysis of experimental data obtained in this study.

In the bulk diffusion test (explained later in detail in Chapter 3), chloride ions penetrate into the concrete solely by diffusion. Diffusion of chloride ions into concrete is governed by Fick's Second Law as expressed by Equation 2.10. As concrete matures and additional hydration occurs the chloride diffusion coefficient of concrete was found to reduce with time as expressed in Equation 2.14, as discussed earlier. This varying diffusion coefficient with age is not often considered when evaluating the results of a bulk diffusion test and a constant diffusion coefficient is often assumed instead, represented by Equation 2.11. By fitting Equation 2.11 to the chloride profile a single diffusion value is determined, and this diffusion value is the average of the changing diffusion coefficient over the testing period, D_{AVG}. The average diffusion coefficient will occur at some point during the test period, and it is therefore useful to be able to establish at what age the instantaneous diffusion coefficient is equal to the average diffusion coefficient. In order to determine this age, one needs to realize that the average diffusion coefficient determined from each test will be (Stanish and Thomas, 2003):

$$D_{AVG} = \frac{\int_{t_1}^{t_2} D_{ref}\left(\frac{t_{ref}}{t}\right)^m dt}{\int_{t_1}^{t_2} dt} \qquad [2.16]$$

where t_1 and t_2 represent the age of the concrete at the start and completion of the bulk diffusion test, respectively. D_{ref}, t_{ref} and m are constant for a specific concrete and therefore can be taken outside the integral. This results in Equation 2.17 (Stanish and Thomas, 2003):

$$D_{AVG} = \frac{D_{ref} t_{ref}{}^{m} \int_{t_1}^{t_2} t^{-m} dt}{\int_{t_1}^{t_2} dt} \qquad [2.17]$$

Solving these integrations yields an expression for the average diffusion coefficient (Stanish and Thomas, 2003):

$$D_{AVG} = D_{ref} t_{ref}^{m} \frac{t_2^{1-m} - t_1^{1-m}}{(1-m)(t_2 - t_1)} \qquad m \neq 0, 1 \qquad [2.18a]$$

$$D_{AVG} = D_{ref} t_{ref}^{m} \frac{\ln\left(\frac{t_2}{t_1}\right)}{t_2 - t_1} \qquad m = 1 \qquad [2.18b]$$

If m is equal to 0, the diffusion value does not change with age. In this instance, the diffusion coefficient at any age is equal to the average diffusion coefficient. When m= 1, the concrete is termed as 'self-blocking', and the chloride profile remains constant (Maage et al., 1996). This value of m=1 is proposed as an upper limit for the value of m. This is one of the differences between considering average diffusion coefficients and instantaneous ones (Stanish and Thomas, 2003). When instantaneous diffusion coefficients are used, this limit is not present (Stanish and Thomas, 2003). There is no reason that values of m of 1 or greater could not occur. This apparent 'self-blocking' effect only occurs when average diffusion coefficients are used because when Equation2.11 was derived it was derived for a constant diffusion coefficient. It is mathematically incorrect to then substitute a time-dependent diffusion coefficient in that solution (Stanish and Thomas, 2003). Additionally, the effective age at which the average diffusion coefficient occurs, t_{eff}, can be determined by using Equation 2.14 (Stanish and Thomas, 2003):

$$D_{AVG} = D_{ref} \left(\frac{t_{ref}}{t_{eff}} \right)^{m} \qquad [2.19]$$

Equating Equations 2.18 and 2.19 and solving for t_{eff} results in (Stanish and Thomas, 2003):

$$t_{eff} = \left[\frac{(1-m)(t_2 - t_1)}{t_2^{1-m} - t_1^{1-m}} \right]^{1/m} \qquad m \neq 0, 1$$

$$t_{eff} = \frac{t_2 - t_1}{\ln\left(\frac{t_2}{t_1}\right)} \qquad m = 1 \qquad [2.20]$$

Equation 2.20 can be used to determine at what age the average diffusion coefficient will occur based upon the bulk diffusion test conditions (the age of the concrete at the beginning and end of the immersion period) and the rate of change of the diffusion coefficient with time (Stanish and Thomas, 2003).

2.4.8 Using bulk diffusion data to determine diffusion vs. age parameters

According to Stanish and Thomas (2003) there are two basic approaches used to evaluate the service life of a structure exposed to chloride ions. The first approach is to use average diffusion coefficients (Weyers, 1998 and Maage et al., 1996). In this approach, the diffusion coefficient at any given age is the average diffusion coefficient at that age from the beginning of exposure to the chloride environment. The chloride concentration at any given depth is then calculated using Equation 2.11. In this case, the instantaneous diffusion is of no interest and the diffusion coefficients can be directly determined from bulk diffusion tests with no additional calculations and the m values can be calculated by fitting the results to Equation 2.14.

The second method involves the use of instantaneous diffusion coefficients, and to therefore apply a finite difference approach using Equation 2.10. A model using this approach was developed at the University of Toronto (Bentz et al., 1996). Using this method the diffusion coefficients and m-values need to be determined for the instantaneous diffusion values and not the average diffusion values determined by bulk diffusion techniques. This is more difficult mathematically to determine but is a more powerful approach (Stanish and Thomas, 2003). When the average diffusion coefficient is used to estimate the service life, it is assumed that the conditions are identical. For example, the age at which the concrete is first exposed to chloride ions is identical, the surface concentration is constant throughout the life of the structure and the surface concentration is identical in both cases. If this is not the case, then the average diffusion coefficients obtained from the test results are inaccurate (Stanish and Thomas, 2003). The average diffusion coefficients are a function of both the material properties of the concrete and the test conditions. However, if the instantaneous diffusion coefficient is used, this is not the case. The instantaneous diffusion coefficient is a property of only the materials. The use of instantaneous diffusion coefficients and a finite difference approach therefore allows for the inclusion of varying environmental parameters (Stanish and Thomas, 2003). It is therefore a more powerful approach. The procedure to use bulk diffusion tests to determine the required instantaneous diffusion coefficients and m-values is presented in the following (Stanish and Thomas, 2003).

The equations established previously to determine the effective age of the average diffusion coefficient during a bulk diffusion test are now used to determine the parameters required to describe concrete diffusion coefficients according to Equation 2.14. The two independent unknowns, m and the reference diffusion coefficient need to be determined. The information available for each of the bulk diffusion test is the age at which the concrete was first exposed to chlorides (t_1), the age at which the test was ended (t_2) and the average diffusion coefficient between these two ages (D_{AVG}). This average diffusion coefficient is the result of fitting the chloride profile obtained during the bulk diffusion test to Equation 2.11. To establish the diffusion parameters (m and D_{ref}), the following iterative procedure can be followed (Stanish and Thomas, 2003):

1. Assume a value of m.
2. For each bulk diffusion test, calculate the effective age from Equation 2.20 using the assumed value of m and the test parameters.
3. Determine the logarithms of the average diffusion coefficients (D_{AVG}) and the effective ages from Step 2 for each test.

4. Determine the value of m from the negative slope of the line of best fit using the logs of the average diffusion coefficients as the y-values and the logs of the effective ages as the x-values.
5. Repeat Steps 2 through 4 with the new value of m. When the m-value determined from Step 4 is equal to the m- value used in Step 2, the value of m is established for the concrete.
6. The intercept of the line of best fit will be the log of the1-day diffusion coefficient (if age is given in days). Correct to the reference age using Equation 2.14 and the value of m just determined.

In this manner, the parameters required to completely describe the change in diffusion coefficient with age according to Equation 2.14 can be determined (Stanish and Thomas, 2003).

2.5 Chloride migration

Migration is the movement of charged substances under the action of an electrical field. Due to the slow nature of diffusion, researchers and practitioners commonly accelerate the diffusion process with the use of an electrical potential difference, applied across a concrete specimen. This is generally termed chloride migration. The equations and principles relating to chloride migration are discussed in the following sections, as they relate to commonly used test methods such as the Rapid Chloride Permeability Test (ASTM C1202), the Rapid Migration Test (CTH Test) (Tang and Nilsson, 1991), the South African Chloride Conductivity Index test (Streicher and Alexander, 1995), and accelerated chloride threshold tests (ASTM C1202).

2.5.1 General migration theory

Information for the discussion on general migration theory in this section was taken from Gardner (2006).

Under a gradient of electrical potential, ions will move along the direction of the gradient, depending on the valence of the ions, at an average velocity v_m:

$$v_m = u\frac{\partial \phi}{\partial x} \qquad [2.21]$$

where u is the ion mobility.

Einstein related the ion mobility to the ion valence (z) and a general diffusion coefficient:

$$u = D.\frac{zF}{RT} \qquad [2.22]$$

where F is the Faraday constant (96480 J/(V.mol), R is the gas constant (8.314 J/(mol.K) and T is the absolute temperature (K). If the number density of chloride ions in a solution is N, then the number of chloride ions passing through an area A in a time Δt is given by $(A.v_m.\Delta t).N$. The flux of the chloride ions, J_m, under the action of an electric field can then be calculated by

$$J_m = \frac{(A.v_m.\Delta t).N}{A.\Delta t} = N.v_m \qquad \text{(number of chlorides/m}^2_{\text{solution}}\text{.s)} \qquad [2.23]$$

or

$$J_m = c.v_m = c.D.\frac{zF}{RT}.\frac{\partial \phi}{\partial x} \qquad \text{(g}_{Cl}\text{/m}^2_{\text{solution}}\text{.s)} \qquad [2.24]$$

where c is the concentration of free chlorides.

The external field is assumed to be constant, i.e. $\frac{\partial \phi}{\partial x} = \frac{U}{L}$, where U is the externally applied electrical potential.

Hence, $J_m = D.\frac{zFU}{RTL}.c$ [2.25]

Equation 2.25 is suitable for pure migration. The main assumptions in this equation are that the Einstein relation is valid for a concentrated solution and the external electrical field is constant.

2.5.2 Steady state migration of chlorides into concrete

In the case of a steady state process constant flux occurs and the flux is independent of distance and time, provided that the chloride concentration in the bulk solution remains constant. The diffusion coefficient can therefore be expressed as below (Gardner, 2006).

$$D = \frac{JRTL}{zFUc} \qquad [2.26]$$

Or if the area of concrete is used for the calculation of the flux, Equation 2.26 becomes:

$$D_{ssm} = \frac{RTL}{zFUc}.J_{concrete} = \frac{RTL}{zFUc}.J_{0m}.\varepsilon = D_0\varepsilon = D_{ss} \qquad [2.27]$$

Where D_{ssm} is the non-steady state migration coefficient, D_{ss} is the steady state diffusion coefficient, J_{0m} is the migratory flux through the pore solution and D_0 is the diffusion coefficient per unit cross sectional area of pore solution. Equation 2.27 therefore shows that the diffusion coefficient from a steady state migration test is identical to that from a steady state diffusion test.

2.5.3 Non-steady state migration

The non-steady state is more complex as the three dimensional cement matrix has varying permeability and porosity properties and chloride binding further complicates the fundamental process.

In the non-steady state process:

$$\frac{\partial c}{\partial t} = -\frac{D_0}{1+\frac{\partial c_b}{\partial c}} \cdot \frac{zFU}{RTL} \cdot \frac{\partial c}{\partial x} = -D_{nssm} \cdot \frac{zFU}{RTL} \cdot \frac{\partial c}{\partial x} \quad [2.28]$$

For a particular time duration t, the chloride front will move to a distance x_f, and reach a maximum concentration of c_0(concentration of the bulk solution). Therefore Equation 2.28 becomes:

$$D_{nssm} = \frac{D_0}{1+\frac{\int_0^{c_b} c_b}{\int_0^{\gamma_0 c_0} dc}} = \frac{RTL}{zFU} \cdot \frac{\int_0^{x_f} dx}{\int_0^{t} dt} \quad [2.29]$$

Which can be simplified to:

$$D_{nssm} = \frac{D_0}{\left(1+\frac{c_b}{\gamma_b c_0}\right)} = \frac{RTL}{zFU} \cdot \frac{x_f}{t} \quad [2.30]$$

Where $0 \leq \gamma_b \leq 1$ and is effectively an active coefficient for chloride binding during migration.

From chloride binding theory:

$$\frac{c_b}{\gamma_b c_0} = K_b \frac{W_{gel}}{\varepsilon} \quad [2.31]$$

where W_{gel} is the hydrated gel content of the concrete (kg_{gel}/m^3), ε is the porosity of the concrete, and K_b is the chloride binding constant during non-steady state (NSS) migration ($m^3_{solution}/kg_{gel}$):

$$K_b = \frac{f_b}{1000}\left(\gamma_b c_0\right)^{\beta-1} \quad [2.32]$$

where f_b and β are adsorption binding constants.

This produces the final equation:

$$D_{nssm} = \frac{D_0}{\left(1 + K_b \frac{W_{gel}}{\varepsilon}\right)} = \frac{RTL}{zFU} \cdot \frac{x_f}{t} \qquad m^2{}_x/s \qquad [2.33]$$

D_{nssm} is relatively constant whereas $D_{nss}$is not, as previously mentioned.

2.6 Mechanisms of chloride binding

The combined mechanisms of chloride transport and binding are complex. In concrete, chlorides are present in any of the following forms; (i) acid soluble chlorides: this is the total amount of chlorides present in concrete or the amount of chlorides that are soluble in nitric acid, (ii) bound chlorides: these are chlorides chemically bound with the hydration products of the cement (e.g. C_3A tricalcium aluminate or C_4AF tetracalciumaluminoferrite) and the loosely bound chlorides with the C-S-H gel, (iii) free or water soluble chlorides, which refer to free chloride ions within the pore solution of the concrete and which are extractable in water under defined conditions (Nagataki, 1993). The relationship between these various chloride concentrations is as follows:

$$c_{TOTAL} = c_{FREE} + c_{BOUND} \qquad [2.34]$$

where c is the concentration in kg/m^3, moles/volume of kg/kg. The free chlorides are given per volume of solute (kg/m^3 solution). The bound and total amounts of chlorides are often given per mass of binder or concrete.

It is the free chloride ions which can move through the concrete, and which can possibly destroy the passive film on the surface of the steel bar and initiate corrosion. When free chloride ions from the environment penetrate into the concrete, some of them will be immobilised by the hydration products - the process of chloride binding. Although the mechanisms of chloride binding are not quite clear, it is believed that both physical adsorption and chemical reactions are involved. Chloride binding is essentially the removal of chloride ions from the solution through interaction with the concrete matrix. Chlorides can be bound chemically through a reaction with C_3A to form calcium chloro-aluminates (Boddy et al., 1999).The large surface area of the hydrate gel provides plentiful sites for physical binding, while “Friedel’s salt” is commonly thought to be a major product of chemical binding. The bound chlorides are generally thought to be ‘harmless’ to the reinforcement. This binding effect also retards the transport process of the free chloride ions. Therefore, the effect of chloride binding must be taken into account when studying chloride transport in concrete.

The nature of the concrete chemistry is important in determining the migration of chloride through concrete and thus the level of chloride present at the steel. Chloride binding may further influence chloride transport through partial blocking of pores due to the formation of the calcium chloro-aluminates. All mineral cements bind chlorides to some degree and this strongly influences the rate at which chlorides penetrate the concrete when exposed to chlorides from an external source. Chloride binding effectively removes chlorides from the transport process resulting in changes to the pore solution concentration and thus the gradient driving ionic diffusion (Glass et al., 1997).

In principle, chloride binding helps prevent or delay corrosion activation in reinforced concrete in two ways(HETEK-53, 1996):

- It decreases the rate of chloride ingress into the concrete since the chloride binding process reduces the concentration of chloride ions in the pore solution available for transportation. At low concentrations the binding process is very effective, removing nearly all free chlorides from the pore solution.
- Ions dissolved in the pore solution are believed to initiate corrosion. The total amount of chlorides (bound and free) which can be tolerated in concrete at the depth of the reinforcement is therefore assumed to be a function of the chloride binding capacity. If this assumption is right, a higher chloride binding capacity implies that a higher total amount of chlorides (by weight of binder) corresponds to a given critical concentration of free chlorides in the pore solution.

When designing for and predicting the service life of a concrete structure, two variables are necessary to characterise the chloride binding capacity (Tang and Nilsson, 1993):

- Chemical binding capacity - The alumina content and total binder content gives an indication of the amount of alumina available to chemically bind chlorides. The chemical binding studies discussed show clear evidence of chemical binding occurrence and its dependence on cement content and composition.
- Physical adsorption capacity – The internal surface area of the matrix available to physically adsorb chloride ions.

2.6.1 Chloride binding isotherms

A chloride binding isotherm can be defined as the quantitative relationship between bound (or total) chlorides and free chlorides at a constant temperature. Chloride binding isotherms are therefore used to characterise the gel's ability to bind ions at increasing chloride concentrations. These isotherms do not distinguish between adsorption and chemical binding but give a global indication of the gel's ability to interact with and immobilise chloride ions.

Two isotherms are commonly used to express the relationship between free and total chlorides at a particular temperature. These are expressed below.

The Langmuir Isotherm (Glass et al., 1998)

$$c_t = c_b + M_{Cl} V c_f \qquad [2.35]$$

where c_b is the bound chloride ions, c_t is the total concentration of chloride ions, M_{Cl} is the atomic mass of chlorine, V is the pore solution volume and c_f is the free chloride concentration

Freundlich Isotherm (Glass et al., 1997)

$$c_b = \kappa (c_f)^{1/n} \qquad [2.36]$$

Where κ and n are constants dependent on binding capacity.

The above isotherms were developed originally to describe gas adsorption onto solids. The Langmuir isotherm was derived for the adsorption of a monolayer of gas onto a solid, whereas the Freundlich isotherm is an empirical description of the multi-layer adsorption process (Glass et al, 1997).

Glass et al.(1997) found that the Langmuir isotherm predicted the relationship between total and free chloride concentration more accurately, but the Freundlich isotherm was simple and easy for practical applications. It was also found to be superior when applied to instances where a high level of chloride binding occurred (e.g. where a supplementary cementitious material was used, with high chloride binding capacity).

A study conducted by Tang and Nilsson (1993) found that the relationship in their study obeyed the Freundlich isotherm at free chloride concentrations higher than 0.01 mol/l and that it obeyed the Langmuir isotherm at concentrations lower than 0.05 mol/l. This implies that at low concentrations, monolayer adsorption occurs, and at concentrations above 0.05 M, complex adsorption involving multiple, interacting adsorption layers occurs. This in turn corresponds to the findings of Glass et al. (1997).

2.6.2 Measurement of chloride binding

Different methods for measuring chloride binding have been established. These methods can generally be classified into two types: measurement of total-free chloride relationship, and measurement of bound-free chloride relationship.

Pore solution expression technique

This technique is widely used and it measures the total chloride content and the free chloride concentration of a concrete specimen under investigation. The concrete sample placed in an expression device and compressed in a compression machine which effectively squeezes out the pore solution out of the sample. This solution is collected and analysed to determine the free chloride concentration. Total chloride contents can then be determined from another sample and the amount of bound ions can be calculated using the following equation:

$$Cl_{total} = Cl_{expressed\ solution} + Cl_{bound} \qquad [2.37]$$

Glass and Buenfeld (1995) and Glass *et al.* (1996) found that the free chloride concentrations of the expressed pore solutions were higher than the equilibrium solution. They accounted this to the destruction of the microstructure and compressive forces which resulted in the disruption of loosely bound or adsorbed chloride ions. These results were confirmed by Nagataki*et al.* (1992) and Tritthart (1989).

Equilibrium method

The equilibrium method is a more direct measurement for chloride binding. This method involves submerging a sample of concrete or mortar, either whole or crushed in a certain amount of chloride solution of known concentration until equilibrium is reached and measuring the equilibrium concentration in the storage solution as the free chloride ion concentration:

$$[Cl^-]_{pore\ solution} = [Cl^-]_{external\ solution} = [Cl^-]_{free}\ (mg_{chlorides} / ml) \qquad [2.38]$$

The amount of bound chlorides can then be calculated using mass balance considerations.

This method has the advantage of not disrupting the microstructure during analysis, however the time-consuming nature of obtaining equilibrium is a disadvantage and it relies on the assumption that equilibrium between the pore and external solution occurs and is maintained.

2.6.3 Factors affecting chloride binding

It is possible to identify a number of factors which influence the amount of bound chlorides, as discussed in the following sections.

Temperature

Studies conducted by Roberts (1962) and Larsson (1995) indicate that the amount of bound chlorides decreases as temperature increases. For physical adsorption an increased temperature increases the thermal vibration of the absorbates (chloride ions) resulting in more unbound absorbates (Tang, 1996). In terms of the chemical reaction, even though an increased temperature increases the rate of the reaction it may also increase the solubility of the reaction products (Friedel's salt) which in turn results in more reactants (chloride ions) to be free at equilibrium (Tang, 1996). Therefore, both the physical adsorption and the chemical reaction tend to decrease chloride binding at higher temperatures.

Type of binder

Various binder types are incorporated into concrete mixes to improve the properties of the concrete mix and for economic benefits. Their chemical compositions are significant as they have the ability to change the chemistry, microstructure, resulting performance and durability of the concrete (Vagelis et al., 2000). The total content of alumina and iron oxide in binder dominates chemical binding, whereas the fineness of the hydration gel dominates physical binding (Tang and Nilsson, 1992). Lambert et al. (1985) found that chloride binding of the cement paste increased with increasing C_3A content of the cement, and the amount of free chlorides in the pore water increased when sulphate was added. Therefore, varying the binder composition can change the binding potential of a concrete mix.

Tang and Nilsson (1991) reported that the capacity of chloride binding strongly depends on the amount of C–S–H gel in the concrete, regardless of w/c ratio and the amount of aggregates. Binders containing mineral admixtures such as silica fume (SF), pulverized fly ash (FA) or ground granulated blast furnace slag (GGBS) enhance the formation of more gel thereby offering larger surface areas available for adsorption. In addition, fly ash and slag react to calcium aluminate hydrates which also might form Friedel's salt (Justnes, 1998).

It is therefore vital to understand the varying compositions of the various binder systems and their effect on chloride binding. Table 2.4 shows the common binder types found in South Africa and their chemical compositions.

Table 2.4: Typical South African cement and cement extender compositions (Mackechnie et al, 2003; Mackechnie and Alexander, 2000 and Addis and Owens, 2001)

Oxides	OPC	CS	GGBS	FA	CSF
CaO	67.2	37.2	34.0	4.7	0.6
SiO_2	22.3	30.8	35.5	54.1	92.0
Al_2O_3	4.4	16.0	15.4	32.9	1.5
MgO	1.01	13.7	9.4	1.3	0.6
TiO_2	0.22	0.51	1.2	1.7	-
Fe_2O_3	3.4	0.87	0.98	3.3	1.2
MnO	0.08	0.09	0.88	-	-
K_2O	0.56	0.35	0.87	0.6	0.6
Na_2O	0.21	0.12	0.16	0.6	-
SO_3	0.58	3.19	2.49	0.4	-

Ground Granulated Blastfurnace Slag (GGBS)

GGBS is a by-product of the blast furnace process used to produce iron and its main constituents include silica and alumina from the iron ore, and lime added as a fluxing agent (Addis and Owens, 2001). The use of GGBS results in a decrease in porosity of the concrete as a result of the formation of finer hydrated products and in turn results in a higher physical binding capacity (Soroka, 1993). The addition of GGBS to Portland cement slightly increases the amount of CSH gel due to its slightly higher silica content (Table 2.5). However, the amount of aluminium oxide present is far greater in a GGBS-containing mix, and as the amount of aluminium oxide present is fundamental to chemical chloride binding i.e. the formation of Friedel's Salt, the addition of GGBS increases the chemical binding potential. This has been shown in a number of studies conducted by Dhir *et al* (1996); Glass *et al* (1997) and Birnin-Yauri and Glasser (1998).

Dhir *et al.* (1996) found that for a replacement level of 66.7% GGBS, the chloride binding capacity was significantly increased when compared to that of an OPC control mix when exposed to a 5 M sodium chloride solution (shown in Figure 2.8). Dhir *et al*. (1997) concluded from this work that the changes observed in chloride diffusion were a result of the high alumina content of the GGBS which resulted in the formation of Friedel's Salt which in turn chemically binds a significant portion of the chloride ions. This large increase in chloride binding capacity would therefore lower the free chloride concentration in the matrix, resulting in a lower rate of diffusion and, therefore a longer service life.

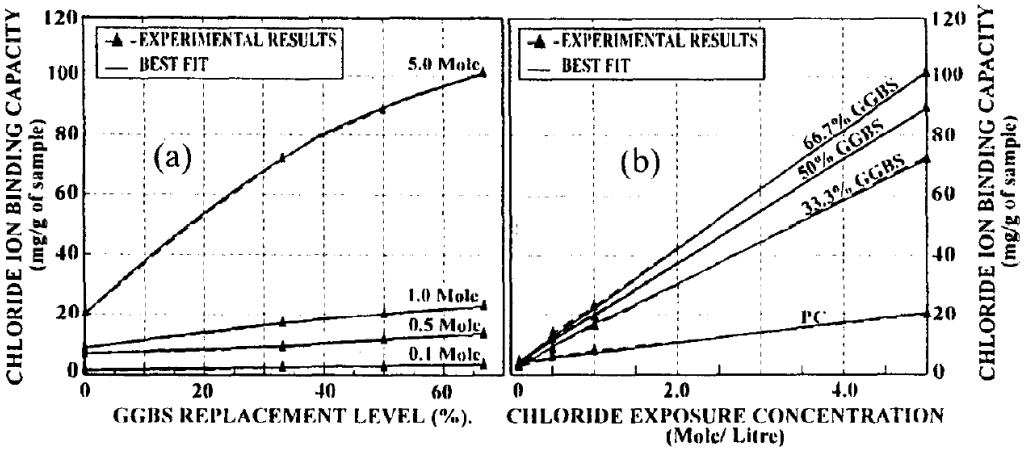

Figure 2.8: The effect of GGBS replacement on the chloride binding capacity of concretes (Dhir et al, 1996)

Work conducted by Luo *et al.* (2003) confirmed Dhir *et al*. (1996) findings that the inclusion of GGBS results in a significant increase in the chloride binding of the concrete mix. They also found a decrease in chloride binding capacity in the presence of sulphates. This is as a result of the sulphate and chloride ions competing to occupy binding sites available in the microstructure.

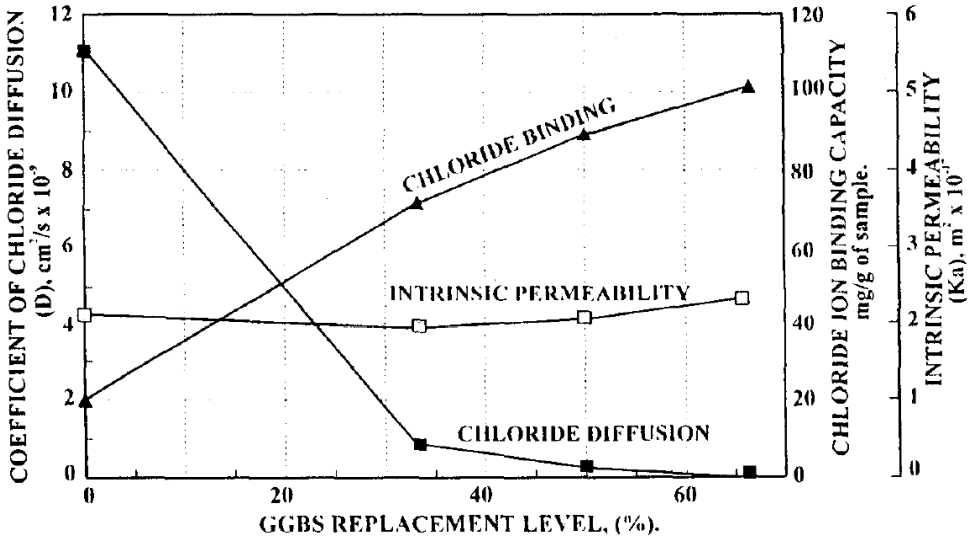

Figure 2.9: The effect of GGBS replacement on permeability, chloride binding capacity and chloride diffusion (Dhir *et al.*, 1996)

Ground Granulated Corex Slag (GGCS)

GGCS is a by-product of the Corex process at the Saldanha steel plant in the Western Cape, South Africa. GGCS has a similar chemistry and characteristics as Ground Granulated Blastfurnace Slag (GGBS). However, analysis showed that GGCS has higher CaO, Al_2O_3 and MgO concentrations than GGBS, and lower levels of SiO_2, and hence GGCS is expected to have a higher hydraulic activity than GGBS of equivalent fineness (Mackechnie et al, 2003).

Optimum chloride resistance of concrete containing GGCS is assumed to be achieved at replacement levels of 50% and above (Mackechnie *et al,* 2003). The improved chloride resistance of GGCS concrete may be a result of the denser microstructure and increased chloride binding by aluminate phases.

Condensed Silica Fume (CSF)

CSF is the condensed vapour from the ferrosilicon smelting process. It is extremely fine and therefore when used as a cement extender it improves the microstructure and pore structure of a concrete. CSF is high in silica (92% by mass) and the by-products of the initial CSH reaction react with the additional silica provided by the CSF to form more CSH gel. This in turn improves the transport properties of the concrete mix and hence the service life of a structure.

Studies conducted by Arya *et al.* (1990), Arya and Xu (1995), Delagrave *et al.* (1997), and Page and Vennesland (1982) show that CSF replacement results in a reduction of chloride binding capacity and that the chloride binding capacity of CSF containing mixes are inferior to mixes containing other extenders such as GGBS and FA. Some experimental results obtained by Arya and Xu (1995) are shown in Figure 2.10.

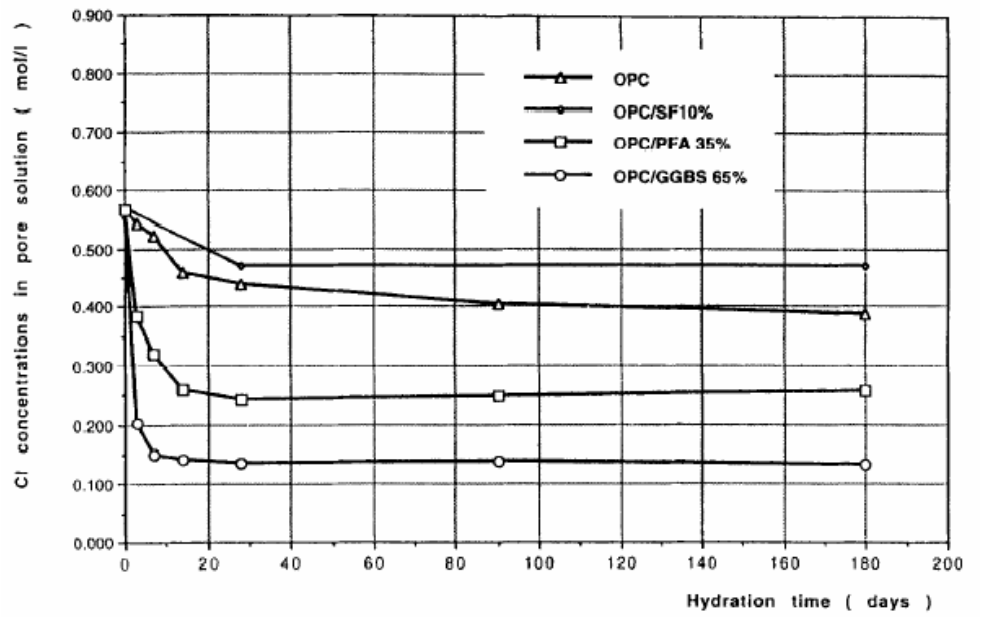

Figure 2.10: Pore solution chloride concentration of different extender mixes exposed toa 3% chloride solution (Arya and Xu, 1995)

It is assumed that the reduction in chloride binding capacity in CSF concrete is a result of two mechanisms. Firstly, the substitution of CSF lowers the amount of alumina in the concrete mix available for hydration and subsequently for chloride binding, and, secondly, the densification of the CSH gel lowers the effective pore surface area in the microstructure and this in turn lowers the physical and chemical binding potentials by making the AFm phases (monoferrite alumina phase) less accessible.

Fly Ash (FA)

FA is extracted by electrostatic precipitators from the flue gases of furnaces fired with pulverized coal. It is made mostly of silica and alumina and this chemical composition is what makes it

useful as a supplementary cementitious extender. The spherical nature and the high silica content of fly ash which reacts with the CH by-product to form further CSH gel improves the density of the matrix. The relatively high alumina content of fly ash is also beneficial to chemical chloride binding. However, the benefits of FA replacement only become apparent after 28 days, which is a result of the latent hydraulic property of FA.

Ngala *et al.* (1995) showed that FA replacement improves values for porosity chloride diffusivity (D_{cl}) and oxygen diffusion (D_o). The difference in chloride diffusivity between the plain OPC mix and the FA mix was accounted to the less permeable matrix of the FA concrete, as well as the increased chloride binding capacity of the matrix.

The literature contains a variety of discussions on improved chloride resistance of concrete containing FA (Ngala *et al*., 1995; Thomas and Matthews, 2004; Thomas and Bamforth, 1999; Song *et al.*, 2008; Tamimi *et al.*, 2008). Thomas and Matthews (2004) conducted experiments on concrete prism samples exposed to marine environments for a period of 10 years and showed that FA significantly reduces the chloride profiles obtained, indicating that the movement of the chloride front through the concrete is significantly slowed down, hence retarding diffusivity and diffusion coefficients (Figure 2.11).

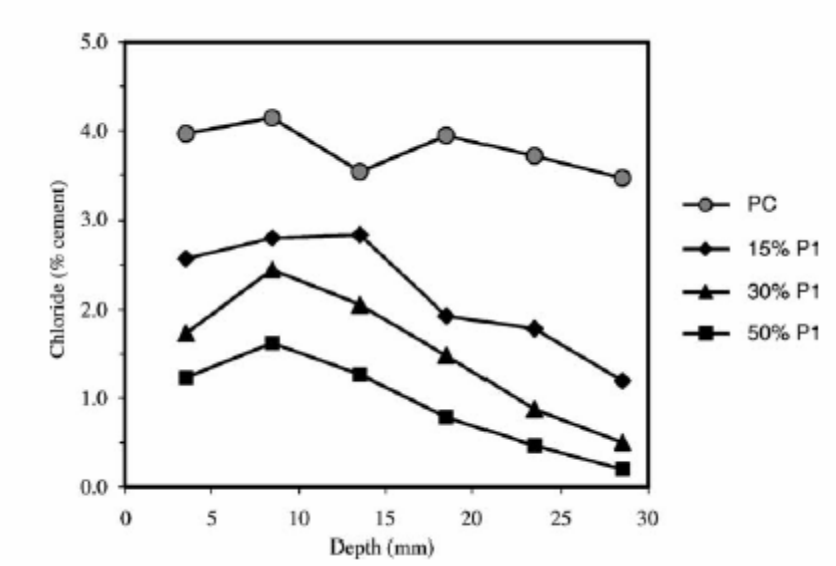

Figure 2.11: Effect of FA on chloride profiles (Thomas and Matthews, 2004)

Alkalinity

The composition of the pore solution is decisive for chloride binding. It is therefore important to consider the concentration of other ions present in the solution. Tuutti (1982), Tritthart (1989), Byfors (1990), Page *et al.* (1991) and Sandberg and Larsson (1993) found that the hydroxide concentration i.e. the pH, of the pore solution has a significant influence on chloride binding since the hydroxide ions "compete" for the binding sites with the chloride ions. (Tang 1993). The chloride binding capacity has been experimentally shown (Sandberg 1993, Byfors 1990) to be affected by the alkalinity and the sulphate ion concentration of the pore solution. Since hydroxide ions are removed from concrete in a similar way as chloride and sulphate ions are transported into it, the chloride binding capacity is affected by the pore solution chemistry, a property which

is time dependent. It has been shown that the higher the hydroxide concentration the lower the chloride binding.

2.6.4 Consideration of chloride binding in the modelling of chloride ingress

As discussed in the previous sections, chloride binding has a positive impact on the durability of a concrete structure. It removes chloride ions from the pore solution thereby decreasing diffusion rates as a result of a decreased chloride front concentration.

A denser, less permeable pore structure brought about by the use of supplementary cementitious extenders affect the resulting transport properties of the matrix. The superior binding capacities of FA, GGCS and GGBS retard the movement of ions through the matrix, thereby significantly reducing diffusion coefficients (generally to an order of magnitude lower than CEM 1 controls). GGCS enhances chloride binding capacity through the addition of further alumina to the mix. This in turn slows the diffusion process by lowering the amount of free chloride ions available to facilitate reinforcement corrosion. GGCS has similar properties to GGBS. CSF increases the density of the cement matrix due to its high silica, and this significantly denser microstructure slows the diffusion process physically. FA also refines the pore structure of the matrix, providing a physical impediment to chloride transport.

In order to correctly establish chloride transport mechanisms in concretes exposed to the marine environment, chloride binding should be considered and factored into quality control tests and modelling. Attempts to include chloride binding into the characterization of concrete mixes have for example been presented by Nguyen *et al.* (2006); Martin-Perez *et al.* (1998) and Saetta *et al*. (1993). However, their studies showed that chloride binding is a very complex process and that it is difficult to precisely account for chloride binding in a way that would make service life estimation of concrete structures in the marine environment more accurate. Most authors do therefore not explicitly include chloride binding modelling in the characterization of concrete mixes for service life prediction, but rate concrete mixes based on their overall resistance to chloride ingress. This simplifaction has proven to result in satisfactory results with respect to service life modelling (e.g. Ferreira *et al.*, 2004; Thomas and Bentz, 2000; Bamforth, 1999; Mangat and Molloy, 1994) and will therefore be adopted in this research. The decision to adopt a more simplified approach was based on making the model accessible to engineers as a design tool for a wide range of general applications. Accounting for multi-mechanistic transport and chloride binding in partially saturated concrete requires detailed knowledge of on site-specific conditions and a wide range of material properties that are usually not available to the engineer at the design stage. It is however important that the principles and mechanisms of chloride binding be understood in order to understand the contributing factors to improved chloride resistance of concretes containing blended cements.

2.7 Critical chloride threshold levels

This threshold chloride concentration or critical chloride concentration (C_t) is defined as the as the minimum total acid soluble chloride content of the concrete at the depth of the reinforcement which results in active corrosion of the reinforcement. Both for the design of new structures and for condition assessments of existing structures, knowledge of a reliable C_t value is of great importance as the remaining service life of a structure is often considered as the time required

to reach the chloride threshold value at the depth of the steel reinforcement. In service life modelling, C_t has been identified to be one of the most decisive input parameters (Tang and Gulikers, 2007). Despite the multitude of studies undertaken, many aspects of chloride induced reinforcement corrosion in concrete are still incompletely understood and no general agreement on a C_t value has been achieved. Results reported in literature scatter over a large range (Ann and Song, 2007, Glass *et al*., 1997 and Breit, 1998). This is a result of differing definitions, measuring techniques and testing conditions, and also as a result of the stochastic and complex nature of initiation of pitting corrosion.

It is important to bear in mind from a practical point of view that it is very difficult or almost impossible to measure the free chloride content or the pH of the concrete pore solution. Accurate values are therefore often unknown. It is comparatively much simpler to determine the total chloride content and to relate it to the weight of concrete or cement. For the purposes of this research, it was therefore decided to best present chloride thresholds in the form of total chloride by mass of binder.

2.7.1 Parameters influencing chloride threshold values

Chloride threshold concentration is a function of the pH, or conversely the OH^- ion concentration. The chloride threshold value required for corrosion to occur has been the subject of a considerable amount of debate over the recent years, and a value of 0.4% by mass of cement is often used (Bamforth, 1999). It is however important to understand that it cannot be represented by a single value, and that it is in fact dependent on a number of factors, namely:

- w/b ratio:

  The w/b ratio as well as the degree of hydration has an effect on the porosity of the concrete paste and therefore the availability of moisture and oxygen at the reinforcement. It has been shown that the threshold chloride content increases with decreasing w/b ratio (Hansson and Sorensen, 1990; Pettersson, 1995 and Poupard *et al.*, 2004). Both the porosity and the moisture content are reflected by the electrical resistivity, a parameter that has been found to empirically correlate with chloride threshold values in a more recent study (Morris et al., 2004).

- Binder type:

  The type of binder affects corrosion initiation by determining the amount of chloride that is available in the pore solution as a result of chloride binding and by affecting the pH of the pore solution. Certain binders also may increase the electrical resistivity of the concrete or improve the characteristics of the steel-concrete interface by forming a denser microstructure.

  Fly Ash (FA). Thomas (1996) found lower C_t values for reinforced concrete specimens after exposure to a marine environment for up to four years when they contained FA, i.e the tolerable chloride content decreased with increasing substitution of OPC with FA. Similarly, Oh et al. (2003) measured lower chloride thresholds with increasing addition of FA. In contrast, Schiessl and Breit (1996) reported higher chloride threshold values for concretes containing FA, and Alonso et al. (2002) did not find significant differences in C_t when replacing cement with FA. A clear influence of FA addition on chloride threshold values has therefore not yet been established.

Silica Fume (SF). In comparison with Ordinary Portland cement (OPC), lower chloride threshold values have been reported for SF containing cement (Pettersson, 1992 and Manera et al, 2008). The partial replacement of OPC with SF reduces the amount of aluminate phases and thereby the ability of the cement to bind chloride. But since the addition of SF also leads to a refinement of the pores, the effect of physical adsorption is more pronounced in SF containing binders.

Blast furnace Slag (BS). Work done by Gouda and Halaka (1970) reported lower chloride threshold values for concrete specimens containing slag when compared to specimens containing OPC cement. The use of BS increases the chloride binding capacity due to improved chemical and physical binding (Arya et al, 1990; Dhir et al, 1996; Luo et al, 2003).

- pH of the pore solution:

  The pH of the pore solution initially depends mainly on the type of binder, but is affected at later stages as carbonation, leaching and hydration proceeds. The presence of Portlandite is the reason for the pH of the pore solution to be as high as 12.5 but the presence of NaOH and KOH can increase it further to values above 13.5. The formation of a cement rich layer at the steel-concrete interface stabilises the high pH and contributes to the passivity of steel in concrete. Hydroxide ions have an inhibiting effect against chloride induced corrosion thereby influencing chloride threshold (Venu et al., 1965, Hausmann, 1967 and Gouda, 1970).

- Binding capacity of the cement paste:

  The capacity of the hydration products to bind chlorides affects the critical chloride content when expressed in terms of total chlorides. Since bound and free chlorides are suggested to be connected by a chemical equilibrium, also bound chloride present a corrosion risk by acting as a reservoir of chloride that might dissolve at altered conditions (Glass et al., 2000). The degree of chloride binding depends on many factors among which some are related to the binder type, as discussed in previous sections.

- Exposure conditions i.e temperature and relative humidity:

  Both water and oxygen are required for the corrosion process and therefore a lack of one of them is sufficient to inhibit corrosion. Since the moisture content regulates the availability of water and oxygen at the steel surface, it can be regarded as a global, environmental influencing factor for chloride thresholds. In the case of water saturated concrete as well as in dry concrete, higher chloride concentrations are required to initiate corrosion; the situation most favourable for corrosion initiation is in the range 90-95% relative humidity (Schiessl and Lay, 2005) or concrete exposed to wetting/drying cycles (Tuutti, 1993). The amount of water in the concrete pores also affects the distribution between free and bound chlorides and therefore determines the concentration of free chloride in the pore solution and hence the chloride threshold value.

2.7.2 A brief summary of critical chloride contents in literature

Numerous publications in connection with C_t can be found in the literature. Chloride thresholds based on the total chloride content are the most consistent, in the range of 0.17 to 2.2% total Cl by weight of binder (Pettersson 1995). Tables 2.5 – 2.7 show the scatter of critical chloride threshold value results obtained by different researchers for different concrete types.

Table 2.5: Reported chloride threshold values in total chloride content per weight of binder (Angst and Vennesland, 2009)

Cl	Cement type	Reported value (total chloride content per weight of binder)	Reference
A	OPC	0.4	Richartz, 1969
A	OPC, GGBS	1.0….3.0	Gouda *et al.*, 1970
D	various cements	0.2….1.4	Stratfull *et al.*, 1975
A	OPC	0.4….0.8	Locke et al., 1980
A	OPC	0.25...0.5	Elsener *et al.*, 1986
A	OPC	0.1….0.19	Hope *et al.*, 1987
D	various cements	0.4….1.37	Hansson *et al.*, 1990
A/D	various cements	0.5…..2.0	Schiessl *et al.*, 1990
A/D	OPC, SRPC	1.5…..2.5	Lambert *et al.*, 1991
D	OPC, FA	0.2…..0.7	Thomas, 1996
A	OPC	1.24…3.08	Alonso *et al.*, 2000
D	various cements	0.73	Alonso *et al.*, 2002
D/M	SRPC	0.15…0.23	Castellote *et al.*, 2002
M	OPC	0.02…0.24	Trejo *et al.*, 2003
A	OPC, SF		Manera *et al*., 2008
min...max		**0.02....3.08**	

A = chloride added to the mix

D/M = chloride introduced into hardened samples by diffusion/capillary suction (D) or migration (M)

Chloride threshold levels vary extensively in field exposed concrete (Table 2.7) as a result of the varying microclimate at the steel surface. As a result, the chloride threshold level depends on the concrete cover and on the physical bonding between the concrete and the reinforcement. Carbonation of concrete can also reduce the threshold level by reducing the pH and the chloride binding capacity of the cement paste (Ferreira, 2004).

As a result of the uncertainties associated with the threshold level, national codes and recommendations tend to be conservative. They do not take into account the effect of exposure conditions, cover size and w/c ratio. In Great Britain, BS 8110 and in Norway, NS 3420, a maximum of 0.4% total chloride by weight of cement is allowed in normal concrete. In America, the ACI recommends a maximum of 0.2% total chloride by weight of cement (Glass, 1995).The European standard EN 206-1 restricts the chloride content to 0.2 to 0.4% chlorides by mass of binder for reinforced concrete and 0.1 to 0.2% for prestressed concrete. These limits, however, are not proper chloride threshold values, but rather practical guidelines for the production of fresh concrete.

Table 2.6: Some critical chloride threshold concentrations as reported in the literature

Chloride threshold value (% by mass of binder)	Remarks	Reference
0.17 - 1.4	Field	Stratful et al. (1975)
0.2 - 0.4	Varied with pH	Cady (1990)
0.2 - 1.5	Field	Vassie (1984)
0.25	Field	West (1985)
0.25 - 0.5	Laboratory	Elsener (1986)
0.3 - 0.7	Field	Henriksen (1993)
0.4	Varied with cement type	Brown (1982)
0.4	Outdoors	Bamforth (1994)
0.4 - 1.6	Laboratory	Hansson (1990)
0.48 - 2.02	Varied with cement type and admixtures	Schiessl (1990)
0.5	Outdoors	Thomas (1990)
0.5 - 1.4	Laboratory	Tuutti (1993)
0.5 - 2.0	Laboratory	Schiessl (1990)
0.6	Laboratory	Locke, Siman (1980)
0.6 - 1.4	Varied with cement type, curing, water to binder ratio, admixtures, etc	Hansson (1990)
0.9 - 1.8	w/b 0.30 - 0.40, pH 3.0 - 13.8, Cl/OH=3 - 6, vairied with pH, cement pozzolan	Pettersson (1993)
1.6 - 2.5	Laboratory	Lambert (1991)
1.8 - 2.2	Field	Lukas (1985)

Chlorides that enter the concrete after it has hardened are more harmful than those that are present in the concrete from the start as admixtures or contamination of aggregates (assuming these cast-in chlorides do not exceed the threshold value). This is because a proportion of any chloride ions present in freshly mixed concrete will combine with tricalcium aluminate in the cement and will not be available for initiating corrosion. Experiments using cast in chlorides have suggested that there is no specific level at which corrosion is initiated, but rather that the corrosion rate increases gradually as the chloride level increases and that some corrosion will occur if free chlorides are present at the steel interface (Dhir et al. 1996).

In literature it is stated that there is very little difference in the water-soluble chloride content required to initiate corrosion in equivalent strength Portland cement and fly ash concrete, it is however the rate at which the chloride ions are transported to the site once corrosion has been

initiated that is important (Angst et al, 2008). The diffusion coefficient is therefore an important parameter in determining the rate of corrosion.

Table 2.7: Published C_t values from real structures

C_t (total Cl^- by% mass of binder)	Chloride cation	Cement type	Year	Reference
0.2 – 1.4	Na	NR	1975	Stratfull et al. (1975)
0.25 – 1.5	Na	NR	1984	Vassie (1984)
0.1 – 0.19	Ca, Na	OPC	1987	Hope and Ip (1987)
0.96 – 1.96	Ca	OPC	1989	Treadaway et al. (1989)
0.7	Seawater	OPC	1996	Thomas et al. (1996)
0.2 – 0.65	Seawater	FA	1996	Thomas et al. (1996)
0.4 – 1.5	Seawater	SRCP, FA, SF, GGBS	1998	Sandberg (1998)
0.2 – 0.4	Na	NR	2000	Zimmermann (2000)
0.72	Seawater	NR	2001	Fluge (2001)
0.4 – 1.3	Na	OPC	2004	Morris et al. (2004)
0.1 – 1.96	**min……max**			

2.8 Detection and quantification of chlorides in concrete

2.8.1 General

This section covers the detection and analysis of chloride contents in concrete. As discussed in previous sections, chloride ingress into reinforced concrete is as a result of a number of mechanisms, namely diffusion, absorption, capillary action, and chloride binding, of which diffusion is considered dominant. In order to understand and quantify the chloride transport properties of concrete it is important determine the apparent chloride ion diffusion coefficient (D_a) of the concrete mix under investigation. D_a is a measure of the chloride resistance capacity of the concrete and is affected by a number of factors which including mix materials, construction practices, age and exposure conditions. The surface chloride concentration (C_s) which is a measure of the accumulation of chlorides on the concrete surface which gives the diffusion process its driving potential is also an important measurable property. These two values are characteristic properties that are used in service life prediction models to predict the time to corrosion initiation and the inherent durability of reinforced concrete exposed to chloride environments (Stanish and Thomas, 2003).

2.8.2 Chloride profiling and chloride contents

A chloride profile is defined as a measured or predicted distribution of chlorides at a certain time in a part of a structure or in a specimen. It is represented in the form of a curve showing the total amount of chlorides as a function of depth (Figure 2.12).

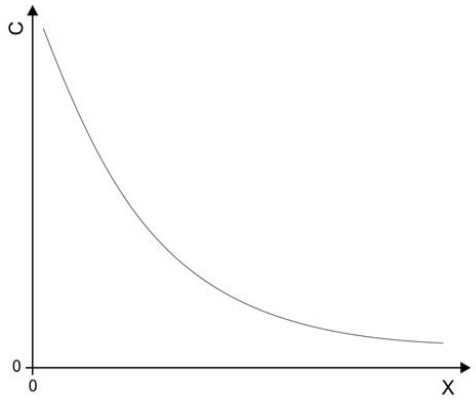

Figure 2.12: Typical chloride profile in concrete (c = chloride concentration, x = depth from the concrete surface)

Chlorides penetrate concrete mainly by the process of diffusion which means that the content of chlorides is largest at the exposed surface and decreases with increasing depth. The slope of the profile gets smaller as the depth increases. At the surface of the concrete a certain amount of chlorides are present, and this is the initial/surface chloride concentration of the concrete (C_S).

The concentration of free chlorides in the pores of the concrete surface is usually assumed to be equal to the concentration of chlorides in the surrounding environment. The amount of bound chlorides is related to the concentration of free chlorides in the pore liquid. Consequently, the profile of bound chlorides and the profile of the total amount of chlorides follow the profile for the free chlorides. The binding of chlorides is different for different concretes depending on the concrete composition and the type of binder, as discussed in previous sections. The binding properties will influence the shape of the chloride profiles. In Figure 2.13 the effect of binding is shown as a comparison of chloride profiles for two concretes which differ only with respect to chloride binding properties. The concrete with a higher binding capacity will have higher total chloride content at the concrete surface, since the amount of bound chlorides is larger. On the other hand, the penetration depth in that concrete will be smaller because more of the chlorides that penetrate are bound, which will delay the penetration (Ferreira, 2004).

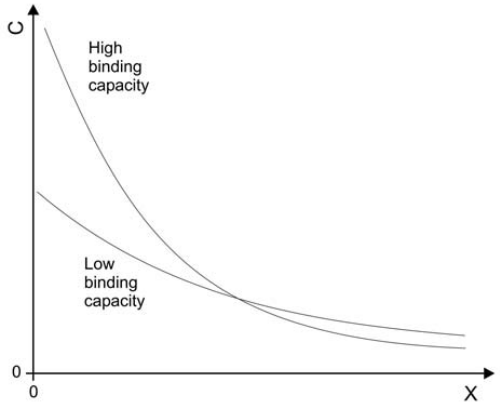

Figure 2.13: Chloride profiles for two concretes with different chloride binding properties

However, measured chloride profiles do not always have the simple theoretical shape as expected from pure diffusion. Lower chloride content is frequently found close to the surface and a maximum in chloride content is found at some depth (Figure 2.14).

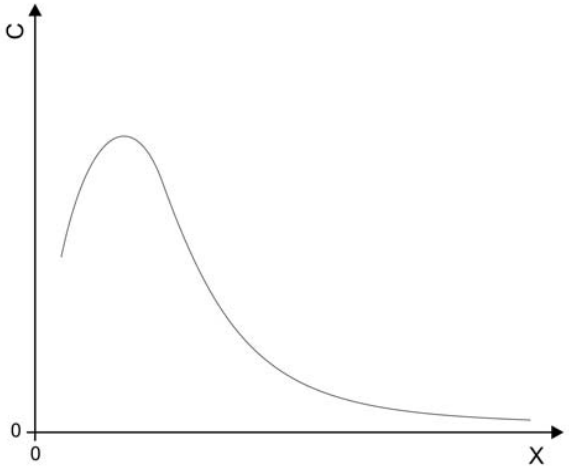

Figure 2.14: A more realistic chloride profile with a lower content at the surface and a maximum at a certain depth

The shape of the chloride profile in Figure 2.14 may have several explanations. Variations in the environmental conditions could cause such a shape, with water movement and evaporation concentrating chlorides at some depth and washing out chlorides from the surface near region. Other explanations include carbonation and leaching of substances other than chlorides, both of which influence the binding properties. The first point of the chloride profile is often omitted from the regression analysis because of a variety of possible interfaces close to the outer surface of the concrete. Ideally the profile should include at least six individual measurements, covering the full range of chloride concentrations encountered in the sample (Lee and Chisholm, 2005; ASTM C 1543, 2003).

The total chloride ion content of concrete is usually determined using acid-soluble titration techniques. Total chloride ion contents are usually measured by obtaining dust samples by either grinding or drilling concrete surfaces at required depth intervals which are then are analysed for their chloride ion content.

Modelling of chloride ion ingress through diffusion is commonly based on Fick's laws of diffusion, which were discussed previously in Section 2.3.

2.8.3 Bulk diffusion testing

The bulk diffusion test as described in ASTM C1556-03 (2004) is one of the most common tests used to determine the apparent chloride diffusion coefficient of concrete. Cylindrical specimens (100 x 100 mm) are firstly sealed on all sides except the top face and saturated in calcium hydroxide solution until no further mass change is observed. Samples are then submerged in a 2.8M NaCl solution for a minimum of 35 days to allow chloride ions to penetrate into the concrete solely by diffusion. After this time chloride profiling is done at regular intervals to obtain the acid soluble chloride ion content of the concrete at the different profile levels which are then analysed to determine the surface chloride concentration (C_s) and the corresponding apparent chloride diffusion coefficient (D_a) by fitting Equation 2.11 to the measured chloride ion contents by means of a non-linear regression analysis using the method of least squares. The principles and test procedures of the bulk diffusion test are discussed in more detail later in Chapter 3.

2.8.4 Reported values of chloride diffusion coefficients of concrete mixes

A range of published values of chloride diffusion coefficients (D_c) found in literature is presented in Table 2.8. The data was mostly derived from tests done on laboratory samples.

Results show that concretes containing only OPC yield chloride diffusion coefficients in the order of 10^{-12} m^2/s and concretes containing slags and fly ash yield values that are significantly lower.

Work done by Chalee and Jaturapitakkul (2008) showed that the replacement of OPC with FA, as well as a decrease in w/b ratio, resulted in lower diffusion coefficient values. However, w/b ratio had more effect than fly ash replacement on reducing D_c. Oh and Jang (2007) also investigated the effect of OPC replacement by fly ash on D_c, and their conclusions were similar indicating that fly ash replacement reduced D_c values by 15% - 50%. Yang (2004) also found D_c to increase with increasing w/b ratio. The addition of supplementary cementitious materials like FA and slag resulted in a significant decrease of D_c. Stanish and Thomas (2003) used bulk diffusion tests to determine the effect of fly ash replacement on D_c values. Their results also indicate that there is a significant decrease in D_c values when FA is substituted for OPC.

Nokken et al. (2006), Hong and Hooton (1999) and Mangat and Molloy (1994) studied the effect of time on D_c. Significant decreases in Dc values with increased concrete age in blended concretes were observed. Hong and Hooton and Nokken et al. reported a reduction of D by up to 42% and 46% respectively within a period of 8 months, and Mangat and Molloy (1994) reported a decrease in D_c values of plain OPC concretes of up to 80% within a similar period of time.

Table 2.8: Review of diffusion coefficient values stated in the literature

Concrete mix		Exposure time (days)	Diffusion coefficient D_c (10^{-12} m^2/s)	Reference
Binder	w/b			
OPC	0.45	730	5.00	Chalee and Jaturapitakkul (2008)
15% FA	0.45		1.40	
OPC	0.55		5.70	
15% FA	0.55		1.60	
OPC	0.4	105	6.44	Oh and Jang (2007)
20% FA	0.4		5.66	
OPC	0.4	90	11.75	Nokken et al. (2006)
8% SF	0.4		3.30	
10% FA	0.35		2.73	
12% FA	0.4		2.79	
15% FA	0.33		2.20	
OPC	0.4	140	6.13	
OPC	0.4	365	6.26	
8% SF	0.4		1.33	
10% FA	0.35		1.00	
12% FA	0.4		1.22	
15% FA	0.33		1.39	
OPC	0.65	90	10.20	Gardner (2006)
50% CS	0.65		2.28	
OPC	0.45	90	16.39	Yang (2004)
20% GGBS	0.45		6.13	
20% FA	0.45		3.51	
OPC	0.55		23.35	
20% GGBS	0.55		7.13	
20% FA	0.55		5.24	
OPC	0.5	180	5.53	Stanish and Thomas (2003)
25% FA	0.5		1.56	
56% FA	0.5		1.53	
OPC	0.5	270	5.03	
25% FA	0.5		1.23	
56% FA	0.5		1.40	
OPC	0.5	455	5.98	
25% FA	0.5		0.96	
56% FA	0.5		0.76	
OPC	0.5	1550	3.22	
25% FA	0.5		0.58	
56% FA	0.5		0.51	
OPC	0.58	90	1.56	
OPC	0.58	270	1.53	

Table 2.8, continued: Review of diffusion coefficient values stated in the literature

Concrete mix		Exposure time (days)	Diffusion coefficient D_c (10^{-12} m^2/s)	Reference
Binder	w/b			
OPC	0.66	180	9.50	Thomas and Bamforth (1999), site exposure
30% FA	0.54		4.30	
70% FA	0.48		7.50	
OPC	0.66	365	3.00	
30% FA	0.54		2.00	
70% FA	0.48		2.90	
OPC	0.66	720	7.60	
30% FA	0.54		1.90	
70% FA	0.48		1.90	
OPC	0.66	1095	5.60	
30% FA	0.54		1.10	
70% FA	0.48		0.99	
OPC	0.66	2190	10.00	
30% FA	0.54		0.81	
70% FA	0.48		1.00	
25% GGBS	0.4	120	3.46	Hong and Hooton (1999)
25% GGBS	0.4	365	2.01	
OPC	0.58	28	5.53	Mangat and Molloy (1994)
OPC	0.58	90	1.56	
OPC	0.58	270	1.53	

Site exposure conducted by Thomas and Bamforth (1999) also indicated reduced diffusion coefficients with time and FA substitution. The data obtained in this study showed that at early ages (eg. 1 month), the diffusivity of concrete containing 25% to 30% FA may be expected to have similar chloride ion diffusivity as an equivalent grade OPC concrete, however, after approximately 2 years the diffusivity of FA concrete in in the order of a magnitude lower than the OPC and it further decreases to two orders of magnitude lower after 100 years. This should have a significant impact on the long-term performance of concrete in chloride environments and on the interpretation of data from short-term (or accelerated) tests. Slag concretes indicated a much higher diffusion coefficient at very early ages but would behave in a similar fashion to FA with time.

2.9 Service life design of concrete structures

Inadequate durability is by far the most common cause of premature failure of concrete structures. However, often very little attention is placed on durability in the design process. Durability is usually covered by prescriptive code requirements based on previous code clauses, which have been reformulated where case histories have shown problems. However, this approach is suspect when applied to new materials or to design lifes longer than relevant experience. Largely in recognition of these shortcomings, service life prediction is currently an area of significant international research.

2.9.1 Serviceability of corroding concrete structures

With reference to service life requirements for structures, Eurocode 1 (1994) states the following:

“A structure shall be designed and executed in such a way that it will, during its intended life with appropriate degrees of reliability and in an economic way:

- remain fit for the use which it is required; and
- sustain all actions and influences likely to occur during execution and use”.

Service life is also defined as the time for which a structure is expected to be able to fulfil its requirements with sufficient reliability with or without periodic inspection and maintenance and without unexpected high costs for maintenance and repair (CEN 1999). Concrete structures are usually expected to have long service life as they often require large investments. It is therefore necessary to have an understanding of the design, materials used, deterioration and future maintenance.

Several different definitions for service life are used. In DuraCrete (1997), three different types of service lives are defined:

- Technical service life: the technical service life is the time in service until a defined unacceptable state of deterioration is reached
- Functional service life: the functional service life is the time in service until the functional performance of the structure becomes obsolete, due to changed requirements from e.g. authorities or the owner
- Economic service life: the economic service life is the time in service until it is economically more viable to replace the structure than to maintain it

Andrande (1995) also defined service life in quantitative terms:

- Required service life: this is the service life specified to meet the user's requirements (e.g. as stated in the client's brief for a project or in a performance specification). Required service life is defined corresponding to the requirements given in common regulations, codes and standards in addition to possible special requirements of the client.
- Design life: this is the period of use intended by the designer (e.g. as stated by the designer to the client to support specification decisions).

Most factors affecting reinforced concrete deterioration are time dependent in their effect. It is therefore somewhat surprising that very few or no standards or codes of practice for design of reinforced concrete structures currently contain any indication of the expected service life from these structures. This omission is, however, rapidly being addressed.

The ideal service life situation occurs when ageing is so slow that the structure maintains satisfactory serviceability for the anticipated service life without unexpected high costs for maintenance. To cope with aggressive exposure conditions, care shall be taken during all phases of the design and execution of the structure to take advantage of available knowledge regarding exposure and deterioration of concrete structures. Controlling the durability of reinforced concrete structures will therefore be a fundamental challenge for future engineers. The outcome of this designing for durability will be a tailor made service life design with the possibility to update the service life using results of tests and measurements throughout the

lifetime of the considered structure. Inspection and testing are therefore integral parts of the durability design. This means that structures shall be designed to be accessible, inspectable and maintainable (Rostam 2001).

2.9.2 Basis for durability design

Traditionally, codes of practise contain requirements for design which are formulated directly in terms of the load carrying capacity of the considered element, and durability has often been considered as being of secondary importance. Durability design of reinforced concrete structures is in general based on simple deem-to-satisfy rules, related to a crude environmental classification (Duracrete, 1999). Examples of such deem-to-satisfy rules are the requirements for minimum cover, maximum water/binder ratio, cement type etc. These deem-to-satisfy rules are however not able to provide the engineer with an explicit relationship between performance and service life, instead he is to assume that the structure would achieve an acceptably long, but unspecified service life.

Like the procedure for load design, the design for durability needs to be performance based and the designer should be able to adjust or adapt his structural design to cope with the aspects of environmental aggressivity and relate this to a specified design service life. Two main design strategies for durability can be followed (Duracrete, 1999):

- Avoid the degradation threatening the structure based on the type and aggressiveness of the environment. This can be done by changing the micro environment e.g. by applying membranes, coatings etc; by selecting non-reactive, or inert materials e.g. stainless steel reinforcement, coated reinforcement, non reactive aggregates, sulphate resistant cements etc; or by inhibiting detrimental reactions e.g.cathodic protection.
- Select an optimal material composition and structural detailing to resist, for a specified period of use, the degradation threatening the structure.

It should be noted however, that the preventative measures suggested in Strategy 1 do not provide a total solution and little knowledge is available for the various protective measures. Hence, Strategy 2 is the more preferred option. When designing for durability, conscious choices of cement type, concrete mix parameters (especially w/c ratio), concrete cover, curing (moisture and temperature control) and geometry of the exposed parts of the structure needs to be made, all adapted to the identified aggressiveness of the environment, which will aid in achieving a satisfactory service life of these structures.

2.9.3 Service life limit states

The concept of service life requires the end of the design life of the structure to be defined. It is usually some level of damage caused by the deterioration process, e.g. depassivation of reinforcing steel and initiation of corrosion, or a level of cracking caused by corrosion. A rational way to determine the service life of a concrete structure is to define a performance for the structure in question. The performance criteria may for example be related to a required function or the appearance of the structure. Usually the performance criteria are defined as limit states. According to DuraCrete (1999), a limit state is defined, as ”the border that separates desired states from the undesired or adverse states in situations, acceptable to the owner, which a structure may be subjected to during its lifetime”.

The limit states identified in structural codes are the serviceability limit state (SLS) and the ultimate limit state (ULS). The SLS is defined as the limit between the state where the performance of the structure is acceptable and the state where the structure is no longer serviceable. Examples of SLS are the onset of corrosion, crack widths, spalling, vibrations, aesthetics, etc. The ULS is defined as the limit between the state where the structure is able to carry the loads acting on it and the state where the structure has collapsed, for example due to excessive material degradation. Examples of ULS are collapse, buckling, and instability of the structure.

EN 1990 defines the limit states as the point beyond which the structure no longer fulfils the relevant design criteria. These limit states define the 'failure criteria' dealt with in the design. The failure criteria for the ULS is linked to structural resistance, while the end of SLS can be characterized by a 'Design Service Life' i.e number of years. The failure criteria for the ULS are fairly well defined in the Eurocodes. The failure criteria for the SLS of a concrete structure should be quantified on the basis of design materials. The fundamental requirement for a structure is that during the intended service life the probability to exceed the specified limit states are sufficiently small (Beeby, 1993). Often ULS and SLS are coupled, e.g. if corrosion of reinforcement is initiated, where first an aesthetic problem occurs, with rust stains on the surface of the structure (SLS), then cracking and spalling due to the formation of corrosion products (SLS), and finally collapse of the structure due to reduction of the cross-section area of the reinforcement (ULS).

2.9.4 Limit states of degradation for corrosion

When designing for durability, the first step is the definition of the desired or required performance of the structure. The required target service life and the event which identifies the end of the service life need to be identified and defined. A number of limit states have been proposed to define critical points in the deterioration of a structure as shown in Figure 2.15. Those proposed include initiation of corrosion, initiation of cracking, a limiting crack width, loss of steel section to a defined level, and loss of structural integrity (Cairns, 2003).

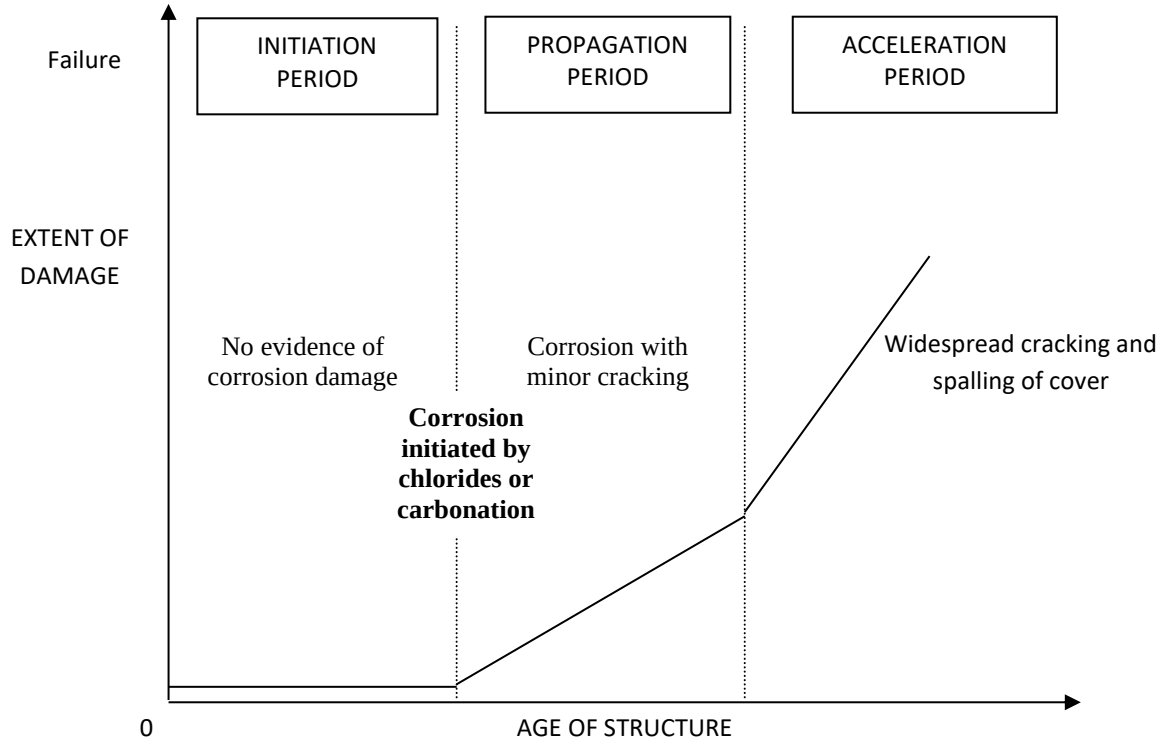

Figure 2.15: Three-phase corrosion damage model (Tuutti, 1992)

The different phases in the three-phase corrosion damage model are defined as follows (Tuutti, 1992):

- Initiation period: Depassivation of the reinforcement. This is the period before there is any evidence of corrosion damage, during which negligible corrosion deterioration occurs. During this period chloride ions or the carbonation front advance into the cover concrete and reach the level of the reinforcing steel inducing depassivation. The initiation phase ends when the chloride concentration at the reinforcement reaches a certain critical threshold value. Depassivation does not necessarily represent an undesirable state, however, this event must have occurred before corrosion will begin.
- Propagation period: Cracking of concrete. In this stage active corrosion begins, expansive corrosion products accumulate, and cracking of the concrete cover occurs. In this case the service life can include a certain propagation period of corrosion activity during which the cross-sectional area of the reinforcement is progressively reduced. Dominant factors affecting the rate of corrosion are the quantity of oxygen in the dissolved state, the moisture present and the electrical resistance of the concrete. The crack width depends on the amount of corrosion, the cover/diameter ratio, the concrete quality and the position of the rebar. The propagation time ends when a certain selected or determined allowable crack width has been reached.
- Acceleration period: Spalling of cover concrete and finally collapse. In this stage the rate of corrosion is accelerated due to the easy access of oxygen and water through cracks present in the cover concrete. Continued corrosion after cracking may lead to

delamination and spalling of the cover concrete. Spalling of concrete is usually considered an unacceptable condition, however it does not necessarily lead to collapse of the structure. Based on existing literature spalling is said to occur when a crack width of approximately 1 mm has been reached. Collapse of a concrete structure will occur if the load carrying capacity of the element is reduced sufficiently due to ongoing corrosion, by further cross-sectional loss of the concrete or steel, or loss of bond between concrete and steel.

For the purposes of this study, the service life of a structure is determined as the beginning of the propagation phase.

2.10 Models for service life design

Reinforcement corrosion in concrete is the predominant factor in the premature deterioration of reinforced concrete structures, leading to ultimate structural failure (Broomfield, 1997, Schiessel, 1988). Failure does not necessarily mean structural collapse, but also loss of serviceability characterized by concrete cracking, spalling, and excessive deflection of structural members. Therefore, there is a clear need that models be developed to determine the effect of the whole corrosion process (initiation to propagation) on structural performance so that the safe service life of corroded reinforced concrete structures can be predicted. Accurate service life prediction of reinforced concrete structures can assist designers and owners to achieve a cost-effective strategy in the design and management of concrete structures in aggressive environments. For service life prediction to be possible, the progress of deterioration mechanisms likely to be contributing to loss of serviceability must be modelled. The model is the set of equations and boundary conditions used to represent the mechanism. Because of the dependence of most deterioration mechanisms on transport of deleterious agents in the concrete, most models of deterioration mechanisms are essentially models of transport processes. Service life is related to the relevant transport parameters and environmental loadings, and transport parameters are defined by the properties of the concrete (Glanville, 1997). If the model is simple, it may be possible to obtain an analytical solution, involving the simple substitution of values into an equation to make a prediction. If an analytical solution is not possible, a numerical solution is required, generally an iterative computer-based approach. The term *modelling* is used to describe selection of the model, selection and development of a solution and application of the solution to make predictions (Glanville, 1997). Initially a model and solution are selected and then the corresponding transport coefficients are determined. Ideally, solutions should involve only known or measurable variables (Glanville 1997). Improvements could be made to existing service life models so that they can better simulate or represent site behaviour of reinforced concrete structures (Shi et al., 2012).

Chloride-induced reinforcement models vary in levels of complexity from simple analytical models assuming uniaxial diffusion into a homogeneous concrete, to more sophisticated numerical models which consider depth and time dependent changes in concrete properties, chloride binding, leaching, etc. The approaches adopted by the different models vary considerably and consequently there can be significant variances between the solutions produced by individual models.

2.10.1 Deterministic and probabilistic models

The performance of a structure, expressed with a limit state, can be solved either with deterministic or probabilistic methods. With deterministic methods, only one single value is used as input data for each of the parameters in the model, e.g. mean values. With probabilistic methods, mean values, statistical uncertainties and statistical distribution functions, are used as input data for the parameters in the model.

In Figure 2.16, the difference in predicted service life is shown when deterministic methods or probabilistic methods are used. The bearing capacity or strength, R, and the load, S, vary over time. Both functions are expressed with mean-values and statistical uncertainties expressed as a statistical distribution function. The mean values of R(t) and S(t) are characterized by the dotted lines. The mean service life is reached when the mean values of R(t) and S(t) cross each other, while the service life determined with probabilistic methods is dependent of the chosen target reliability, P_{target}. The probability of a certain event can be expressed with a probability function. The probability function is defined by events and it can be extended with the use of random variables. The probability functions can be both linear and non-linear. If many independent random variables, with arbitrary distribution functions, are summarized the sum will, according to the "central limit theorem", be normally distributed.

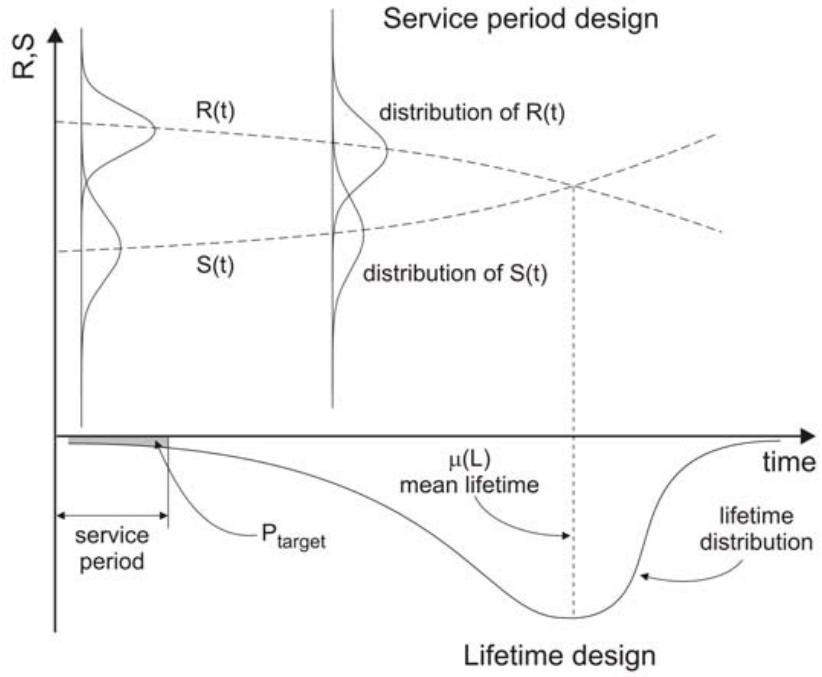

Figure 2.16: Service life predicted with only mean values and mean values and scatters of the parameters in the prediction models (DuraCrete, 1999)

For the purposes of this research a deterministic approach is followed due to its simplicity and practicality. A full probabilistic approach was not the focus of this research as such an approach would have to consider the variability in the environment, constituent materials, construction procedures, etc. This work focuses on the relationship between short-term chloride conductivity testing and long-term chloride ingress in real structures, as discussed in the chapters to follow.

Major difficulties related to the use of probabilistic modelling of the deterioration mechanisms are connected to the lack of good relevant data. In order to achieve reliable results from the computations, the applied uncertainty of the various parameters must be quantified. Generally a huge amount of data is available. The challenge is to sort out the reliable part of the data and to organize it for use in probabilistic calculations. Up till now there have existed very scarce data for this purpose.

2.10.2 Life 365

Life-365 (Thomas and Bentz, 2000) is a computer program for predicting the service life and life-cycle costs of reinforced concrete exposed to chlorides. This software presents an initial life cycle cost model based on an existing service life model developed at the University of Toronto. Life-365 makes three separate calculations based on the input parameters:

- Chloride concentrations are calculated at rebar depth for increasing exposure times in a selected geographic location and predicts the time to the onset of corrosion, commonly called the initiation period, which is when the chloride concentration at the rebar depth reaches the threshold concentration for corrosion.
- The propagation period is set up at 6 years for black steel and 20 years for epoxy coated steel. The model calculates the time to first repair, as the sum of the initiation and propagation periods. The total of the two is the time for corrosion damage to first reach an unacceptable level. The repair schedule after the first repair depends on the propagation period.
- Life cycle costs are estimated based on the initial concrete parameters and future repair costs for a specified “design” age.

The initiation period is the time it takes for chloride ions to penetrate the concrete cover and initiate corrosion at the depth of the steel reinforcement. This is the time required for the critical threshold concentration to reach the rebar depth from chloride on the surface. This model determines a maximum surface chloride concentration, and the time taken to reach that maximum based on the type of structure and expected salt and weather exposure on an annual basis for the geographic location selected by the user. The temperature and age of the structure also affect the diffusion coefficient and are taken into account. The base case assumed by the model is plain Portland cement concrete with no special corrosion protection applied. The model also allows for the use of corrosion preventative measures like corrosion inhibitors, epoxy coated steel and stainless steel.

Life-365 software is based on 1-dimensional and 2-dimensional finite difference calculations using Fick’s second law, where the apparent diffusion coefficient is adjusted each time step applying Equation 2.14 (compare Section 2.4.4).

The time to first repair, is predicted by Life-365 by considering the properties of the concrete, the nature of any corrosion protection strategy and details of the environmental exposure. The following values are assumed in this software for Portland cement concrete with no special corrosion protection applied (Maheswaran et. al, 2004):

$$D_{PC} = 1x10^{(-12.06+2.4w/c)} \qquad [2.39]$$

Where Portland cement is assumed to have a m value of 0.2 and C_t = 0.05% (by mass of concrete); where $C_t$is the threshold chloride content for corrosion initiation. Life-365 applies a reduction factor to the D value calculated for PC concrete based on the level of silica fume (%SF) in the concrete:

$$D_{SF} = D_{PC} e^{(-0.165SF)} \quad [2.40]$$

This relationship is only valid up to replacement levels of 15% silica fume. The model will not compute diffusion values (or make service life predictions) for higher levels of silica fume (Maheswaran et. al, 2004).

Life-365 assumes that silica fume has no effect on either m or C_t (Maheswaran et. al, 2004). Neither fly ash nor slag is assumed in Life-365 to affect the early-age diffusion coefficient, D28, or C_t. However, the rate of reduction in diffusivity is affected, hence the value of m. The following equation is used in Life-365 to modify the value of m based on the level of Fly ash (%FA) or slag (%SG) in the mix (Maheswaran et. al, 2004).

m=0.2+0.4(%FA/50+%SG/70) [2.41]

This relationship is only valid up to replacement levels of 50% fly ash or 70% slag, and thus m <0.6. The model will not compute diffusion values (or make service life predictions) for higher levels of these materials.

Life-365 accounts for the use of corrosion inhibitors, membranes and sealers. Membranes and sealers are assumed to impact the rate of chloride build-up only. It is assumed in the model that the rate of damage build up is lower when epoxy coated steel is present and these effects are dealt by modifying the propagation period (Maheswaran et. al, 2004). The initiation period is not influenced by the presence of epoxy coated steel. A chloride threshold of 0.5% (by mass of concrete) is assumed for grade 316 stainless steel in the current version of Life-365.

The cost and extent of the first repair, i.e percentage of area to be repaired; and the cost, extent and schedule of future repairs are decided by the user. The user is responsible for providing the information on the cost of the concrete mixes, repairs and discount rate. The total life cycle costs are then calculated as the sum of the initial construction costs and the discounted future repair costs over the life of the structure. Future repair costs are calculated on a ‘present worth’ basis using the discount rate, provided by the user. All predicted future costs over the entire design life of the structure are calculated in this manner and added to the initial costs to give total life cycle costs. Cash flow diagrams are available in Life-365 and show the estimated cash flow over the design life of the structure. These costs are however not discounted to present worth, but are corrected (increased) for inflation.

There are limitations however, in using this software: (a) this software needs to be used as a black-box when using it for prediction of chloride profiles; (b) the user has limited influence on the way the calculations are performed and cannot modify the model; and (c) it would not be possible for the user to incorporate this software as a part of another analysis, as the results from this software have to be fed into other analyses manually. For example, Monte Carlo simulation of the diffusion processes, typically carried out to estimate the reliability of the service life of a structure would be almost impossible to perform. The solutions provided by Life-365 are

intended to be helpful when comparing different designs for reinforced concrete structures exposed to chlorides. However, the calculated service life and life cycle cost information produced by the model should not be taken as absolute values. Many assumptions have been made to simplify the model, such that the solution only approximates actual conditions.

2.10.3 DuraCrete

DuraCrete (BE95-1347, 1997) is a performance-based service life design methodology for reinforced concrete structures. With this design methodology it is possible to model the complete service life for a reinforced concrete structure i.e. from casting, until degradation has put the structure into and adverse state. The service life is modelled as initiation and propagation of reinforcement corrosion, consequences of reinforcement corrosion and finally structural consequences, using Fick's second law of diffusion to determine diffusion coefficients of concrete types based on mix proportions. This model involves a limit state formulation for chloride induced corrosion initiation which can be simplified by stating that failure (i.e. corrosion initiation) occurs when the chloride content at the reinforcement surface (C) is greater than the critical (threshold) chloride content (C_t). According to the DuraCrete model for chloride transport, the chloride content at the steel C(x,t) is a time dependent function described by:

$$C(x,t) = C_S - (C_S - C_i)erf\left[\frac{x}{2\sqrt{KD_0 t\left(\frac{t_0}{t}\right)^{n_{cl}}}}\right] \qquad [2.42]$$

Where C_S is the chloride surface content (% by mass of concrete or cement); C_i is the initial chloride content (%); x is the depth of the reinforcing steel (m); D_0 is the diffusion coefficient (m^2/s) at time t_0 (s, usually 28 days); K is an environmental coefficient; n_{Cl} is an ageing component and erf is the error function, stemming from solving Fick's Second Law of diffusion.

This model can be applied in the design stage of new structures by inserting into equation 2.42 values for the design cover depth, the expected surface chloride content (based on experience, e.g. from DuraCrete tables) and experimentally determined chloride diffusion coefficients of trial concrete mixes. This allows calculating the point in time when C(x,t) reaches C_{crit}, whose value is also taken from experience or tables. The input values for cover depth and chloride diffusion coefficient are varied until the calculation indicates that corrosion initiation is postponed until the end of the desired service life period.

DuraCrete also uses the same methodology for assessment of existing structures. However, for existing structures some of the input parameters are different. For example, one of the limit parameters for the model is the measured value of the diffusion coefficient of 28 day old concrete. It is not possible to measure this value on concrete that is already 20 years old. On the other hand, the chloride surface content and the cover depth and their statistical distribution can be established experimentally; hence their values can be measured and do not have to be assumed such as in the design stage.

The probabilistic methods used in this model takes into account the scatter and distribution type of the input variables and the required reliability (or probability of failure) of the result. However, the statistical quantification in the DuraCrete project has shown difficulties in quantifying the environmental actions in the mathematical prediction models (Lindvall, 2001). It is hard to find data on the same concrete composition exposed in different environments (both marine and road conditions), which makes it difficult to quantify differences between different environments. Thus, there is a need for good data where the same type of concrete is exposed in different environments.

2.10.4 Computer-Integrated Knowledge System

The National Institute of Standards and Technology (USA) provides a Computer-Integrated Knowledge System (CIKS) with the goal of predicting the service life of reinforced concrete structures exposed to chloride ions. The diffusion rate at which these chloride ions can reach the steel is one of the controlling factors in determining how long such a structure will last. Starting from the mix proportioning process, the system proceeds to predict chloride ion diffusivity coefficients and to finally predict the ingress profiles or time to corrosion initiation for a reinforced concrete structure exposed in a specific environment (Bentz et al., 1996). Based on the trial mix proportions, the program predicts the value for the chloride ion diffusivity (D) of the concrete. The prediction of chloride ion diffusivity from the mix proportions is based on a statistically designed computer experiment which identifies water/cement ratio (w/c), volume fraction of aggregates, and degree of hydration as the three main variables influencing the diffusivity of a conventional concrete mix without mineral admixtures (Bentz et al., 1996). From these results an equation is developed for estimating chloride ion diffusivity coefficients using these three variables. An estimation of the 90 percent confidence limits for the estimated D value, based on regression of the developed equation, is also determined. The estimated D value is then employed in Fick's second law and the service life of a reinforced concrete structure exposed to an external source of chlorides is determined. The diffusion coefficients predicted in this model are verified using site and laboratory data.

2.10.5 Clinconc

The Clinconc model is mainly used in the Scandinavian countries. It was, for example, applied to the concrete design of the Oresund Bridge between Sweden and Denmark. Clinconc is essentially based on the current knowledge of physical and chemical processes involved in chloride transport and binding in concrete.

This model is made up of two main procedures (Tang and Nilsson, 1999):

- Simulating free chloride transport through the pore solution in concrete by using a chloride diffusion equation with the free chloride concentration as the driving potential, and
- Calculating the distribution of the total chloride content in concrete by considering non-linear chloride binding isotherms including the significant effects of both alkalinity and temperature.

The equation for the flux is given by Fick's first law and the concentration profiles are obtained by solving mass balance equations. In this model the main input data include the non-steady migration coefficient which is a function of the depth, time and temperature, concrete mix design (cement, water, aggregates etc), workmanship, and exposure conditions (chloride concentrations, temperature etc). The chloride binding phenomena, including the pH and the

temperature effects are accounted for by a Freundlich type of chloride binding isotherm (Tang and Nilsson, 1993). The only parameter that must be measured is the chloride diffusion coefficient by using the CTH rapid method, which has recently been accepted as a Nordic standard test method (Nordtest, 1999). The effects of temperature, curing age and concrete skin (laitance layer) on diffusivity are also taken into account. This model is verified with data from up to five years field exposure. It seems however that the model underestimates chloride penetration into concrete containing Fly Ash binder, probably due to an underestimated diffusivity by the laboratory test (Tang and Nilsson, 1993). The modelled chloride profiles are in good agreement with the measured ones, even though further study is needed to clarify the expansion coefficient for the concrete containing silica fume and other pozzolanic additions (Tang, 2008).

Advantages of this model are that only one of the input data needs to be measured, chloride diffusivity, which can be obtained from a short-term test method e.g. the standard non-steady state migration test (Tang and Nilsson, 1993) and the model takes into account a maximum of physical and chemical phenomena. The model, however, appears complicated which may limit its practical application.

2.10.6 UCT model

This service life model known as the UCT Service Life Model, of specifying concrete performance with respect to chloride resistance was developed by Mackechnie (2001). This approach uses a combination of characterisation index testing of laboratory concretes and on-site marine exposure of various concrete types (including different cement extenders) to develop an empirical model which predicts the time to initiation of corrosion in a marine environment. The prediction model allows early age properties of concrete to be related to the potential durability performance of the material under a range of marine conditions. Durability index tests (Alexander et al., 1999) such as chloride conductivity, water sorptivity and oxygen permeability are used as the governing factors for determining the service life of a structure. These durability index tests are sensitive to changes in concrete pore structure and are therefore able to characterise the material properties of concrete at early ages, in terms of the resistance of the cover concrete to the ingress of fluids and ions. These properties are then used for comparative purposes and related to long term durability properties of the concrete in service (Mackechnie, 1997). This prediction model is therefore based on the relationship between early age concrete properties, validated with long term chloride contents from marine concrete structures.

The service life of a structure in the marine environment is determined in the following manner (Mackechnie, 1997):

- Chloride conductivity values of the concrete mix are obtained
- Long term diffusion coefficients are predicted using chloride conductivity results.
- Chloride surface concentrations are predicted from measured data.
- Chloride profiles are calculated using a modified form of Fick’s second law (Equation 2.43)

$$C_x = C_s\left(1 - erf\left[\frac{x}{2\sqrt{D_i t^{1-m}}}\right]\right) \qquad [2.43]$$

where:

- C_x concentration at depth x measured normal to the section at time t expressed by% weight of binder (g/m^3)
- C_s projected surface chloride concentration determined by regression analysis expressed by% weight of binder (g/m^3)
- erf error function
- x depth measured normal to the surface (m)
- D_i diffusion coefficient at one second (m^2/s)
- t time of exposure (s)
- m empirical material coefficient relating to the reduction in D_c with time t

The approach allows for time-dependent diffusion coefficients based on binder type, with slag and fly ash concretes having larger reduction factors (m) than OPC and silica fume concretes. A range of values for m were determined from short term marine exposure samples. Determinations of these values were done by regression analysis of plots of the logarithms of diffusion coefficients and time.

Figure 2.17 shows a graphical solution of Equation 2.43 using a nomogram, allowing for greater flexibility than the error function equation. An estimation of the time to corrosion activation is then made once chloride levels at the reinforcement have been predicted. Activation of corrosion is assumed to occur at chloride levels of 0.4% by mass of cement.

Figure 2.18 shows the prediction model for different concretes with a cover to reinforcement of 60 mm. Environmental exposure conditions are also defined by the model as shown in the Table 2.8.

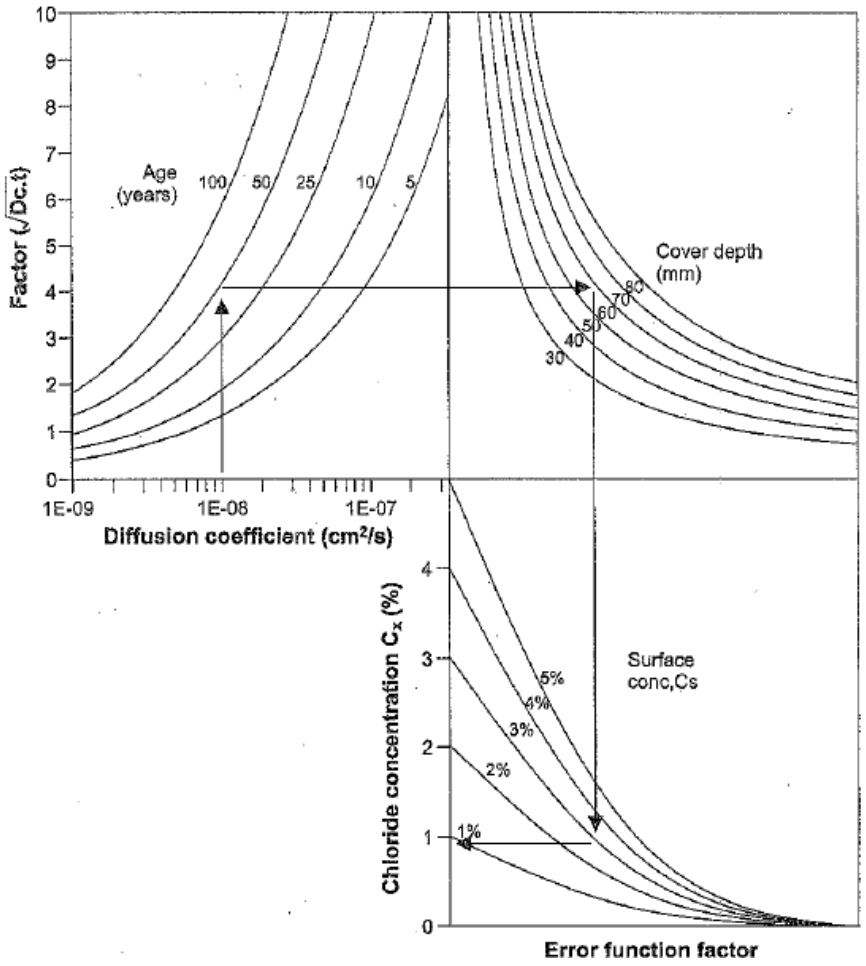

Figure 2.17: Nomogram format of the South African chloride prediction model (Mackechnie, 2001)

Table 2.8: Classification of marine exposure categories

Marine exposure category	Marine tidal and splash	Marine spray zone
Extreme	Structure exposed directly to sea water with heavy wave action and/or abrasion.	N/A
Very severe	Structure exposed directly to sea water under sheltered conditions with little wave action.	Structure within 500m of shore exposed to heavy wave and onshore wind.
Severe	N/A	Structure located near shore (>500m) in an exposed marine location
Moderate	N/A	Structure in a sheltered location within 1km of shore or anywhere within 30km of coast

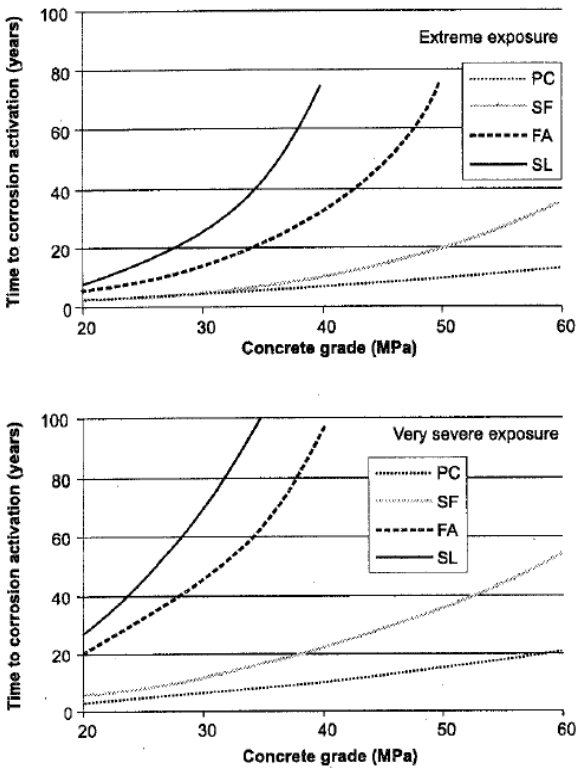

Figure 2.18: Time to corrosion activation for different moderately cured concretes with 60 mm concrete cover (Mackechnie, 2001)

2.11 Closure

The need to provide concrete with sufficient durability has stimulated the development of models to predict service life. These models are based on parameters defining concrete permeation or resistance to penetration. In general, chloride diffusion coefficients derived from analytical solutions to differential equations are used. This approach has however several limitations as the reproduction of real boundary and initial conditions by the differential equations is not obvious or easy. Also, the approaches adopted by the different models vary considerably and consequently there can be significant variances between the solutions produced by individual models. Therefore, a need has been identified to develop a “standard model”. This can equip engineers with confidence in decision making in regard to the design, maintenance and repair of corroded reinforced concrete structures. The solutions provided by such a model are intended as approximations to be used as a guideline in designing a reinforced concrete structure exposed to chlorides. Assumptions must be made to simplify the model and make it accessible to engineers who may not have specific expertise in the area of chloride transport and reinforcement corrosion.

3.Experimental methods

3.1 General

This chapter presents details of the experimental tests conducted, material constituents and proportions, and environmental exposure conditions used in the laboratory and on site.

The quantification of this work is based on information about the response of the concrete to material influences and environmental actions. The presently used chloride ingress prediction models include in detail the material effects but fail to explicitly take account of environmental actions. This requires knowledge about how the environmental actions vary with time over a structure and how this influences the long-term chloride ingress characteristics (i.e. surface concentrations and apparent diffusion coefficients). Information about variations in the environmental exposure in different regions in South Africa, and across different exposure conditions in the respective marine environments, is currently not available. Additionally, data on chloride ingress into concretes with different binder types from long-term exposure tests are missing, which makes it difficult to predict long-term performance of modern concretes in South African marine environments.

For the purposes of this research, the most significant parameters in the prediction model for chloride ingress are divided into two main classes:

- Material influences
- Environmental influences

Material influences are assessed by casting concretes with different types of binder at different w/b ratios. The laboratory bulk diffusion tests samples were placed under submerged conditions in a 2.8 M NaCl solution. Bulk diffusion tests were conducted at various mature ages. Relationships obtained between the above parameters with age were established. By choosing different binder types, binder contents, w/b ratios, etc., it is then possible to determine the material influences. The designer can predict how the material choice and mix design will influence the performance of the structure.

Environmental influences follow from the conditions at the location of the structure. The quantification of this work is based on information about the response of the concrete to environmental actions, i.e. chloride penetration profiles measured with the various exposure condition classes. Concrete specimens of different mix proportions were placed at two coastal sites in South Africa, including differing exposure classes at each location. At regular intervals, samples were retrieved, and chloride profiles were obtained and analysed to determine diffusion coefficients and surface concentrations of chlorides at various ages.

3.2 Materials used

The materials sourced are typical materials used in concretes made for marine environments in South Africa. Six different binder types were used in this research. In order to determine the influences of the environment on concrete durability, samples were cast in a standard/fixed environment (UCT laboratories) using specific fixed mix designs presented in Section 3.3.

3.2.1 Cementitious binders

The Portland Cement (PC) used for this investigation was a CEM I 42.5 N. Five other supplementary binder types typical to South Africa were also used in this investigation, Fly ash (FA), Ground Granulated Blast furnace Slag (BS), Ground Granulated Corex Slag (CS), Condensed Silica Fume (SF) and Super-Pozz® (SP), with each type coming from a single production batch. Typical oxide compositions of the binders are shown in Table 3.1 and further details on the various binders are provided below.

Table 3.1: Chemical compositions of binders (%) (Mackechnie et al., 2003, Mackechnie and Alexander, 2000, Addis and Owens, 2001)

Oxides	CEM I 42.5[1]	FA[2]	BS[3]	CS[4]	SF[5]	SP[6]
CaO	65.29	4.40	34.0	37.12	0.60	4.40
SiO_2	21.59	52.80	35.5	34.10	92.0	53.5
Al_2O_3	4.54	34.10	15.4	13.94	1.50	34.3
Fe_2O_3	3.47	3.60	0.98	1.06	1.20	3.60
SO_3	2.21	0.10	2.49	4.94	-	-
MgO	1.24	1.10	9.40	11.59	0.60	1.00
K_2O	0.68	0.50	0.87	0.69	0.60	0.80
TiO_2	0.29	1.60	1.20	0.61	-	-
Na_2O	0.12	0.40	0.16	-	-	-
Mn_2O_3	0.11	0.10		4.94		-
P_2O_5	0.11	0.30		0.00		-
Cl	0.01	-	-	-	-	-
C	-	0.80	-	-	-	<0.30

[1] CEM I 42.5 (PC): Riebeek West PPC, Western Cape

[2] Fly Ash (FA): Lethabo Thermal Power Station, Free State

[3] Ground Granulated Blastfurnace Slag (BS): Vanderbijl Park Steel Plant, Gauteng

[4] Ground Granulated Corex Slag (CS): Saldanha Steel Plant, Western Cape

[5] Silica Flume (SF)

[6] Super-Pozz® (SP): Ash Resourses

CEM I, 42.5N (PC)

Plain Portland cement binder (PC) complying with the requirements of SANS 50197-1:2000 was used: CEM I, 42.5N from Riebeek West PPC factory in the Western Cape Province. The main raw materials used in the manufacture of Portland cement are oxides of lime, silica, aluminium and iron. The oxide composition, in terms of the Portland cement used in this study, is shown in Table 3.1.

Ground granulated blast furnace slag (BS)

Ground granulated blast furnace slag (BS) is a by-product of the blast furnace process which is used to produce iron. It has been found to comply with the requirements of SANS 1491-1:2005

BS consists mainly of silica and alumina, derived from the iron ore, and lime or dolomitic lime added as a fluxing agent. If the slag is cooled rapidly, it assumes a glassy, and thus reactive state. The manufacture of BS consists of quenching (i.e. granulating) the hot slag with water, and then milling it to a fine powder. The oxide composition, in terms of the BS used in this study, is shown in Table 3.1. Concrete made with BS cement sets and hardens more slowly than concrete made with ordinary Portland cement, depending on the amount of BS in the cementitious material, but also continues to gain strength over a longer period in production conditions. This results in lower heat of hydration and lower temperature rises, and therefore makes avoiding cold joints easier. Use of BS significantly reduces the risk of damages caused by alkali-silica reaction (ASR), due to the lower alkali concentration in the cement paste, provides higher resistance to chloride ingress thus reducing the risk of reinforcement corrosion, and provides higher resistance to attack by sulphate and other chemicals. Typical substitutions of BS for PC in marine concretes are 50 %.

Ground granulated corex slag (CS)

Corex slag (CS) from the Saldanha Steel plant in the Western Cape is a premium latent hydraulic binder complying with the requirements of SANS 1491-1:2005. CS is reported to be more reactive than that produced in conventional blast furnaces mentioned above (Beushausen *et al.*, 2012). There is only one such plant in South Africa, i.e. that situated in Saldanha Bay. The oxide composition, in terms of the CS used in this study, is shown in Table 3.1. Typical substitutions of CS for PC in marine concretes are 50%.

Fly ash (FA)

Fly ash (FA) is an inorganic residue obtained from the flue gases of furnaces at pulverised coal power plants, complying with SANS 1491-1:2005. The spherical shape of fly ash creates a ball bearing effect in the mix, improving workability without increasing water requirements. FA also improves the pumpability of concrete by making it more cohesive and less prone to segregation. In addition, some fly ashes have been shown to significantly decrease heat generation as the concrete hardens and strengthens. FA, as do all pozzolanic materials, generally provide increased concrete strength gain for much longer periods than mixes with portland cement only. Concrete mixes containing FA in concrete have also shown increased life cycle expectancy and increased durability. During the hydration process, fly ash chemically reacts with the calcium hydroxide, forming calcium silicate hydrate and calcium aluminate hydrate, which reduce the leaching of calcium hydroxide and the concrete permeability. FA also improves the impermeability of concrete by permitting lowering the water-to-cement ratio due to the improved workability, which reduces the volume of capillary pores remaining in the mass. The spherical shape of fly ash improves the consolidation of concrete, which also reduces permeability.

FA from Lethabo Thermal Power Station near Vereeniging is a pozzolanic binder complying with the requirements of SANS 1491-2:2005. The oxide composition is shown in Table 3.1. Typical substitutions of FA for OPC in marine concretes are 30%.

Super-Pozz (SP)

Super-Pozz® is a highly reactive alumino-siliceous pozzolan. According to the suppliers, the

product's pozzolanic activity results in increased strength and durability of concrete, whilst the particle size distribution and spherical shape improves workability and results in reduced water content. Super-Pozz is produced by Micron Materials™. The oxide composition is shown in Table 3.1.

Condensed Silica Fume (SF)

Silica fume (SF) is a by-product of the ferrosilicon smelting process complying with SANS 1491-1:2005; it is the condensed vapour from the process. The oxide composition, in terms of the SF used in this study, is shown in Table 3.1. SF is extremely fine and the specific surface is about 20 000 m^2/kg and average particle size is 0.15 µm. As a result of this fineness, particles are strongly attracted to each other and cannot slide or roll over each other to achieve a dense packing. SF therefore has a very low bulk density (about 200 kg/m^3) and consequently is difficult to handle and transport. In order to make the material more manageable, SF is densified by means of electrostatic forces that cause particles to agglomerate into small pellets about 0.5 mm in diameter. In the densified state, bulk density is about 600 kg/m^3. Because of its extreme fineness and high silica content, SF is considered a very effective pozzolanic material. The typical oxide composition, in terms of the SF used in this study, is shown in Table 3.1.

3.2.2 Aggregates

A 9 mm Greywacke stone conforming to SANS 1083:2006 was used as the coarse aggregate. Its characteristics are given in Table 3.2. The values are typical ranges obtained from studies on the properties of South African aggregates reported by Alexander and Davis (1991).

Table 3.2: Typical characteristics of Greywacke aggregate (Alexander and Davis, 1991)

Aggregate property	
Relative density	2.64 – 2.78
10% Fines Aggregate Crushing Value (kN)	299
Unconfined compressive strength (MPa)	297 – 308
Elastic Modulus (GPa)	68 – 77
Coefficient of thermal expansion (x 10^{-6}/˚C)	10.9
Water absorption (%)	0.4

Greywacke is a commonly available coarse aggregate for use in Western Cape concretes including marine construction. The aggregate sample used for this work was obtained from the Peninsula Quarry in the Western Cape. It is formed by thermal metamorphism of the initially argillaceous rocks of the Malmesbury group by the intrusion of plutons of Cape Granite, and as such its distribution is confined to the vicinity of the granite bodies. Greywacke is a fine-grained glassy rock consisting of quartz, feldspar, mica and iron oxides. Greywacke particles are dark/grey-coloured and angular in shape.

"Klipheuwel" sand from a local source of pit sand, conforming to SANS 1083:2006, was used in all mixes as the fine aggregate. The fine aggregate was oven dried at 100°C for 24 hours and air-cooled for another 24 hours before being used for the concrete mixes. Klipheuwel sand is a siliceous pit sand having a very good particle shape and a continuous grading. The concrete

water requirement is low, making it a good sand for concrete. The grading analysis was performed according to SANS 829:2006. It was found that the material grading fell within the limits recommended by SANS 1083:2006, with a fineness modulus of 2.50. A single batch of sand was used throughout this research project.

3.3 Mix proportions

The concrete mix proportions are shown in Table 3.3, as well as the average 28-day compressive strength of 100 mm cube specimens.

Table 3.3: Concrete mix proportions (kg/m^3), 28-day strength values

Binder type	Mix No.	w/c	Water	PC	FA (30%)	BS (50%)	CS (50%)	SF (7%)	SP (15%)	Stone	Sand	$f_{cu,28}$[1] (MPa)
PC	0.4 PC	0.4	180	450	-	-	-	-	-	1000	707	60.0
	0.6 PC	0.6	175	292	-	-	-	-	-	1000	850	33.0
FA	0.4 FA	0.4	170	297	127	-	-	-	-	1000	723	45.5
	0.6 FA	0.6	170	198	85	-	-	-	-	1000	858	33.0
BS	0.4 BS	0.4	180	225	-	225	-	-	-	1000	686	56.0
	0.6 BS	0.6	175	146	-	146	-	-	-	1000	837	32.0
CS	0.4 CS	0.4	180	225	-	-	225	-	-	1000	686	63.0
	0.6 CS	0.6	175	146	-	-	146	-	-	1000	837	41.0
SF	0.4 SF	0.4	180	419	-	-	-	31.5	-	1000	702	64.0
	0.6 SF	0.6	175	272	-	-	-	20.4	-	1000	846	38.0
SP	0.4 SP	0.4	170	361	-	-	-	-	64	1000	687	62.0
	0.6 SP	0.6	170	240	-	-	-	-	43	1000	810	36.0

[1] Average strength obtained by crushing three 100 mm cubes; reported to the nearest 0.5 MPa

The water contents of all the mixes were kept within the range of 170 to 180 kg/m^3. Two w/b ratios of 0.40 and 0.60 were used, yielding binder contents in the order of 450 kg/m^{3}and 292 kg/m^3 respectively. A slump of 75 ± 25 mm was achieved in all mixes, using a PCE-based water-reducing admixture (plasticiser). The coarse aggregate content of all mixes was fixed at 1000 kg/m^3 with the fine aggregate contents adjusted in each mix to obtain the required yield of the concrete. The quantity of cementitious addition substituted for the primary binders was 50% for CS and BS, 30% for FA, 15% for SP and 7% for SF. All mix constituents were mass-batched.

3.4 Specimen manufacture and scheduling of testing

Control specimens containing CEM I, 42.5N Western Cape Portland cement were produced at the two w/b ratios. These are essentially non-marine concrete mix types. This was done to find the behaviour of plain PC concrete and the influence of using supplementary cementitious materials in the marine environment. Concrete was produced using a horizontal forced action

pan mixer of 0.05 m^3 capacity. The pan mixer was charged with coarse aggregate, fine aggregate and binder respectively and the constituents dry mixed before adding water, mixed with the water reducing admixture, until the mix was visually consistent. Slump measurements were then taken. To minimise any effects due to variations in the materials used for the concrete, all casting was done with cement from only one delivery from the cement factory, aggregates from the same two deliveries (sand and stone) and super plasticiser from only one container.

For the bulk diffusion tests, 100 ∅ x 100 mm cylinders were used. For each mix and testing age, three cylinders were sampled, and an average value obtained. Bulk diffusion tests were done at 35 days, and roughly 6 months, 1, 1.5, 2, 2.5, 3 and 3.5 years.

For the durability index tests, 100 mm cubes were cast and the specimens were extracted for tests at 28 days. A further three 100 mm cubes were cast for compressive strength tests for each of the different binder types and concrete grades. Compressive strengths were obtained at 28 days.

For site exposure, 150 mm cubes were cast. Twelve cubes were cast per mix and exposure site or condition, eg. submerged, tidal, splash/spray and air borne. Exposure samples were prepared by slicing the 150 mm cubes in half and all surfaces except the sliced face were coated with epoxy such that there was only one exposure face. Site diffusion tests were performed at 1, 1.5, 2, 2.5, 3 and 3.5 years.

After casting and testing for slump, the concrete specimens were cured under PVC plastic at normal room temperature for 24 hours, at the end of which they were removed from their moulds. Samples for durability index and compressive strength testing were then placed in a water bath for continuous curing in accordance with SANS 5861-3:2006 until testing. Site exposure samples were also cured in the water bath for a further 27 days after demoulding. The temperature of the curing baths was maintained at 23 ± 2 °C. The cylindrical samples for bulk diffusion testing were cured in a $Ca(OH)_2$ water bath solution for 27 days after demoulding (i.e. at 28 days of age), after which they were coated with epoxy resin on the cylindrical sides and bottom face of the test specimen. This was done to ensure that during the diffusion process there would be only one controlled front of diffusion of chlorides. They were then immersed in the NaCl exposure solution as per the provisions of ASTM C1556-04, before chloride profiling. The bulk diffusion samples were kept in an environment room maintained at a relative humidity of 68 ± 5 % and a temperature of 23 ± 2 °C for the entire duration of exposure. The bulk diffusion samples therefore effectively simulated submerged conditions on site, which allowed correlating the lab samples with the submerged site samples.

3.5 Experimental work

The quantification of this work is based on information about the response of the concretes to environmental actions, i.e. chloride penetration profiles. However, the response from the concretes does not only include effects from the environmental actions, but also effects from the material properties with time, e.g. concrete composition. The presently used prediction models do not include the environmental actions in an explicit way, which means that the environmental influence must be quantified with the response from the concrete. This requires knowledge about how the environmental actions vary over a structure with time and how this influences their response. Information about these variations is still scarce and it has been

shown that there can be significant variations, in environmental actions and response. Additionally, data from long-term exposure are largely missing, which makes it hard to assess long-term properties of the concrete.

3.5.1 Environmental exposure (site work)

The quantification of exposure conditions is vital in reducing the variability of results obtained. It is therefore necessary to define and classify the various environmental classes within South Africa. These relate to the conditions at the location of the structure, e.g. saturated vs. unsaturated conditions, and mechanisms i.e. immersed structures as opposed to structures undergoing cyclic wetting and drying, temperature (air and water), humidity, severity of exposure, abrasive effects etc.

The informative examples of the EN 206 exposure classes which appear in the complimentary UK concrete standard to EN 206 (BSI, 2013) were considered. Table 3.4 shows the environmental exposure classes representative of corrosion induced by chlorides from seawater in South Africa (Mackechnie, 1997) and of relevance to this research. The exposure conditions can generally be divided into four zones (i.e submerged, tidal, splash/spray and atmospheric). The tidal and splash/spray are subjected to long-term chlorides with drying and wetting cycles. Due to the coupling effect of convection and diffusion (Yu et al., 2015 and Meijers et al., 2005), the exposure conditions in these two zones are considered the most harsh, with the atmospheric zone being the least (Wu et al., 2017).

In order to determine fundamental influences of the environment on concrete durability, samples were cast in a standard environment (University of Cape Town laboratory) and then placed in the various environments. After curing, the 150 mm cube samples were sliced in half such that a specimen of dimensions 150 x 150 x 75 mm were obtained, all faces except the sliced face were coated with epoxy resin to allow for only one controlled front of diffusion of chlorides. Samples were further sealed on the five-coated faces with a foam material to ensure one-directional chloride ingress into the exposed test face. The specimens were then slotted into steel frames (Figures 3.1, 3.2), which were lowered via steel chains into the various environments discussed in Table 3.4. Six 150x150x75 mm concrete samples were placed in each steel frame.

Two main areas along the South African coastline were chosen as ideal sites, Cape Town and Durban (Figure 3.3). At these sites, samples were placed for all four different exposure classes (submerged, tidal, splash/spray and air borne).

Samples of varying binders specific to the area concerned were cast and placed. 100 mm diameter cores were taken at regular intervals (approximately 1 year, 1.5 years, 2 years, 2.5 years, 3 years, and 3.5 years) and ground and sliced at varying increments to obtain chloride profiles from which surface concentration of chlorides and apparent chloride diffusion coefficients are determined on these samples.

The salinity of seawater typically ranges from 3.2 – 4.0%, with a typical value of 3.5% (expressed as 35 parts per thousand) and is primarily made up of sodium and chloride ions (https://www.sciencelearn.org.nz). Low salinity is found in cold oceans, particularly during the summer season when ice melts. High salinity is found in subtropical areas where evaporation is high and precipitation low. Particularly high salinity is found in arid Mediterranean seas (Figure

3.4). Note Southern Africa's moderate salinity of around 3.5 – 3.6%, which is similar to that of the Atlantic Ocean on the western coastlines of northern Europe.

Table 3.4: Exposure classes relevant to South African conditions (from EN 206 2013)

	Description of the environment	Informative examples applicable to research
XS 1	Exposed to airborne salt but not in direct contact with sea water (< 5 km distance from the sea).	Reinforced and prestressed concrete surfaces in saturated salt air. External reinforced and prestressed concrete surfaces on coastal areas more than 100 m from the sea.
XS 2	Submerged or totally immersed on all sides. Abrasive conditions.	Reinforced and prestressed concrete completely submerged more than 1 m below lowest low water level.
XS 3	Tidal zone (wetted zone). Abrasive conditions.	Reinforced and prestressed concrete surfaces in sea water tidal zones down to about 1 m below lowest low water level.
	Splash/spray zone (< 100 m distance from the sea).	External reinforced and prestressed concrete surfaces less than 100 m from the sea.

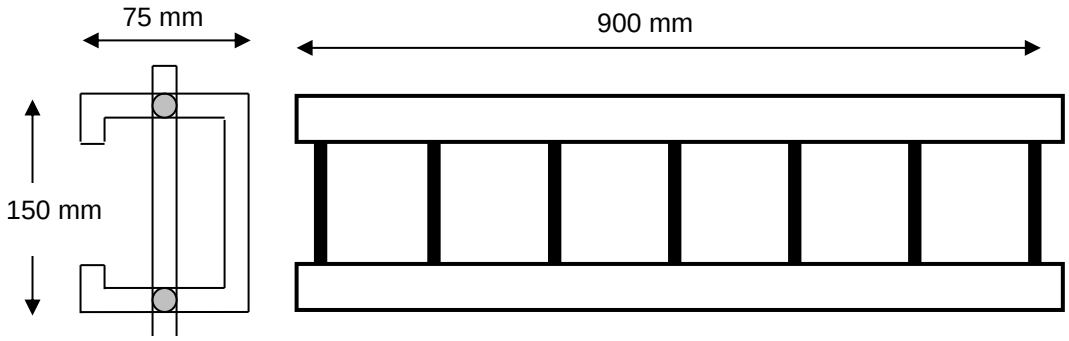

Figure 3.1: Schematics of steel channel frames

Figure 3.2: Typical site samples in steel frames; per mix and exposure condition, 6 samples were manufactured and placed into a single steel channel frame

Figure 3.3: Exposure sites in Southern Africa (from left to right): Walvis Bay, Cape Town, Durban, indicated by the stars (map extracted from www.maps.google.com)

Durban Site

The Durban site was a 4 m high quay wall in the commercial harbour in Durban, exposed to the Indian Ocean where sea temperatures range from 18 to 25°C. Average winter and summer air temperatures range in the region of 18 to 26°C and 20 to 35°C respectively. Submerged samples were lowered via steel chains into the sea. Tidal zone samples were suspended with steel chains just below the high tide mark while the splash/spray zone samples were located on the top most level of the sea wall about 4 m above the mean sea level as illustrated in Figures 3.5 and 3.6. Binder types tested at this site were PC, BS and FA. They were chosen as they are typical of the concrete binders used in this exposure region.

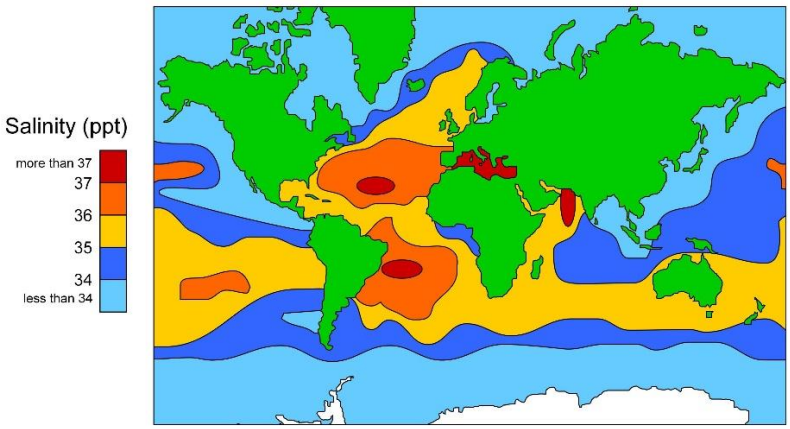

Figure 3.4: Map showing the salinity of the oceans (https://www.sciencelearn.org.nz/resources/686-ocean-salinity)

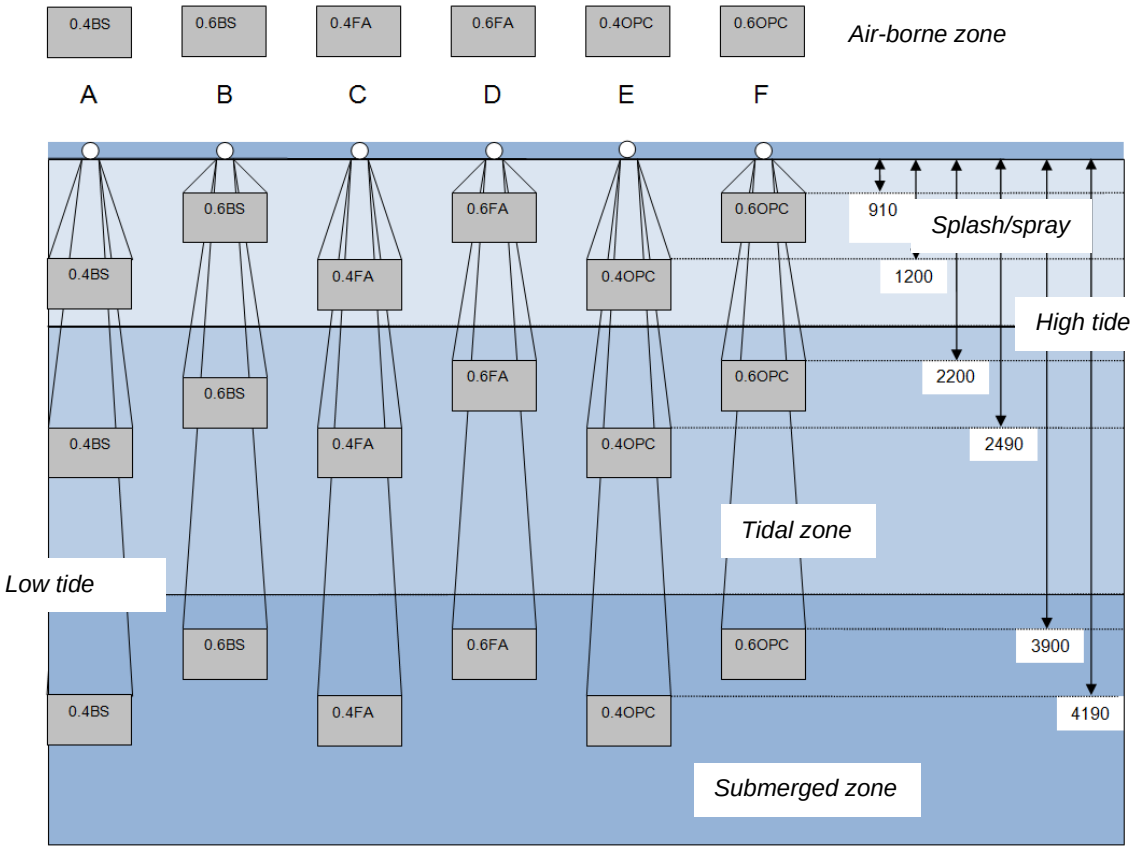

Figure 3.5: Schematic of sample layout in Durban

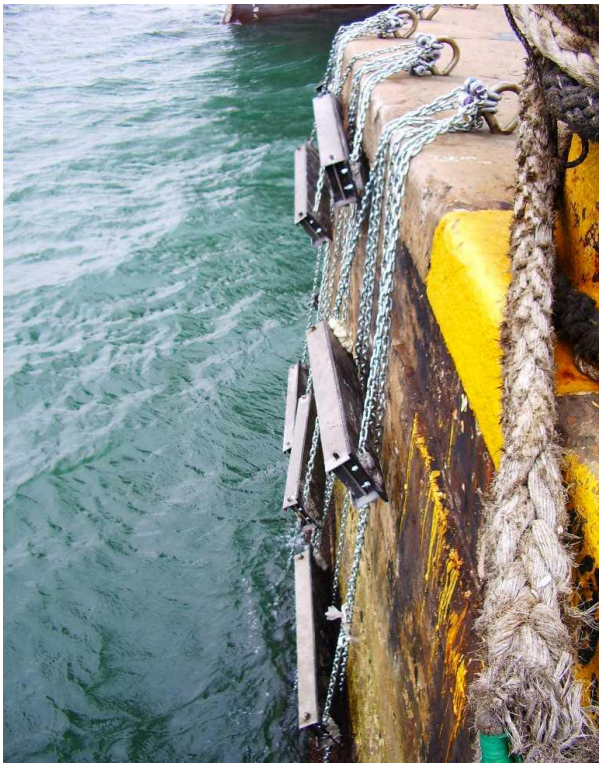

Figure 3.6: Arrangement of site exposure samples in Durban harbour

Cape Town Site (Granger Bay)

The exposure site at Granger Bay in Cape Town was chosen due to the exposed nature of the area, which is prone to heavy wave action and strong winds. This site is exposed to the Atlantic Ocean where sea temperatures range from 12 to 15°C due to presence of the cold Benguela current off the Cape West Coast. Average winter and summer air temperatures range in the region of 7 to 20°C and 15 to 27°C respectively. Submerged samples were placed via steel chains into the sea, tidal zone samples were suspended using chains just below the high tide mark and splash/spray zone samples were located on top of a sea wall (Figure 3.7). Air borne samples were placed at some distance < 5 km away from the sea. Binder types tested were PC, CS, FA, SF, and SP.

Figure 3.7: Arrangement of splash/spray site exposure samples in Cape Town, on top of a sea wall (pictures shows low tide conditions)

3.5.2 Experimental tests

3.5.3 Bulk diffusion test, laboratory samples

Bulk diffusion tests were conducted on all concrete mixes by being exposed to a laboratory saline environment (Bulk Diffusion test) for 35 days, 6 months, 1, 1.5, 2, 2.5, 3 and 3.5 years. Two specimens were tested per mix as per the provisions of ASTM C1556-04 (2004). The cylindrical specimens (100 mm depth and 100 mm diameter) were initially moist cured for 28 days and specimens were then sealed on all sides with epoxy resin except for the exposure face. Specimens were then immersed in saturated calcium hydroxide water bath until the mass did not change by more than 0.1 % in 24 hours. The samples were then submerged in a 2.8 M NaCl solution (Figure 3.8), for a minimum of 35 days.

To evaluate the chloride contents at various depths into the concrete, samples were ground at various depth increments using a custom-modified mechanical mill with a diamond tipped bit. This was done in increments of 1 to 3 mm over the first 16 mm into the sample. The samples were placed such that the axis of advance of the bit was perpendicular to the surface of the sample. At depths greater than 16 mm, where such small depth increments were not deemed necessary for the chloride profiling, the samples were dry-sliced using a diamond saw. A 2-mm blade was used for the dry slicing technique and as a result 2 mm was lost from the sample between depths during slicing. Table 3.5 shows the sampling depths at 90 days. As a result of the early exposure age, samples were profiled at smaller increments as opposed to the samples profiled at approximately 1, 1.5, 2, 2.5, 3 and 3.5 years, shown in Table 3.6. Potentiometric titration was then done to determine the total acid-soluble chloride contents at the profile levels.

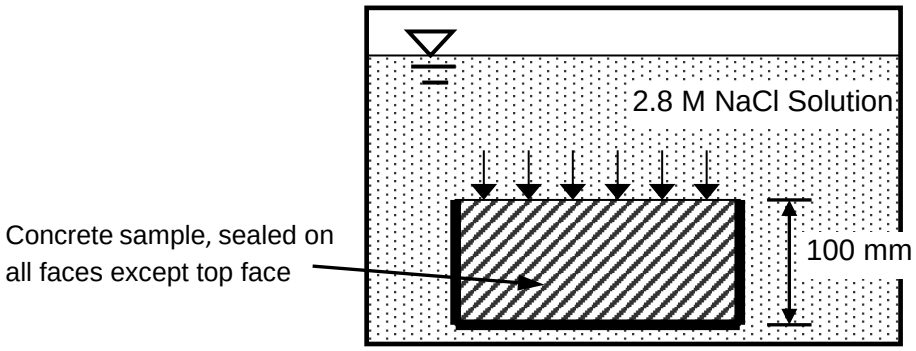

Figure 3.8: Schematic of the Bulk Diffusion Test

Table 3.5: Sampling depths for chloride content analysis, 90 days exposure (depth increments, grinding versus slicing)

Depth	Sampling depth (mm)	Average depth (mm)	Method
1	0-1	0.5	Grinding
2	1-3	2	Grinding
3	3-5	4	Grinding
4	5-7	6	Grinding
5	7-10	8.5	Grinding

6	10-13	11.5	Grinding
7	13-16	14.5	Grinding
8	16-20	18	Slicing
9	20-30	25	Slicing
10	30-40	35	Slicing
11	40-50	45	Slicing

Table 3.6: Sampling depths for chloride content analysis, at approximately 1, 1.5, 2, 2.5, 3 and 3.5 year exposure (depth increments, grinding versus slicing)

Depth	Sampling depth (mm)	Average depth (mm)	Method
1	0-2	1	Grinding
2	2-5	3.5	Grinding
3	5-10	7.5	Slicing
4	10-15	12.5	Slicing
5	15-20	17.5	Slicing
6	20-25	22.5	Slicing
7	25-30	27.5	Slicing
8	30-40	35	Slicing
9	40-50	45	Slicing
10	50-60	55	Slicing
11	60-70	65	Slicing

3.5.4 Chloride testing on site samples

Site samples exposed at Durban and Cape Town were tested for time-dependent chloride ingress in real exposure conditions. Per mix and exposure condition, 6 concrete blocks (150 x 150 x 75 mm) were available, as shown in Figure 3.2. At 6-months intervals, core specimens (100 mm diameter) were removed from the blocks on site (Figures 3.9 – 3.11). As seen in the photographs, samples from the submerged zone showed significant barnacle growth (a mix of encrustations, mussels, slime and small animals) which over the exposure period of 3.5 years increased to an average thickness of about 5 mm (estimated, not measured). Such barnacle growth was observed only in the submerged zone in Durban.

After completion of coring on site, core specimens were labelled, wrapped in cling wrap and transported to the laboratory for chloride profiling. The same method as discussed in Section 3.5.2.1 was used for titration testing. Each specimen was ground or cut into 11 depth increments as indicated in Table 3.6. For each core specimen and depth increment, 3 powder samples were tested for chloride content and the average value used in the analysis.

Figure 3.9: Removing of core samples on site (Durban)

Figure 3.10: Removing of core samples on site (Durban); note the growth of barnacles on the samples (in the submerged zone)

Figure 3.11: Core samples (Durban); bottom row: specimens from submerged zone (with barnacle growth), middle row: splash/spray zone (slightly discoloured), top row: splash/spray zone ("clean" samples")

3.5.5 Chloride profile fitting technique

The values of surface concentration and apparent chloride diffusion coefficient are determined by fitting Equation 3.1 to the measured chloride ion contents by means of a non-linear regression analysis using the method of least squares.

$$C(x,t) = C_S - (C_S - C_i).erf\left(\frac{x}{\sqrt{4.D_a.t}}\right) \qquad (3.1)$$

Where:

C(x,t) = Chloride concentration at depth x and exposed time t, mass %

C_S = Projected chloride concentration at the interface between the exposure liquid (2.8 M NaCl solution) and test specimen that is determined by the regression analysis, mass %

C_i = Initial chloride-ion concentration of the cementitious mixture prior to submersion in the exposure solution (2.8 M NaCl solution), mass %

x = Depth of the exposed surface, m

D_a = Apparent chloride diffusion coefficient, m^2/s

t = Exposure time, s

erf = Error function (see Section 2.3.3)

3.5.6 Compressive strength tests

The compressive strengths of the concrete mixes were obtained by performing standard cube (100 mm) compressive strength tests. The specimens were tested at 28 days according to SANS 5863:2006. All the tests were performed using a manually-operated hydraulic AMSLER

compression machine at a loading rate of 0.3 ± 0.1 MPa/sec. The test results are included in Table 3.3.

3.6 Long-term chloride ingress data from field structures

Long-term chloride ingress data was also used to help calibrate the chloride ingress model used in this research, as discussed later in Chapter 5. The data was obtained from various condition assessment projects recently carried out by the Concrete Materials and Structural integrity Research Unit at UCT, as part of consultancy projects (unpublished). All of the considered structures are exposed to marine environments along the west coast of Southern Africa. Chloride testing was performed on core samples removed from the structures, using Potentiometric titration to determine the total acid-soluble chloride contents. A summary of the investigated structures is presented in Table 3.7.

The exact ages of the structures investigated are not known; the estimated ages shown in the table are based on information received from the various clients for whom the work was carried out. Structures with an estimated age of 45 – 50 years were selected in order to perform the comparison to 50-year predicted chloride profiles from experimental work carried out in this research, as discussed in detail in Chapter 5. No information on the mix designs was available. However, all measurements were done on structural elements of large concrete structures, and in the comparison of site data with experimental data obtained in this research, the assumption is made that these structures represent a structural concrete with a w/c ratio of about 0.40, which represents a common w/c ratio used for structural marine concrete in Southern Africa. Unfortunately, data on compressive strength, which would have assisted in estimating the w/b ratio, was not available.

During the time when the structures were constructed, the only available cement type in Southern Africa was a CEM I type cement (“Ordinary Portland Cement”). The test results are therefore expected to represent a PC concrete. The measured chloride concentrations for the various structures are shown in Figure 3.12.

Table 3.7: Summary of site structures investigated for long-term chloride penetration

no	Type of structure	Age (years)[1]	Location	Exposure
1	Sea Wall	~ 45	Cape Town	Splash/spray
2	Harbour wall	~ 50	Cape Town	Splash/spray
3	Harbour wall	~ 45	Walvis Bay	Tidal
4	Piles	~ 50	Walvis Bay	Tidal

[1] Age at testing

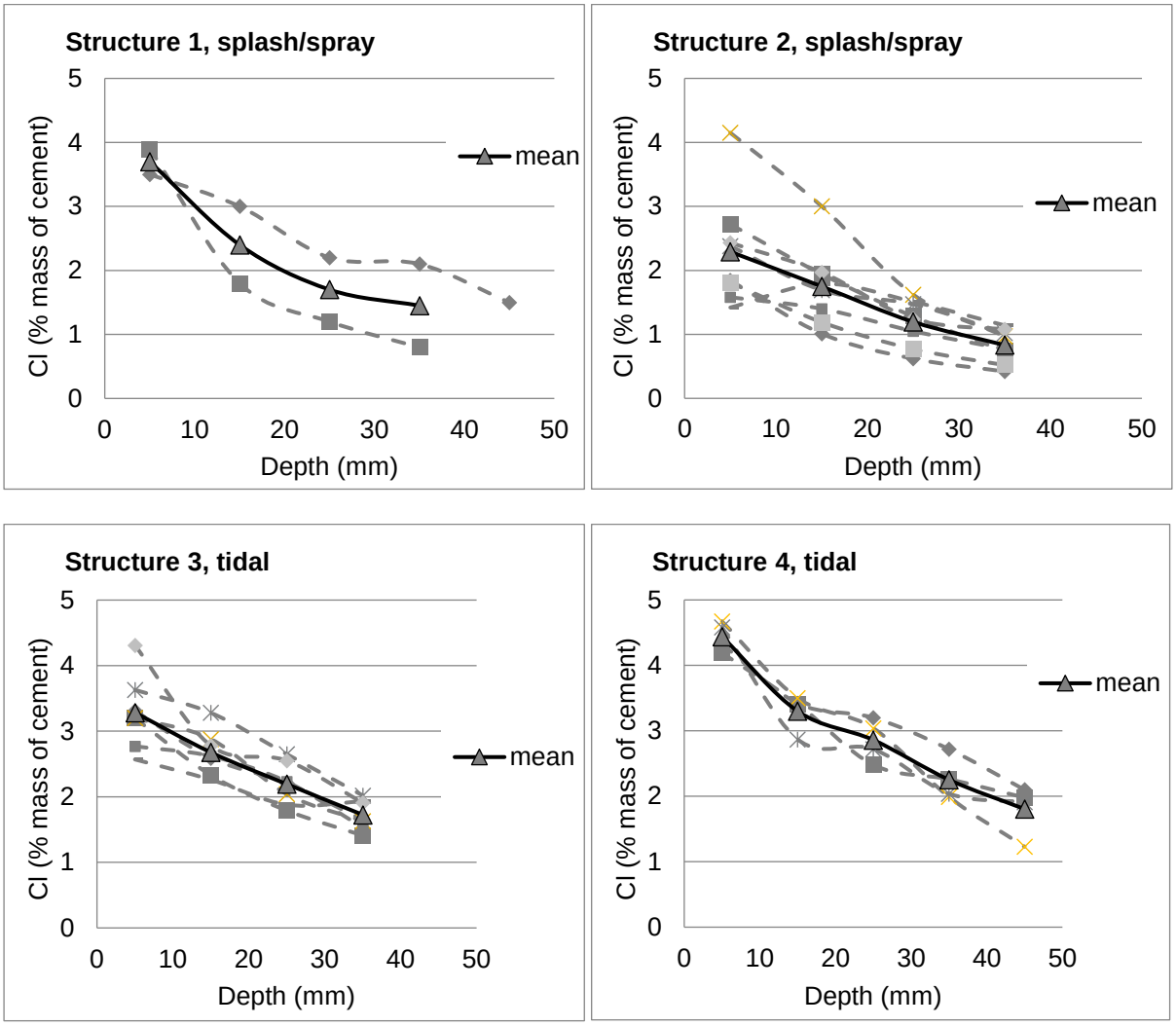

Figure 3.12: Long-term chloride ingress data obtained from actual structures

The graphs in Figure 3.12 contain individual results obtained from core samples as well as the mean values calculated from the individual results. In general, a large scatter in results was observed, despite the fact that samples were removed from locations with the same environmental exposure condition. This highlights the uncertainty usually involved in chloride ingress predictions, which is related to the influence of micro-climatic conditions on chloride ingress and the general variability of concrete.

3.7 Summary and scope of experimental work

In this chapter an outline of the experimental programme was provided. The concrete mixes and materials used were introduced and their proportions given. Details of the tests were also presented, which included the bulk diffusion test, chloride titration on powder samples (retrieved from samples exposed to the laboratory or site conditions), durability index tests, and compressive strength tests. The casting and configuration of the specimens for chloride testing resulted in the following variables being defined:

- Two w/b ratios (w/b = 0.40 and 0.60)
- Six different binder types (PC, BS, CS, FA, SP, SF)

- Varying exposure conditions:
    - Laboratory (bulk diffusion test, ASTM C1556-04)
    - Durban harbour
        - Submerged, tidal, splash/spray, and air-borne exposure
    - Cape Town harbour
        - Submerged, tidal, splash/spray, and air-borne exposure

A summary of the test specimens for chloride testing is provided in Table 3.8. A total of 456 core specimens were tested for chloride profiling (11 depth increments each, 3 powder samples per depth increment), resulting in completion of approximately 15,000 chloride titration tests.

Table 3.8: Summary of test specimens used for time-dependent chloride testing

Mix designation	Binder type	w/b ratio	Exposure conditions				Test intervals[2]	Total no. of specimens
			lab	CT[1]	D[1]	total		
PC 0.4	PC	0.4	1	4	4	9	6	54
PC 0.6		0.6	1	4	4	9	6	54
BS 0.4	BS	0.4	1		4	5	6	30
BS 0.6		0.6	1		4	5	6	30
CS 0.4	CS	0.4	1	4		5	6	30
CS 0.6		0.6	1	4		5	6	30
FA 0.4	FA	0.4	1	4	4	9	6	54
FA 0.4		0.6	1	4	4	9	6	54
SP 0.4	SP	0.4	1	4		5	6	30
SP 0.6		0.6	1	4		5	6	30
SF 0.4	SF	0.4	1	4		5	6	30
SF 0.6		0.6	1	4		5	6	30
								456

[1] Exposure conditions in CT and Durban: submerged, tidal, splash/spray, and air-borne

[2] Test intervals approximately 1, 1.5, 2, 2.5, 3, and 3.5 years; in addition, laboratory samples were tested after 90 days

4.Experimental results and discussion

4.1 Introduction

The experimental programme for this research included measuring the ingress of chloride ions into various types of concrete in different marine environments, as discussed in Chapter 3. The measurements were taken at roughly 6-month intervals for a period of 3.5 years. These were used to identify time-dependent chloride profiles in relation to binder type, w/b ratio and exposure condition. Regression analysis of the chloride profiles was done using Fick's second law of diffusion, which yielded the input parameters needed for the modelling of time-dependent chloride ingress:

- Apparent diffusion coefficient D_a (obtained from the curvature of individual chloride profiles)
- Chloride surface concentration C_s (obtained by extrapolating the chloride profiles to the concrete surface)
- m-values and n-values, which describe the change in D_a and C_s over time, respectively (obtained from analysing the change in D_a and C_s over the experimental duration)

The analysis of the chloride ingress data was aimed at identifying the influence of the concrete mix properties and the environmental exposure conditions on chloride ingress. In order to rate the research to be of high practical relevance, four different marine exposure conditions were investigated in both Durban and Cape Town. In each of these locations, concrete samples were made using binder types that were of relevance to the locality, which resulted in a total of eighteen different concretes (nine binder types and two w/b ratios) each of which were exposed to four different marine exposure zones.

The main emphasis of the data analysis was placed on using the obtained time-dependent D_a and C_s values in a service life prediction model, based on Fick's 2nd Law of diffusion, to predict the time to corrosion initiation, where the latter was defined as the time when chloride concentrations exceeded the (assumed) critical chloride threshold. In this way, the chloride measurements obtained over the 3.5 years of exposure allow predicting the time to reinforcement corrosion initiation with respect to cover depth, binder type, w/b ratio and environmental exposure class.

The service life modelling is discussed at a later stage in Chapter 5. Figure 4.1 illustrates the experimental and analytical strategy followed in this research.

In the following sections, chloride contents are always expressed as percentage by mass of binder.

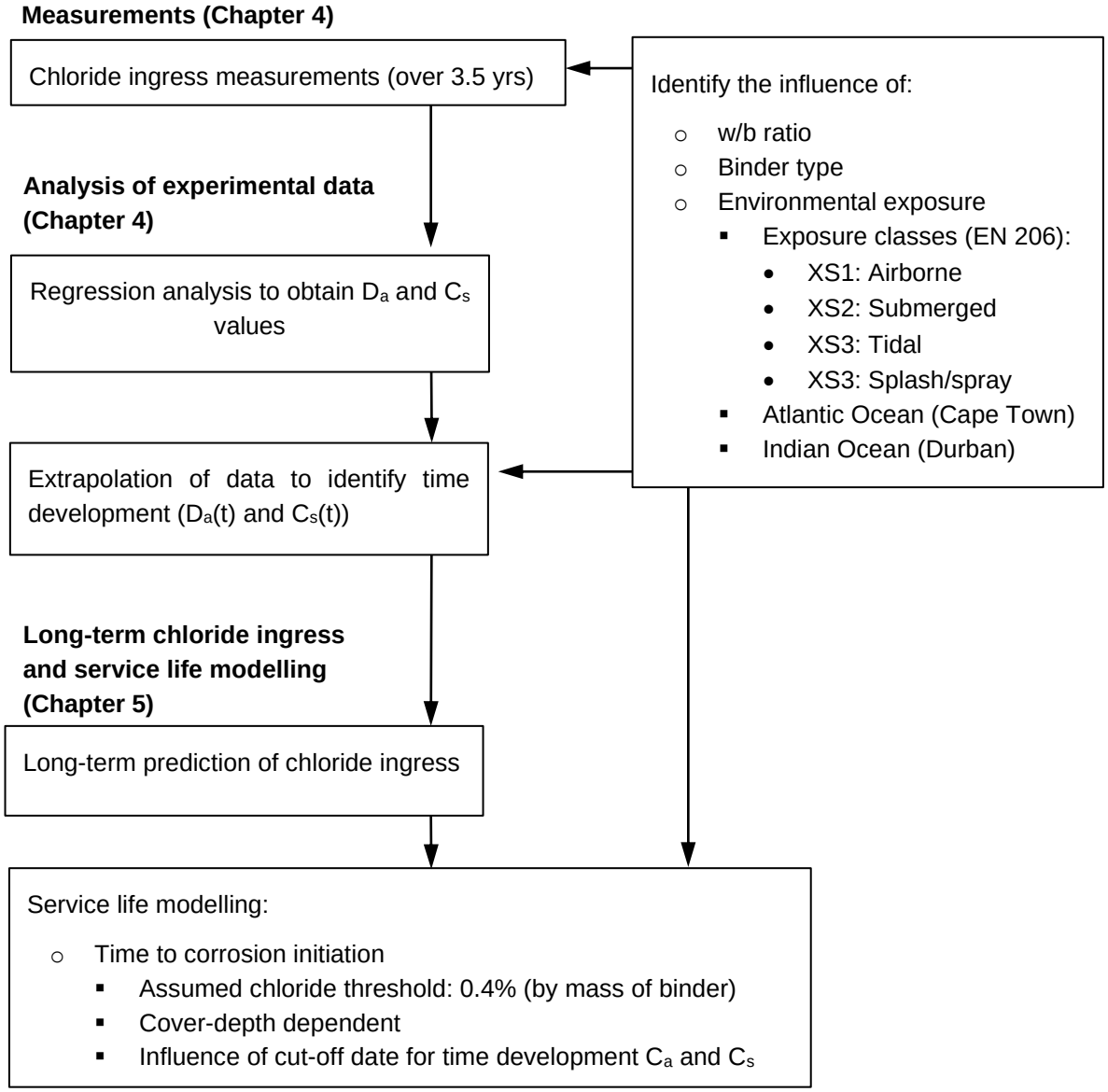

Figure 4.1: Flowchart for the experimental and analytical strategy adopted in this research

4.2 Methods of data presentation and interpretation

4.2.1 Interpretation of chloride profiles

Time-dependent chloride profiles were obtained by measuring chloride contents (% by mass of binder) on concrete core samples that were removed from the test specimens at roughly 6 month intervals, for a total exposure period of approximately 3.5 years. Commonly, each core was tested using potentiometric titration on powder samples retrieved from 10 depth increments over a total depth of 50 mm (compare Section 3.5.1). This resulted in an individual chloride profile for each sample for a given exposure time. Figure 4.2 shows typical examples of chloride profiles. All chloride profiles established in this manner (for all concrete types, exposure conditions and test ages) are included in Appendix A.

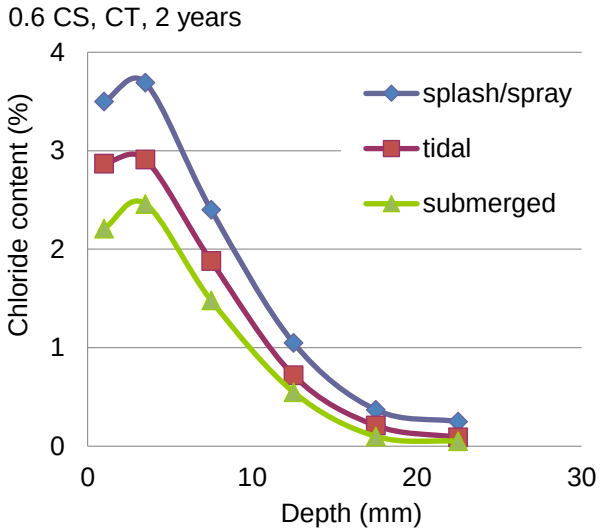

Figure 4.2: Example of typical chloride profiles (exposure site: Cape Town, CS concrete with w/b = 0.6), after approximately 2 years of exposure

The calculation of apparent diffusion coefficients (regression analysis, see Section 4.2.2) first required determining and excluding outlier values from the individual chloride profiles. Measured chloride concentrations at certain depths (i.e. certain data points on the chloride profile) were therefore removed from the curve if they were considered not to represent the chloride ingress characteristics of the particular sample. Two adjustments were made to the chloride profiles of all samples: firstly, removing the first data point, and secondly, “cutting” the “tail” of the curve, as discussed in the following paragraphs.

The first data point on the curve (i.e. the chloride content in the first depth increment (1 mm at younger test ages and 3 mm at older test ages)) of most samples indicated a lower chloride concentration, compared to the subsequent depth increment. This “dip” in the chloride profile close to the surface is a commonly observed phenomenon (compare Section 2.6.2) that is linked to near-surface effects such as washing out, wetting/drying cycles and the ‘skin’ effect (Lee and Chisholm, 2005). Including the first depth increment in the regression analysis would have resulted in a flatter chloride profile and hence a higher diffusion coefficient. In line with recommendations given in the literature (e.g. ASTM C 1543, 2003) the first data point was thus always excluded in the regression analysis.

The “tail” of the chloride profile was considered to consist of data points that were lying beyond the first depth at which zero chloride content was measured. In the regression analysis it was noted that including these data points forced the chloride profile curve to become flatter, which correspondingly resulted in lower extrapolated chloride surface concentrations and higher diffusion coefficients (Figure 4.3), which was considered not to represent the chloride ingress behaviour of the concrete. The chloride ingress characteristic of the concrete was therefore assumed to be best represented by regression analysis of data points ranging from the second depth increment to the first depth increment with close to zero chloride content (Figure 4.4).

In addition to making these adjustments to the measured data prior to regression analysis, some chloride profiles required exclusion of outliers. A chloride concentration at a certain depth was considered an outlier if it visually did not fit the chloride profile indicated by the remainder of the

data. Outliers were identified in less than 10% of the measured chloride profiles. In all cases where a data point was considered an outlier, explanations and reasons are provided (see Appendix A, which contains all individual chloride measurements as well as all chloride profiles).

Measured data (max. 30 sets)		
Depth No.	Depth mm	Cl content mass%
1	1	2.690
2	3.5	3.600
3	7.5	2.230
4	12.5	0.740
5	17.5	0.240
6	22.5	0.120
7	27.5	0.070
8	35	0.080
9	45	0.050
10	55	0.130

Exposure data	
Exposure time t, days:	1277.0
Initial chloride content C_i, mass%:	

Curve-fitting conditions	
Curve-fitting **start** from the depth No.:	1
Curve-fitting **end** at the depth No.:	
Exposure boundary:	One-side
Thickness of specimen, mm:	75

Curve-fitting results	
Surface Cl content C_s, mass%:	**3.643**
Transport coefficient D_a, m^2/s:	**6.27E-13**
R^2 (for selected data):	0.909

Data for calculated curve	
Depth mm	Cl content mass%
0	3.643
2.4	3.055
4.8	2.49
7.2	1.97
9.6	1.51
12	1.121
14.4	0.805
16.8	0.559
19.2	0.374
21.6	0.242
24	0.151

Measured data (max. 30 sets)		
Depth No.	Depth mm	Cl content mass%
1	1	2.690
2	3.5	3.600
3	7.5	2.230
4	12.5	0.740
5	17.5	0.240
6	22.5	0.120
7	27.5	0.070

Exposure data	
Exposure time t, days:	1277.0
Initial chloride content C_i, mass%:	

Curve-fitting conditions	
Curve-fitting **start** from the depth No.:	2
Curve-fitting **end** at the depth No.:	
Exposure boundary:	One-side
Thickness of specimen, mm:	75

Curve-fitting results	
Surface Cl content C_s, mass%:	**5.242**
Transport coefficient D_a, m^2/s:	**3.62E-13**
R^2 (for selected data):	0.997

Data for calculated curve	
Depth mm	Cl content mass%
0	5.242
1.2	4.682
2.4	4.133
3.6	3.603
4.8	3.1
6	2.633
7.2	2.205
8.4	1.822
9.6	1.484
10.8	1.191
12	0.941

Figure 4.3: Measured chloride concentrations and resulting chloride profiles from regression analysis, top: including all data points, bottom: reduced number of data points (screenshot from data sample)

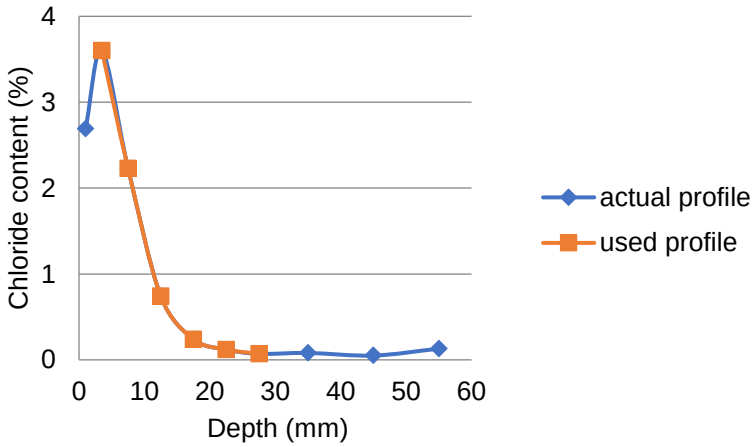

Figure 4.4: Chloride profile data points used in regression analysis, compare Figure 4.3

The regression analysis of measured chloride ingress data yields the input parameters for the equation describing Fick's second law of diffusion, i.e. the theoretical chloride surface

concentration (C_s) and the apparent diffusion coefficient (D_a), as discussed in Sections 4.2.2 and 4.2.3.

It needs to be noted that D_a and C_s, if obtained based on experimental data (as done in this research) must always be considered in conjunction with each other. The regression analysis applied to obtain D_a and C_s from the measured chloride profiles assumes a certain relationship between D_a and C_s. Therefore, in terms of chloride ingress prediction, D_a is a construct of C_s and vice versa, and it would be invalid to consider either parameter in isolation. The combined consideration of D_a and C_s in service life modelling of RC structures is discussed in Ch. 5.

4.2.2 Calculation of apparent diffusion coefficients D_a

Calculation of a chloride profile in terms of D_a and C_s from experimental points usually follows the following procedures. Firstly the chloride profile is obtained from the samples collected by grinding the concrete cores obtained in the required increments. The chloride content is then obtained by acid extraction in nitric acid solution followed by potentiometric titration against silver nitrate. The chloride concentration of each sample is then obtained as a percentage of chloride by mass of binder. This then gives the chloride profile at the time when the specimens are removed from the exposure environment. D_a is determined by fitting the error function solution to Fick's Second Law, for non-steady state diffusion in a semi-infinite medium as described in Section 3.5.1 (see Figure 4.3). When analysing the chloride profile, the sum of the squared differences between the fitted and the actual data for the chloride content of each sample is minimised by adjusting the regressor variable. Once a best fit is achieved, D_a is calculated, where D_a is the gradient of the best-fit curve. D_a (apparent diffusion coefficient) is the global diffusion coefficient involved in Fick's second law, which takes chloride binding into account. D_a reflects the influence of all possible transport mechanisms and environmental effects acting on the concrete that have contributed to establishing the chloride profile. It does not yield an instantaneous measure of the current resistance to chloride penetration. Instead, it reflects the 'time-averaged' performance of the concrete over the period between first exposure of the structure and the time when the chloride profile was determined. D_a and C_s are time-dependent, and the values are influenced by binder type, w/b, exposure condition and even weathering. Time dependency is associated with on-going hydration of the cement matrix. Capillary pore volume and its connectivity are important in assessing chloride transport, and capillary pores reduce and are partially blocked as the cement matrix hydrates, which implies a loss of path for chloride ions. D_a can decrease with time (i.e. degree of hydration) and C_s can increase as a result of the increase in chloride binding and the build-up of chlorides on the surface. For the purposes of this research the time-dependent model of D is shown in Equation 2.15.

Once values of D_a are calculated from the chloride profiles, they are plotted against average time on a log-log scale, and m is the negative gradient of the resulting best-fit line. The equation resulting from the best-fit line represents the time-dependent development of D_a.

4.2.3 Prediction of time-dependent chloride surface concentrations C_s

As mentioned above, the measured chloride profiles were analysed using regression analysis. The chloride surface concentration (C_S) is the projected chloride surface concentration at the exposed surface. The resulting chloride profile was used to predict chloride concentrations at various depths in the concrete. Since the regression analysis is based on measured data, the

predicted chloride profiles (using the calculated D_a and C_s) generally correspond reasonably well to the measured chloride ingress when depths away from the concrete surface are considered. However, the extrapolated chloride surface concentrations resulting from regression analysis are 'hypothetical' values with little resemblance of actual measured chloride surface concentrations.

As discussed in Section 4.2.1, the regression analysis is commonly carried out disregarding the measured chloride concentration near the surface. The curve fitted to the experimental data based on regression analysis is therefore, in terms of actual performance in the field, only valid for depths away from the surface. Due to the shape of the predicted chloride profile, which corresponds to a power function, the extrapolation of the curve on to the y-axis (i.e. the concrete surface, at a depth of 0 mm) results in the prediction of an unrealistically high chloride surface concentration. This is unproblematic when D_a and C_s are used together as input parameters in Fick's second law of diffusion to predict chloride concentrations close to the level of the reinforcement, as both D_a and C_s are only "valid" in conjunction with each other, as already discussed in Section 4.2.1. However, when discussing the influence of various material and environmental parameters on C_s, as done in Chapter 2 and Chapter 5, it needs to be kept in mind that the predicted surface concentrations are only 'hypothetical' values.

The "measured" chloride surface concentrations generally increased over the exposure duration of 3.5 years. The trend lines fitted to the time-development of C_s allow extrapolation of values beyond the measurement period. Similar to what was observed for D_a values, it was also proposed that the time development of chloride surface concentrations followed a power function. However, it appears questionable to assume that chloride surface concentrations continue to increase indefinitely during the service life duration of a concrete structure in the marine environment. Literature states that C_s can increase as a result of the increase in chloride binding and the build-up of surface chlorides (Uji et al, 1990). Also, the nature of the interaction with the chloride environment is key to the various levels of the surface chloride content. The surface chloride concentration of concrete constantly exposed to seawater may not change with time due to chemical equilibrium, but at the tidal zone C_s can be increased by wetting and drying cycles (Bamforth, 1993). Long-term monitoring of C_s from concrete structures shows that the order of C_s with regard to contact with seawater is tidal>splash>atmospheric zone (Uji et al, 1990). Several models exist for the time-dependent nature of C_s (as discussed in Chapter 2), however, these models do not consider an initial build-up of chlorides on the surface of the cover concrete at an early age of concrete exposure to a salt environment. Using these models, short-term C_s values are underestimated, and long-term C_s values are over-estimated (Song et al, 2008). It seems therefore more realistic to assume that chloride surface concentrations eventually cease to increase further and reach a constant value i.e. follow a power function. The time at which such a constant C_s is attained was not determined in this research, as it clearly lay beyond the end of the experimental period of 3.5 years. The question of which C_s value to use in this service life modelling, i.e. the question of whether there is an appropriate "cut off" time for C_s (and also for D_a) beyond which values are assumed to remain constant, is discussed in more detail in Chapter 5.

The experimental data on C_s are thus used in two different ways:

- Firstly, estimate surface concentrations that can actually be expected in-situ (obtained from literature and real structures), based on w/b ratio, binder type, exposure condition

and time. With this, the influence of w/b, binder type and exposure condition can be identified, which will help develop a better understanding on these effects.
- Secondly, for each of the concretes and exposure conditions investigated, the predicted development of hypothetical chloride surface concentrations (based on extrapolated trend lines obtained with the experimental data), is used in connection with the development of the apparent diffusion coefficients to make a service life estimate.

4.2.4 Presentation of experimental data

The experimental investigation comprised testing concretes with combinations of various binder types and water/binder ratios under different marine and laboratory exposure conditions in Durban and Cape Town. Water/binder ratios and basic mix design parameters were the same for Durban and Cape Town exposure sites (compare Chapter 3). However, different binder types were used in both locations (CEM I and FA both in Durban and Cape Town, GGBS only in Durban, and GGCS, SF and Superpozz only in Cape Town). Further, due to differences in ambient temperature, relative humidity, and possible slight variations in salinity of the seawater (compare Section 3.5.1), chloride ingress characteristics were expected to be different in the two exposure locations. Considering this large range of experimental variables, results obtained from samples exposed in Durban and Cape Town are first analysed in separate sections. In these sections, the general methods of analysis and influence of parameters investigated are explained. In this manner, the influences of water/binder ratio, binder type and marine exposure classes on the time-development of chloride surface concentrations and chloride diffusion coefficients are investigated separately for Durban and Cape Town in Section 4.3. A comparison of results obtained from both exposure locations is subsequently done in Section 4.3.11, aiming at highlighting the influence of the prevailing environmental conditions. This is considered to have practical relevance as national codes and guidelines commonly do not take into account that different marine regions within a country may represent different degrees of aggressive exposure linked to the influences of ambient environmental conditions.

The large amount of experimental data from the three exposure sites (Durban, Cape Town, and laboratory exposure) over the duration of the research resulted in the generation of a great number of spread sheets for data analysis, as well as a very large number of graphs for the comparison of the influence of various experimental parameters. In order to present the experimental data and the related analysis in a comprehensible manner, the number of figures and tables included in Chapter 4 has been kept to a minimum. Reference is made to additional figures and tables in the appendices where appropriate.

4.3 Experimental results and analysis: site exposure

From the Durban and Cape Town exposure sites, samples were retrieved at roughly 1 year initially, and every six months thereafter for a total period of 3.5 years, resulting in measured chloride profiles at 6 different time intervals. Chloride profiles were analysed to obtain apparent chloride diffusion coefficients D_a and chloride surface concentrations C_s, as discussed in Section 4.2. Individual chloride profiles are included in Appendix A. Section 4.3.2 contains a summary of chloride profiles after one year of exposure, highlighting general trends with regard to the influence of binder type, water/binder ratio and exposure condition on chloride ingress. Subsequent sections contain the presentation and analysis of time-dependent values for D_a and

C_s. The influences of concrete mix properties (w/b ratio and binder type) and exposure conditions on time-dependent chloride ingress are discussed in view of service life modelling for reinforced concrete structures in the marine environment.

In Durban, specimens made with GGBS and a water/binder ratio of 0.4 (BS 0.4), situated in the submerged and splash/spray exposure zones, were unfortunately lost in a storm that damaged large parts of the port. Data for these samples are therefore only available up to an exposure duration of 2 years. Similarly, for some of the samples exposed to airborne chlorides in Durban (PC 0.6, BS 0.6, and BS 0.4) experimental data is only available for the first 2 years as some of the metal cages carrying the test specimens were apparently stolen. This, however, did not prevent conclusions being drawn for these sites and exposure conditions.

4.3.1 Chloride profiling

Detailed chloride profiles for all samples and test ages are presented in Appendix A. A few examples are discussed here to highlight some of the most important trends and to compare the various parameters influencing chloride ingress into the concrete. This allows interesting observations on the time-development of chloride ingress in relation to binder type, w/b ratio and exposure conditions.

4.3.2 Time-dependency of chloride ingress

Figure 4.5 shows a comparison of the time-dependent chloride ingress of PC concrete (w/b = 0.6) in the submerged exposure zones in Durban and Cape Town. Similarly, Figure 4.6 shows the same for BS and CS samples. It can clearly be seen that chloride concentrations across all depth increments increase with time, which is a result of increasing chloride surface concentrations C_s and diffusion into the concrete. The increase in C_s is indicated by the upward "shift" of the curves with time. The diffusion coefficient D_a is related to the curvature of the chloride profiles and a flattening slope is expected with time (corresponding to a decrease in D_a with time). The slope of the chloride profiles is relatively constant in the PC samples, indicating that the change in D_a over time is relatively small. In contrast, the chloride profiles of BS and CS concrete clearly show the decrease in D_a as the profiles become increasingly steeper as time proceeds. The time development of D_a with respect to various binder types and exposure conditions is analysed and discussed in more detail in Sections 4.3.5 and 4.3.6.

Figure 4.6 shows an anomaly in the data, with chloride concentrations measured on BS concrete in Durban after approximately 3.5 years being lower than those measured after approximately 3 years, at depths greater than 10 mm. This is assigned to differences in the respective specimens (e.g. differences in compaction or coarse aggregate content in sample) and not considered to represent a noteworthy trend.

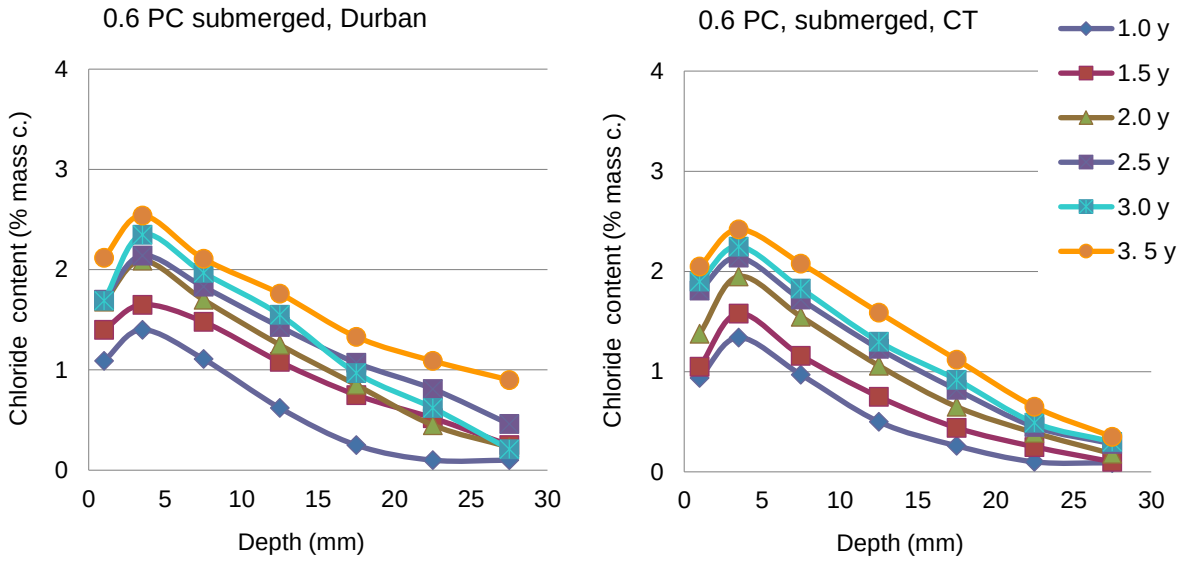

Figure 4.5: Typical time development of chloride profiles in Durban, submerged environment, concrete with w/b = 0.6: CEM I (left) and GGBS (right)

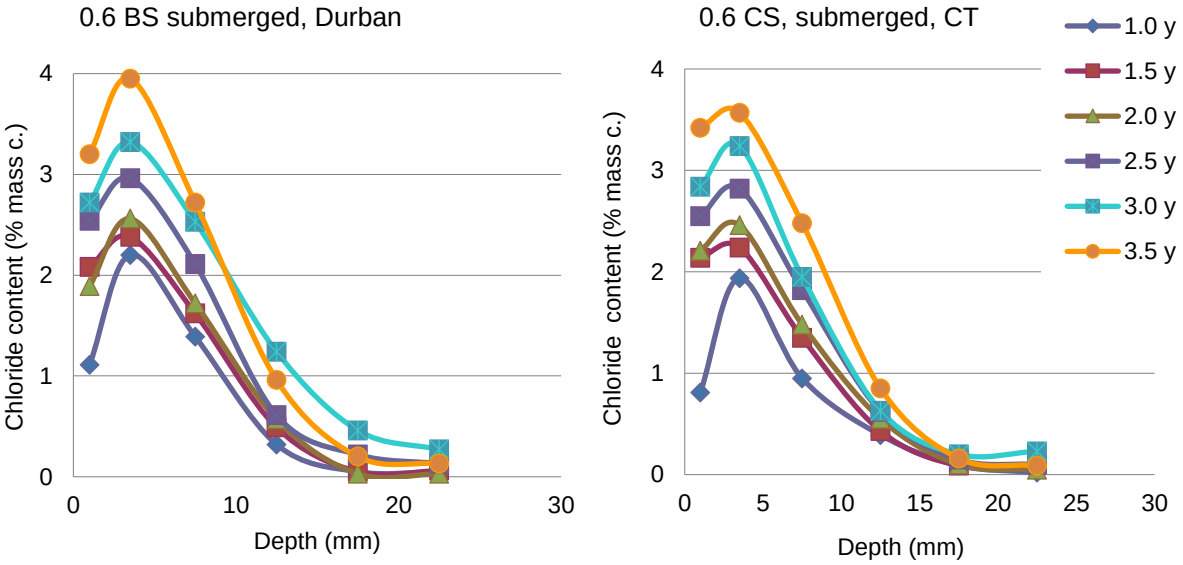

Figure 4.6: Typical time development of chloride profiles in Cape Town, submerged environment, concrete with w/b = 0.6: CEM I (left) and GGCS (right)

4.3.3 The influence of binder type and w/b ratio

It is interesting to use Figures 4.5 and 4.6 to compare the overall distribution of chloride concentrations of the PC and slag concretes. The use of blast furnace or corex slag (at 50% cement replacement) resulted in a significantly higher chloride concentration at the surface, compared to the respective plain CEM I concrete (PC), however also significantly lower chloride concentrations deeper inside the specimens. The higher chloride surface concentration in BS and CS concrete, compared to plain PC concrete, can be linked to the effects of higher chloride

binding (the effect of different absorption properties can be ruled out as water sorptivity and porosity results for BS, CS and PC concretes were generally similar).

The steep decrease in chloride content through the depth of the slag concretes, compared to the chloride profiles of the PC concrete, is linked to lower diffusion coefficients. The overall result of this somewhat contradicting phenomenon is that BS and CS concrete can be expected to perform much better in chloride environments than PC concrete. The reason for this is that the reinforcement is commonly located at depths of at least 20 mm or more, i.e. in regions where chloride concentrations are much lower in concrete containing slag, compared to plain PC concrete.

The influence of various binder types on chloride ingress is further highlighted in Figures 4.7 and 4.8. These figures show that PC concrete generally has the lowest chloride concentrations in surface regions, compared to concretes containing various supplementary cementitious materials, but significantly higher chloride ingress deeper inside the concrete.

For the Durban samples (Figure 4.7), the comparison of BS and FA concrete indicates a better performance of BS concrete, however only with regards to the chloride surface concentration and the chloride contents in the first roughly 10 mm. Beyond the first 10 mm (roughly), the performance is similar. Similarly, Cape Town samples indicated that concrete containing slag has the best overall performance (Figure 4.8). The effect of binder type on chloride ingress is explored in detail in Chapter 5 for all exposure conditions.

Figures 4.7 and 4.8 further allow assessing the influence of w/b ratio on chloride ingress as considerably lower chloride concentrations were measured for the concretes with w/b = 0.4 (on the right of Figures 4.7 and 4.8), compared to concrete with w/b = 0.6 (on the left). This also is investigated in detail in Chapter 5.

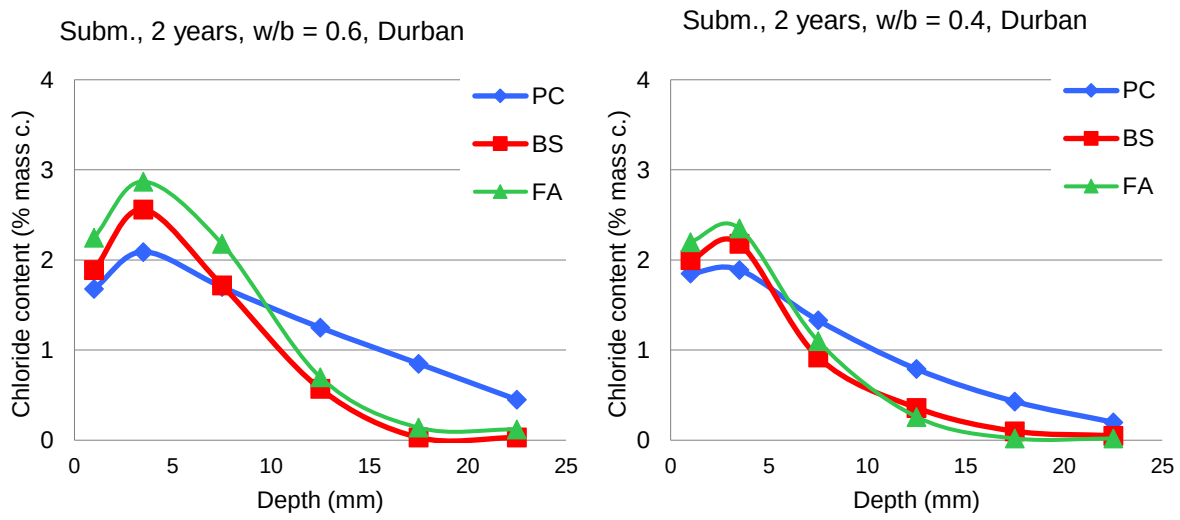

Figure 4.7: Typical influence of binder type on chloride profiles after 2 years, submerged environment: w/b = 0.6 (left) and w/b = 0.4 (right) (Durban)

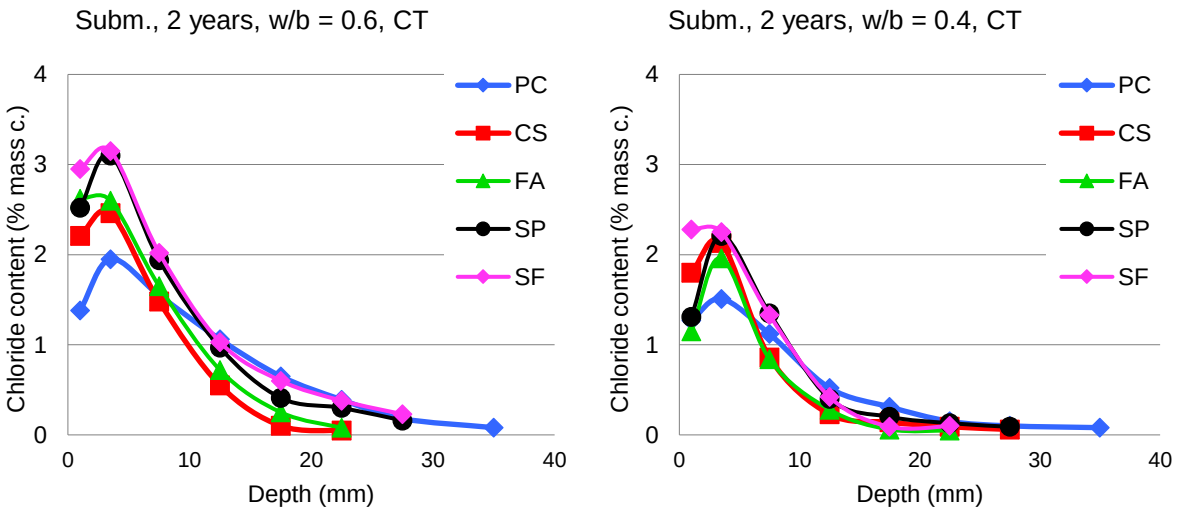

Figure 4.8: Typical influence of binder type on chloride profiles after 2 years, submerged environment: w/b = 0.6 (left) and w/b = 0.4 (right) (Cape Town)

4.3.4 Chloride ingress versus exposure condition

As expected, the exposure condition was found to have a significant influence on chloride ingress. Figures 4.9 and 4.10 show examples, comparing chloride ingress into PC and slag (BS or CS) concretes after 2 years exposure in the different environments. The general trend observed across all samples is that the highest chloride concentrations were measured in the splash-spray zone, followed by the tidal zone and the submerged zone. The lowest chloride concentrations were measured on samples exposed to airborne chlorides.

These trends generally confirm what is expected with regard to the influence of environmental exposure classes. Samples exposed to the tidal zone were placed roughly halfway between high and low tide water levels, which means that during an average tide cycle they were submerged for roughly 6 hours, followed by 6 hours drying. This probably caused the concrete samples to be relatively saturated for most of the time, considering that water takes significantly longer to escape concrete, compared to entering it. The higher chloride ingress in the splash/spray zone, compared to the tidal zone, confirms that frequent and efficient drying supports chloride ingress into concrete that is subjected to regular contact with salt water. This is commonly related to the combined transport mechanisms of sorptivity, convection and diffusion, whereas the predominant mechanism of ingress in the tidal zone samples would have been diffusion. It is therefore to be expected that the chloride profiles of concrete samples exposed to the tidal zone lie in between those of the splash/spray and submerged zones.

It however needs to be noted that samples in the submerged and tidal zones in Durban were overgrown with a relatively dense and strong layer of barnacles and crustaceans (a mix of encrusters: mussels, shells, algae, crabs, etc.; compare Figure 3.10). This may have effectively kept the concrete in the tidal zone saturated with moisture over most of the exposure period.

For the purpose of these discussions, it is interesting to note that the environmental classes stipulated in EN 206 (BSI, 2013) for concrete structures in marine exposure conditions make no distinction between tidal and splash/spray zones, such that class XS3 combines the 2 cases (compare Section 3.5.1). The results of this research indicate that this is a simplification that

needs further consideration. This is discussed further in Chapter 5, based on detailed modelling and analysis of the influence of the exposure environment on time-dependent chloride ingress.

In summary, exposure conditions were found to have a significant influence on chloride ingress. Samples with the highest chloride concentrations were measured in the splash-spray zone and the lowest chloride concentrations were measured in the airborne samples.

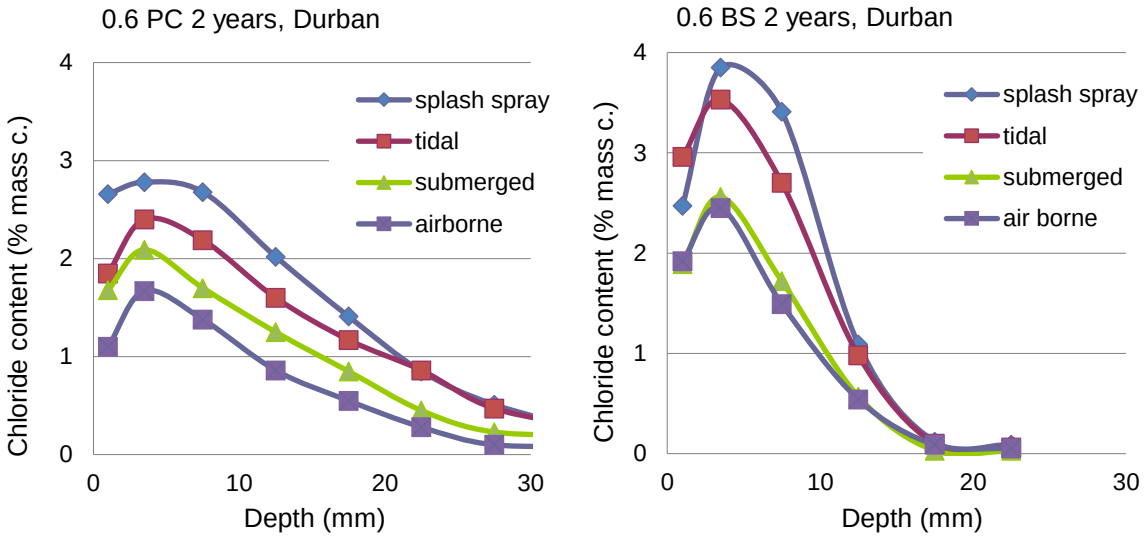

Figure 4.9: Typical influence of exposure condition on chloride profiles in Durban after 2 years, concrete with w/b = 0.6: CEM I (left) and GGBS (right)

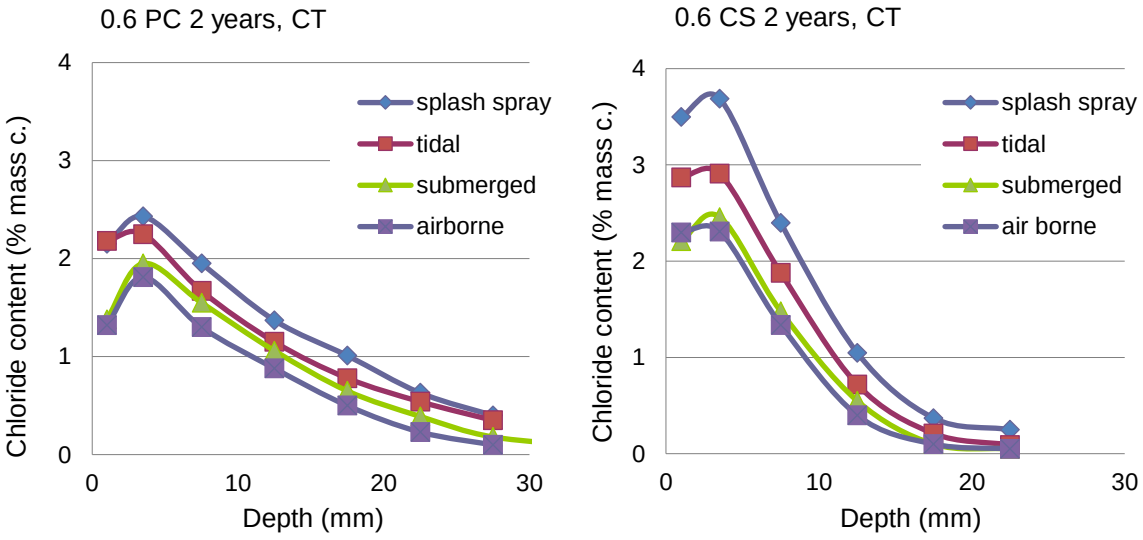

Figure 4.10: Typical influence of exposure condition on chloride profiles in Cape Town after 2 years, concrete with w/b = 0.6: CEM I (left) and GGCS (right)

4.3.5 Time-development of D_a (Durban)

The time-dependent development of the apparent diffusion coefficient D_a is shown in Figures 4.11 to 4.15, for the samples exposed in Durban. The figures compare values obtained for concretes with consistent w/b ratio but different binder types, for specimens exposed to the same environmental condition. In Figures 4.12 - 4.15, the measurements (D_a versus time) were plotted on a log-log curve and trend lines were fitted using the automatic trend line function in MS Excel. The trend lines, which assume linearity on a log-log scale, are of the power type. For illustration purposes, Figure 4.11 first presents the "real" time-development of D_a on a natural scale, using airborne exposure as an example.

Concrete made with plain CEM I had consistently higher diffusion coefficients, compared to FA and BS concretes, as expected. The diffusion coefficients of BS and FA concretes were very similar, as indicated by the close proximity of the respective trend lines. However, BS concrete sometimes showed slightly lower D_a values. The magnitude of the diffusion coefficients was also strongly influenced by the w/b ratio, which also was expected. The influences of binder type and w/b ratio on chloride diffusion are discussed in further detail in Sections 4.3.8 and 4.3.9, respectively.

To determine how well the trend lines for the time-development of D_a fit the experimental measurements, linear regression analysis was carried out and the R^2 value computed (using the automatic functions provided in MS Excel). The exponents of the power-type trend line equations signify the m-values and hence the time-development of D_a. Table 4.1 contains a summary of the trend line equations, R^2 values, and m-values for all parameter combinations.

The table also contains interpolated D_a values for the following ages:

- 35 days, representing $D_{a,35d}$ as the reference short-term value for D_a, as commonly done in literature (compare Eq. 2.15 in Section 2.4.4)
- 1 year, which is used to compare predicted and actual measured values for D_a
- 20 years, representing $D_{a,20y}$ which was later used in service life modelling for BS and FA concretes (as discussed in Chapter 5)

For all concrete types and exposure environments, a decrease in apparent diffusion coefficients over time was observed. The power functions describing the time dependent development of D_a generally fit the measurements reasonably well, with R^2 values commonly around 0.9 indicating a good correlation (Table 4.1). Plotted on a log-log scale, most specimens show a consistent decrease in D_a over the measurement period, with some individual test results only deviating slightly from the trend lines (Fig. 4.12 to 4.15).

As stated previously, samples with w/b= 0.6 in airborne exposure in Durban were lost due to a storm, hence data is only available for the first 3 measurement intervals. For consistency and cross-comparison between test parameters, the time-dependent variation of the D_a value was extrapolated (Figure 4.11, right). It is noted that, strictly, this extrapolation is not valid. However, it was applied to receive complete information for the analysis.

The apparent diffusion coefficients were generally dependent on the various test parameters such as binder type, environmental exposure condition and w/b ratio, which is discussed in detail in the sections to follow. Concerning the time-development, the m-values ranged from 0.29 to 0.86 (Table 4.1) and were dependent mainly on binder type. It was observed, importantly, that the environmental exposure condition did not have a noteworthy influence on

m-values even though it had a very large influence on chloride ingress as such (i.e. chloride concentrations, compare Section 4.3). Generally, m-values were very similar for the various concretes across all four exposure conditions (Table 4.1). Based on this useful observation, m-values obtained for the different concrete types were averaged for the 4 exposure conditions, which allowed for a more general investigation into the influence of binder type and w/b ratio on the change in diffusion coefficient with time (Figure 4.16). The figure presents the standard deviation, which is generally small, confirming that the influence of exposure conditions on the m-values was insignificant.

PC concretes had m-values of around 0.3, indicating a comparatively smaller change in D_a over time compared to BS and FA concretes. This is also obvious from Figures 4.12 to 4.15, in which the linear trend lines of PC concretes are less inclined compared to concretes containing blended binders. Both BS and FA concretes showed m-values of around 0.8, with values for BS concrete being somewhat higher than those for FA concrete. The concretes with higher w/b ratio always showed a slightly higher m-value, compared to concrete with w/b of 0.4, although the difference was small. These observations indicate that the m-value can be thought of as a material characteristic linked to binder type and not depending on concrete strength class or external factors such as chloride exposure condition.

The above comparison of m-values gives a good indication of the time-dependent change in chloride diffusion of the various concretes tested. However, the phenomenon of decreasing D_a with time becomes more notable and quantifiable when values, predicted for different ages, are compared, as done in Figure 4.17. After 20 years of exposure, the predicted apparent diffusion coefficient of PC concretes is close to 20% of the reference value at 35 days. For blended cement concretes, however, the predicted D_a after 20 years of exposure is only 2% of the original value. This illustrates the significant changes in chloride ingress behaviour during the service life of concrete structures, especially for concretes containing fly ash and blast furnace slag.

The data points in the figures correspond to the various testing ages, i.e. 1 year, 1.5 years, 2 years, 2.5 years, 3 years, and 3.5 years.

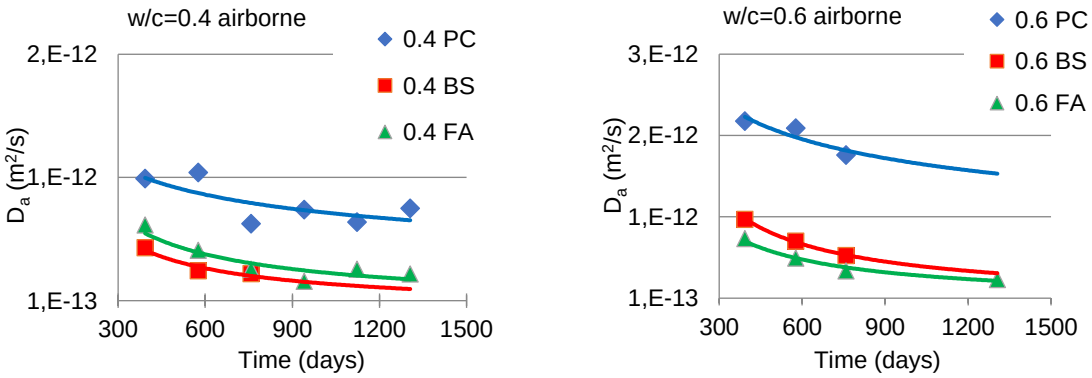

Figure 4.11: Time-dependent variation of D_a (natural scale), Durban, airborne

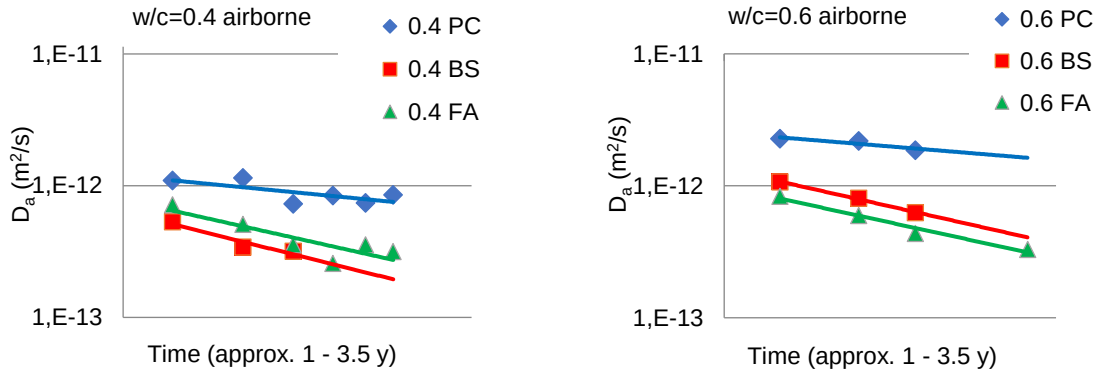

Figure 4.12: Time-dependent variation of D_a (log-log scale), Durban, airborne

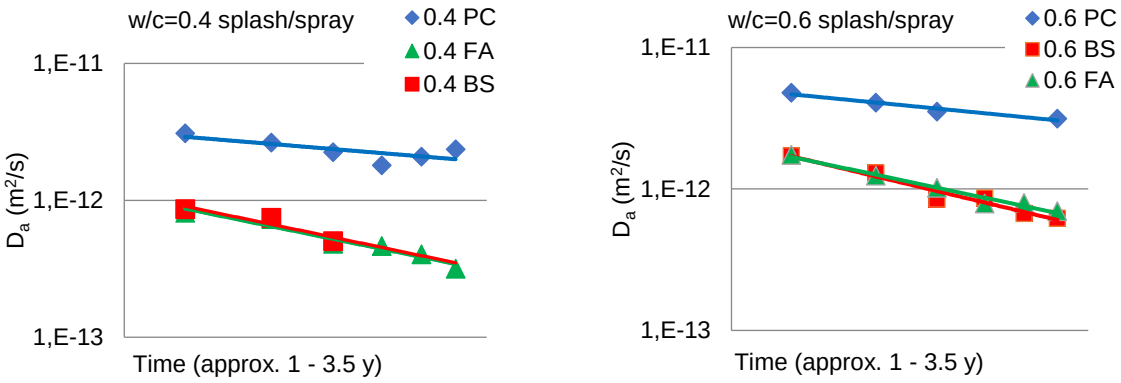

Figure 4.13: Time-dependent variation of Da (log-log scale), Durban, splash/spray

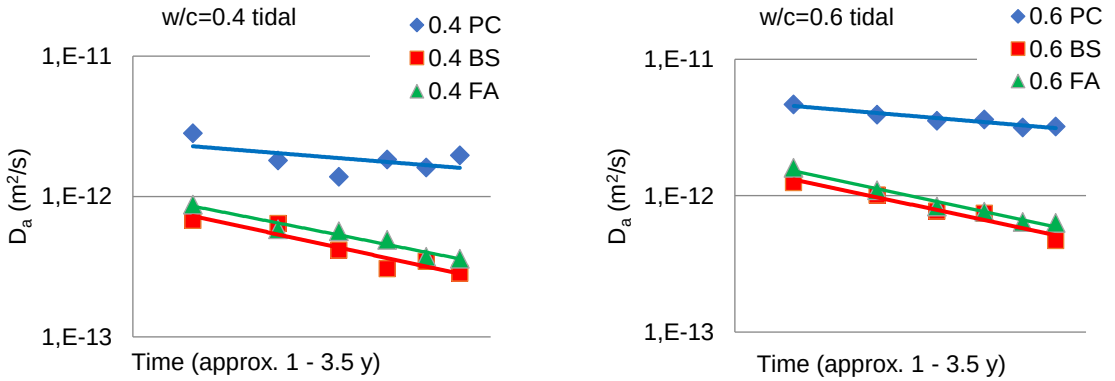

Figure 4.14: Time-dependent variation of Da (log-log scale), Durban, tidal

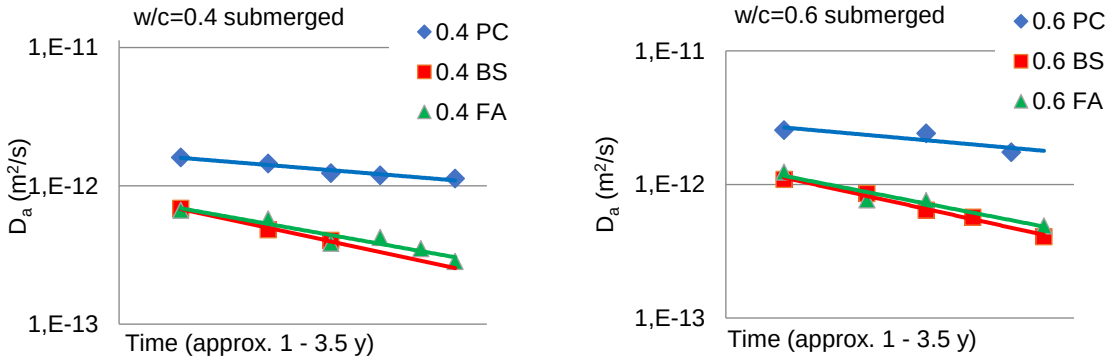

Figure 4.15: Time-dependent variation of Da (log-log scale), Durban, submerged

Table 4.1: Time development of apparent diffusion coefficients (extrapolated from the analysis of experimental results) (Durban samples)

Mix	Exposure	$D_a(t)$ (m^2/s)	R^2	m	$D_{a,\ 35d}$	$D_{a,\ 1y}$	$D_{a,\ 20y}$
0.4 PC	airborne	$7E\text{-}12t^{-0.31}$	0,528	0,31	2,33E-12	1,12E-12	4,44E-13
	splash/spray	$2E\text{-}11t^{-0.31}$	0,866	0,31	6,64E-12	3,21E-12	1,27E-12
	tidal	$1E\text{-}11t^{-0.29}$	0,800	0,29	3,57E-12	1,81E-12	7,58E-13
	submerged	$1E\text{-}11t^{-0.31}$	0,952	0,31	3,32E-12	1,61E-12	6,34E-13
0.6 PC	airborne	$1E\text{-}11t^{-0.29}$	0,826	0,29	3,57E-12	1,81E-12	7,58E-13
	splash/spray	$4E\text{-}11t^{-0.35}$	0,960	0,35	1,15E-11	5,07E-12	1,78E-12
	tidal	$3E\text{-}11t^{-0.31}$	0,931	0,31	9,96E-12	4,82E-12	1,90E-12
	submerged	$2E\text{-}11t^{-0.33}$	0,834	0,33	6,19E-12	2,85E-12	1,06E-12
0.4 BS	airborne	$6E\text{-}11t^{-0.8}$	0,911	0,80	3,49E-12	5,35E-13	4,87E-14
	splash/spray	$1E\text{-}10t^{-0.79}$	0,885	0,79	6,03E-12	9,46E-13	8,87E-14
	tidal	$8E\text{-}11t^{-0.78}$	0,891	0,78	5,00E-12	8,03E-13	7,76E-14
	submerged	$9E\text{-}11t^{-0.82}$	0,989	0,82	4,88E-12	7,13E-13	6,11E-14
0.6 BS	airborne	$1E\text{-}10t^{-0.81}$	0,996	0,81	5,61E-12	8,41E-13	7,43E-14
	splash/spray	$3E\text{-}10t^{-0.86}$	0,964	0,86	1,41E-11	1,88E-12	1,43E-13
	tidal	$1E\text{-}10t^{-0.78}$	0,954	0,78	6,25E-12	1,00E-12	9,70E-14
	submerged	$2E\text{-}10t^{-0.82}$	0,911	0,82	1,08E-11	1,58E-12	1,36E-13
0.4 FA	airborne	$5E\text{-}11t^{-0.71}$	0,859	0,71	4,01E-12	7,58E-13	9,04E-14
	splash/spray	$9E\text{-}11t^{-0.77}$	0,941	0,77	5,83E-12	9,58E-13	9,54E-14
	tidal	$6E\text{-}11t^{-0.72}$	0,950	0,72	4,64E-12	8,58E-13	9,92E-14
	submerged	$4E\text{-}11t^{-0.67}$	0,911	0,67	3,69E-12	7,68E-13	1,03E-13
0.6 FA	airborne	$9E\text{-}11t^{-0.78}$	0,972	0,78	5,62E-12	9,03E-13	8,73E-14
	splash/spray	$2E\text{-}10t^{-0.76}$	0,977	0,76	1,34E-11	2,26E-12	2,32E-13
	tidal	$2E\text{-}10t^{-0.78}$	0,974	0,78	1,25E-11	2,01E-12	1,94E-13
	submerged	$9E\text{-}11t^{-0.72}$	0,940	0,72	6,96E-12	1,29E-12	1,49E-13

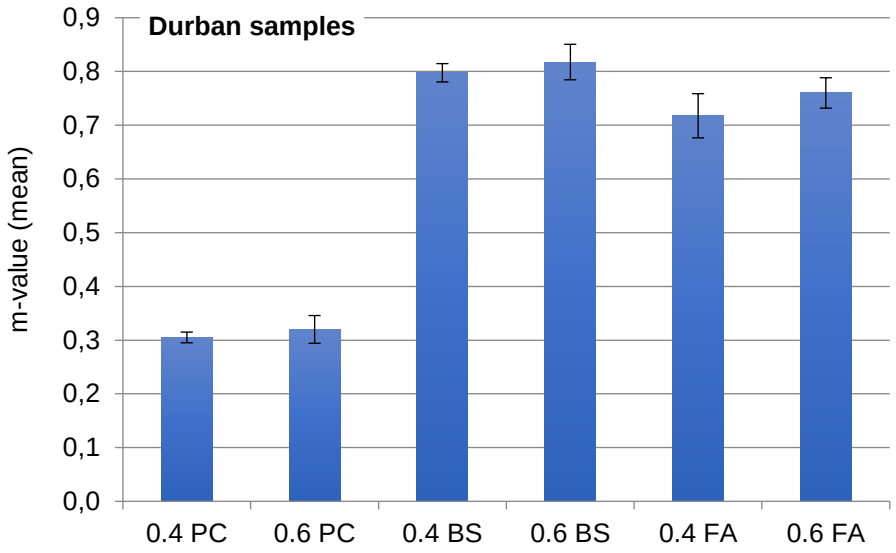

Figure 4.16: Comparison of average m-values (averaged for all 4 exposure conditions; ±1 STDVs are indicated in the figure by the whiskers) (Durban samples)

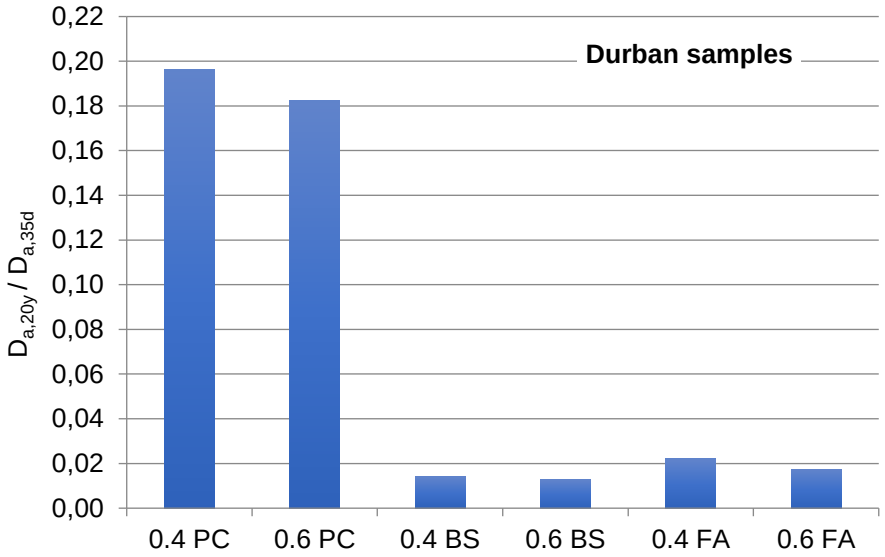

Figure 4.17: Time development of D_a - ratio between apparent diffusion coefficients at 20 years ($D_{a,20y}$) and 35 days ($D_{a,ref}$), (values were averaged for all 4 exposure conditions) (Durban)

4.3.6 Time-development of D_a (Cape Town)

Following the same procedures discussed in the previous Section 4.3.5, this section discusses the time-development of the apparent diffusion coefficient D_a for the samples exposed in Cape Town (Figures 4.18 to 4.21). Generally, similar trends as already discussed in Section 4.3.5 were observed. Therefore, in order to avoid unnecessary repetition of observations, the discussions below are kept to the minimum.

The general trend shows that CEM I concretes have the highest diffusion coefficient, followed by concretes containing SF and SP, respectively. Concrete made with CS and FA had very similar diffusion coefficients, which were generally lower than those of the other mixes. As already observed on the Durban samples, the magnitude of the diffusion coefficients was strongly influenced by the w/b ratio, as expected.

Linear regression analysis was carried out and the R^2 value computed (Table 4.2). Again, for all concrete types and exposure environments, a decrease in apparent diffusion coefficients over time was observed. The m-values ranged from 0.26 to 0.84, which are very similar values as observed for the Durban samples and were again dependent mainly on binder type and not much influenced by exposure condition. The m-values obtained for the different concrete types were averaged for the 4 exposure conditions, as shown in Figure 4.22. The m-values are very similar to those measured on the Durban samples (compare Fig. 4.16), with PC concretes having m-values of around 0.3 and CS, FA and SP concretes generally showing m-values close to 0.8. Concrete containing SF, which was not tested in the Durban environment, had m-values close to 0.6.

Based on the values shown in Table 4.2, the comparison of predicted short- and long-term apparent diffusion coefficients is illustrated in Figure 4.23. Similar to the Durban samples (Figure 4.17), the predicted apparent diffusion coefficient of PC concretes after 20 years of exposure is close to 20% of the reference value at 35 days. For blended cement concretes with FA, SF and CS, D_a after 20 years of exposure is below 2% of the original value. For concrete containing SF, the 20-year value of Da is about 5% of the short-term value.

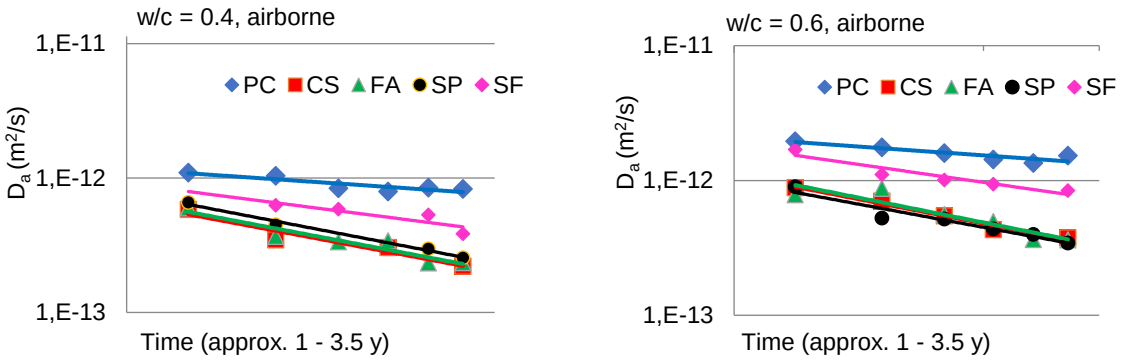

Figure 4.18: Time-dependent variation of D_a (log-log scale), Cape Town, airborne

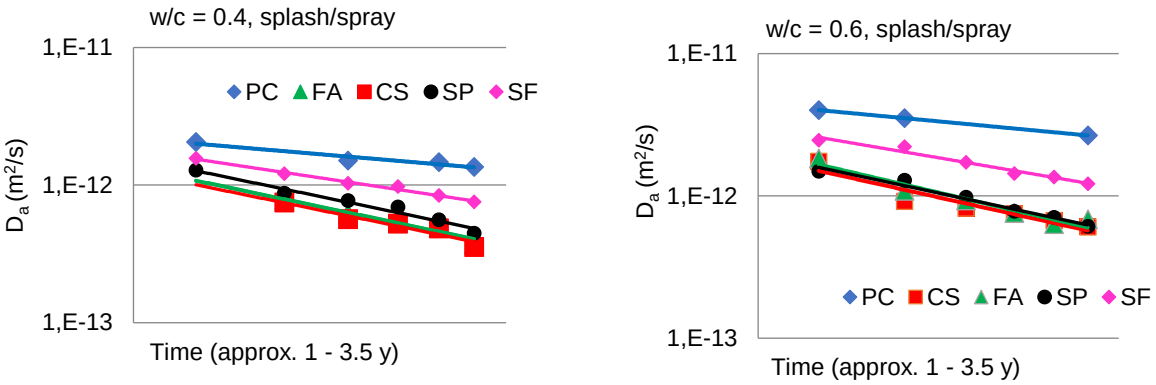

Figure 4.19: Time-dependent variation of Da (log-log scale), Cape Town, splash/spray

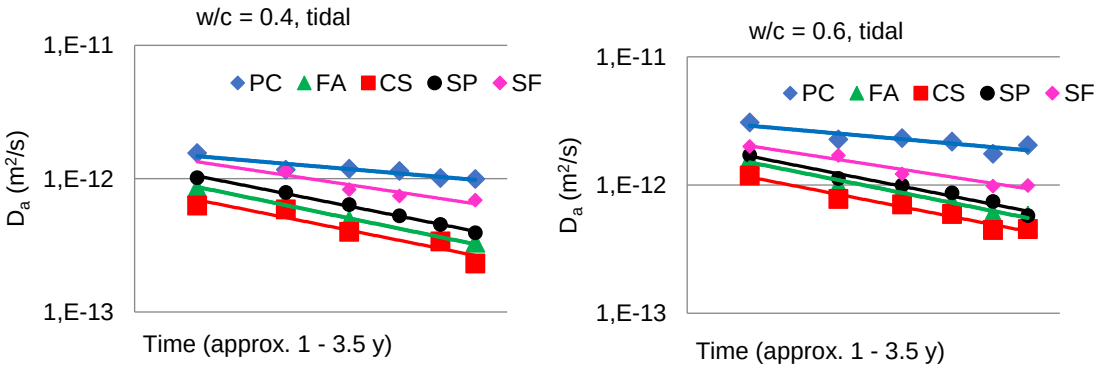

Figure 4.20: Time-dependent variation of Da (log-log scale), Cape Town, tidal

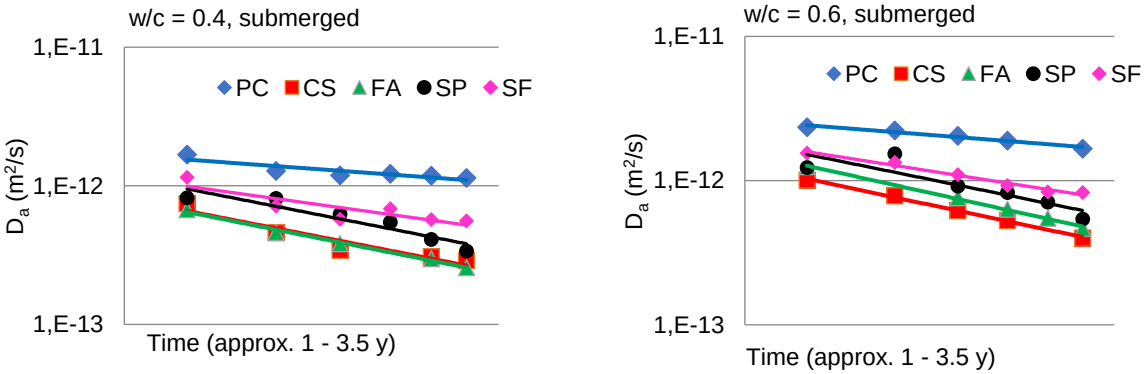

Figure 4.21: Time-dependent variation of Da (log-log scale), Cape Town, submerged

Table 4.2: Time development of apparent diffusion coefficients (extrapolated from the analysis of experimental results) (Cape Town samples)

Mix	Exposure	Da(t) (m^2/s)	R^2	m	$D_{a,\ 35d}$	$D_{a,\ 1y}$	$D_{a,\ 20y}$
0.4 PC	airborne	$5E\text{-}12t^{-0.26}$	0.877	0.26	1.98E-12	1.08E-12	4.95E-13
	splash/spray	$1E\text{-}11t^{-0.32}$	0.937	0.32	3.21E-12	1.51E-12	5.80E-13
	tidal	$1E\text{-}11t^{-0.34}$	0.879	0.34	2.99E-12	1.35E-12	4.86E-13
	submerged	$8E\text{-}12t^{-0.28}$	0.890	0.28	2.96E-12	1.53E-12	6.63E-13
0.6 PC	airborne	$1E\text{-}11t^{-0.27}$	0.804	0.27	3.83E-12	2.03E-12	9.06E-13
	splash/spray	$3E\text{-}11t^{-0.34}$	0.999	0.34	8.96E-12	4.04E-12	1.46E-12
	tidal	$3E\text{-}11t^{-0.36}$	0.889	0.36	8.34E-12	3.59E-12	1.22E-12
	submerged	$1E\text{-}11t^{-0.28}$	0.961	0.28	3.70E-12	1.92E-12	8.28E-13
0.4 CS	airborne	$4E\text{-}11t^{-0.73}$	0.927	0.73	2.98E-12	5.39E-13	6.05E-14
	splash/spray	$1E\text{-}10t^{-0.79}$	0.918	0.79	6.03E-12	9.46E-13	8.87E-14
	tidal	$8E\text{-}11t^{-0.8}$	0.905	0.80	4.65E-12	7.13E-13	6.49E-14
	submerged	$6E\text{-}11t^{-0.75}$	0.910	0.75	4.17E-12	7.19E-13	7.60E-14
0.6 CS	airborne	$8E\text{-}11t^{-0.75}$	0.982	0.75	5.56E-12	9.58E-13	1.01E-13
	splash/spray	$2E\text{-}10t^{-0.8}$	0.904	0.80	1.16E-11	1.78E-12	1.62E-13
	tidal	$1E\text{-}10t^{-0.81}$	0.966	0.81	5.61E-12	8.41E-13	7.43E-14
	submerged	$1E\text{-}10t^{-0.77}$	0.997	0.77	6.47E-12	1.06E-12	1.06E-13
0.4 FA	airborne	$5E\text{-}11t^{-0.74}$	0.905	0.74	3.60E-12	6.35E-13	6.92E-14
	splash/spray	$1E\text{-}10t^{-0.81}$	0.940	0.81	5.61E-12	8.41E-13	7.43E-14
	tidal	$1E\text{-}10t^{-0.82}$	0.989	0.82	5.42E-12	7.92E-13	6.79E-14
	submerged	$6E\text{-}11t^{-0.76}$	0.991	0.76	4.02E-12	6.77E-13	6.95E-14
0.6 FA	airborne	$9E\text{-}11t^{-0.77}$	0.854	0.77	5.83E-12	9.58E-13	9.54E-14
	splash/spray	$3E\text{-}10t^{-0.84}$	0.941	0.84	1.51E-11	2.11E-12	1.71E-13
	tidal	$2E\text{-}10t^{-0.83}$	0.975	0.83	1.05E-11	1.49E-12	1.24E-13
	submerged	$2E\text{-}10t^{-0.80}$	0.996	0.80	1.16E-11	1.78E-12	1.62E-13
0.4 SP	airborne	$6E\text{-}11t^{-0.75}$	0.988	0.75	4.17E-12	7.19E-13	7.60E-14
	splash/spray	$2E\text{-}10t^{-0.8}$	0.966	0.80	1.16E-11	1.78E-12	1.62E-13
	tidal	$1E\text{-}10t^{-0.79}$	0.996	0.79	6.03E-12	9.46E-13	8.87E-14
	submerged	$9E\text{-}11t^{-0.75}$	0.887	0.75	6.25E-12	1.08E-12	1.14E-13
0.6 SP	airborne	$6E\text{-}11t^{-0.71}$	0.931	0.71	4.81E-12	9.10E-13	1.08E-13
	splash/spray	$2E\text{-}10t^{-0.77}$	0.976	0.77	1.29E-11	2.13E-12	2.12E-13
	tidal	$2E\text{-}10t^{-0.82}$	0.971	0.82	1.08E-11	1.58E-12	1.36E-13
	submerged	$1E\text{-}10t^{-0.74}$	0.880	0.74	7.20E-12	1.27E-12	1.38E-13
0.4 SF	airborne	$2E\text{-}11t^{-0.5}$	0.864	0.50	3.38E-12	1.05E-12	2.34E-13
	splash/spray	$5E\text{-}11t^{-0.58}$	0.989	0.58	6.36E-12	1.63E-12	2.87E-13
	tidal	$5E\text{-}11t^{-0.60}$	0.863	0.60	5.92E-12	1.45E-12	2.40E-13
	submerged	$2E\text{-}11t^{-0.53}$	0.859	0.53	3.04E-12	8.77E-13	1.79E-13
0.6 SF	airborne	$4E\text{-}11t^{-0.55}$	0.896	0.55	5.66E-12	1.56E-12	3.00E-13
	splash/spray	$1E\text{-}10t^{-0.62}$	0.970	0.62	1.10E-11	2.58E-12	4.02E-13
	tidal	$9E\text{-}11t^{-0.64}$	0.954	0.64	9.25E-12	2.06E-12	3.03E-13
	submerged	$5E\text{-}11t^{-0.57}$	0.976	0.57	6.59E-12	1.73E-12	3.14E-13

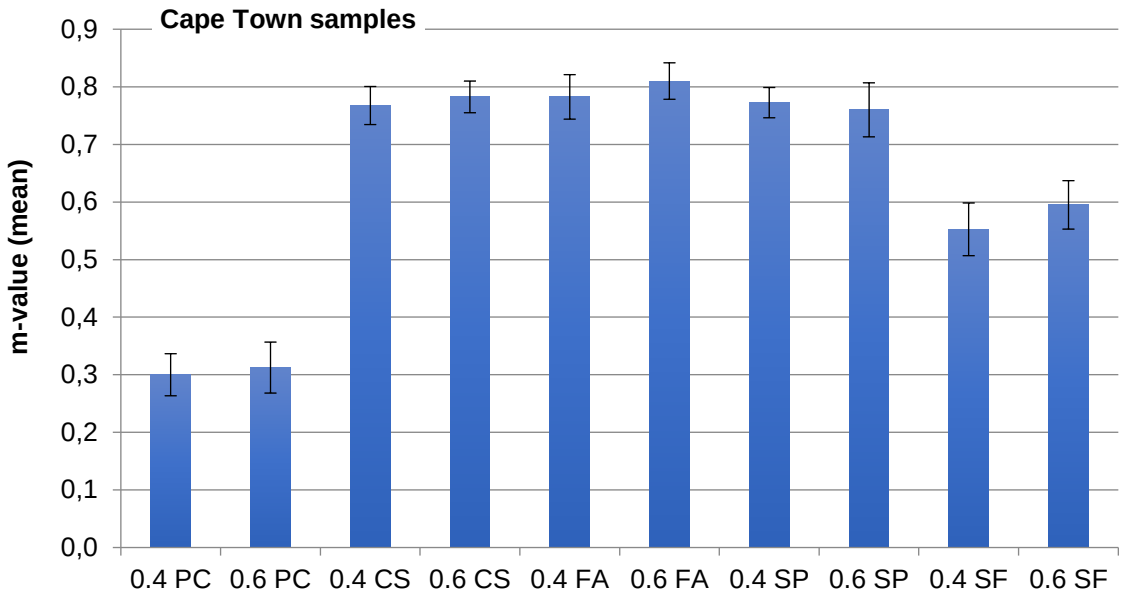

Figure 4.22: Comparison of average m-values (averaged for all 4 exposure conditions, ±1 STDVs are indicated in the figure by the whiskers) (Cape Town samples)

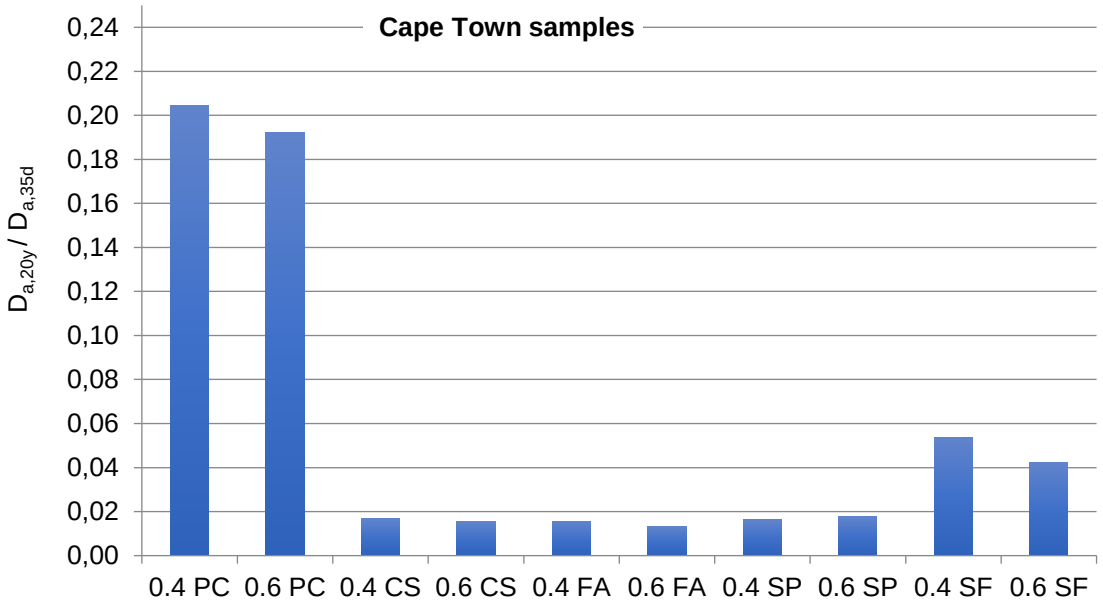

Figure 4.23: Time development of D_a - ratio between apparent diffusion coefficients at 20 years ($D_{a,20y}$) and 35 days ($D_{a,ref}$), (values were averaged for all 4 exposure conditions) (Cape Town)

4.3.7 Model predictions versus experimental measurements on D_a

The experimental data for chloride ingress was used to establish equations $D_a(t)$ to predict the time-development of the apparent diffusion coefficient, as discussed in Section 4.3.6 and shown in Table 4.2 above. To verify that the prediction models (which are based on all data obtained at different time intervals) are properly calibrated and hence a good representation of actual experimental results (at a particular point in time), predicted and measured values at roughly 1 year and 3.5 years (to be precise, 393 days and 1,306 days, which corresponds to the times of

measurement) were compared. Figure 4.24 shows the outcome of the comparison for 1 year and 3.5 years, using the splash/spray zone in Durban as an example. The measured diffusion coefficients generally correspond closely to the predicted values, which shows that the modelled values of $D_a(t)$ are a good representation of the chloride ingress behaviour over the 3.5 years of measurements. For the data presented in the figures below, the predicted value for D_a was generally slightly higher than the measured one, which is related to the general scatter of data points around the predicted values, and which has no practical significance.

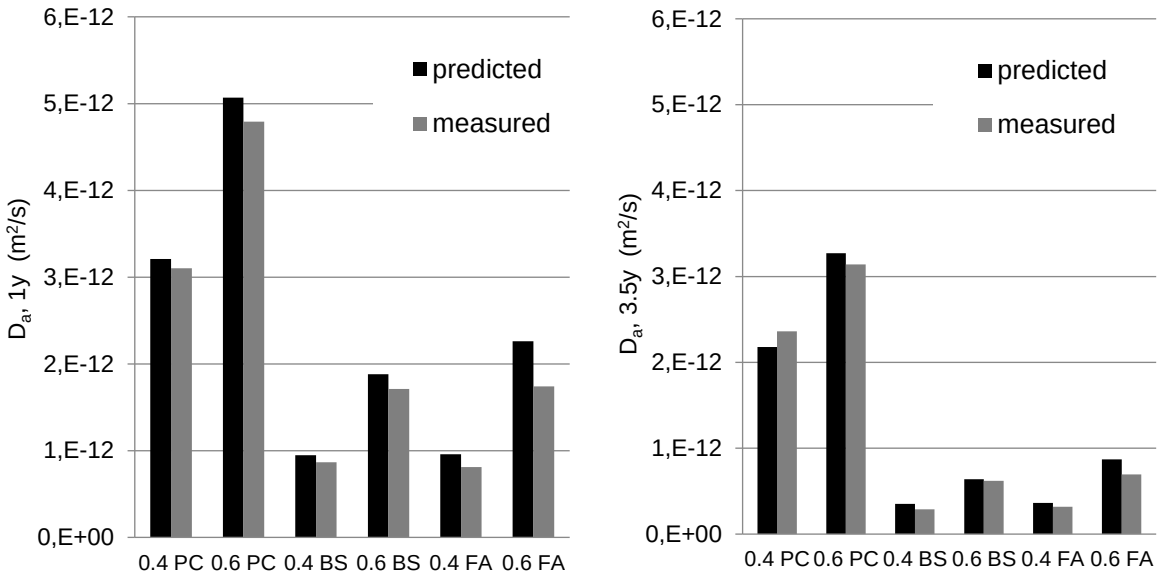

Figure 4.24: Time-dependent values of Da; Comparison of measured and predicted values (left: 1 year exposure, right: 3.5 years exposure)

4.3.8 Influence of binder type on D_a

For determining the influence of binder type on the apparent diffusion coefficient, D_a values predicted for a 20-year exposure period were compared (Figures 4.25 – 4.28). The 20-year value was taken as a reference as this was later used as a realistic alternative in the service life modelling for blended cement concretes, as discussed in detail in Chapter 5.

As expected, concretes made with plain Portland cement had significantly higher diffusion coefficients, compared to concretes with blended cements. For the Durban samples, the comparison of BS and FA concrete shows that the BS consistently has a lower diffusion coefficient (for all exposure zones and for both w/b ratios). In the Cape Town environment, concrete made with FA and CS had the lowest D_a values, followed by concrete made with SP and SF. However, note that the influence of binder type on actual chloride ingress needs to be investigated with consideration of the chloride surface concentration, as discussed in Chapter 5. The diffusion coefficient in isolation is not a representative indicator of the influence of binder type on chloride ingress.

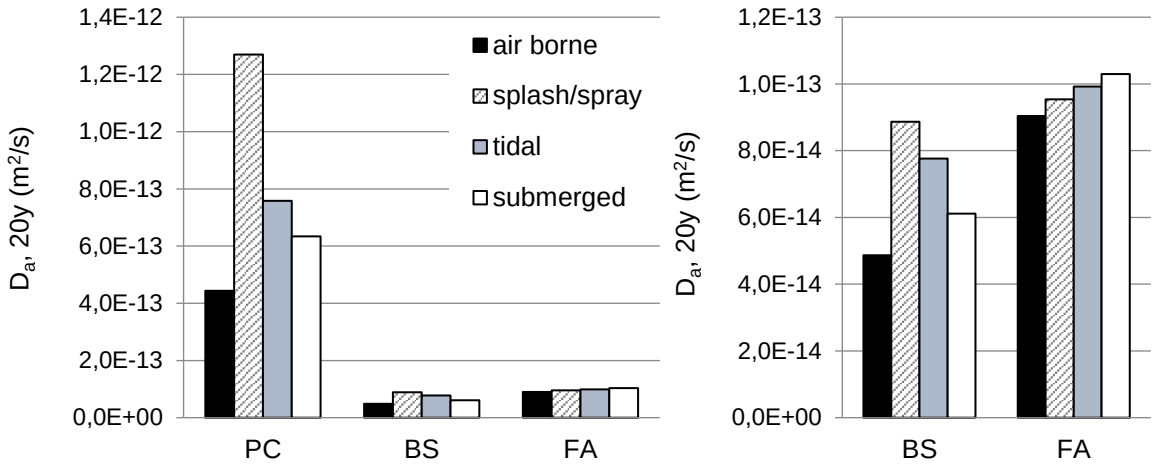

Figure 4.25: The influence of binder type on the predicted D_a values at 20 years, for concretes with w/b = 0.40 (the right-hand graph is an upscale from the left graph, for BS and FA concrete) (Durban)

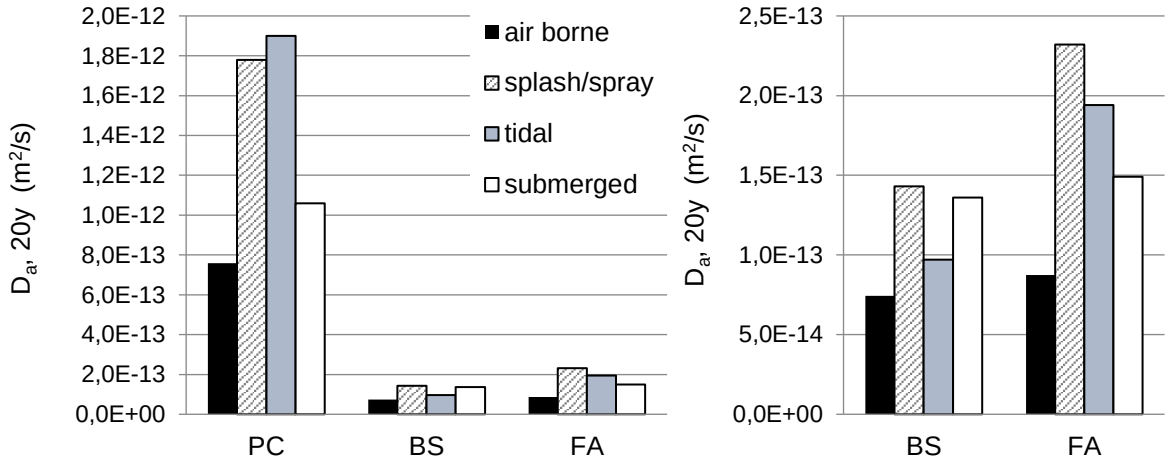

Figure 4.26: The influence of binder type on the predicted D_a values at 20 years, for concretes with w/b = 0.60 (the right-hand graph is an upscale from the left graph, for BS and FA concrete) (Durban)

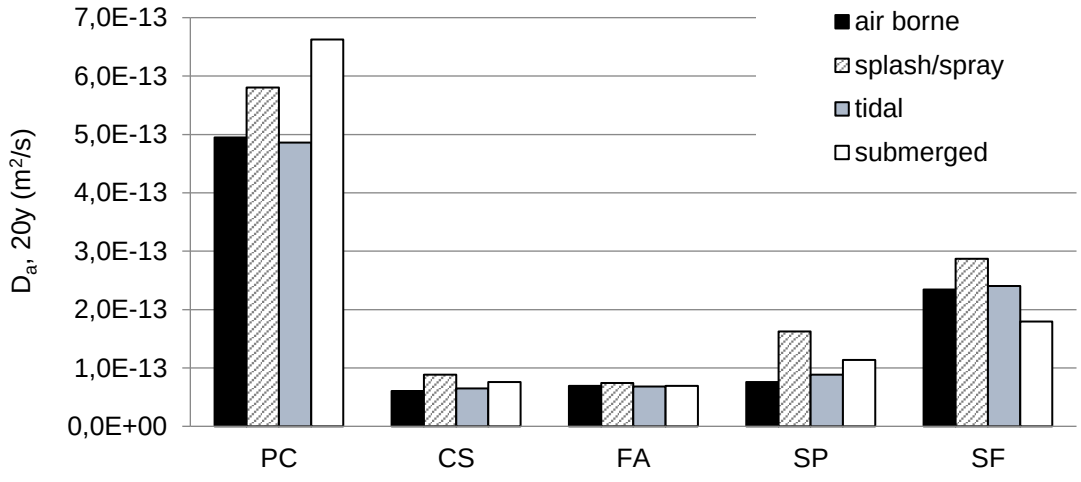

Figure 4.27: The influence of binder type on the predicted D_a values at 20 years, for concretes with w/b = 0.40 (Cape Town)

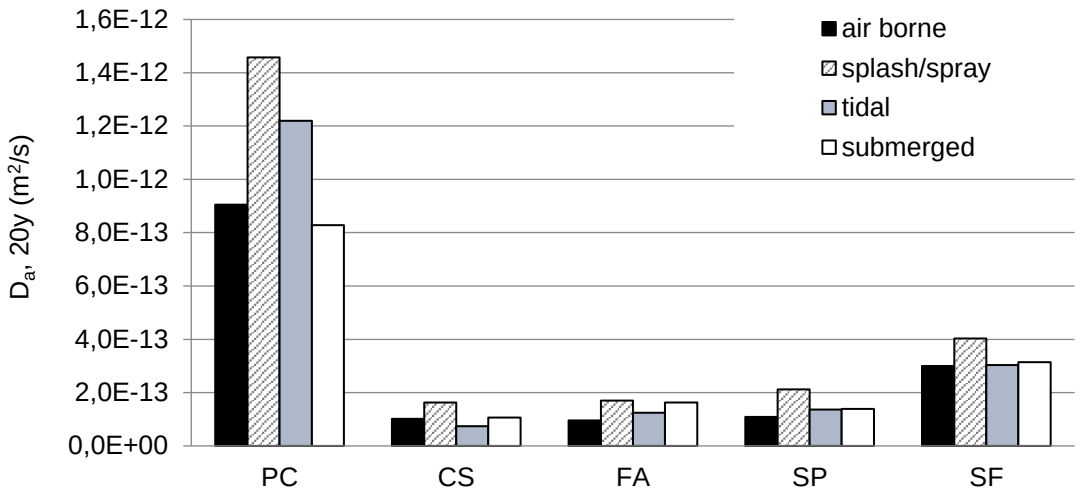

Figure 4.28: The influence of binder type on the predicted D_a values at 20 years, for concretes with w/b = 0.60 (Cape Town)

4.3.9 Influence of w/b ratio on D_a

To determine the influence of w/b ratio on the diffusion coefficient, the ratio between D_a values obtained for w/b = 0.6 and w/b = 0.4 was calculated (again using 20 years exposure time as the reference), as shown in Figures 4.29 and 4.30. The exposure condition had no clear influence on the ratio between $D_{a,20y,0.6}$ and $D_{a,20y,0.4}$, with values ranging seemingly randomly between 1.0 and 2.5 for the various binder types. Calculating the average ratio between diffusion coefficients obtained for the two w/b ratios for all exposure conditions yields the following results:

- PC concrete, Durban: $D_{a,20y,0.6}$ / $D_{a,20y\ 0.4}$, average = 1.8 (1 STDV 0.5)
- BS concrete, Durban: $D_{a,20y,0.6}$ / $D_{a,20y\ 0.4}$, average = 1.7 (1 STDV 0.4)
- FA concrete, Durban: $D_{a,20y,0.6}$ / $D_{a,20y\ 0.4}$, average = 1.7 (1 STDV 0.6)
- PC concrete, Cape Town: $D_{a,20y,0.6}$ / $D_{a,20y\ 0.4}$, average = 2.0 (1 STDV 0.6)
- CS concrete, Cape Town: $D_{a,20y,0.6}$ / $D_{a,20y\ 0.4}$, average = 1.5 (1 STDV 0.3)
- FA concrete, Cape Town: $D_{a,20y,0.6}$ / $D_{a,20y\ 0.4}$, average = 2.0 (1 STDV 0.5)
- SP concrete, Cape Town: $D_{a,20y,0.6}$ / $D_{a,20y\ 0.4}$, average = 1.4 (1 STDV 0.1)
- SF concrete, Cape Town: $D_{a,20y,0.6}$ / $D_{a,20y\ 0.4}$, average = 1.4 (1 STDV 0.2)

In terms of the diffusion coefficient, the binder type had no apparent influence on how much “better” a concrete with lower water/binder ratio performs, as indicated by the above numbers. This is also illustrated by the very similar ‘m’ values (Tables 4.1 and 4.2) for any given binder type. The 20-year diffusion coefficient of concretes with w/b = 0.6 was on average roughly 1.7 times higher, compared to concretes with w/b = 0.4, with no clear trend related to binder type. The influence of w/b ratio on actual chloride ingress needs to be evaluated under consideration of the chloride surface concentration, as discussed in Chapter 5.

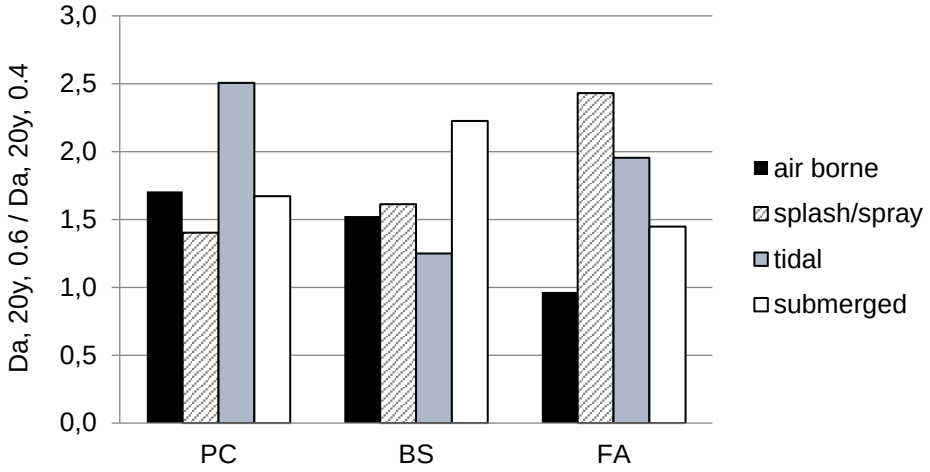

Figure 4.29: Influence of w/b ratio on the apparent diffusion coefficient $D_{a,20y}$ (Durban)

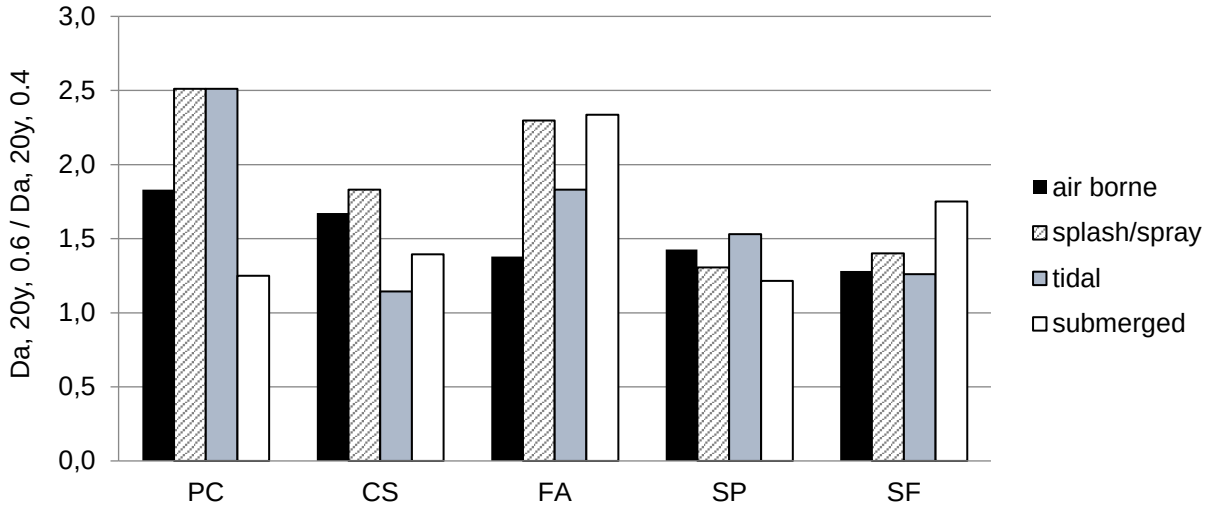

Figure 4.30: Influence of w/b ratio on the apparent diffusion coefficient $D_{a,20y}$ (Cape Town)

4.3.10 Influence of environmental exposure on D_a

Figures 4.31 – 4.33 show a comparison of $D_{a,20y}$ values obtained in relation to the exposure environment. The lowest diffusion coefficients were generally obtained for airborne exposure. With respect to the other 3 exposure classes, no consistent trend was observed.

In literature, as discussed in Chapter 2, the diffusion coefficient is generally considered a material parameter independent of environmental exposure, i.e. the diffusion coefficient is constant across different exposure classes. Consequently, the different chloride ingress behaviour resulting from different exposure conditions is a result only of the different chloride surface concentrations, as well as temperature, other transport mechanisms, binding, etc. The data obtained indicates that this may be an over-simplification that needs further consideration, as generally lower diffusion coefficients in the air-borne and submerged zones were established, compared to splash/spray and tidal exposure zones.

Overall, across all samples tested in Cape Town and Durban, no consistent trend with regard to the influence of environmental exposure condition on chloride diffusion coefficient could be

established. Consequently, for the modelling of chloride ingress into concrete, the assumption that the diffusion coefficient is a sufficiently inherent material parameter independent of the environmental exposure condition appears to be reasonable, despite the seemingly slightly lower and higher values for D_a in the air borne and splash/spray zones, respectively. Further research would be required to establish whether there is in fact a statistically significant difference in diffusion coefficients in these different exposure zones.

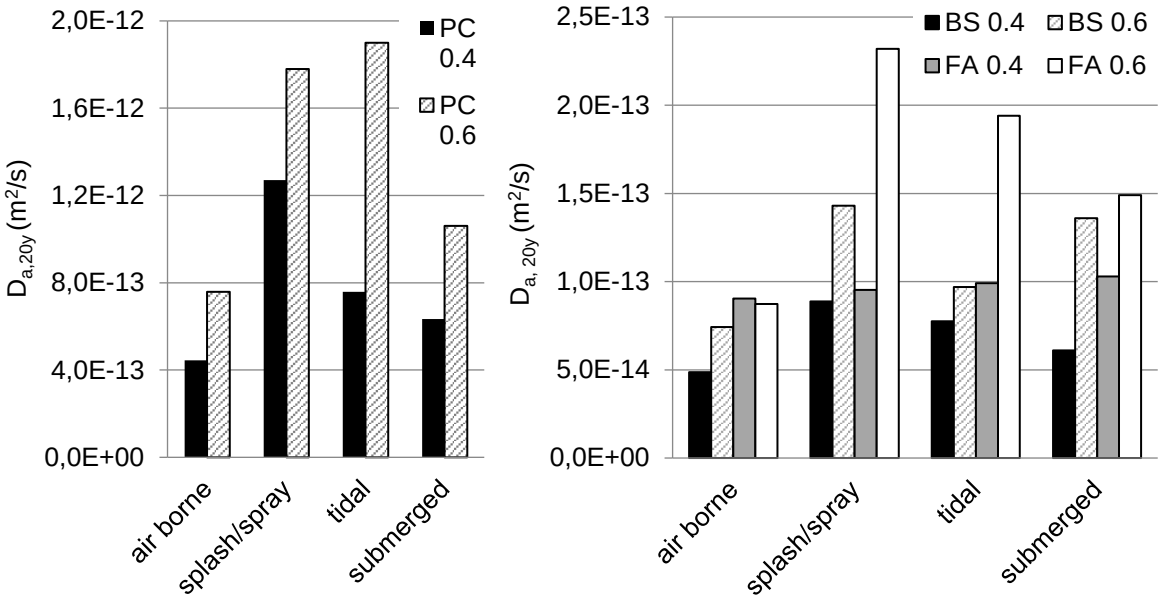

Figure 4.31: Influence of exposure condition on $D_{a,20y}$ (Durban)

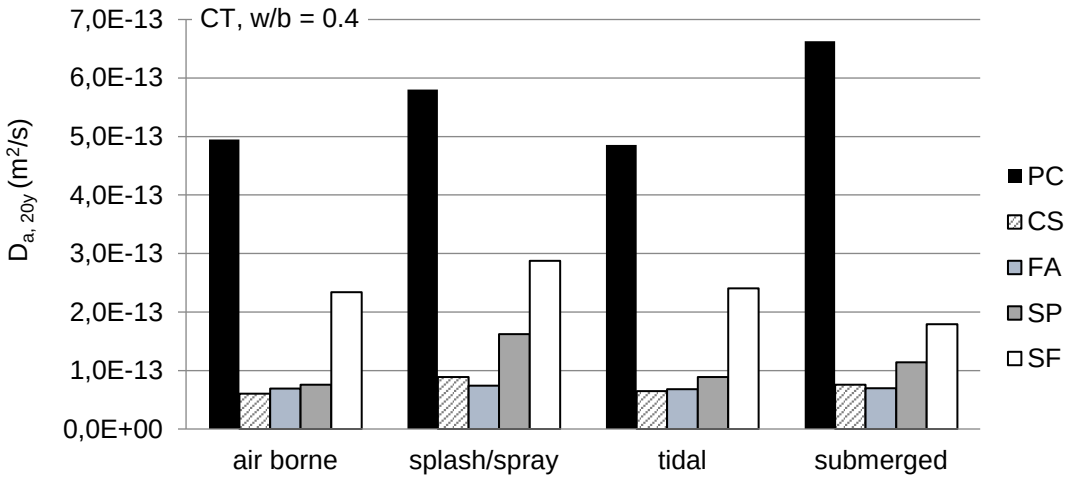

Figure 4.32: Influence of exposure condition on $D_{a,20y}$ (Cape Town, w/b = 0.4)

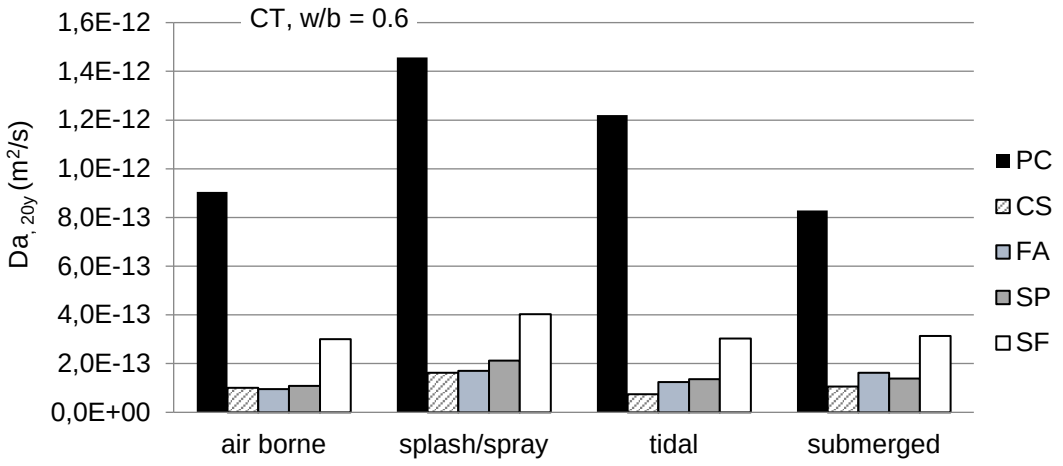

Figure 4.33: Influence of exposure condition on $D_{a,20y}$ (Cape Town, w/b = 0.6)

4.3.11 Chloride diffusion coefficients: Durban versus Cape Town

The previous section compared chloride ingress in the various exposure zones that differentiate between direct and indirect exposure to seawater. The results indicate that the exposure zones do not significantly influence the diffusion coefficients of the concrete. Consequently, for concrete exposed to various exposure zones in a certain ambient environment, diffusion coefficients can be considered a constant basic material characteristic. This is an important aspect to consider in chloride ingress modelling, where chloride profiles are usually predicted based on two parameters only, namely chloride surface concentrations and diffusion coefficients. The results discussed in the previous section indicate that the exposure zones influence chloride ingress mostly through their effect on chloride surface concentrations, while diffusion coefficients are not significantly affected. This aspect is discussed in more detail in sections to follow.

Samples in Durban and Cape Town had been exposed to the same range of exposure zones, but different ambient environmental conditions related to water and air temperatures, relative humidity, and salinity of sea water (compare Section 3.5.1). The only binder types that were used both in Durban and Cape Town exposure sites were PC and FA concretes. The comparison of diffusion coefficients calculated for samples exposed in Durban and Cape Town, for these two concretes, is shown in Figures 4.34 and 4.35. The results indicate that ambient exposure conditions have a significant effect on diffusion coefficients, especially in the exposure zones related to regular wetting and drying cycles, i.e. splash/spray and tidal zones. In these zones, diffusion coefficients obtained in Durban were notably higher that those obtained in Cape Town, for all 4 concretes (PC and FA concrete at 2 w/b ratios).

A detailed analysis of which ambient exposure characteristic is the most dominant influence on chloride diffusion coefficients in concrete was not within the scope of this research. However, assuming that samples directly exposed to seawater (tidal and splash/spray zones) in Durban and Cape Town probably have similar moisture conditions independent of ambient relative humidity, indicates that the ambient temperature may have been the dominating influence.

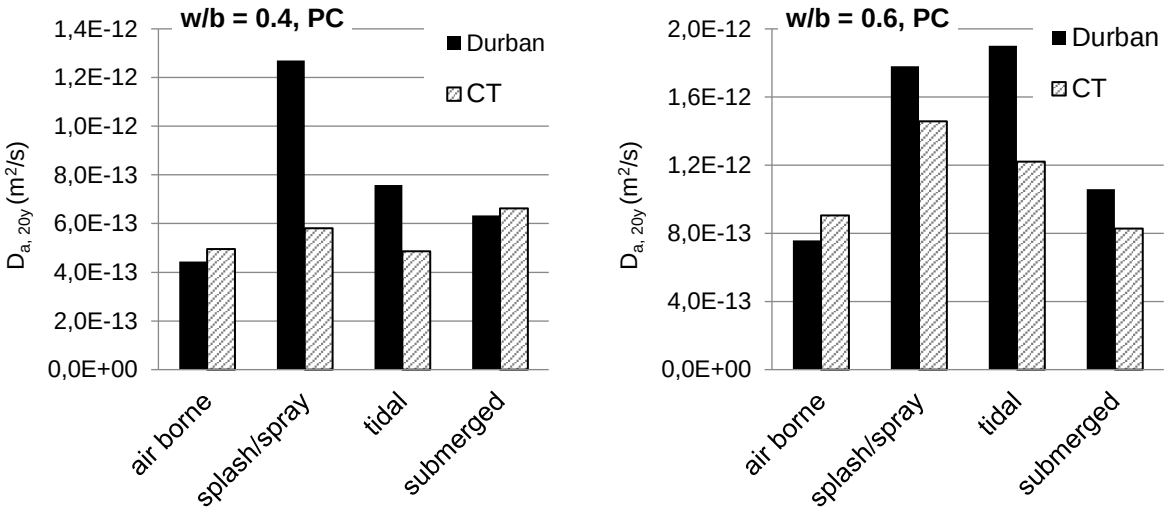

Figure 4.34: Comparison of $D_{a,20y}$ obtained in CT and Durban exposure zones, PC concrete

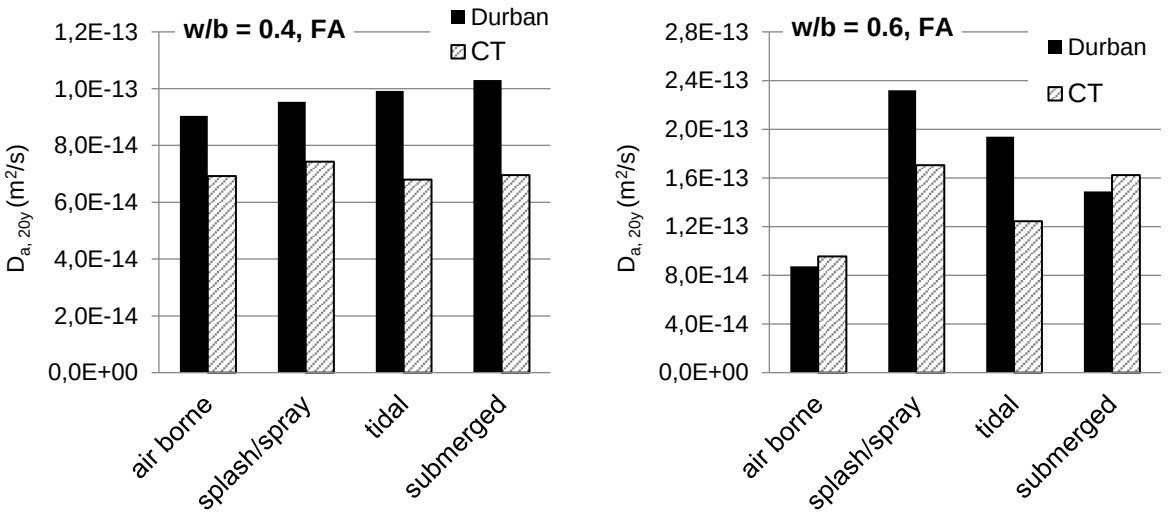

Figure 4.35: Comparison of $D_{a,20y}$ obtained in CT and Durban exposure zones, FA concrete

4.3.12 Chloride surface concentrations C_s, general considerations

In the modelling of chloride ingress into concrete using Fick's second law of diffusion, the chloride surface concentration C_s is as important a parameter as the chloride diffusion coefficient. The latter is a representation of the slope of the chloride profile, while the surface concentration determines the scaling of the chloride profile. For example, at a constant diffusion coefficient, doubling the chloride surface concentration results in twice as high chloride contents throughout the depth of the concrete (i.e. a scaling factor of 2).

While literature contains many discussions on chloride diffusion coefficients (time development, influencing parameters, etc.), very limited information is available with respect to parameters influencing C_s. In particular, very little or no information is available on the combined influence of exposure conditions and binder type on time-dependent chloride surface concentrations in concrete situated in the marine environment. The present experimental data, however, allows these aspects to be explored in this work.

This research produced data for the time development of both D_a and C_s with respect to various marine exposure conditions, binder types and w/b ratios. Considering the importance of C_s for the modelling of chloride ingress into concrete, the discussion on influencing parameters on C_s, which is presented in the following sections, is of a similar structure as the discussion on chloride diffusion coefficients in previous sections.

The actual surface concentration of the samples was measured as the average chloride concentration in the first 2 mm depth interval, as is common in the bulk diffusion test. In the regression analysis of chloride profiles, this first depth interval was omitted due to the 'bend over' effect, as discussed in Section 4.2.1. In the analysis of C_s values, it needs to be kept in mind therefore that extrapolated surface concentrations are a hypothetical construct resulting from the extrapolation of chloride profiles to the concrete surface, applying Fick's second law of diffusion to characterize the chloride profile (which assumes an exponential function); they are not referring to an 'actual' material parameter. As a result, high values of C_s can simply be an indication of a low diffusion coefficient (a low diffusion coefficient results in a steep chloride profile, which when extrapolated to the surface results in a high surface concentration).

Figure 4.36 illustrates the above considerations. The figure represents two typical chloride profiles in concrete, where the data points represent individual measurements and the exponential trend lines simulate the curve fitting using Fick's second law of diffusion. In the fictitious example, both profiles have the same concentration at the first depth increment of 3 mm (indicated by the round marker). The curve termed "Case 1" relates to a higher diffusion coefficient, indicated by the less steep profile, compared to the curve termed "Case 2". When the exponential trend line is extrapolated to the y-axis (i.e. the "surface"), a higher surface concentration is predicted for the concrete that has a lower diffusion coefficient ("Case 2").

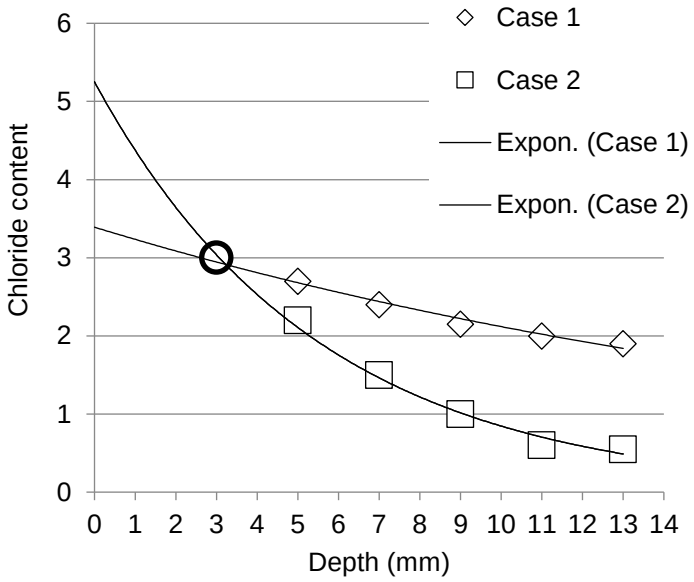

Figure 4.36: Illustration of the effect of different diffusion coefficients on extrapolated values for C_s

It would therefore be misleading to consider C_s as an actual material parameter. It can merely be considered a parameter in the modelling of chloride profiles, at least if it is calculated on the basis of extrapolation of experimental results to the y-axis of the chloride ingress profile, as done in this research. Nonetheless, the discussion in the following sections is based on the extrapolated values of C_s, as these are the values that will later be used in the service life model (Chapter 5).

A more realistic picture of chloride contents in the surface region is obtained when measured chloride concentrations at 3.5 mm depth are considered. The discussion on measured chloride concentrations is included in the following sections as this was considered to add clarity to chloride ingress characteristics.

4.3.13 Time development and magnitude of C_s (Durban)

The measured time-dependent development of the (extrapolated) chloride surface concentration C_s is as shown in Figures 4.37 to 4.41 (Durban samples). The figures compare values obtained for concretes with consistent w/b ratio but different binder types and for specimens exposed to the same environmental condition. In Figures 4.38 to 4.41, the measurements (C_s versus time) are presented on a log-log curve and trend lines are fitted using the automatic trend line function in MS Excel. The trend lines, which are linear on a log-log scale, are of the power type. For illustration purposes, Figure 4.37 presents the "real" time-development of C_s on a natural scale, using air borne exposure as an example.

Concrete made with plain CEM I had consistently lower extrapolated surface concentrations, compared to FA and BS concretes. The surface concentrations of BS and FA concretes were very similar, as indicated by the close proximity of the respective trend lines.

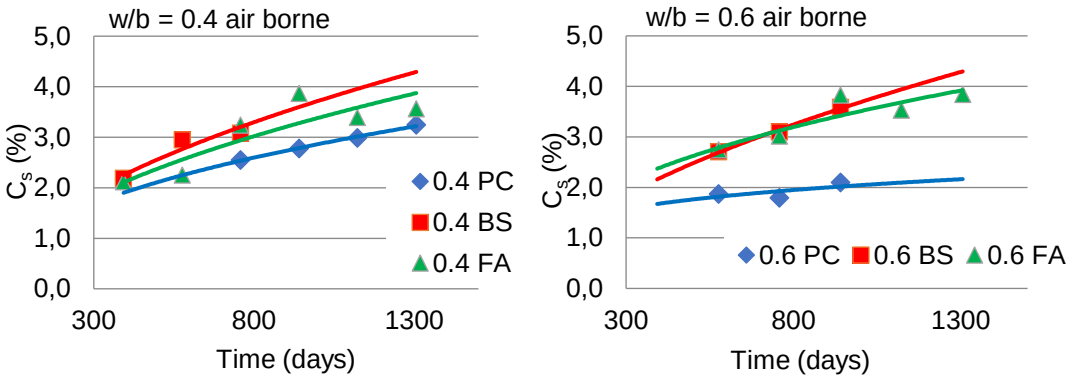

Figure 4.37: Time-dependent variation of C_s (natural scale), Durban, air-borne

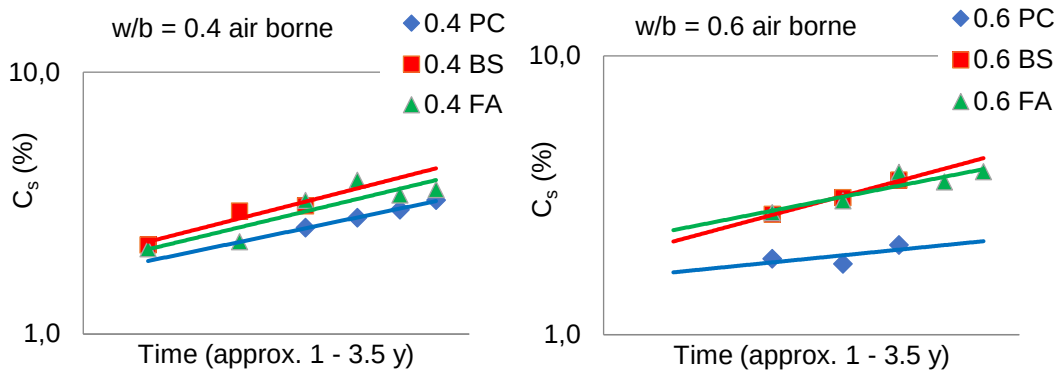

Figure 4.38: Time-dependent variation of C_s (log-log scale), Durban, air-borne

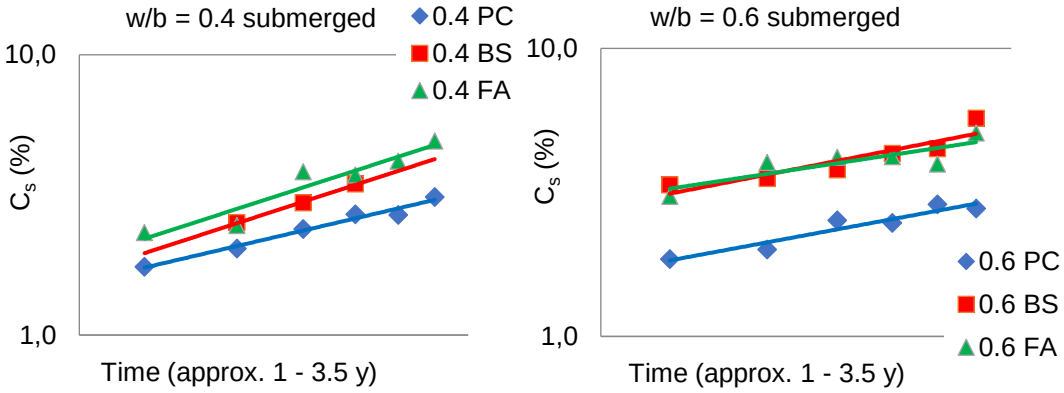

Figure 4.39: Time-dependent variation of C_s (log-log scale), Durban, submerged

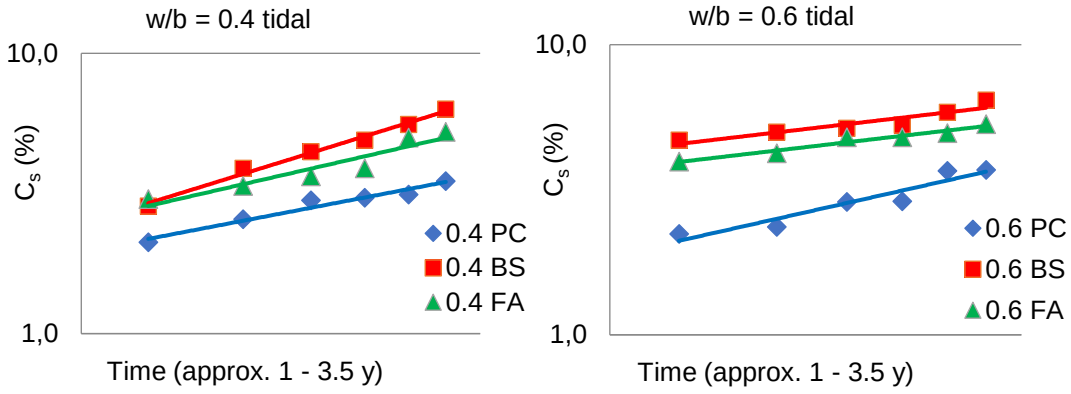

Figure 4.40: Time-dependent variation of C_s (log-log scale), Durban, tidal

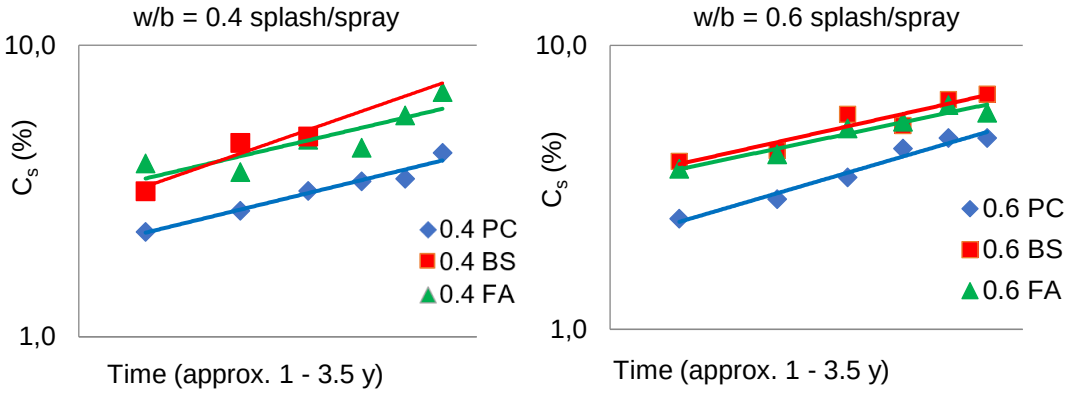

Figure 4.41: Time-dependent variation of C_s (log-log scale), Durban, splash/spray

To evaluate how well the trend lines for the time-development of C_s fit the experimental measurements, linear regression analysis was carried out and the R^2 value computed (using the automatic functions provided in MS Excel). The exponents of the power-type trend line equations signify the n-values and hence the time-development of C_s. Table 4.3 contains a summary of the trend line equations, R^2 values, and n-values for all parameter combinations. The table also contains extrapolated C_s values for the following ages:

- 2 years (to compare measured and predicted chloride concentrations)
- 20 years, representing $C_{s,20y}$ which was later used as a realistic alternative in service life modelling for blended cement concretes (as discussed in Chapter 5)

The n-value ranged from 0.15 to 0.68 for the different concrete types and exposure conditions. No clear correlation was observed between exposure condition and n-value, with minimum and maximum n-values for the different concretes relating randomly to different environments. To compare the change in C_s with time for the various concretes, n-values were averaged for all exposure conditions of the respective concretes, as shown in Figure 4.42 (left). Also shown in Figure 4.42 (on the right) is the correlation between chloride surface concentrations predicted for 20 years and 2 years.

Considering the generally large scatter in n-values across all different environments (see Figure 4.42), it must be understood that the comparisons presented in Figure 4.42 are for illustration purposes only. Nonetheless, it can be observed from the figures that the blended concretes with a low w/b ratio (i.e. FA and BS concretes with w/b = 0.4) have the highest n-value, which corresponds to the largest change in C_s over time. The other concretes had n-values of around 0.4, resulting in an increase in chloride surface concentrations from 2 to 20 years of roughly 100-200%. Intuitively, this magnitude of the increase in C_s seems realistic.

However, the actual values for C_s are unrealistically high, especially at later ages (Table 4.3). After 2 years of exposure, predicted values exceed 6% by mass of cement for some of the concretes, which already is unrealistic. After 20 years of exposure, the modelled predicted chloride concentrations are commonly as high as 10% by mass of cement, or more, which seems not representative of actual chloride ingress into concrete. This again highlights the fact that predicted chloride surface concentrations (based on extrapolation of the chloride profile to the concrete surface) are a theoretical construct that facilitates the modelling of chloride ingress into the concrete, but not a representation of actual values, as discussed earlier.

Table 4.3: Time development of (extrapolated) chloride surface concentrations, Durban

Mix	Exposure	Cs (t)	R^2	n-value	$C_{S,\ 2y}$	$C_{S,\ 20y}$
0.4 PC	air borne	$0.138t^{0.438}$	0,87	0,44	3,17	6,79
	splash/spray	$0.133t^{0.474}$	0,96	0,47	3,95	9,02
	tidal	$0.212t^{0.389}$	0,96	0,39	3,43	6,75
	submerged	$0.109t^{0.463}$	0,98	0,46	2,99	6,70
0.6 PC	air borne	$0.72t^{0.154}$	0,40	0,15	2,17	2,83
	splash/spray	$0.063t^{0.607}$	0,97	0,61	4,84	13,94
	tidal	$0.137t^{0.457}$	0,91	0,46	3,60	7,98
	submerged	$0.191t^{0.378}$	0,91	0,38	2,85	5,51
0.4 BS	air borne	$0.09t^{0.537}$	0,91	0,54	4,19	10,69
	splash/spray	$0.056t^{0.679}$	0,90	0,68	7,20	23,52
	tidal	$0.067t^{0.629}$	0,98	0,63	6,03	18,03
	submerged	$0.042t^{0.643}$	1,00	0,64	4,18	12,80
0.6 BS	air borne	$0.21t^{0.426}$	0,99	0,43	4,42	9,29
	splash/spray	$0.235t^{0.466}$	0,90	0,47	6,59	14,84
	tidal	$1.092t^{0.238}$	0,86	0,24	5,99	9,07
	submerged	$0.288t^{0.398}$	0,84	0,40	4,96	9,93
0.4 FA	air borne	$0.101t^{0.507}$	0,80	0,51	3,80	9,18
	splash/spray	$0.225t^{0.458}$	0,74	0,46	5,96	13,23
	tidal	$0.175t^{0.467}$	0,90	0,47	4,94	11,15
	submerged	$0.047t^{0.641}$	0,91	0,64	4,61	14,08
0.6 FA	air borne	$y=0.244x^{0.401}$	0,86	0,40	4,30	8,64
	splash/spray	$y=0.27x^{0.436}$	0,94	0,44	6,11	13,05
	tidal	$y=0.953x^{0.237}$	0,95	0,24	5,19	7,85
	submerged	$y=0.511x^{0.31}$	0,72	0,31	4,69	8,05

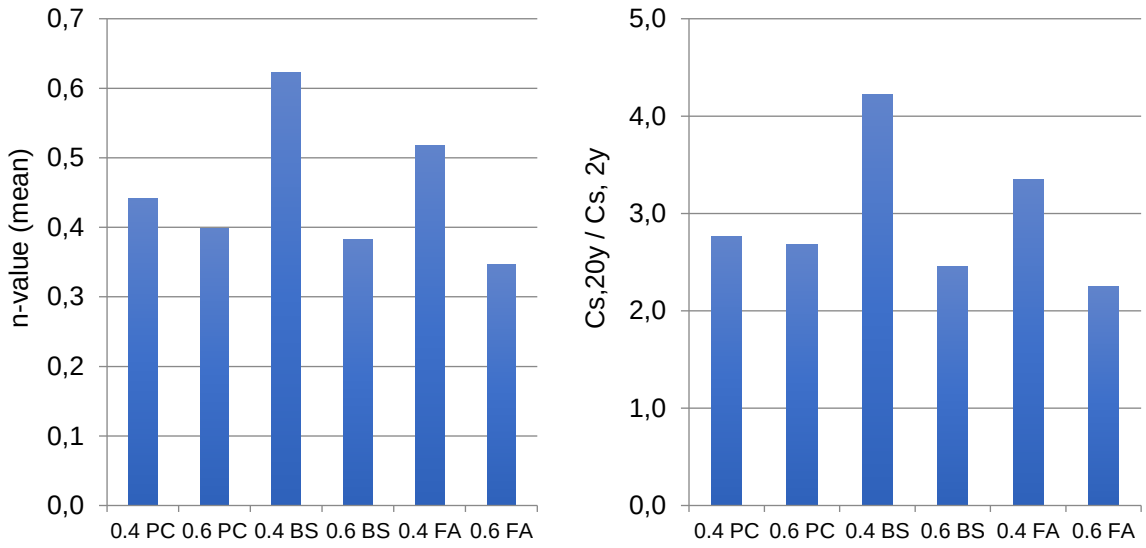

Figure 4.42: Time development of C_s (left: n-value, right: $C_{s,\ 20y}$ / $C_{s,\ 2y}$), mean values for all exposure conditions Durban

4.3.14 Time development and magnitude of C_s (Cape Town)

The time-dependent development of (extrapolated) chloride surface concentrations C_s measured on the Cape Town samples is shown in Figures 4.43 to 4.46.

As already observed on the Durban samples, concrete made with plain CEM I had consistently lower predicted surface concentrations, compared to concretes made with blended cements. The surface concentrations of the concretes made with blended cements were generally similar, as indicated by the close proximity of the respective trend lines.

Similar to Table 4.3 (Durban samples), Table 4.4 contains a summary of the trend line equations, R^2 values, n-values, and extrapolated C_s values for the ages of 2 and 20 years. The n-value ranged from 0.35 to 0.66 for the different concrete types and exposure conditions.

For the Durban samples, no clear correlation was observed between exposure condition and n-value, with minimum and maximum n-values for the different concretes relating randomly to different environments, as discussed in Section 4.3.13. However, interestingly, for the Cape Town samples, a clear trend was observed, with n-values being consistently higher for air borne and submerged exposure zones, compared to splash/spray and tidal zones. This is further discussed in a later section.

To judge the development of n-values over time, n-values were averaged for all exposure conditions for the respective concretes, as shown in Figure 4.47. It is interesting to note that the Durban samples (compare Figure 4.42) showed a larger range of average n-values whereas the average n-values for the Cape Town samples generally ranged from 0.4 – 0.5. For the Cape Town samples, no clear trend with regards to the influence of concrete type on n-value could be established, except that the concrete made with SP and SF showed a slightly lower n-value compared to the other concretes.

The predicted increase in chloride surface concentrations between 2 years and 20 years was about 100% - 150%, as shown in Figure 4.48.

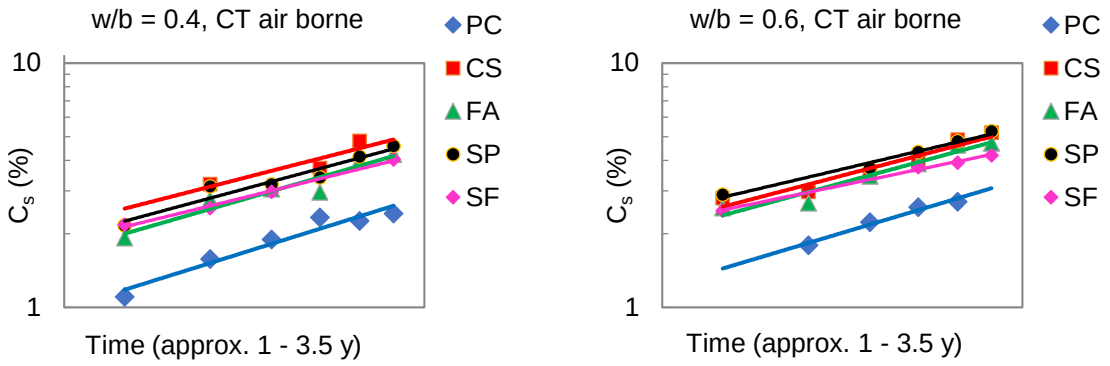

Figure 4.43: Time-dependent variation of C_s (log-log scale), Cape Town, airborne

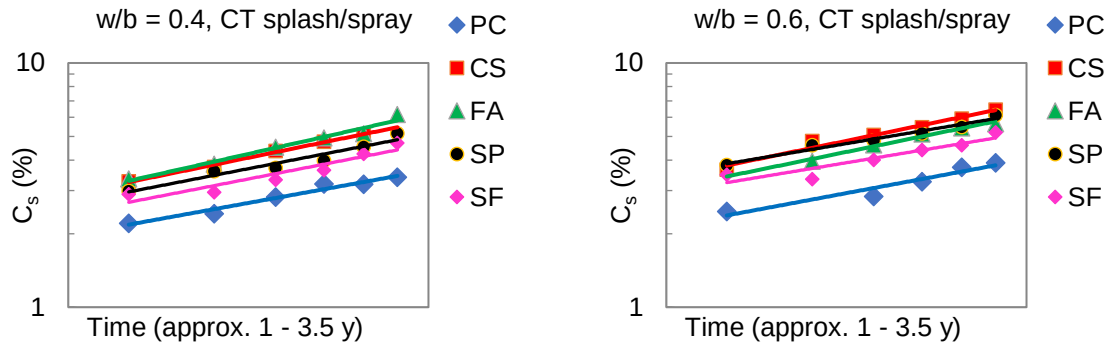

Figure 4.44: Time-dependent variation of C_s (log-log scale), Cape Town, splash/spray

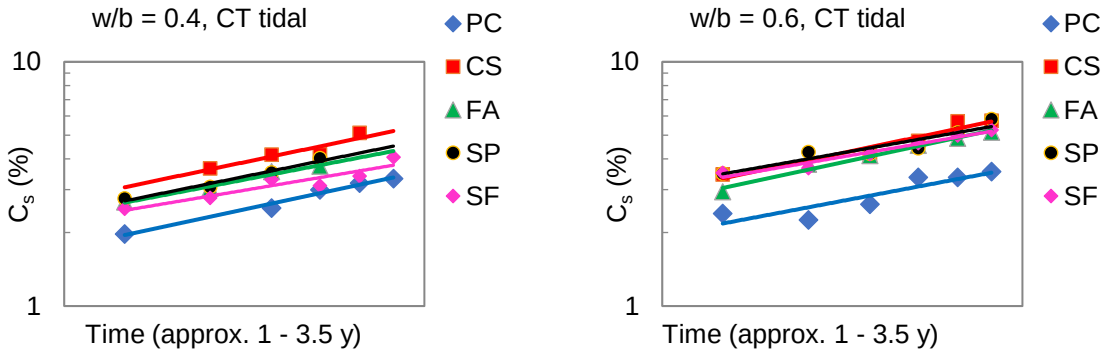

Figure 4.45: Time-dependent variation of C_s (log-log scale), Cape Town, tidal

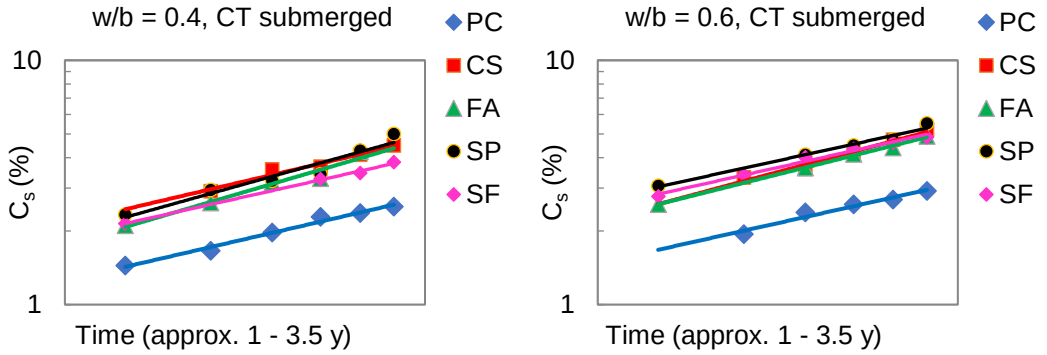

Figure 4.46: Time-dependent variation of C_s (log-log scale), Cape Town, submerged

Table 4.4: Time development of (extrapolated) chloride surface concentrations, Cape Town

Mix	Exposure condition	Cs (t)	R^2	n value	$C_{S,\ 2y}$	$C_{S,\ 20y}$
0.4 PC	air borne	$0.023\ t^{0.658}$	0.94	0.66	2.2	8.0
	splash/spray	$0.221\ t^{0.382}$	0.97	0.38	4.2	6.6
	tidal	$0.132\ t^{0.45}$	0.98	0.45	3.8	7.2
	submerged	$0.077\ t^{0.488}$	0.98	0.49	2.7	5.9
0.6 PC	air borne	$0.033\ t^{0.63}$	0.90	0.63	2.7	9.0
	splash/spray	$0.190\ t^{0.418}$	0.95	0.42	4.5	7.8
	tidal	$0.226\ t^{0.393}$	0.96	0.39	4.6	7.5
	submerged	$0.100\ t^{0.47}$	0.98	0.47	3.2	6.5
0.4 CS	air borne	$0.099\ t^{0.542}$	0.84	0.54	4.8	12.3
	splash/spray	$0.247\ t^{0.431}$	0.97	0.43	6.3	11.4
	tidal	$0.219\ t^{0.441}$	0.86	0.44	5.9	11.1
	submerged	$0.059\ t^{0.59}$	0.96	0.59	3.8	11.2
0.6 CS	air borne	$0.096\ t^{0.551}$	0.93	0.55	5.0	12.9
	splash/spray	$0.282\ t^{0.435}$	0.97	0.44	7.3	13.5
	tidal	$0.233\ t^{0.445}$	0.93	0.45	6.4	12.2
	submerged	$0.087\ t^{0.566}$	0.97	0.57	4.9	13.4
0.4 FA	air borne	$0.052\ t^{0.609}$	0.92	0.61	3.8	11.7
	splash/spray	$0.192\ t^{0.475}$	0.97	0.48	6.3	13.1
	tidal	$0.236\ t^{0.404}$	0.98	0.40	5.1	8.6
	submerged	$0.051\ t^{0.617}$	0.96	0.62	3.9	12.3
0.6 FA	air borne	$0.077\ t^{0.573}$	0.94	0.57	4.5	12.6
	splash/spray	$0.258\ t^{0.432}$	0.98	0.43	6.6	12.0
	tidal	$0.205\ t^{0.451}$	0.98	0.45	5.9	11.3
	submerged	$0.110\ t^{0.527}$	0.99	0.53	4.9	11.9
0.4 SP	air borne	$0.076\ t^{0.567}$	0.93	0.57	4.3	11.8
	splash/spray	$0.256\ t^{0.409}$	0.94	0.41	5.7	9.7
	tidal	$0.206\ t^{0.43}$	0.97	0.43	5.2	9.4
	submerged	$0.068\ t^{0.587}$	0.94	0.59	4.3	12.6
0.6 SP	air borne	$0.145\ t^{0.496}$	0.98	0.50	5.4	12.0
	splash/spray	$0.465\ t^{0.354}$	0.97	0.35	7.5	10.8
	tidal	$0.377\ t^{0.371}$	0.88	0.37	6.7	10.2
	submerged	$0.193\ t^{0.460}$	0.98	0.46	5.8	11.6
0.4 SF	air borne	$0.096\ t^{0.518}$	0.99	0.52	4.1	9.6
	splash/spray	$0.230\ t^{0.411}$	0.98	0.41	5.2	8.9
	tidal	$0.296\ t^{0.354}$	0.88	0.35	4.8	6.9
	submerged	$0.128\ t^{0.471}$	0.99	0.47	4.1	8.4
0.6 SF	air borne	$0.185\ t^{0.435}$	0.88	0.44	4.8	8.9
	splash/spray	$0.398\ t^{0.35}$	0.87	0.35	6.3	9.0
	tidal	$0.386\ t^{0.362}$	0.96	0.36	6.5	9.7
	submerged	$0.170\ t^{0.0.47}$	0.99	0.47	5.4	11.1

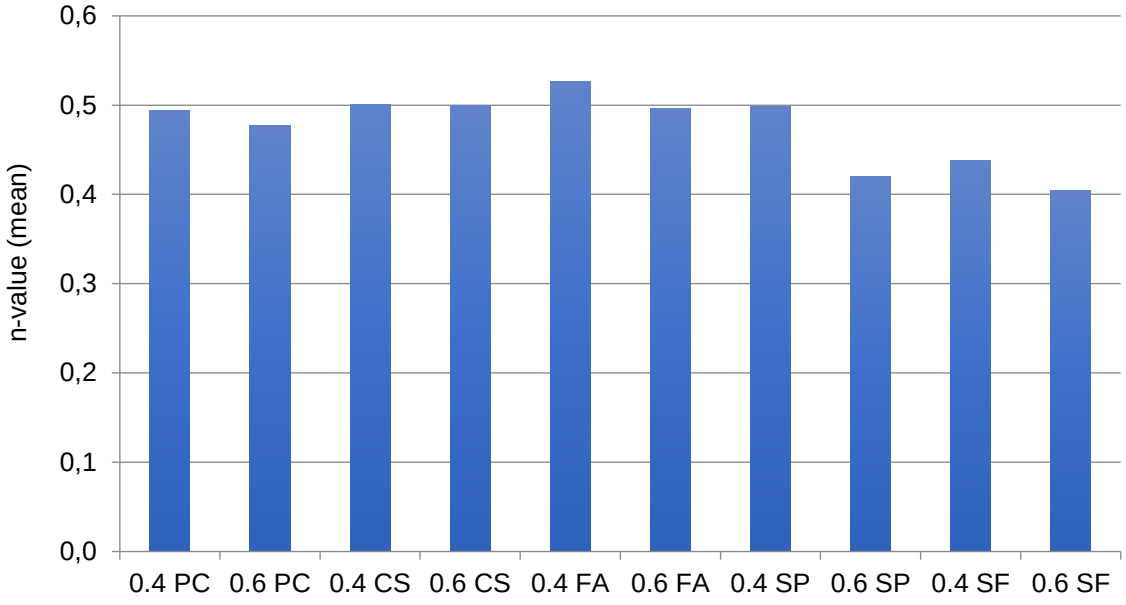

Figure 4.47: Time development of chloride surface concentration, n-value, mean values for all exposure conditions, Cape Town

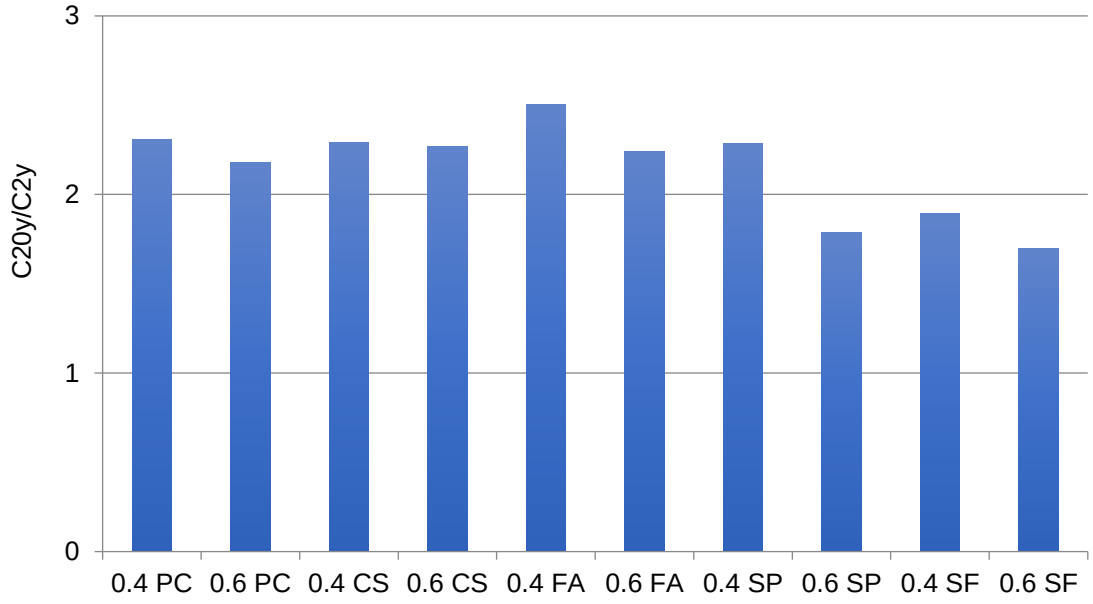

Figure 4.48: Time development of chloride surface concentration, $C_{s,}$ 20y/$Cs_{,2y}$, mean values for all exposure conditions, Cape Town

4.3.15 Influence of w/b ratio, binder type and exposure on measured C_s (Durban)

To determine the influence of various parameters on chloride surface concentrations, measured values for chloride concentrations are considered first. Since the first depth increment of the measurements (1 – 2 mm depth) was not included in the analysis (see Section 4.2.1), measurements from the second depth increment are used (2 – 5 mm, with a mean depth of 3.5 mm). This near-surface chloride concentration is considered to give a good indication on factors influencing chloride surface concentrations. Figure 4.49 shows chloride concentrations at 3.5

mm depth after approximately 2 years of exposure in relation to binder type, w/b ratio and environmental exposure. The period of 2 years was chosen as this was the last exposure age at which samples from all concrete types and exposure conditions were available (afterwards, some samples were lost in Durban, as discussed at the beginning of Section 4.3).

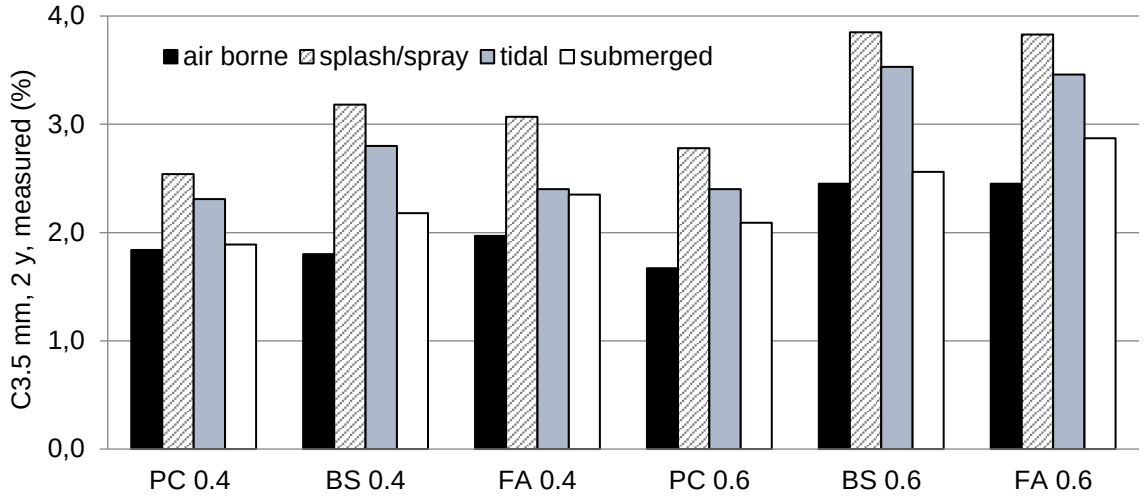

Figure 4.49: Chloride concentrations measured at 3.5 mm depth (average) after 2 years in Durban

The test results show a clear trend with regard to the influence of environmental exposure condition on chloride surface concentrations. For all concretes, the highest values were measured in the splash/zone, followed by the tidal, submerged and air borne zones. Higher chloride concentrations were generally measured in concretes with higher w/b ratios (about 25-30% higher in FA and BS concrete with w/b = 0.6, compared to w/b = 0.4, on average across all exposure zones), although this trend was not very pronounced for PC concrete (only 5% difference). Comparing the influence of binder type showed that PC concretes had the lowest chloride surface concentrations. No practical difference was observed between the BS and FA concretes.

Compared to actual values measured at 3.5 mm depth, the predicted values for C_s after 2 years of exposure (Figure 4.50) show similar trends with respect to the influence of binder type. Similarly, the rating of the severity of the exposure zones was the same for both predicted and measured values. However, the influence of w/b ratio is not as pronounced for the predicted values of C_s (only 15-20% difference between w/b ratios of 0.4 and 0.6 for BS and FA concrete and no difference for PC concrete, on average from all 4 exposure zones).

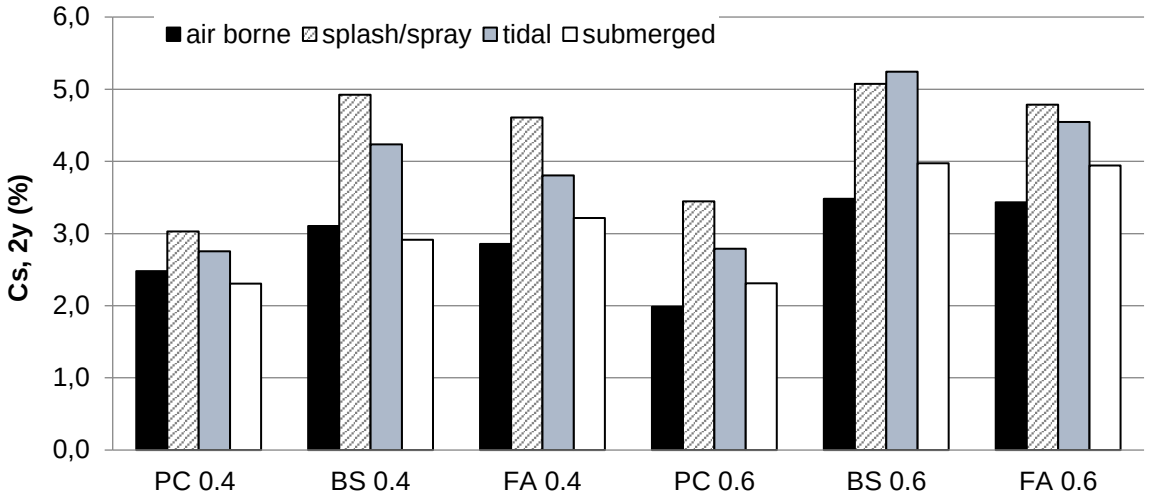

Figure 4.50: Chloride surface concentrations predicted for 2 years of exposure in Durban

The difficulties and inaccuracies in modelling long-term chloride surface concentrations based on regression analysis of short-term chloride profiles as done in this research, is evident from Figure 4.51. The figure shows the predicted values for C_s after 20 years of exposure. It is immediately obvious that the magnitude of chloride concentrations is unrealistically high. It is also interesting to note that while predicted values of C_s for 2 years showed similar trends with respect to the influence of w/b ratio, binder type and exposure class, compared to actually measured values (at 3.5 mm depth), this is not the case for predicted values at 20 years. For example, the influence of the exposure class is not as clear or as pronounced as it is for the 2-year values. Similarly, the influence of binder type seems somewhat skewed, with BS concrete having significantly higher C_s values compared to FA concrete, especially at a w/b ratio of 0.4, while the 2 binders perform very similarly at younger ages. The most obvious discrepancy is seen when values for concretes with different w/b ratio are compared. Actual measurements (and also predicted values) after 2 years of exposure show the expected trend of higher chloride concentrations in concrete with higher w/b ratio. However, the values predicted for 20 years of exposure show the opposite trend, with significantly higher values for C_s in concretes with a lower w/b ratio. This trend makes little sense from a concrete technology perspective but is linked to the nature of the time-dependent modelling.

As stated earlier, values of C_s are a construct of the diffusion coefficient (i.e. the slope of the predicted chloride profile). It was shown in Section 4.3.2 that the diffusion coefficient decreases with time, especially for blended cement concretes, which corresponds to an increasingly steeper chloride profile. This consequently results in a comparatively higher increase in C_s in concretes with lower diffusion coefficients, compared to concretes with higher diffusion coefficients. Hence, C_s in concretes with lower w/b ratios eventually "overtakes" C_s in concretes with higher w/b ratios. It is therefore important to again stress that predicted values for C_s are hypothetical and only to be used in combination with predicted diffusion coefficients in the modelling of chloride ingress. However, they do not resemble actual chloride surface concentrations in concrete.

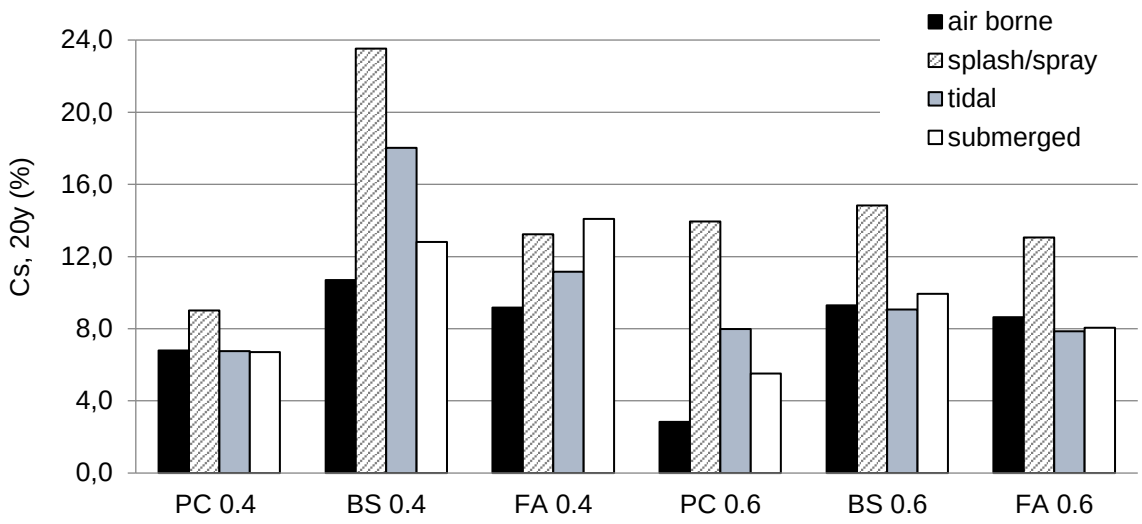

Figure 4.51: Chloride surface concentrations predicted for 20 years of exposure in Durban

4.3.16 Influence of w/b ratio, binder type and exposure on C_s (Cape Town)

Figures 4.52 and 4.53 show measured chloride concentrations at 3.5 mm depth after approximately 2 years of exposure in Cape Town, for w/b ratios of 0.4 and 0.6, respectively. The figures confirm the same trends already discussed in the previous section for the Durban samples. The highest values were measured in the splash/spray zone, followed by the tidal, submerged and air borne zones. Concretes with a higher w/b ratio of 0.6 had about 30% higher values compared to concrete with w/b = 0.4. This was observed for all binder types. Further, PC concretes had the lowest chloride surface concentrations at typically below 2% while surface concentrations for concretes containing other binder types typically ranging between 2 and 3%.

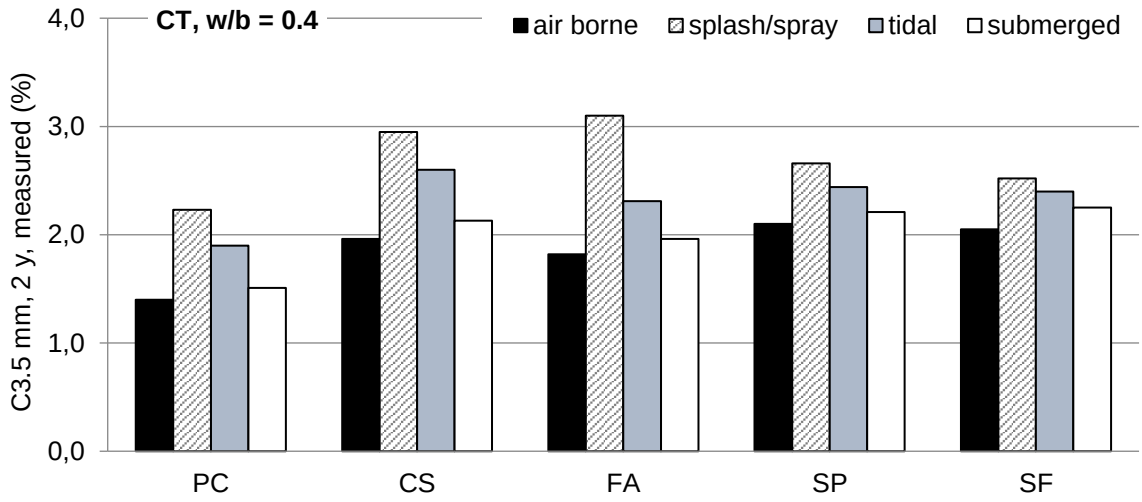

Figure 4.52: Chloride concentrations measured in 3.5 mm depth (average) after 2 years of exposure in Cape Town (w/b = 0.4)

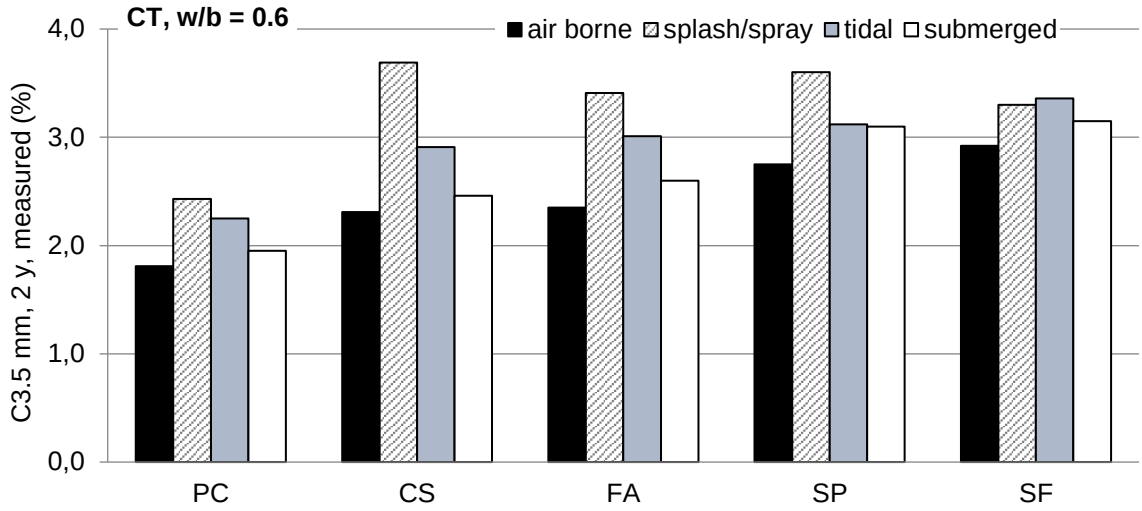

Figure 4.53: Chloride concentrations measured in 3.5 mm depth (average) after 2 years of exposure in Cape Town (w/b = 0.6)

4.3.17 Chloride surface concentrations in Durban versus Cape Town

The difference in near-surface chloride concentrations measured after roughly 2 years (576 days) in Durban and Cape Town is shown in Figures 4.54 and 4.55, for PC and FA concretes, respectively. The results indicate that surface concentrations can generally be expected to be higher in Durban. Similar to what was discussed in Section 4.3.11, this can be ascribed mainly to the higher ambient temperatures in Durban.

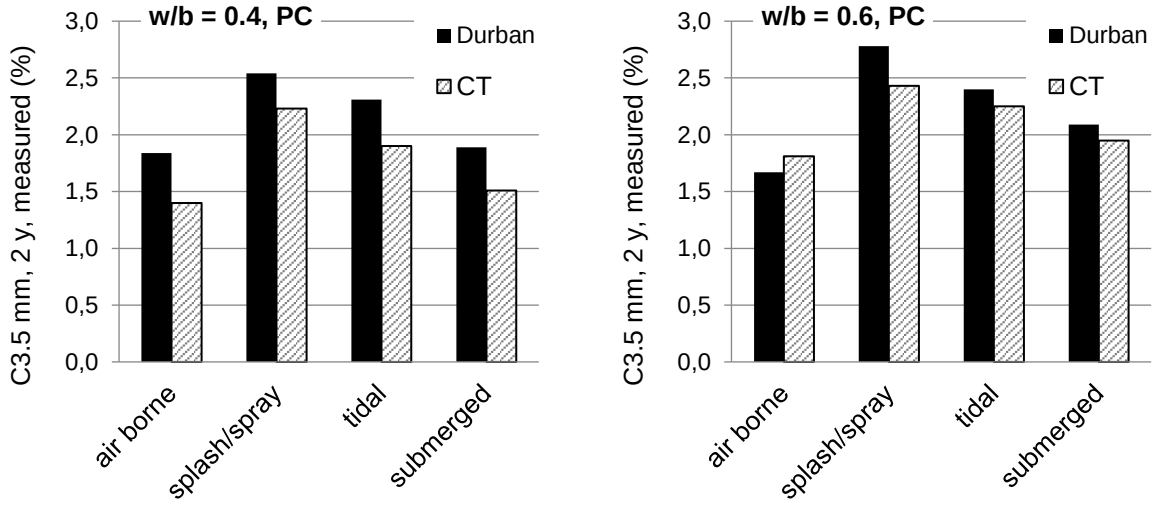

Figure 4.54: Comparison of chloride surface concentrations measured after 2 years in Durban and Cape Town, PC concrete

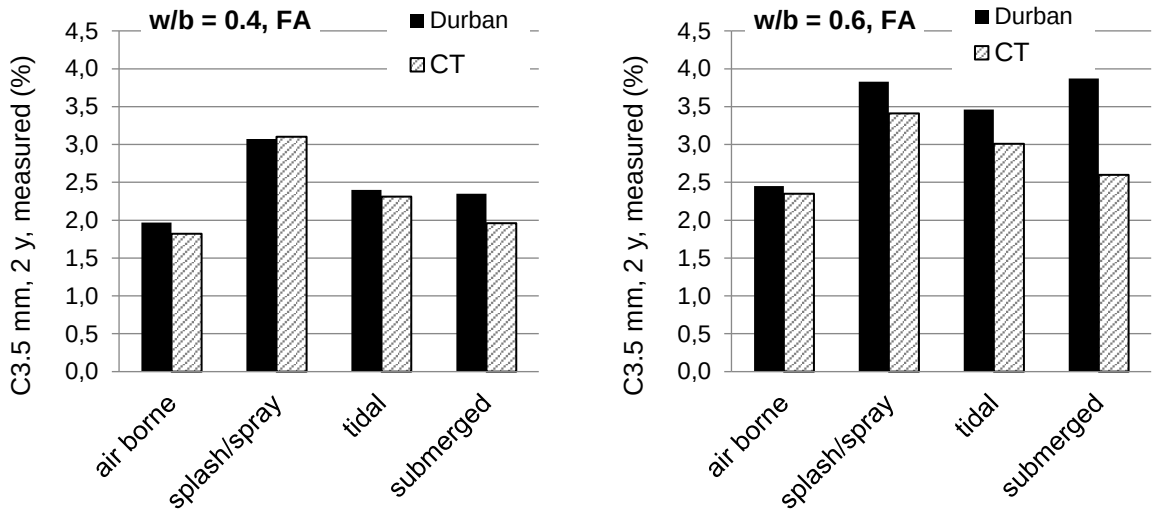

Figure 4.55: Comparison of chloride surface concentrations measured after 2 years in Durban and Cape Town, FA concrete

4.4 Laboratory exposure

In the Durban environment, concretes with 3 different binder types (PC, FA, BS) were exposed to natural marine exposure conditions. In Cape Town, 5 different binder types were used (PC, FA, CS, SP, SF), 2 of which (PC and FA) were identical to the ones used in Durban. Concretes with all of the 6 different binder types and both w/b ratios of 0.4 and 0.6 were also tested for chloride ingress characteristics under standard laboratory conditions. Samples were immersed in a chloride bath, which had the same salt concentration as that measured in the Atlantic Ocean in Cape Town and a constant temperature of 23°C (compare Chapter 3). The time-dependent chloride ingress was measured over a period of approximately 3.5 years. To interpret the data, the same analytical methods were applied as those discussed in previous sections for the site-exposed samples. Per testing age, 2 samples of the particular concrete were tested, and the mean values used in the analysis.

The chloride profiles showed the same time-dependency as discussed in Section 4.3.2 for the site-exposed samples, with chloride concentrations increasing with time throughout the sample depth. Detailed chloride profiles for all samples tested can be found in the Appendix.

The following sections contain a summary of the test results and an analysis of the time-dependent development of D_a and C_s. The underlying aim of testing samples after laboratory exposure was to compare results to site-exposed samples and evaluate if laboratory testing can be used to predict in-situ chloride ingress characteristics.

4.4.1 Diffusion coefficients

The time-dependent development of the apparent diffusion coefficient D_a is shown in Figure 4.56. Table 4.5 contains a summary of the trend line equations, R^2 values, and m-values for all concretes, as well as extrapolated D_a values for 20 years. The power functions describing the time dependent development of D_a fit the measurements very well. The R^2 values were mostly greater than 0.95, indicating a better consistency compared to the site samples, which had a correlation factor of around 0.9 (compare Section 4.3.5).

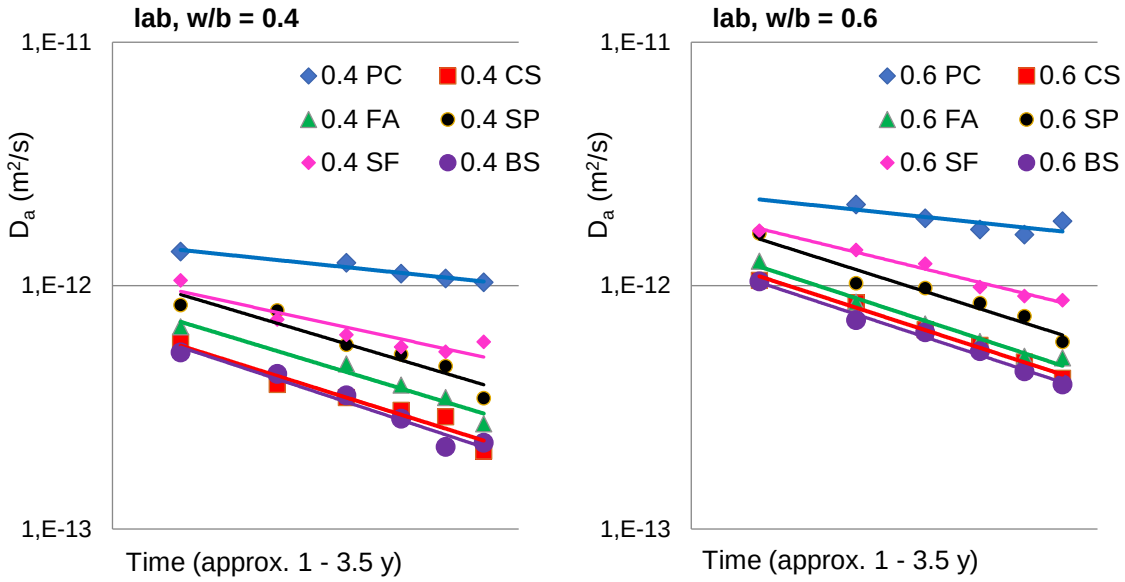

Figure 4.56: Time-dependent variation of D_a (log-log scale), laboratory exposure

Table 4.5: Time development of apparent diffusion coefficients (extrapolated from the analysis of experimental results) (laboratory exposure)

Mix	$D_a(t)$ (m^2/s)	R^2	m	$D_{a,\ 35d}$	$D_{a,\ 20y}$
0.4 PC	$6E\text{-}12t^{-0.24}$	0,96	0,24	2,56E-12	7,10E-13
0.6 PC	$1E\text{-}11t^{-0.25}$	0,57	0,25	4,11E-12	1,08E-12
0.4 CS	$5E\text{-}11t^{-0.74}$	0,95	0,74	3,60E-12	6,92E-14
0.6 CS	$1E\text{-}10t^{-0.77}$	0,99	0,77	6,47E-12	1,06E-13
0.4 BS	$6E\text{-}11t^{-0.78}$	0,96	0,78	3,75E-12	5,82E-14
0.6 BS	$1E\text{-}10t^{-0.78}$	0,99	0,78	6,25E-12	9,70E-14
0.4 FA	$5E\text{-}11t^{-0.72}$	0,96	0,72	3,87E-12	8,27E-14
0.6 FA	$1E\text{-}10t^{-0.78}$	0,98	0,78	6,34E-12	9,89E-14
0.4 SP	$6E\text{-}11t^{-0.71}$	0,91	0,71	4,81E-12	1,08E-13
0.6 SP	$1E\text{-}10t^{-0.75}$	0,95	0,75	6,95E-12	1,27E-13
0.4 SF	$2E\text{-}11t^{-0.51}$	0,85	0,51	3,26E-12	2,14E-13
0.6 SF	$6E\text{-}11t^{-0.58}$	0,98	0,58	7,63E-12	3,45E-13

Corresponding to what was observed for the site-exposed samples, concrete made with plain CEM I had significantly higher diffusion coefficients, compared to concrete with supplementary cementitious materials. Further, the different performance of the various concretes made with supplementary binders was consistent with what was observed on site. Concrete made with slag (BS or CS) had the lowest diffusion coefficients, followed by FA, SP and SF. The diffusion coefficients were further strongly influenced by the w/b ratio, as expected.

Figures 4.57 and 4.58 compare the extrapolated diffusion coefficients at 20 years in relation to the 2 exposure sites, for concretes with w/b ratios of 0.4 and 0.6, respectively. The site results in the figures represent the submerged exposure zone, which is closest to the exposure conditions in the laboratory. The measured diffusion coefficients are generally very similar for

the various binder types. This indicates that laboratory testing can not only be used to qualitatively distinguish between various binder types and w/b ratios, but also gives a good quantitative estimate of chloride diffusion coefficients in real submerged exposure conditions.

The close correlation between diffusion coefficients measured in the 3 exposure sites is somewhat surprising, considering the differences in temperatures (23°C for lab exposure, 12-15°C in Cape Town and 18-25°C in Durban).

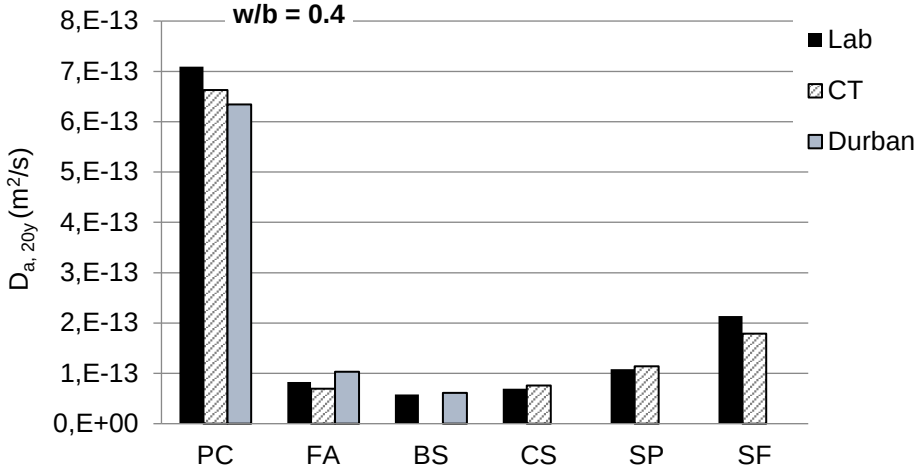

Figure 4.57: Comparison of $D_{a,20y}$ values for lab versus site exposure, w/b = 0.4 (submerged)

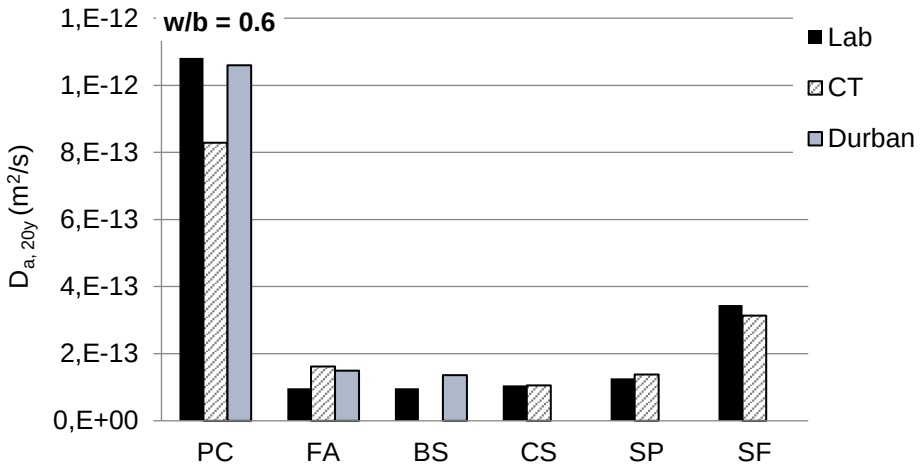

Figure 4.58: Comparison of $D_{a,20y}$ values for lab versus site exposure, w/b = 0.6 (submerged)

The m-values measured in the laboratory-exposed samples were very similar to those measured on site (Figure 4.59), with values measured on lab-exposed samples consistently slightly lower than those measured on the respective site samples.

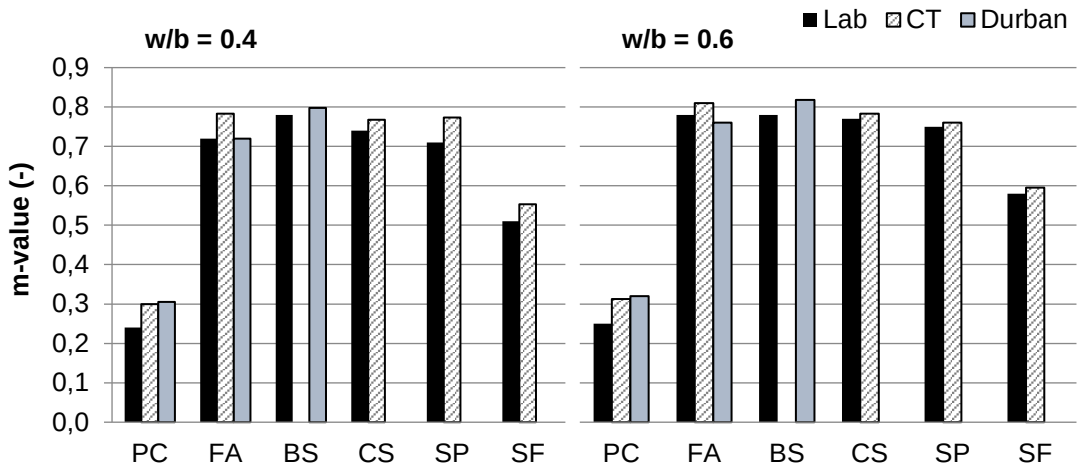

Figure 4.59: Comparison of m-values for all concretes tested

4.4.2 Chloride surface concentrations

The measured time-dependent development of the (extrapolated) chloride surface concentrations C_s is shown in Figure 4.60 and quantified in Table 4.6. Similar to the site samples, the chloride surface concentrations increase steadily with time. The n-value ranged from about 0.4 to 0.6, which is the same range as observed on the site samples. No clear trend with regards to binder type and w/b ratio could be established. Similarly, site samples did not allow establishing any clear trends concerning various influence factors (compare Sections 4.3.14 and 4.3.13).

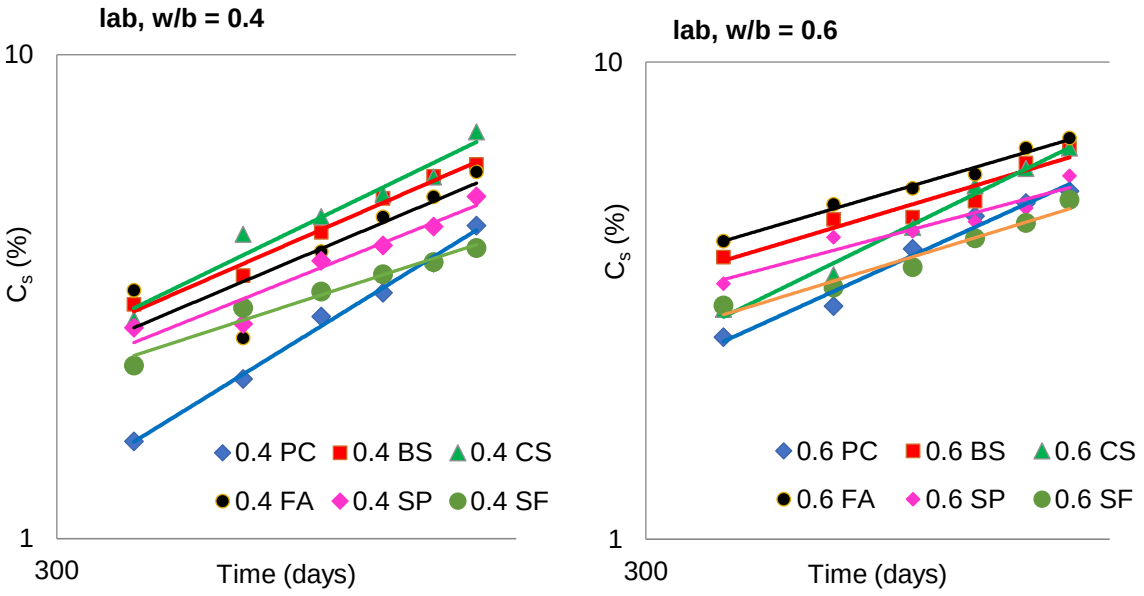

Figure 4.60: Time-dependent variation of C_s (log-log scale), lab exposure

Table 4.6: Time development of (extrapolated) chloride surface concentrations, lab exposure

Mix	Cs (t)	R^2	n value	$C_{S,\ 20y}$
0.4 PC	$0.023t^{0.658}$	0,94	0,66	8,0
0.6 PC	$0.221t^{0.382}$	0,97	0,38	6,6
0.4 CS	$0.132t^{0.45}$	0,98	0,45	7,2
0.6 CS	$0.077t^{0.488}$	0,98	0,49	5,9
0.4 BS	$0.033t^{0.63}$	0,90	0,63	9,0
0.6 BS	$0.190t^{0.418}$	0,95	0,42	7,8
0.4 FA	$0.226t^{0.393}$	0,96	0,39	7,5
0.6 FA	$0.100t^{0.47}$	0,98	0,47	6,5
0.4 SP	$0.099t^{0.542}$	0,84	0,54	12,3
0.6 SP	$0.247t^{0.431}$	0,97	0,43	11,4
0.4 SF	$0.219t^{0.441}$	0,86	0,44	11,1
0.6 SF	$0.059t^{0.59}$	0,96	0,59	11,2

The comparison of actual (measured) chloride concentrations near the surface (at 3.5 mm depth) indicates that the laboratory samples generally experienced slightly higher chloride surface concentrations, compared to site-exposed samples. Samples exposed to submerged conditions in Cape Town had been exposed to water of the same salt content as laboratory-exposed samples, which allows a direct comparison of values. Similarly, the samples exposed to the Atlantic Ocean in Cape Town did not show any significant abrasion from wave action, which indicates that lab and site exposure conditions were sufficiently similar to make this comparison. The consistently higher chloride surface concentrations in the lab samples (the only exception being concrete containing SF) can probably mostly be related to higher water temperatures in the lab-based samples (23°C, compared to 12-15°C on site in Cape Town).

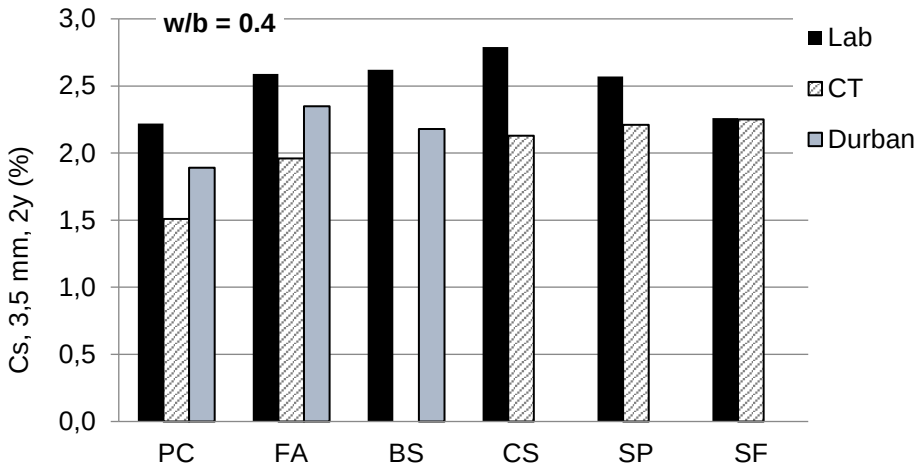

Figure 4.61: Measured chloride concentrations at 3,5 mm depth after 2 years of exposure to submerged conditions, w/b = 0.40

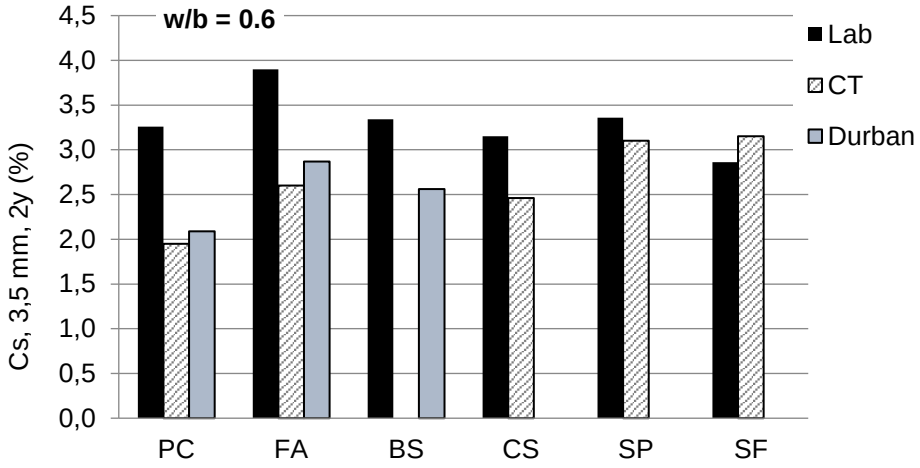

Figure 4.62: Measured chloride concentrations at 3,5 mm depth after 2 years of exposure to submerged conditions, w/b = 0.60

4.5 Summary of main aspects

In this chapter, the method and outcome of the experimental data analysis were presented. Chloride ingress profiles were obtained for several years in various environmental exposure conditions, that is on-site exposure in the Atlantic Ocean in Cape Town and the Indian Ocean in Durban, South Africa. On both exposure sites, concrete samples made from different cementitious binder combinations and 2 water/binder ratios (w/b = 0.4 and 0.6) were exposed to four marine exposure conditions, namely submerged, tidal, spray/splash and air-borne exposure. In the Durban environment, concretes with 3 different binder types (PC, FA, BS) were exposed to natural marine exposure conditions. In Cape Town, 5 different binder types were used (PC, FA, CS, SP, SF), 2 of which (PC and FA) were identical to the ones used in Durban. In addition, concrete samples with all 6 binder types had been exposed to long-term chloride ingress under laboratory conditions. The time-dependent development of chloride ingress was measured and analysed to obtain the development of chloride diffusion coefficients and chloride surface concentrations, in relation to the main experimental variables. These included exposure condition, binder type and water/binder ratio.

4.5.1 Analysis of results

Chloride profiles were analysed using the assumption that chloride ingress relates to the mechanisms characterised by Fick's law of diffusion. Regression analysis of chloride profiles resulted in the identification of time-dependent apparent diffusion coefficients D_a and chloride surface concentrations C_s. In the analysis of chloride ingress data, the first few depth increments (over a depth of typically 0-5 mm) were excluded as they did not represent the overall chloride profile. Consequently, chloride surface concentrations represented the extrapolation of chloride profiles to the outer surface of the concrete, not actually measured values. The analysis of experimental data therefore distinguished between extrapolated chloride surface concentrations and actually measured near-surface chloride concentrations in the samples.

4.5.2 Time development of D_a and C_s

The apparent diffusion coefficient (D_a) and chloride surface concentration (C_s) data produced from the bulk diffusion tests showed the time development of both variables with respect to the various marine exposure conditions, binder types and w/b ratios. D_a is seen to decrease with time in all instances and the corresponding m-value gives a good indication of the time-dependent nature. The m-values appear to be a concrete material property related mostly to binder type; notably, they were found to be independent of the w/b ratio or external factors such as chloride exposure condition. Plain PC concrete had m-values around 0.3, indicating a comparatively small change in D_a with time compared to concrete containing blended cements. Across both w/b ratios and all the various environmental exposure conditions (including exposure in 2 different oceans), concrete containing slag (CS, BS) or fly ash (FA, SP) had m-values of around 0.8. Concrete containing SF had m-values that were consistently at around 0.6.

In most instances, C_s was seen to increase with time with the n-value giving a good indication of this. Measured n-values ranged from 0.15 to 0.68 for the various concrete mixes. In general, clear trends with regards to the influence of concrete type or environmental exposure on n-value could not be established.

4.5.3 Influence of environmental exposure on D_a and C_s

Based on the results discussed in this chapter, it appears to be a reasonable assumption in chloride ingress modelling that, within a certain environment, i.e. a certain geographical location, the diffusion coefficient is a basic material characteristic independent of the environmental exposure class (tidal, splash/spray, airborne, submerged).

However, results also indicated that ambient exposure conditions (RH and temperature) of a certain geographic location have an effect on diffusion coefficients, especially in the exposure zones related to regular wetting and drying cycles, i.e. splash/spray and tidal zones. In these zones, diffusion coefficients obtained in Durban were notably higher that those obtained in Cape Town, for all of the 4 identical concrete types that had been exposed in both locations (PC and FA concrete at two w/b ratios).

For all concrete types, the highest C_s values were measured in the splash/spray zone followed by the tidal, submerged and airborne zones. A higher C_s value was also generally measured in concrete with higher w/b ratio, as expected. Surface concentrations were also found to be generally higher in Durban, which was ascribed to the higher ambient temperatures.

The EN 206 stipulates 3 different exposure conditions for marine environments, i.e. airborne, submerged, and tidal & splash/spray. Notably, tidal and splash/spray exposure classes are combined in the code. The results obtained in this research indicate that this is an oversimplification that needs further consideration. Chloride surface concentrations were measured to generally be significantly higher in the splash/spray zone, compared to the tidal zone. Combined with similar diffusion coefficients in these exposure zones, chloride ingress in the splash/spray zone was generally found to be significantly higher than that measured in the tidal zone.

4.5.4 Influence of binder type on D_a and C_s

The test results confirmed that the cementitious binder type has an influence on chloride ingress in concrete. In general, concretes made with plain Portland cement had a significantly higher diffusion coefficient, compared to concretes with blended cements, as expected. Further, for the Durban samples, concrete containing slag (BS) had consistently lower D_a values, compared to concrete containing fly ash (FA). In the Cape Town environment, the lowest diffusion coefficients were measured for concretes containing slag (CS) and FA, followed by concrete made with SP and SF. However, the influence of binder type on actual chloride ingress needs to be investigated with consideration of the chloride surface concentration. Here it needs to be remembered that the chloride surface concentrations used in the modelling of chloride ingress correspond to the extrapolation of the chloride profile to the concrete outer surface, not to actually measured values. Considering these values, PC concretes generally had the lowest chloride surface concentrations, compared to concrete containing blended cements.

The combined influence of binder type on both D_a and C_s is analysed in detail in the following chapter. In general, mixes containing slag were found to have the lowest chloride ingress, compared to the other mixes. Plain PC mixes were found to have the highest chloride ingress, as expected.

4.5.5 Laboratory data versus site data

Under standard laboratory conditions, samples were immersed in a chloride bath, which had the same salinity as that measured in the Atlantic Ocean in Cape Town and a constant temperature of 23^{o}C. In general, the chloride profiles showed the same time-dependency as identified for the respective samples exposed at the Atlantic Ocean. Similarly, the performance of the various concretes made with supplementary binders was consistent with that observed on site, which was true for the time development and magnitude of both diffusion coefficients and chloride surface concentrations. Overall, the results confirm that laboratory testing can be used to qualitatively distinguish between various binder types and w/b ratios.

5.Chloride ingress modelling and analysis of experimental data

5.1 Introduction

In Chapter 4, time-dependent diffusion coefficients and chloride surface concentrations were established in relation to various experimental parameters including material characteristics and exposure conditions. For service life prediction of reinforced concrete structures in marine environments, most researchers use Fick's laws of diffusion to model long-term chloride ingress (compare Section 2.4). However, model input parameters and associated assumptions vary widely between the various approaches. Most models assume a certain time-dependency for diffusion coefficients, usually based on empirical data analysis. In addition, some of the models assume that chloride surface concentrations change with time, while other models assume constant surface concentrations over the entire exposure period. Details of the various existing models were discussed in Chapter 2.

Long-term chloride ingress modelling in this chapter is based on applying Ficks' laws of diffusion (Equation 2.43, Chapter 2), in which both the apparent diffusion coefficient and chloride surface concentrations were expressed as time-dependent variables. In this manner, long-term chloride profiles could be predicted based on the measured time-dependent development of D_a and C_s.

The experimental data discussed and presented in Chapter 4 indicate that both diffusion coefficients and chloride surface concentrations are time-dependent parameters. Apparent diffusion coefficients decrease with time and chloride surface concentrations increase with time. The time development of both D_a and C_s were linear in a log-log coordinate system. Both magnitude and time-development of D_a and C_s were found to be dependent on environmental exposure conditions, binder type and water/binder ratio. The modelling of long-term chloride ingress into concrete structures therefore needs to recognise these various influencing factors.

Based on the experimental data, values for D_a and C_s could be established based on various parameters. Notably, clear trends were observed for the time development of D_a and C_s, expressed through m- and n-values, respectively. However, the longer-term time development of D_a and C_s could not be established in the period of this study since data was collected over a period of only 4 years. In the modelling of long-term chloride ingress, assumptions therefore need to be made with regard to the time period during which D_a and C_s keep changing. The time-dependency of these two parameters is typically explained as being the result of continuous hydration and chloride binding. These mechanisms are generally assumed to diminish with time, which is why many existing models define a cut-off point for the time development of D_a and C_s. Until this cut-off point is reached, D_a and C_s are assumed to keep changing. After the cut-off point, D_a and C_s are assumed to be constant for the remainder of the service life. There is no consensus in literature with regard to appropriate cut-off points. Some models assume that D_a and C_s keep changing throughout the service life and therefore do not define a cut-off point (Frederiksen et al., 1996) and some models don't assume C_s to change at all and keeps it constant (Costa, 1999, Maheswaran and Sanjayan, 2004, Petcherdchoo, 2013 and Pack et al., 2010). Other models assign cut-off points for both D_a and C_s (Thomas and Bentz, 2001). While some models assume that the cut-off point is reached at the same time for D_a and C_s, other models assume an earlier cut-off point for C_s, compared to D_a (Thomas and Bentz, 2001) and some models assume constant C_s with a varying D_a (Mangat and Molloy, 1994, Maage et al., 1996 and Stanish and Thomas, 2003).

Based on the principles discussed in literature and the experimental data obtained in this research, the modelling proposed in this chapter is based on the following premises:

- Both D_a and C_s are time-dependent parameters (as established in Chapter 4)
- There is a cut-off point beyond which D_a and C_s remain notionally constant for the remainder of the service life
- The cut-off point is the same for D_a and C_s

The latter of the above points is considered to be of significance. As discussed in Chapter 4, D_a and C_s are inter-dependent parameters and cannot be modelled in isolation from each other. In this research, time-dependent chloride profiles were established through regression analysis of measured chloride ingress profiles. In this analysis, chloride surface concentrations at zero mm depth (which cannot be measured) are established based on extrapolation of measured chloride profiles to the concrete surface. They are therefore a theoretical construct, highly dependent on the regression slope of the chloride profile. The slope of the chloride profile is defined by the diffusion coefficient and relies on the starting point on the surface to quantify chloride concentrations inside the concrete. Therefore, due to this co-dependency, it would be inconsistent to assume different cut-off points for D_a and C_s.

The modelling of long-term chloride ingress requires information on the related influence of material characteristics and environmental exposure conditions, which has been established in Chapter 4. However, further analysis is required to define appropriate cut-off points for the time-dependency of D_a and C_s. This is done in the following section.

5.2 Time-dependency of D_a and C_s: cut-off point

5.2.1 Introduction

The literature contains several models that define certain cut-off points for the time-development of chloride surface concentrations and diffusion coefficients (see Section 2.4 in the literature review). No consensus exists on suitable cut-off points. Also there is no sound scientific justification based on which such cut-off points can be defined. It is therefore reasonable to assume that cut-off points are dependent on material characteristics such as binder type, binder content, w/b ratio, penetrability and porosity, etc., as well as on environmental conditions such as exposure zone, temperature, relative humidity, etc. It is therefore impossible to determine accurate cut-off points; consequently, simplifying assumptions need to be made, which assist in modelling long-term chloride ingress as realistically as possible. The strategy adopted in this research is to first model chloride ingress into concrete based on various cut-off points and make an engineering judgement on the validity of the resulting predicted long-term chloride profiles. For this purpose, long-term chloride ingress was modelled as chloride ingress after 50 years of exposure time.

Based on the test results obtained during the first 4 years of exposure, time-dependent values for D_a and C_s were established for all concretes tested, as discussed in Chapter 4. To determine suitable cut-off points for this time development, the following three different scenarios were evaluated:

- D_a and C_s keep changing for a period of 10 years; thereafter they remain constant (50/10/10 – exposure of 50 years / cut-off time for D_a = 10 years / cut-off time for C_s = 10 years))

- D_a and C_s keep changing for a period of 20 years; thereafter they remain constant (50/20/20) - exposure of 50 years / cut-off time for D_a = 20 years / cut-off time for C_s = 20 years))
- D_a and C_s keep changing for the whole period of 50 years (50/50/50)

Considering the many uncertainties in chloride ingress modelling, which relate to the numerous influencing factors and associated assumptions, it was considered sufficient to only evaluate the above three scenarios. A further refinement would probably not result in a higher reliability of the resulting model. For the same reasons, no attempt was made to find cut-off dates for different exposure conditions.

In all three scenarios considered, it was assumed that the cut-off time for D_a and C_s is identical, as discussed above. It will be shown in the following sections that the three different scenarios result in significantly different predictions for long-term chloride ingress. The determination of a cut-off date for the changing D_a and C_s values is therefore a key aspect in long-term chloride ingress modelling. This is an aspect that has not been adequately considered in existing models for the prediction of chloride ingress.

Due to the large amount of data generated in this research, the determination of suitable cut-off points was at first determined for concretes with a w/b ratio of 0.40 for the Cape Town exposure site. A w/b of 0.40 was selected as it was considered a more realistic design value for concretes exposed to the marine environment, compared to a w/b of 0.60. The Cape Town exposure site was selected over the Durban site, as various long-term chloride ingress data exists for structures along the west coast of South Africa and Namibia (see Chapter 3). Due to similar exposure and environmental conditions (water temperature and salinity, ambient temperatures and RH), a comparison of model outcomes and existing data was therefore considered useful in evaluating various model scenarios. A limitation in this regard was that existing long-term chloride ingress data is available only for concretes containing PC as the sole binder type.

5.2.2 Modelling of long-term chloride ingress for Cape Town PC samples

The time-dependent chloride diffusion coefficients D_a and surface concentrations C_s were used to model chloride profiles after 50 years of exposure, see also Section 4.3.2. For illustration purposes, depths into the concrete up to 50 mm were considered, which relates to common cover depths specified for marine structures in South Africa. As discussed in the previous section, three different scenarios regarding the cut-off date were considered. Figures 5.1 and 5.2 show the modelled chloride profiles for PC concrete (w/b = 0.40) in Cape Town, situated in the splash/spray and tidal zones, respectively. For these two exposure conditions, long-term chloride ingress data was available for concrete structures situated on the west coasts of South Africa and Namibia, as discussed in Chapter 3. The site data is also shown in the figures, to help in assessing which of the three scenarios is most realistic.

The modelled surface concentration (at zero mm depth) is not included in the graphical presentation of the experimental data obtained in this research as a result of the low diffusion coefficients of concretes containing supplementary cementitious materials and the associated steep chloride profile which results in predicted surface concentrations (which are based on extrapolation of the chloride profile to the surface, as discussed in detail in Chapter 4) that are generally unrealistically high. The data presentation in the following sections therefore focuses

on depths between 10 mm and 50 mm, for which the predicted chloride concentrations appear reasonably realistic.

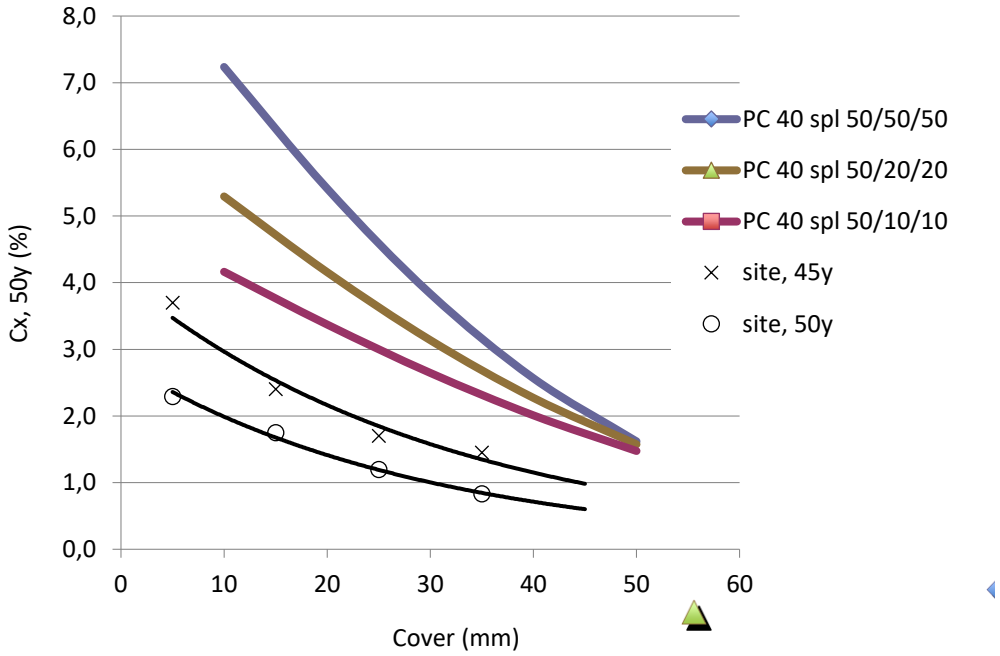

Figure 5.1: Modelling of chloride profiles after 50 years of exposure, CT samples, w/b = 0.40, PC concrete, splash /spray zone; comparison to data from site (mean values)

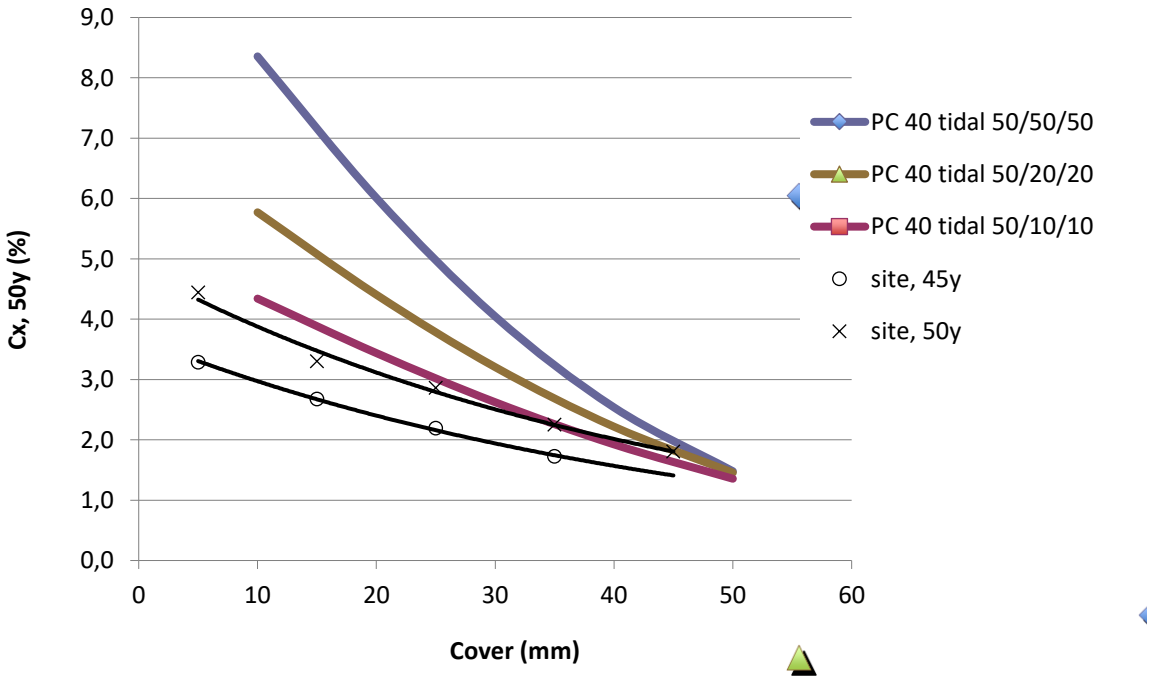

Figure 5.2: Modelling of chloride profiles after 50 years of exposure, CT samples, w/b = 0.40, PC concrete, tidal zone; comparison to data from site (mean values)

For the PC concretes, predicting 50-year chloride ingress with an earlier cut-off date for the development of D_a and C_s results in a decrease in chloride concentrations across all depths. The main reason for this is that D_a does not change much with time (as indicated by a low m-value (compare Section 4.3.2)). In contrast, the surface concentration significantly changes with time (high n-value). Therefore, the change of C_s in PC concretes has a larger influence on the results - as time proceeds, C_s keeps increasing but D_a stays relatively constant, which results in very high chloride values at higher cut-off ages. The chloride concentrations related to the different scenarios are significantly different for the outer approximately 40 mm. However, notably, beyond a (cover) depth of about 40 mm, all scenarios result in very similar chloride concentrations.

The change in chloride surface concentration is also the reason for the observation that chloride contents are higher in the tidal zone (Figure 5.2), compared to the splash/spray zone (Figure 5.1), even though the splash/spray zone produced a higher value for D_a (compare Fig. 4.28). As seen in Table 4.4 in Chapter 4, the n-value in the tidal zone is 0.45, compared to an n value of 0.38 in the splash/spray zone. Hence, the long-term development of the chloride surface concentration is the dominant factor for the differing long-term chloride ingress between tidal and splash/spray zones.

Figures 5.1 and 5.2 indicate that assuming a later cut-off date for D_a and C_s, results in an unrealistically conservative prediction of long-term chloride profiles, i.e. higher chloride values. The comparison of the predicted profiles and long-term chloride ingress in real structures indicates that, from the different scenarios considered, the 50/10/10 scenario is the most realistic as it results in a similar order of magnitude for chloride ingress. It therefore appears appropriate to use a cut-off time of 10 years for PC concretes as opposed to 20 or 50 years. Based on the comparison of experimental modelling with site data shown in Figures 5.1.and 5.2, this assumption appears conservative, as even with a 50/10/10 scenario, modelled chloride concentrations are generally higher than those related to existing long-term data. This is especially the case for the splash/spray zone (Figure 5.1), which is generally of most concern with regard to reinforcement corrosion.

Considering that the chloride profile for the 50/10/10 modelling scenario in Figure 5.1 is appreciably higher than the site data, one could argue that a 50/5/5 modelling scenario should also be investigated. However, considering how close the predicted chloride profile in Figure 5.2 is to the measured data, this would result in an unconservative outcome for the tidal zone. In absence of additional data and a full probabilistic approach, the selection of a 50/10/10 scenario appears appropriate and conservative.

5.2.3 Chloride ingress for Cape Town samples with binary cement blends

To avoid presenting too much data, only the splash zone is considered in this section, since it is the zone most affected by reinforcement corrosion problems. For the other exposure zones, similar trends as discussed below for the splash/spray zone were identified.

For concrete containing Fly Ash, using the scenario 50/10/10 compared to 50/50/50 results in a lower chloride concentration near the surface (in the 10 mm depth) (Figure 5.3, top right), as expected. Further away from the surface, chloride concentrations are significantly higher for the 50/10/10 scenario, compared to 50/20/20 and 50/50/50. The main reason for 50/10/10 yielding much higher chloride values at depth is that D_a changes significantly with time (as indicated by

high m-values, compare Section 4.3.2). Assuming that this change continues throughout the 50 year exposure duration (as done with the 50/50/50 scenario) will therefore result in much steeper chloride profiles and consequently in lower chloride concentrations in depths approximately between 20 mm and 50 mm. Notably, for PC concrete, the opposite trend was observed for the various scenarios, compared to concrete containing Fly Ash, i.e. the 50/10/10 scenario resulted in the lowest chloride concentrations in depths between 10 and 50 mm. Therefore, in contrast to PC concrete, assuming an earlier cut-off date for D_a and C_s in Corex slag results in a more conservative prediction of long-term chloride profiles.

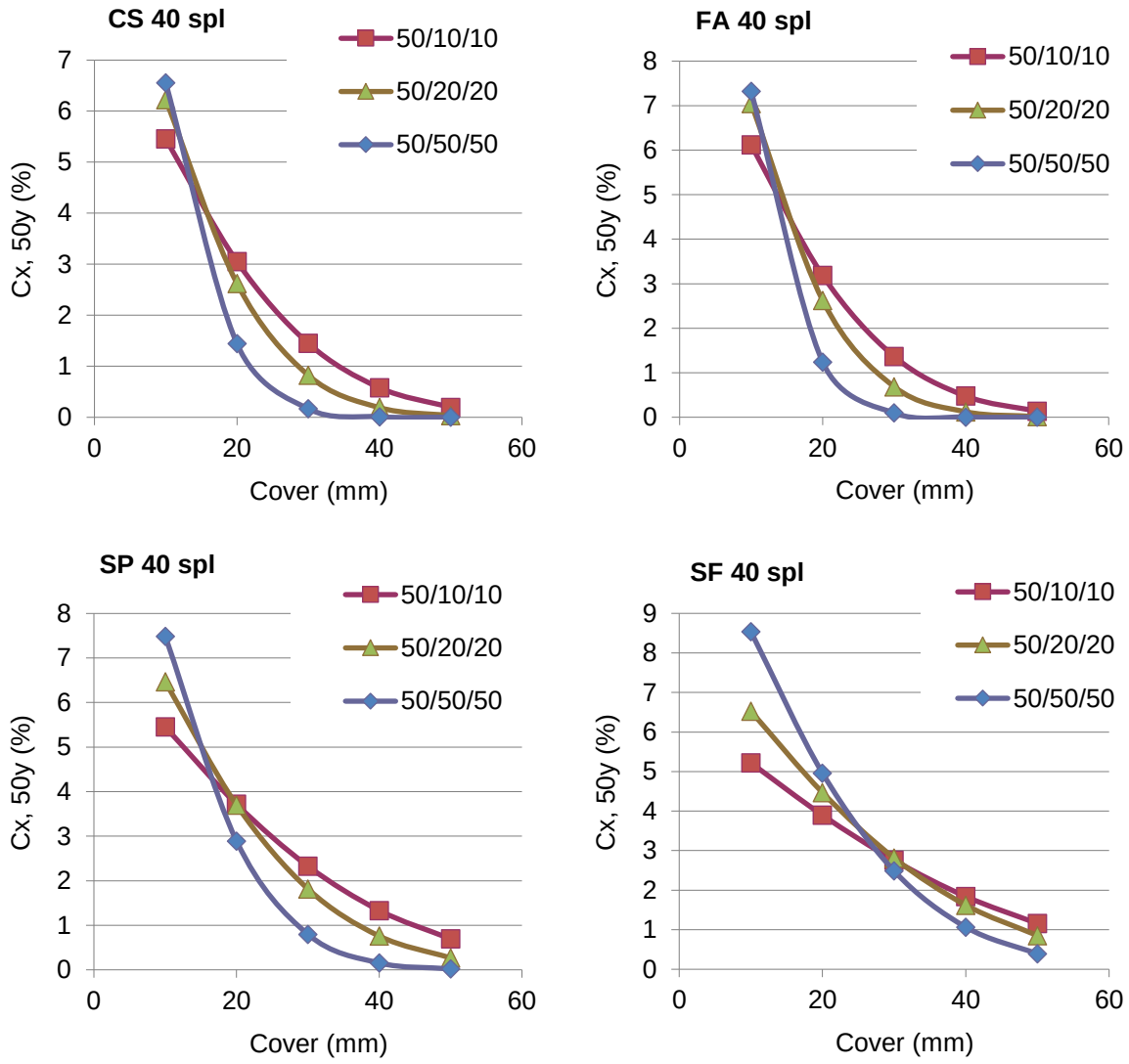

Figure 5.3: Modelling of chloride profiles after 50 years of exposure, CT samples (CS: top left, FA: top right, SP: bottom left, SF: bottom right), w/b = 0.4, splash/spray zone, in relation to different cut-off dates for D_a and C_s. Note that "CS 40 spl" refers to Corex slag at a w/b ratio of 0.40 in the splash/spray zone, etc.

Similar to the significant time-dependent change in D_a, C_S also changes significantly with time for the binary blended concretes. The n-values measured for Corex slag concretes were generally high and of similar magnitude as the n–values obtained for PC concrete. In PC concretes, this was the main reason for the differences in predicted chloride profiles for the

various scenarios, as discussed in Section 5.2.2. However, for concrete containing Corex slag, the change in C_s is counterbalanced by the large change in D_a (in contrast, the change in D_a was small in PC concrete, hence the dominance of the changing C_s). Therefore, the main influence on the different predictions of long-term chloride ingress in relation to the three scenarios for concrete containing Corex slag is the large change in D_a. The assumption that the m-value continuously changes over the full period of 50 years results in very low long-term apparent diffusion coefficients and hence very low apparent chloride concentrations in depths away from the surface.

The low chloride concentrations predicted using the 50/50/50 scenario seem unrealistic (note that close to zero chloride content is predicted from 30 mm cover). In contrast, the 50/10/10 scenario yields chloride concentrations that are on the higher side. Intuitively, from the three scenarios investigated, 50/20/20 appears closest to what might be expected from slag concrete. However, no long-term experimental data are available to justify selecting the 20/20 option in the modelling of long-term chloride ingress in slag concrete. Further research on long-term chloride ingress into concretes with blended cements is required to define the most suitable cut-off date. Until such research data become available, it appears justified to conservatively select the same cut-off date for concretes containing blended cements, as for PC concretes. In the following sections, both scenarios (i.e. 10/10 and 20/20) are used to model chloride ingress and associated service life, where appropriate, to highlight the different outcome resulting from the two scenarios.

Figures 5.4 to 5.7 also show the comparison of the different modelling scenarios for concretes containing CS, FA, SP and SF, respectively. The same trends as discussed above for concrete containing CS are observed, i.e. assuming a later cut-off date results in a less conservative prediction of long-term chloride profiles in depths that are relevant in practice, i.e. depths exceeding 20-30 mm.

The influence of the cut-off point for the time development of C_s and D_a on the predicted service life of reinforced concrete members is discussed further in Section 5.3.

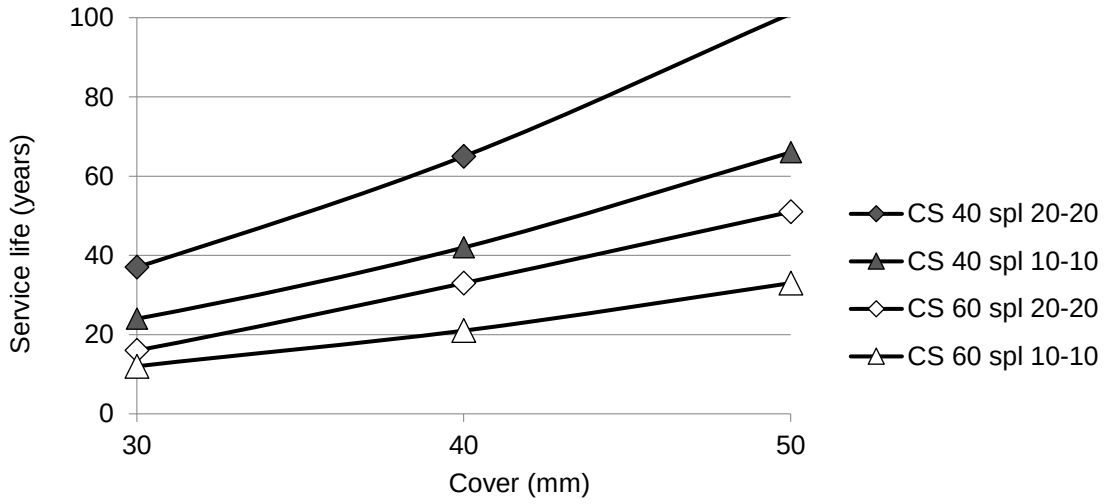

Figure 5.4: Influence of cut-off date for D_a and C_s on service life prediction for CS concrete, CT, splash/spray zone (a chloride threshold value of 0.4% by mass of binder was assumed in the service life prediction)

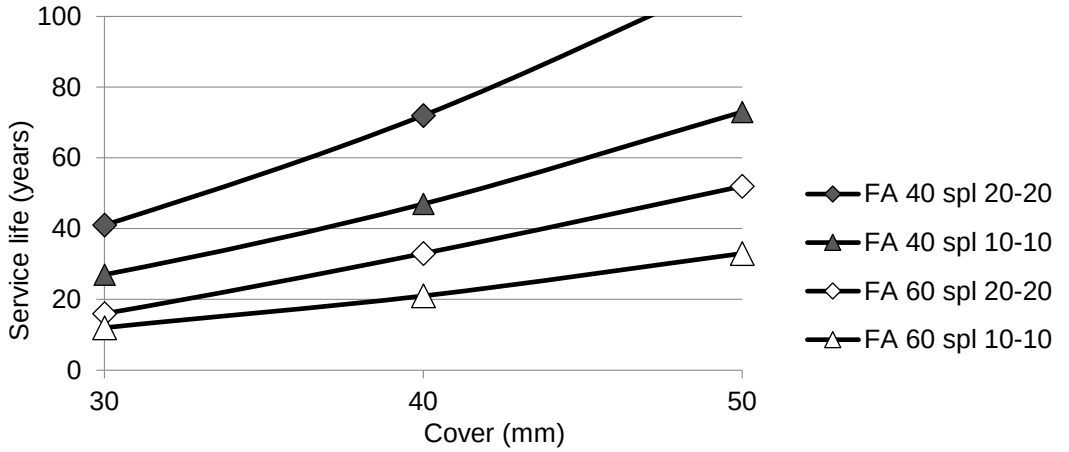

Figure 5.5: Influence of cut-off date for D_a and C_s on service life prediction for FA concrete, CT, splash/spray zone (chloride threshold 0.4%)

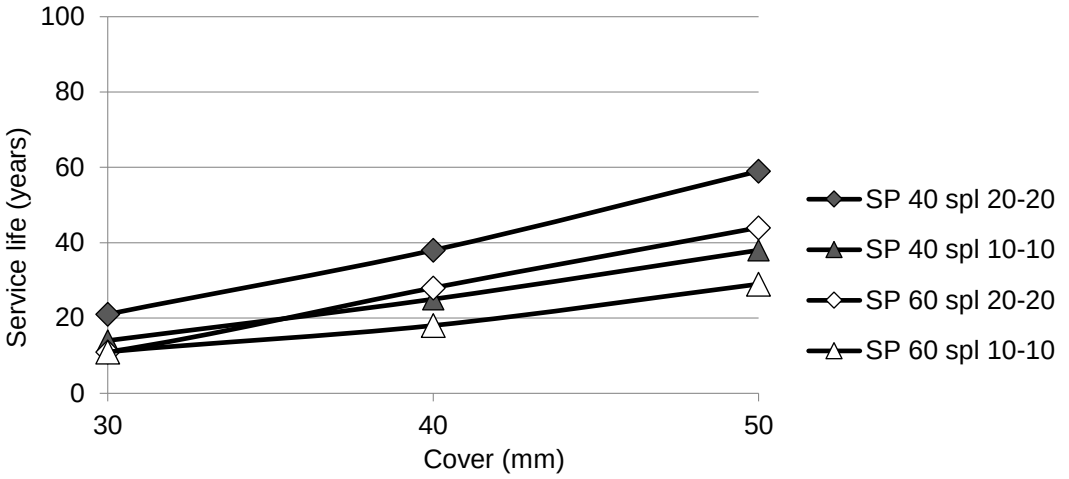

Figure 5.6: Influence of cut-off date for D_a and C_s on service life prediction for SP concrete, CT, splash/spray zone (chloride threshold 0.4%)

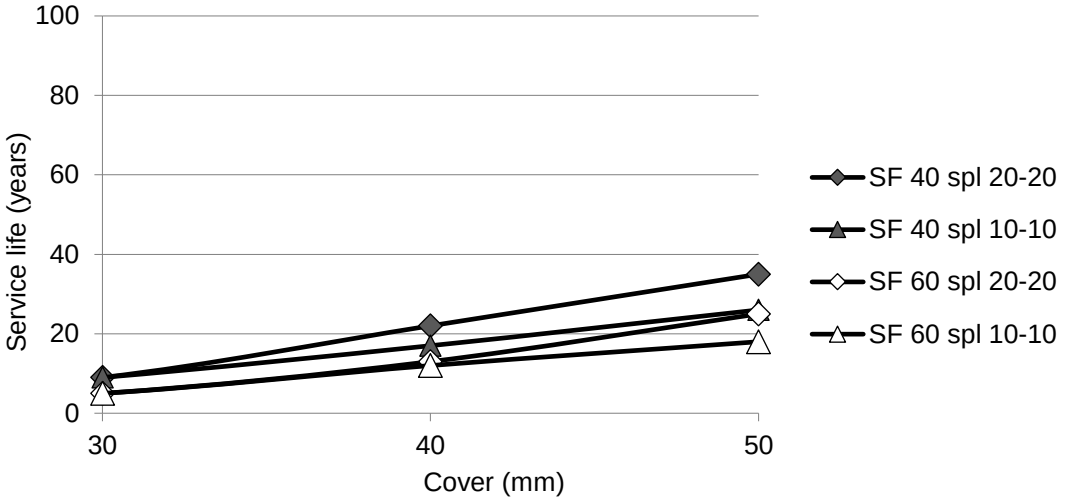

Figure 5.7: Influence of cut-off date for D_a and C_s on service life prediction for SF concrete, CT, splash/spray zone (chloride threshold 0.4%)

5.2.4 Limitations of the proposed modelling with a cut-off date of 10 years

The prediction of time-dependent chloride ingress into concrete is usually obtained using Fick's laws of diffusion, assuming that the diffusion coefficient D_a changes, i.e. reduces, with time, which is expressed with the m-value. With regard to chloride surface concentrations, however, a consistent approach cannot be found in literature. Most researchers assume that C_s is constant throughout the lifetime of the structure and model chloride ingress with a somewhat randomly selected value for C_s, in combination with a time-dependent diffusion coefficient. In contrast to most approaches stated in literature, this thesis argues that, in the modelling of chloride ingress using Fick's laws of diffusion, the values for D_a and C_s are inextricably related. Consequently, both C_s and D_a must be assumed to be time-dependent. The experimental results clearly confirm that both D_a and C_s are time-dependent parameters, with D_a decreasing with time and C_s increasing with time.

With regard to the time-development of the diffusion coefficient, some researchers assume that D_a keeps reducing throughout the lifetime of the concrete, while others assume a "cut-off point after which D_a remains constant. Based on the comparison of experimental results obtained in this research and chloride ingress measurements in real structures, a cut-off point of 10 years was considered to be a realistic and conservative assumption in the modelling of long-term chloride ingress for concrete containing PC as the sole binder. For concrete containing blended cements, long-term chloride ingress data for real structures exposed to the southern African coastline are not available. Therefore, this thesis proposes to initially, in the modelling and parameter comparison, also use the same cut-off date of 10 years for concrete containing blended cements. However, as will be seen later, the modelling with a cut-off point of 10 years results in overly conservative predictions of chloride ingress into concrete containing blended cements. As an alternative, a cut-off date of 20 years is presented where deemed informative, in the discussions to follow in the sections below.

Figures 5.4 to 5.7 indicate the significance of the cut-off date for the time development of D_a and C_s. The figures show the service life duration as the expected time of corrosion initiation, i.e. the time when the chloride concentration at a certain cover depth exceeds the chloride threshold, which is assumed to be 0.4% by mass of cement. As discussed in Chapter 2, there is no general consensus in literature on the chloride threshold and in practice, the threshold may be dependent on many factors, including binder type and characteristics of the reinforcing steel. The threshold value typically used in practice, i.e. 0.4% was therefore used in the modelling in this research.

Time-dependent chloride ingress was modelled using Fick's 2nd law of diffusion (see Eq. 2.10 in Section 2.4), assuming a cut-off time of either 10 years or 20 years for both C_s and D_a. To prevent overload of graphical presentation, only the splash/spray zone is considered here, which is the most aggressive exposure for chloride ingress and rebar corrosion. The figures clearly show the large influence of the assumed cut-off date for D_a and C_s, across all concretes tested. This is most prominently evident in concrete containing C_s, where a later cut-off date (i.e. 20 years versus 10 years) results in the prediction of a significantly longer time until corrosion initiation. This effect is already clear in Figure 5.3, which shows the influence of the cut-off date on chloride profiles. However, the conversion of chloride profiles (Figure 5.3) to predicted service life (Figures 5.4 to 5.7) notably magnifies the effect and places the predictions in an engineering context.

Intuitively, the assumed cut-off date of 10 years appears to be a conservative assumption, which may not necessarily represent the expected durability of blended cement concretes. However, this assumption can be used for chloride ingress modelling until such time when actual data from real structures becomes available. It allows to compare and therefore evaluate the influence of various experimental parameters on chloride ingress, including binder type, w/b ratio, and environmental exposure condition, which is done in the sections to follow.

5.3 Prediction of chloride ingress and related service life duration

5.3.1 Introduction and limitations

To investigate the influence of the various experimental parameters on chloride ingress and the related service life of concrete structures in more detail, long-term chloride ingress was modelled using the determined time-dependent values for D_a and C_s as input parameters in Fick's second law of diffusion (see Eq. 2.10 in Section 2.4). As discussed in previous sections, for PC concrete the long-term modelling of chloride ingress with a cut-off point of 10 years is reasonably realistic, as existing long-term data from actual structures is available to "calibrate" the results obtained in this research. However, for concrete containing binary blends, the long-term modelling of chloride ingress with a cut-off point of 10 years is believed to be overly conservative. As a consequence, the predicted quantitative chloride profiles for concrete with supplementary cementitious materials are probably not showing the full durability potential of the mixes, when it is modelled with a cut-off point of 10 years. Therefore, the evaluation of the influence of binder type on chloride ingress needs to be viewed with caution. However, within a certain group of concretes (e.g. FA concrete, PC concrete, etc.), the approach allows to evaluate the influence of various other parameters, including exposure condition, time, w/b ratio, and cover depth, with reasonable clarity. Where deemed appropriate, modelling of chloride ingress into concrete with blended cements using a cut-off point of 20 years is included in the discussions to follow, in order to highlight the difference between the two approaches.

5.3.2 Time development of chloride profiles

Long-term chloride ingress was modelled using Fick's 2nd law of diffusion, using the predicted chloride surface concentrations and apparent diffusion coefficients, as discussed in the previous sections:

$$C_x(t) = C_s(t)\left(1 - erf\left[\frac{x}{2\sqrt{D_a(t)}}\right]\right) \qquad [5.1]$$

Where:

$C_x(t)$ = Chloride concentration at depth x (% by mass of binder) at time t (with t ≥ 10 years for PC concrete and t ≥ 20 years for blended cement concrete)

$C_s(t)$ = Predicted chloride surface concentration (% by mass of binder) at time t (with t = 10 years for PC concrete and t = 20 years for blended cement concrete)

x = Depth measured normal to the surface (mm)

$D_a(t)$ = Predicted chloride diffusion coefficient (m^2/s) at time t (with t = 10 years for PC concrete and t = 20 years for blended cement concrete)

For illustrative purposes, Figures 5.8 and 5.9 show the chloride profiles predicted for PC and CS concrete (w/b = 0.4) in the splash and airborne exposure zones in Cape Town. A cut-off point of 10 years was used in this modelling.

Chloride profiles for PC concrete show reducing slopes and reducing curvature with time. For PC concrete, the main influence on long-term chloride ingress is diffusion; near-surface chloride concentrations (at 10 mm depth) do not significantly change with time while concentrations deeper inside the concrete significantly increase with time. In contrast, long-term chloride profiles in CS concrete are significantly affected by a change in chloride surface concentrations, while the chloride concentrations at 50 mm do not change much over a period of 50 years. In terms of long-term chloride ingress, the time-dependent chloride profiles of PC concrete tend to "hinge around" the near-surface chloride concentration, while the profiles of CS concrete "hinge around" the chloride concentration at about 50 mm depth.

The chloride profiles in Figures 5.8 and 5.9 further indicate that the two particular exposure zones does not have a very large influence on chloride ingress, especially for PC concrete, with chloride profiles in air borne and splash zones being of similar order of magnitude. This is discussed in more detail in the sections that follow.

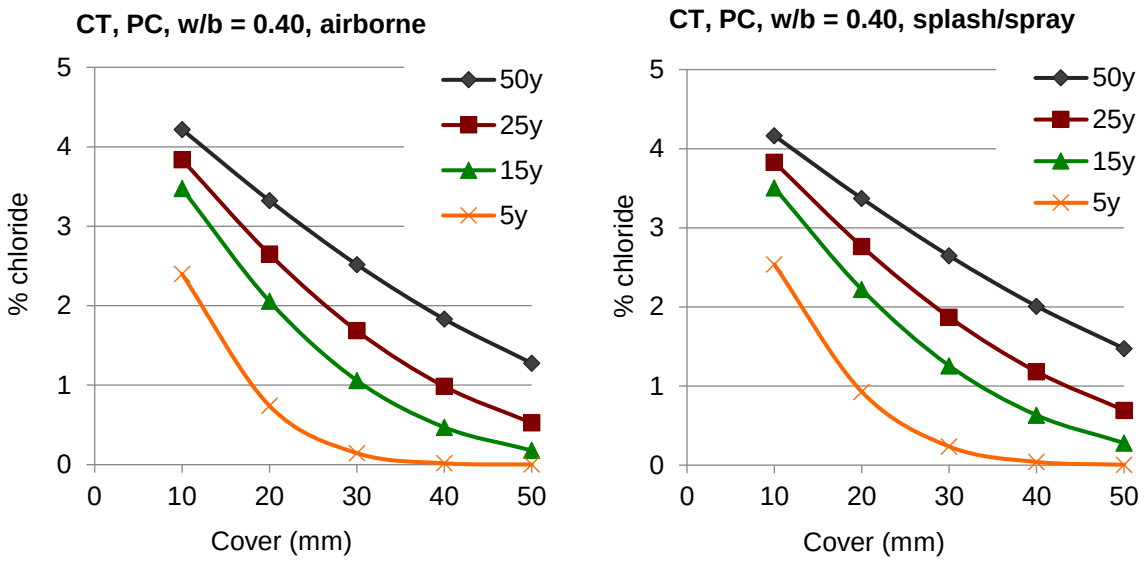

Figure 5.8: Predicted time development of chloride profiles (by mass of cement), CT, PC concrete, air-borne (left) and splash/spray (right), cut-off point: 10 years

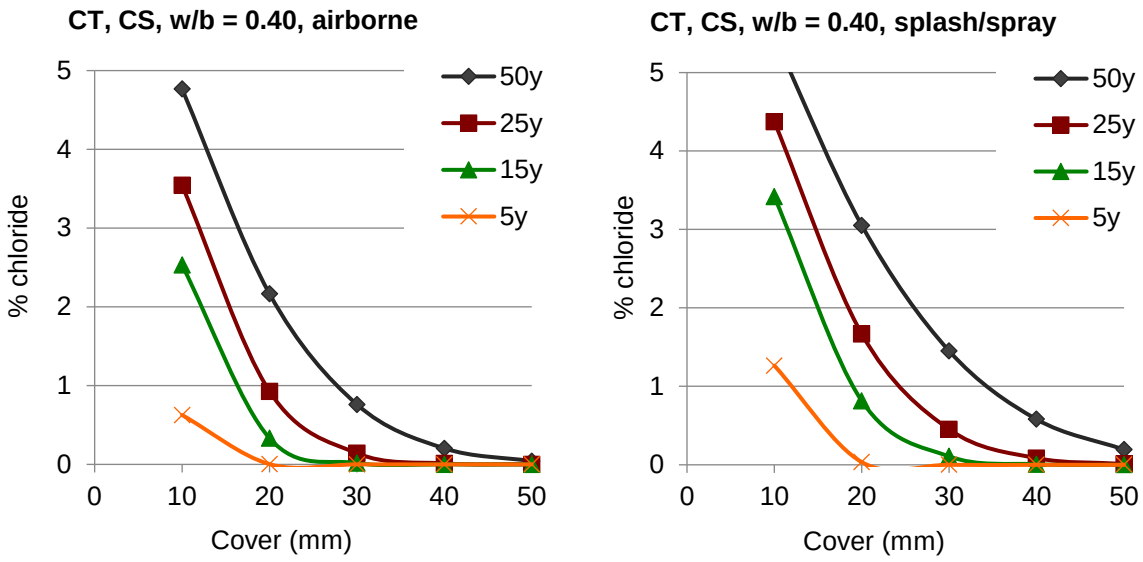

Figure 5.9: Predicted time development of chloride profiles (by mass of cement), CT, CS concrete, airborne (left) and splash/spray (right), cut-off point: 10 years

5.3.3 Influence of binder type

Binder type is known to have a significant influence on chloride ingress into concrete. The experimental data obtained in this research attempt to quantify the influence of binder type on the expected service life duration of concrete structures in the marine environment. As discussed in previous sections, the assumption of suitable cut-off dates for the time development of D_a and C_s has a substantial influence on the predicted long-term chloride ingress. Notably, the assumption that a universal cut-off date can be used for different binder types may not be correct and may alter the results. Therefore, both scenarios, i.e. cut-off points of 10 years and 20 years, are used in the service life predictions presented in the following sections.

Independent of the actual cut-off point assumed, the analytical approach developed in previous sections gives a useful indication of the relative performance of various binder types, indicating which types of concrete are the most suitable for marine exposure conditions and for a given service life.

5.3.4 Influence of binder type (Cape Town)

The predicted chloride profiles in Cape Town (by mass of cement) for an exposure period of 50 years and a cut-off point of 10 years are shown in Figures 5.10 to 5.13. Some general trends with regard to binder type are observed. An interesting observation is that, for each exposure condition and w/b ratio, the chloride concentrations at 10 mm depth are very similar across all concrete types. The difference in performance resulting from the various cement types is mostly evident in the chloride profiles deeper inside the concrete.

PC concrete consistently has the lowest chloride surface concentrations but generally higher chloride concentrations in depths exceeding about 20 mm to 30 mm, compared to all other concrete types. This corresponds to the trends discussed in Chapter 4, i.e. that PC concrete

has lower chloride surface concentrations but higher chloride diffusion coefficients, compared to concrete containing supplementary cementitious materials.

For most environmental exposure zones and w/b ratios, the 50-year chloride profiles of concretes containing CS, FA and SP are very similar across all depths with some variations/anomalies. The chloride profiles for these 3 concrete types tend to approach the x-axis at depths exceeding 50 mm, indicating that the expected chloride concentration beyond 50 mm is small. In contrast, concrete containing SF and PC show a flatter and less curved chloride profile, which corresponds to significantly higher chloride concentrations further inside the concrete. Consequently, SF and PC concrete generally have significant chloride concentrations in depths exceeding 50 mm.

The effect of binder type on chloride ingress is investigated further in Section 5.3.5, in which the influence of binder type on predicted service life is discussed.

The figures indicate that in cover depths between 30-50 mm, the marine exposure condition has very little effect on the predicted 50-year chloride concentrations. This is explored in more detail in Section 5.3.6.

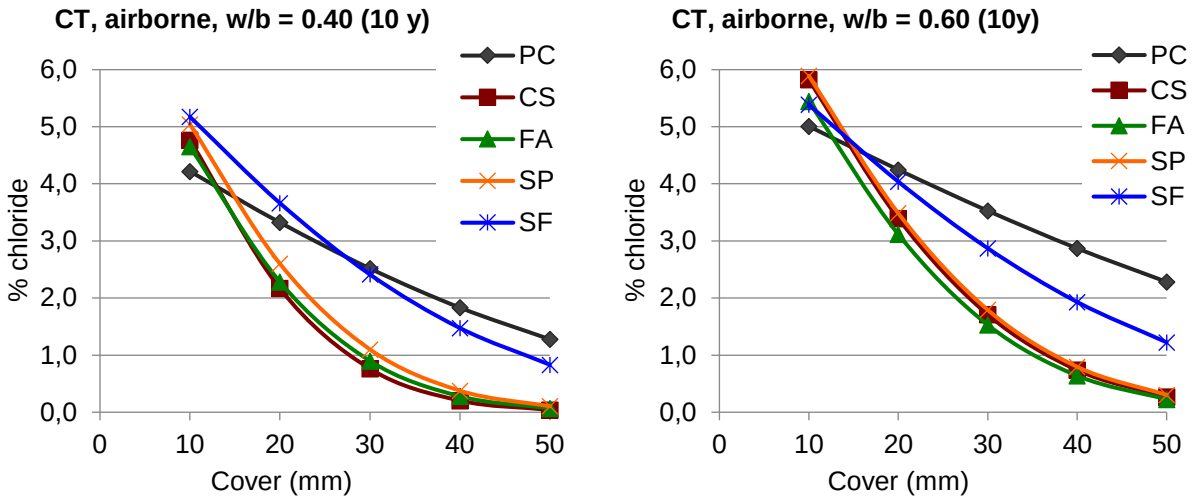

Figure 5.10: Predicted chloride profiles after 50 years, CT airborne, cut-off point: 10 years

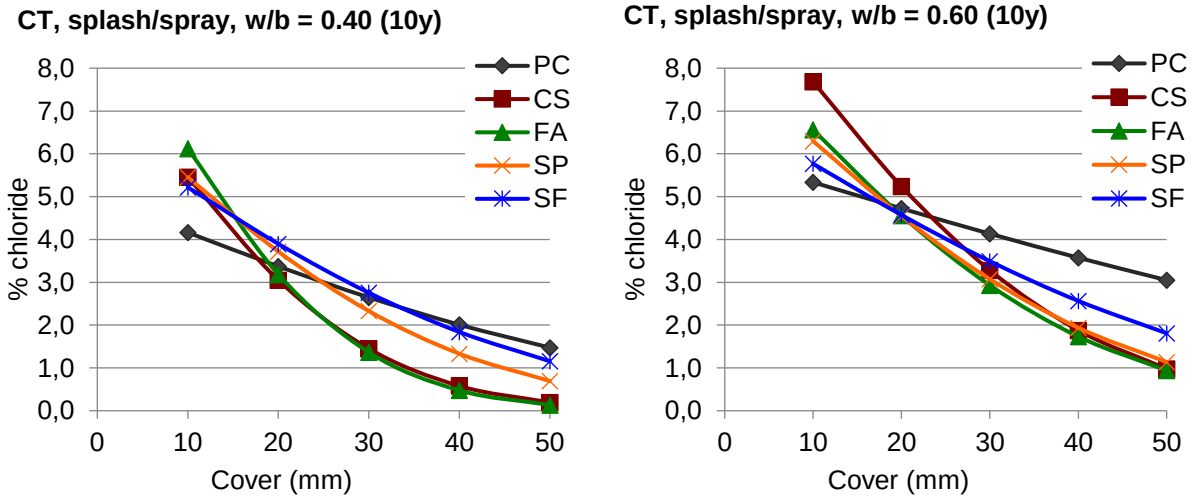

Figure 5.11: Predicted chloride profiles after 50 years, CT splash/spray, cut-off point: 10 years

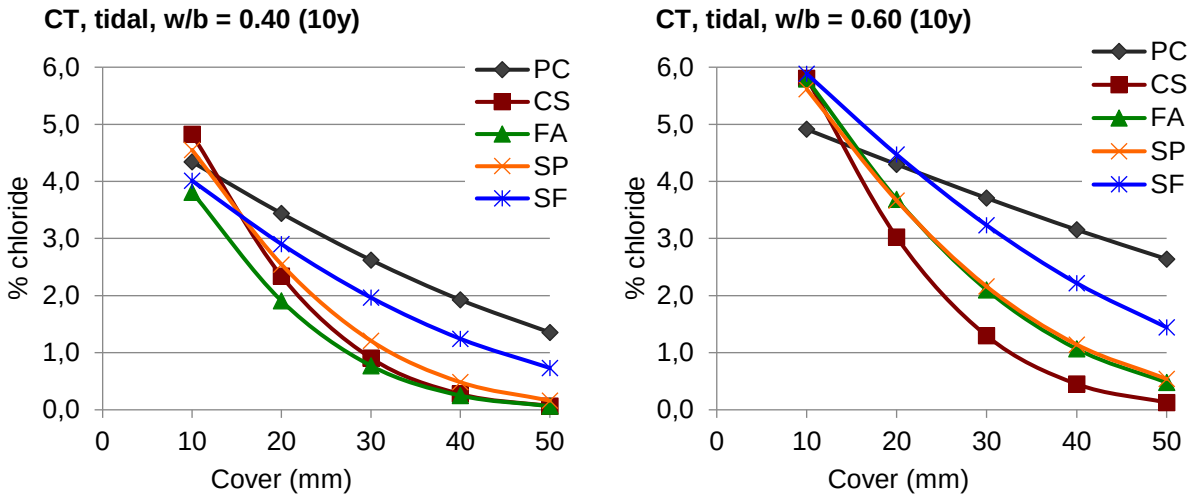

Figure 5.12: Predicted chloride profiles after 50 years, CT tidal zone, cut-off point: 10 years

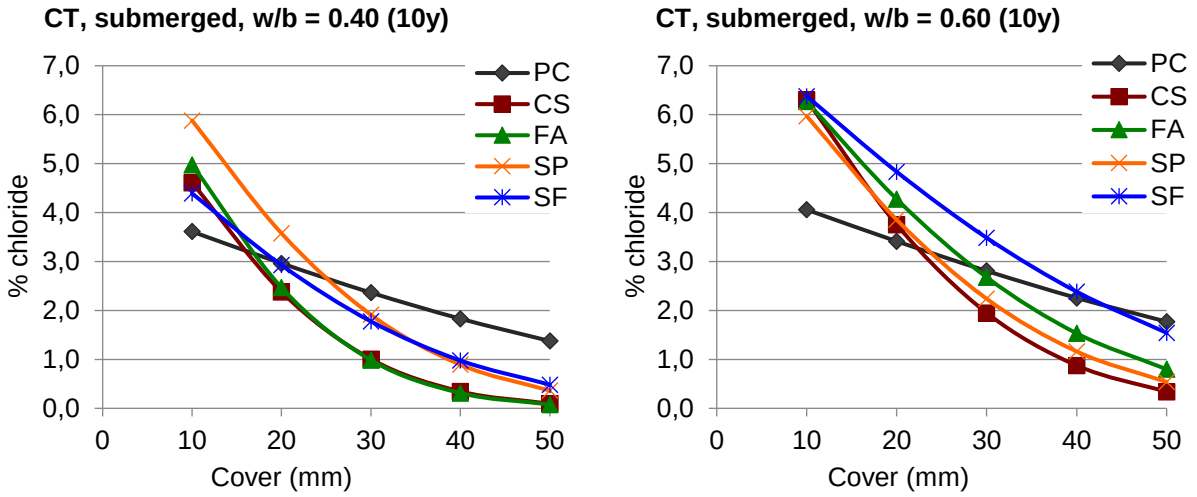

Figure 5.13: Predicted chloride profiles after 50 years, CT submerged, cut-off point: 10 years

Chloride predictions for a cut-off point of 20 years for blended cement concrete

The predicted chloride profiles in Cape Town for an exposure period of 50 years and a cut-off point of 20 years for concretes with blended cements are shown in Figures 5.14 to 5.17. Notably, using this later cut-off point, chloride surface concentrations in blended cement concretes are higher, compared to a cut-off point of 10 years. Consequently, PC concretes (at a cut-off point of 10 years) generally have significantly lower chloride surface concentrations, compared to concrete made with blended cements. The reasons for this have been discussed in previous sections and relate mainly to high n-values in blended concretes, which result in a steady increase in chloride surface concentrations with time (in this case up to 20 years). The other consequence of using a cut-off point of 20 years instead of 10 years for the blended cement concretes is that a lower apparent diffusion coefficient is used in the modelling of long-term chloride ingress, due to high m-values. As an overall result, chloride profiles modelled with a cut-off point of 20 years are much steeper and have higher chloride concentrations at the surface, and at the same time lower chloride concentrations inside the concrete, compared to a cut-off point of 10 years. The only exception to this are the SF concretes, which are not

significantly affected by the different cut-off points, which is due to lower n- and m-values, compared to the other blended cement concretes (compare Chapter 4).

Overall, using a cut-off point of 20 years, compared to 10 years, for blended cement concretes results in a less conservative, but notionally more realistic performance prediction. The difference between PC concrete and concrete made with binary blends becomes more apparent, as predicted chloride concentrations inside the concrete are now significantly lower for the blended cement concretes.

When comparing the performance of CS, FA and SP concretes for a cut-off point of 20 years, a similar picture as for a cut-off point of 10 years is observed, i.e. generally very similar chloride profiles are observed for the predicted 50-year data.

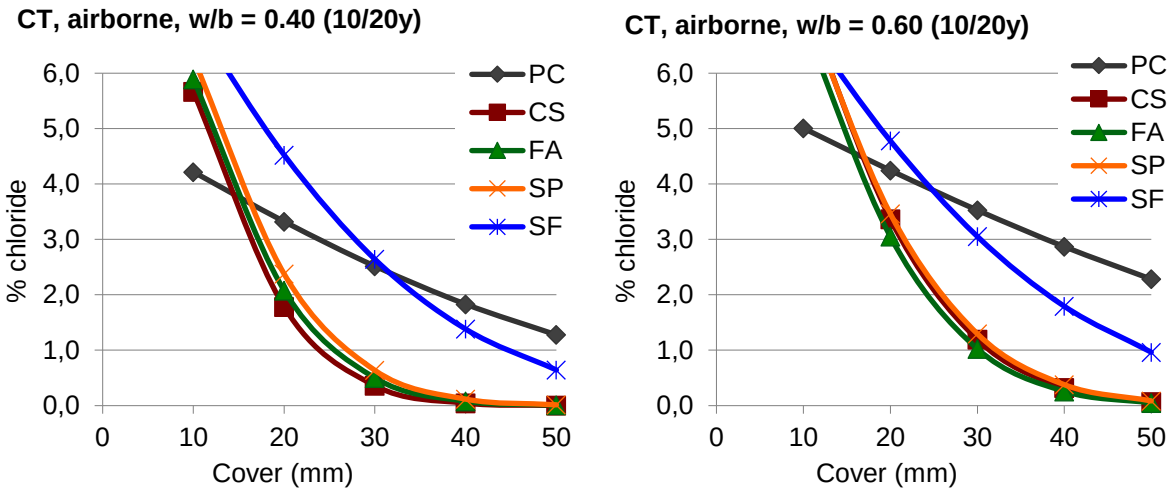

Figure 5.14: Predicted chloride profiles after 50 years, CT airborne, cut-off point: 20 years (blended cement) or 10 years (PC)

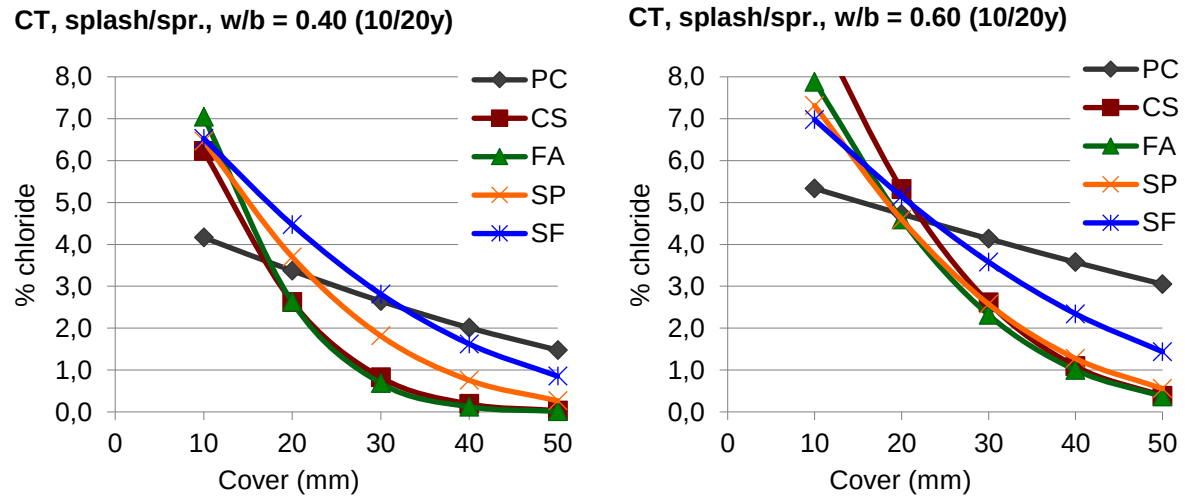

Figure 5.15: Predicted chloride profiles after 50 years, CT splash/spray, cut-off point: 20 years (blended cement) or 10 years (PC)

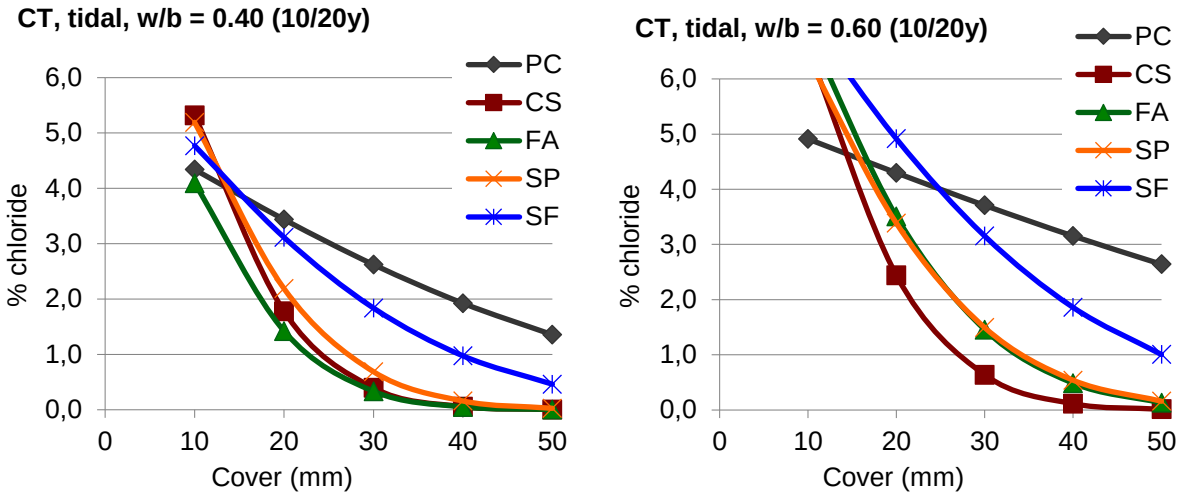

Figure 5.16: Predicted chloride profiles after 50 years, CT tidal zone, cut-off point: 20 years (blended cement) or 10 years (PC)

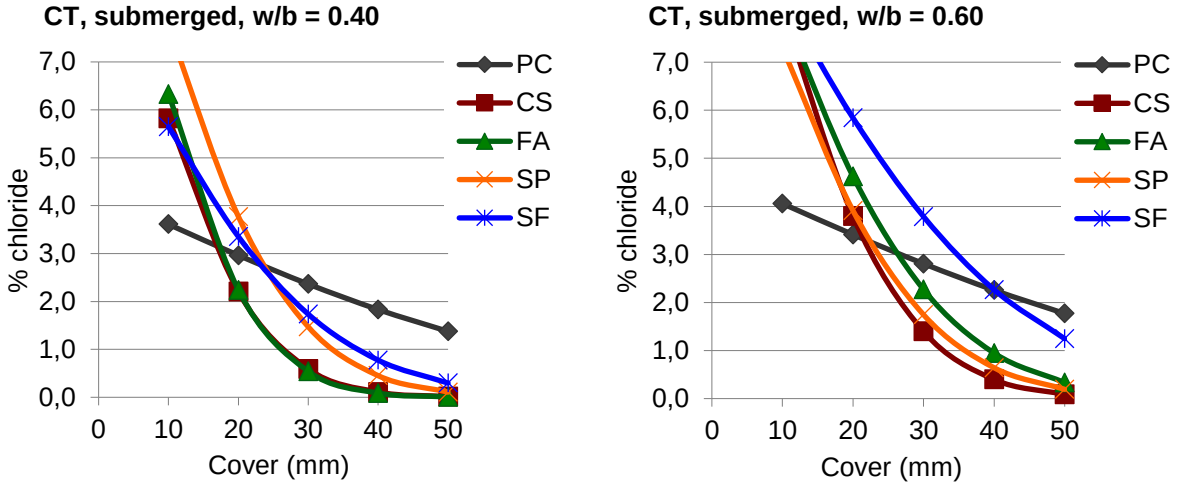

Figure 5.17: Predicted chloride profiles after 50 years, CT submerged, cut-off point: 20 years (blended cement) or 10 years (PC)

5.3.5 Influence of binder type (Durban)

The 50-year chloride profiles predicted for Durban, based on a cut-off point of 10 years, are shown in Figures 5.18 to 5.21. In general, the same trends as discussed for the Cape Town exposure are observed here. The performance of BS and FA concrete was generally similar, PC concrete having significantly higher chloride concentrations. These trends are investigated further in Section 5.3.7.

Figure 5.18 shows an unexpected chloride profile for PC concrete at a w/b ratio of 0.60, which is a result of unexpectedly low measured chloride surface concentrations.

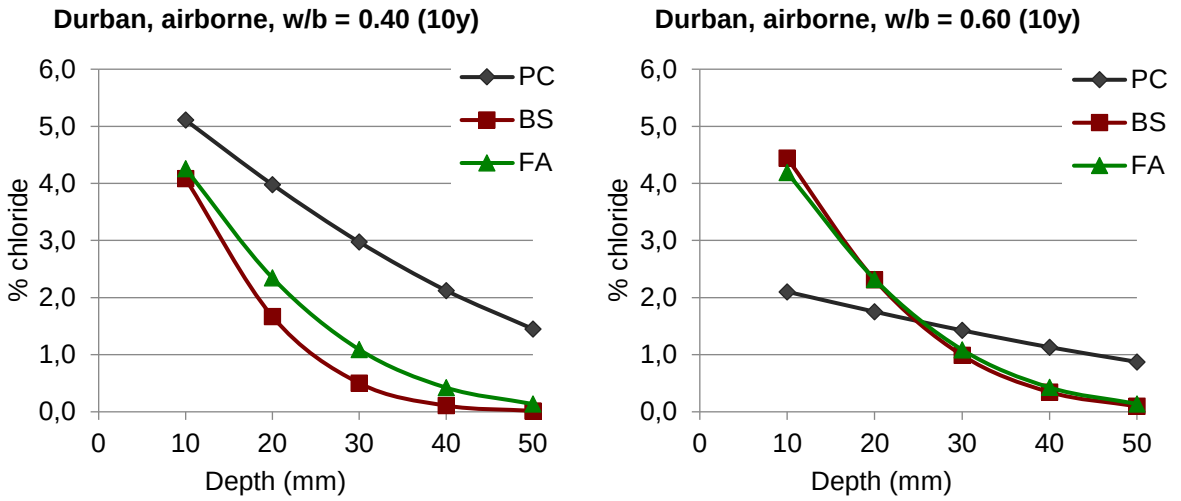

Figure 5.18: Predicted chloride profiles after 50 years, Durban airborne, cut-off point: 10 years

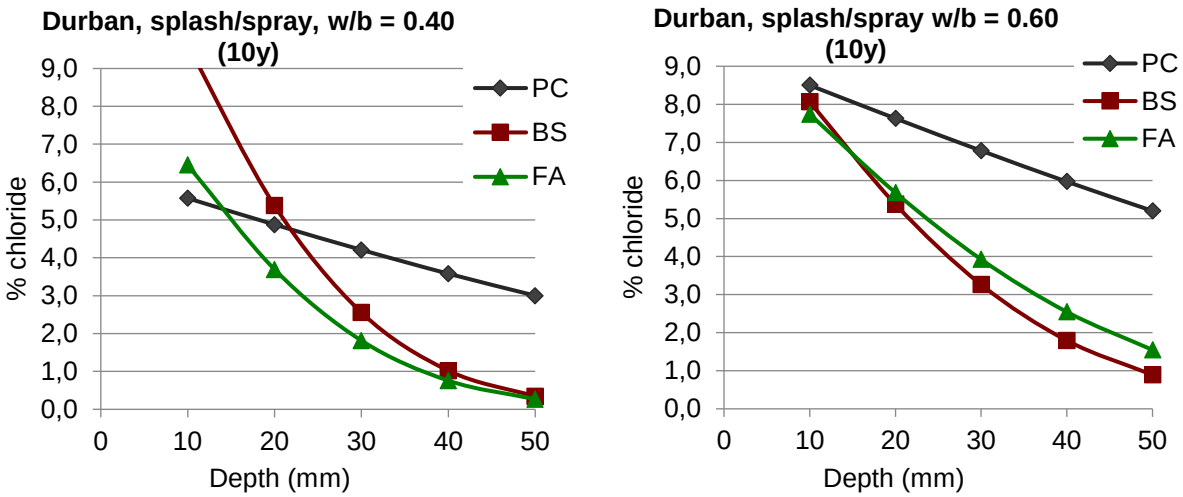

Figure 5.19: Predicted chloride profiles after 50 years, Durban splash/spray, cut-off point: 10 years

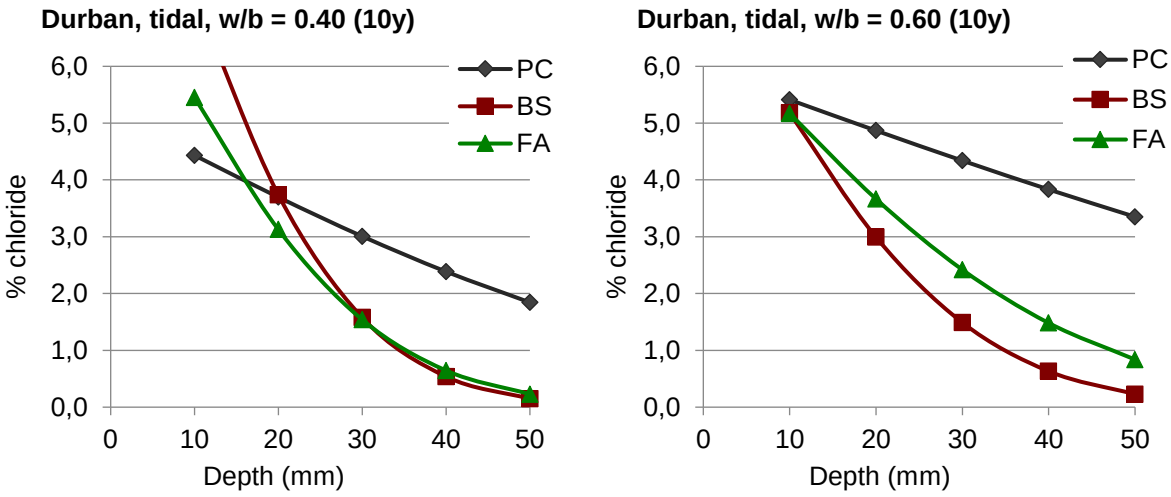

Figure 5.20: Predicted chloride profiles after 50 years, Durban tidal, cut-off point: 10 years

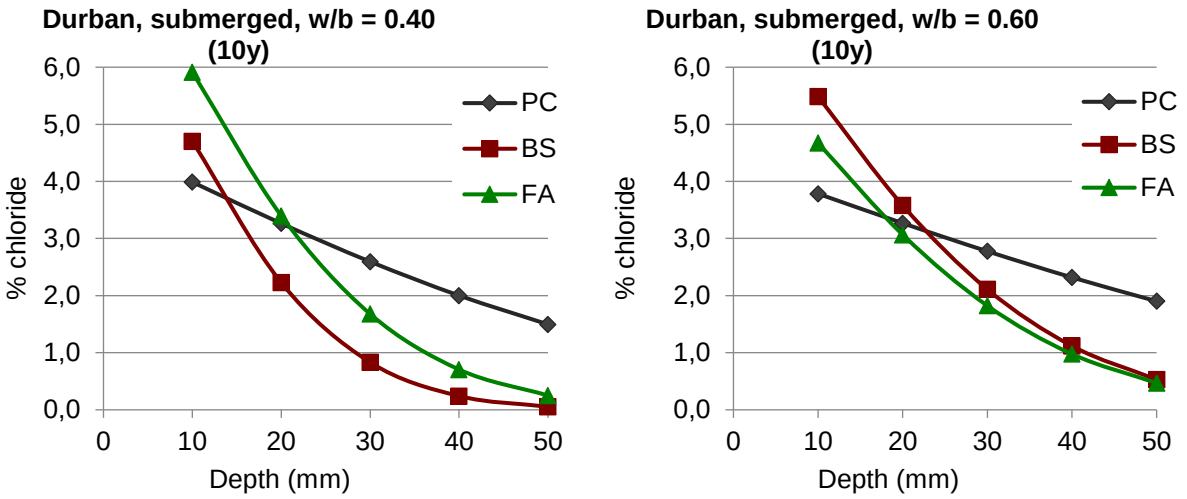

Figure 5.21: Predicted chloride profiles after 50 years, Durban submerged, cut-off point: 10 years

Chloride predictions for a cut-off point of 20 years for blended cement concrete

The predicted chloride profiles for a cut-off point of 20 years for concretes with blended cements in Durban are shown in Figures 5.22 to 5.25. As already observed for Cape Town samples, using this later cut-off point, chloride surface concentrations in blended cement concretes are higher, compared to a cut-off point of 10 years. Again, using a cut-off point of 20 years instead of 10 years for concretes with blended cements results in a less conservative chloride ingress prediction. This aspect is explored in more depth in Section 5.3.8.

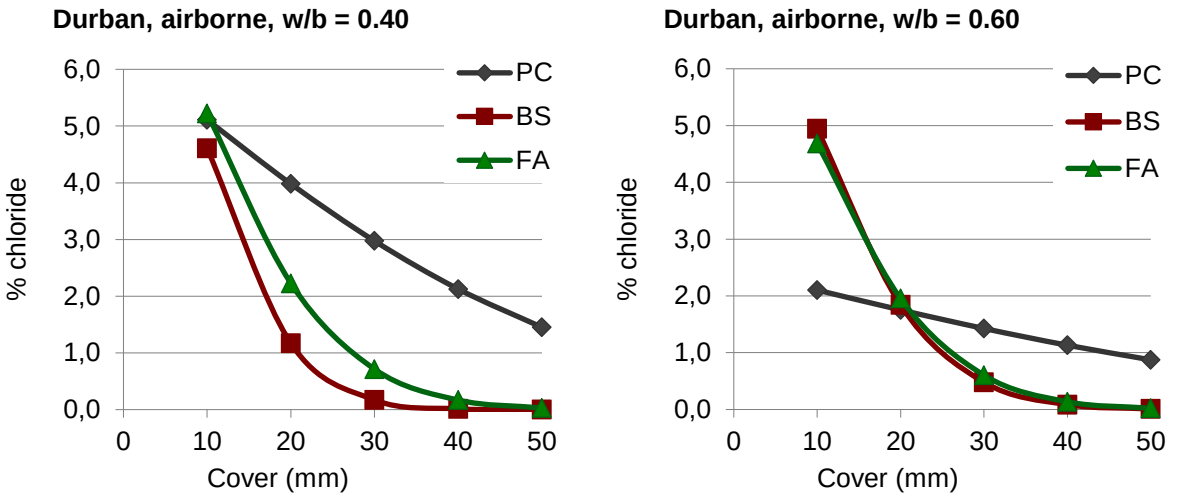

Figure 5.22: Predicted chloride profiles after 50 years, Durban airborne, cut-off point: 20 years (blended cement) or 10 years (PC)

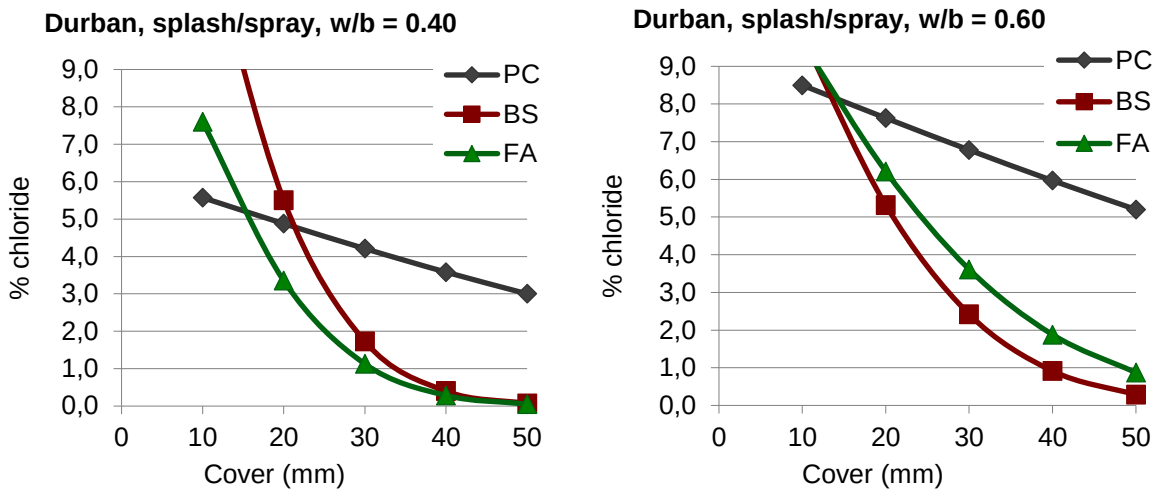

Figure 5.23: Predicted chloride profiles after 50 years, Durban splash/spray, cut-off point: 20 years (blended cement) or 10 years (PC)

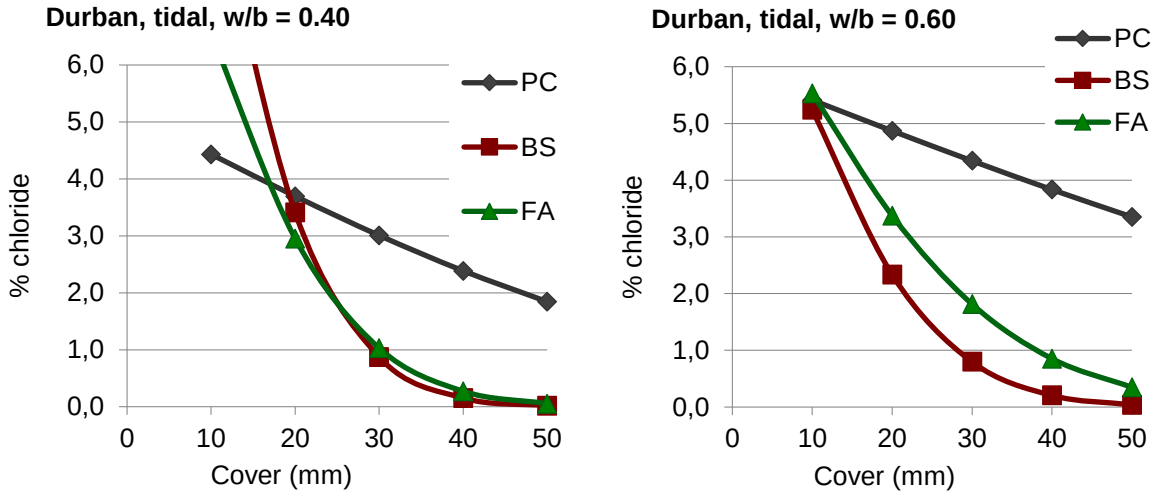

Figure 5.24: Predicted chloride profiles after 50 years, Durban tidal, cut-off point: 20 years (blended cement) or 10 years (PC)

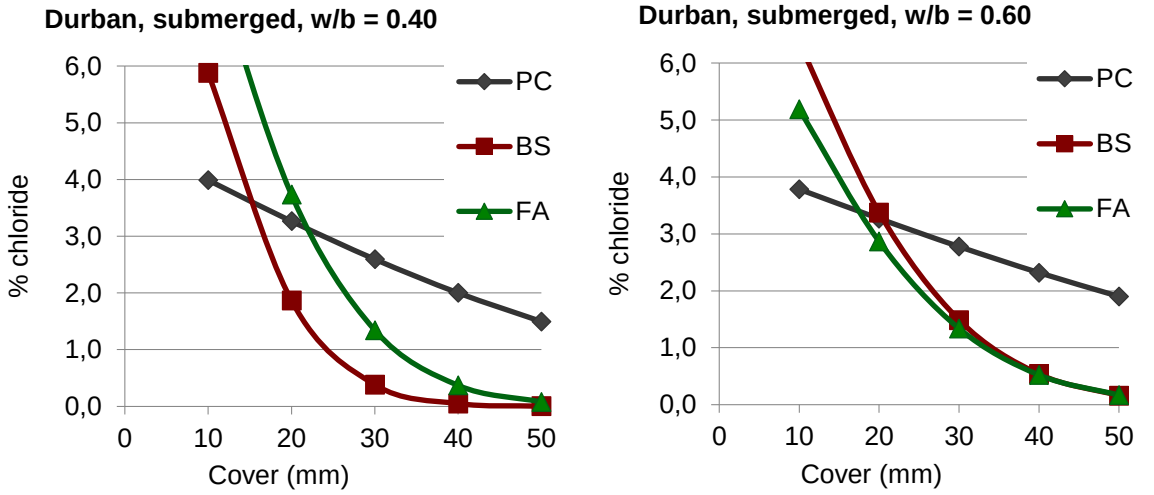

Figure 5.25: Predicted chloride profiles after 50 years, Durban submerged, cut-off point: 20 years (blended cement) or 10 years (PC)

5.3.6 Service life duration (Cape Town)

The long-term chloride profiles discussed in previous sections were used to give a quantitative estimate for the expected service life duration. In the modelling, the end of the service life was assumed to correspond to the time of corrosion initiation, i.e. the time when the chloride concentration at the cover depth to the reinforcing steel exceeds 0.4% by mass of cement. This is a very simplified approach, as reinforcement corrosion and the related service life of concrete structures depends on many factors other than chloride concentration at the depth of the steel, including cracking, concrete resistivity, oxygen and moisture availability, temperature, corrosion propagation and associated damage, etc. Further, concrete with different binder types can be expected to have different chloride threshold values for reinforcement corrosion initiation. However, no common agreement can be found in literature on the quantitative effect of the above-mentioned factors that are known to influence reinforcement corrosion. Consequently, a commonly used approach is to consider the service life duration to correspond to the time when the chloride concentration at the level of the steel exceeds the assumed chloride threshold of 0.4% by mass of cement. In the scope of this research, the same approach was therefore adopted to evaluate the influence of various parameters on the service life of reinforced concrete structures in the marine environment.

The influence of binder type on the predicted service life duration, for a consistent cut-off point of 10 years, is shown in Figures 5.26 to 5.29 for the various marine exposure conditions and water/binder ratios. The influences of w/b ratio and exposure conditions are discussed separately below.

For the Cape Town exposure it was generally observed that concrete containing CS and FA have significantly higher predicted service life durations, compared to the other binder types. For concretes with a w/b ratio of 0.4, the performance of FA and CS concrete is very similar, indicating that the two binder types at the selected PC replacement levels (50% for CS and 30% for FA) result in equally good chloride ingress characteristics. The same was observed for concrete with a w/b ratio of 0.6 in the airborne and splash/spray exposure zones. However, for concrete with w/b of 0.6 in the tidal and submerged zones, CS concrete had notably better performance, compared to concrete containing FA.

Concrete containing SP generally shows slightly less favourable performance compared to concrete containing FA and CS, and more favourable performance compared to PC and SF concrete. The reason for SP to be performing poorer than FA could be related to the alumina content in the binder.

Concrete containing PC always shows the worst performance, as expected. For all exposure conditions and both w/b ratios, the predicted service life duration at 50 mm does not exceed 20 years, which confirms that PC concrete is not suitable for the marine environment. Similarly, concrete containing SF was found to be not suitable for the marine environment, as predicted service life durations were generally below 40 years even at 50 mm cover. The reason for the unfavourable performance of SF concrete relates to low chloride binding capabilities, compared to other blended cements, despite the denser concrete microstructure usually obtained with SF.

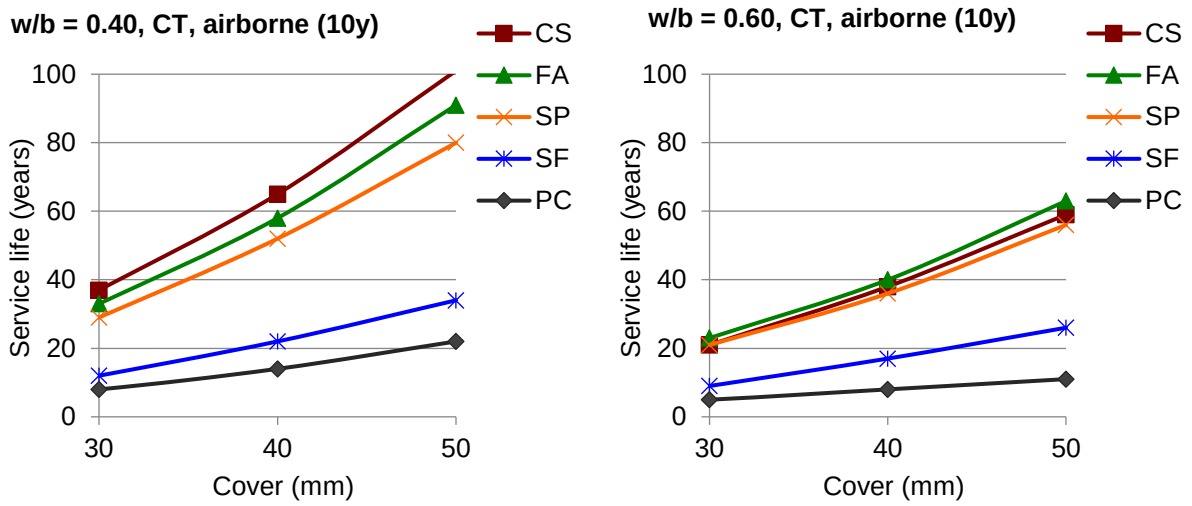

Figure 5.26: Predicted service life versus binder type, CT, airborne exposure, cut-off point: 10 years

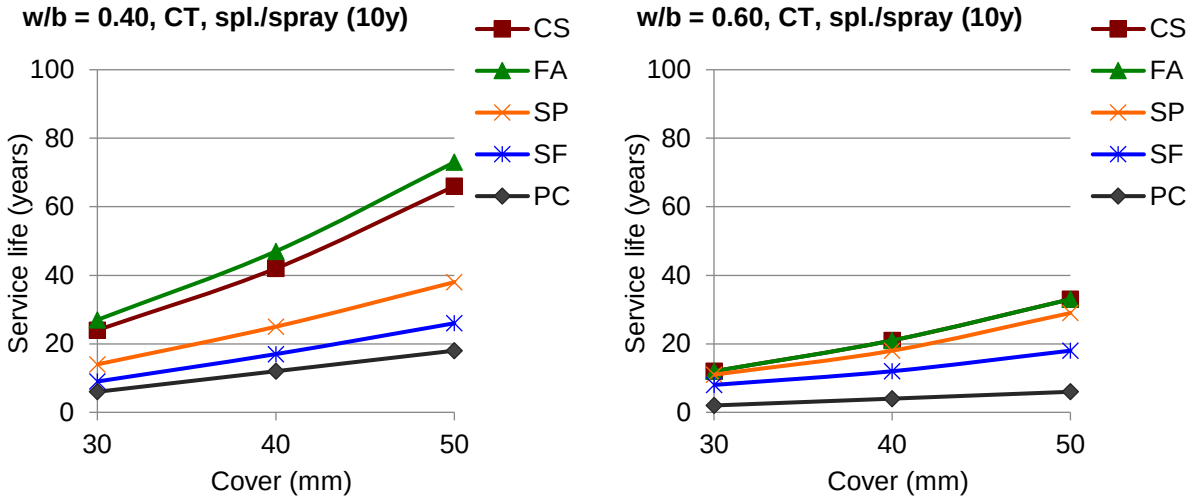

Figure 5.27: Predicted service life versus binder type, CT, splash/spray, cut-off point: 10 years

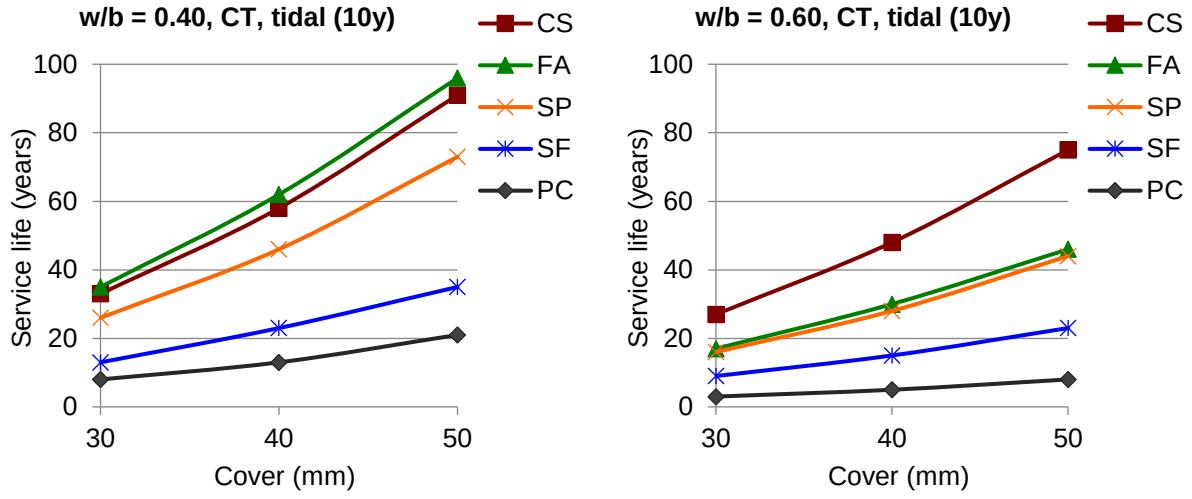

Figure 5.28: Predicted service life versus binder type, CT, tidal exposure, cut-off point: 10 years

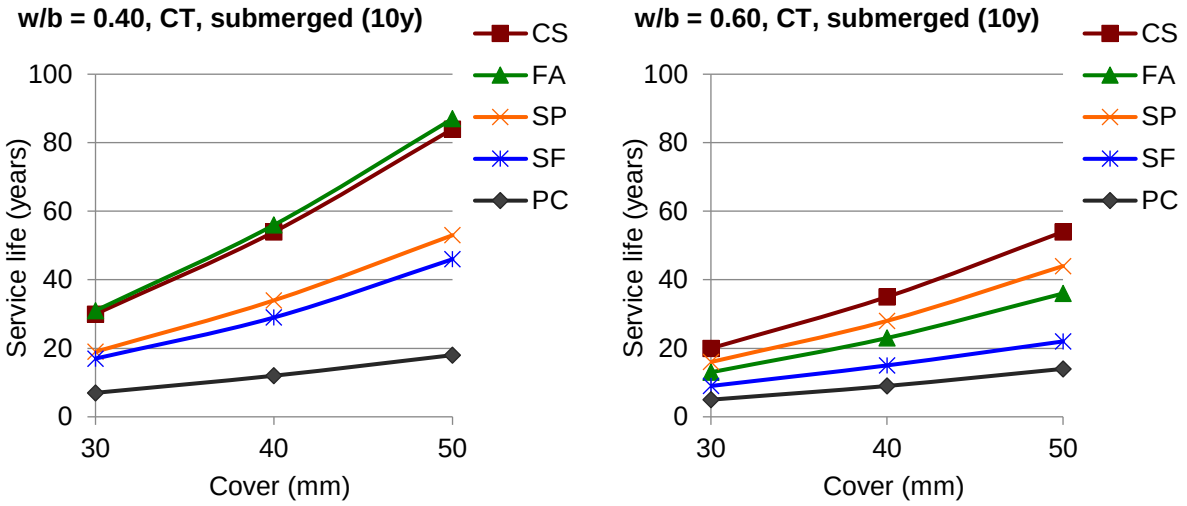

Figure 5.29: Predicted service life versus binder type, CT, submerged, cut-off point: 10 years

Service life predictions for a cut-off point of 20 years for blended cement concrete

The influence of binder type on the predicted service life duration for a cut-off point of 10 years (PC concrete) and 20 years (blended cement concretes) is shown in Figures 5.30 to 5.33. As already discussed in previous sections, the choice of a later cut-off point for blended cement concretes (i.e. 20 years instead of 10 years) results in a less conservative service life prediction. This aspect is analysed and discussed in more detail in Section 5.3.12.

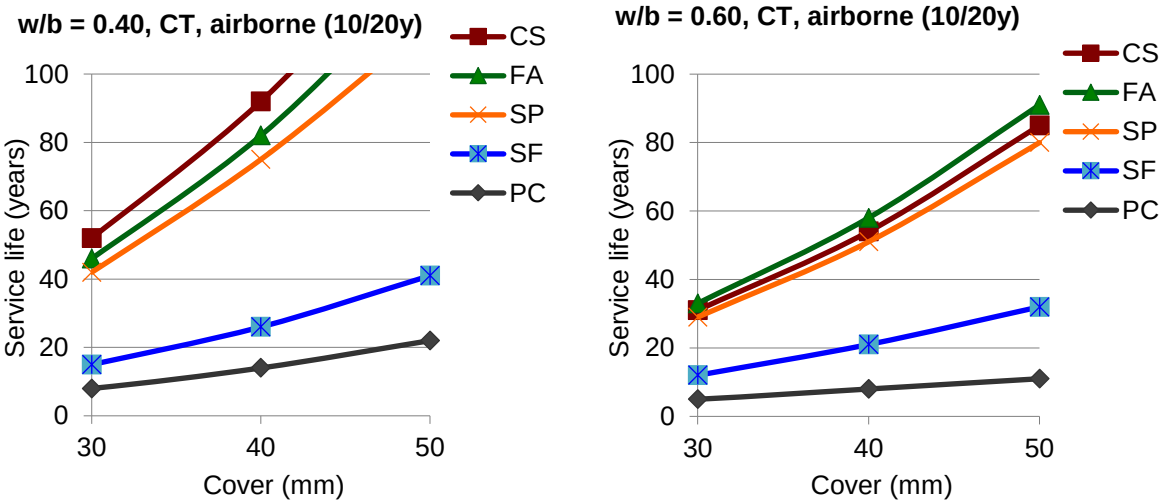

Figure 5.30: Predicted service life versus binder type, CT, airborne exposure, cut-off point: 10 years (PC) or 20 years (blended cements)

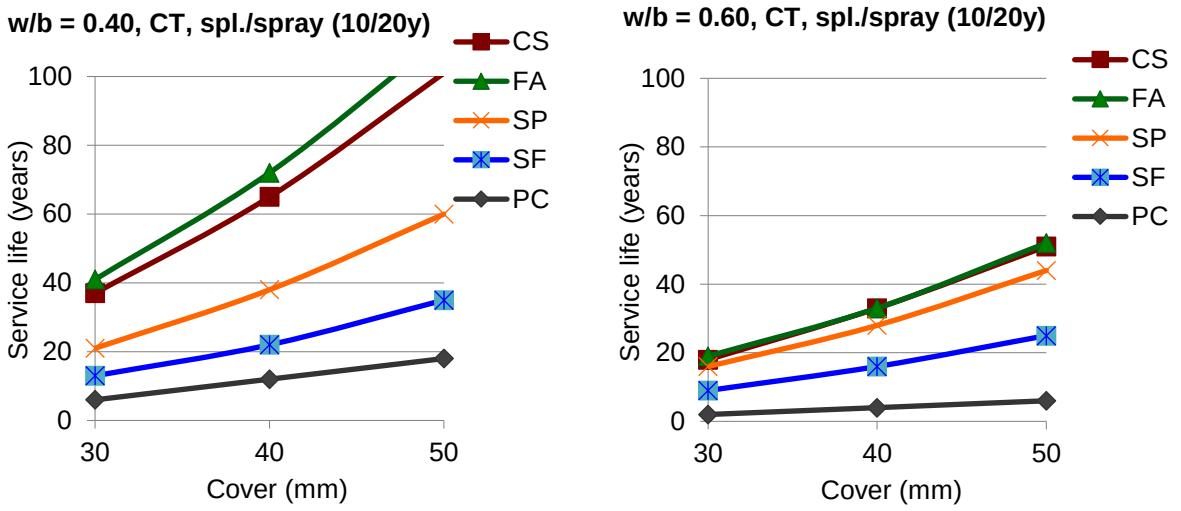

Figure 5.31: Predicted service life versus binder type, CT, splash/spray exposure, cut-off point: 10 years (PC) or 20 years (blended cements)

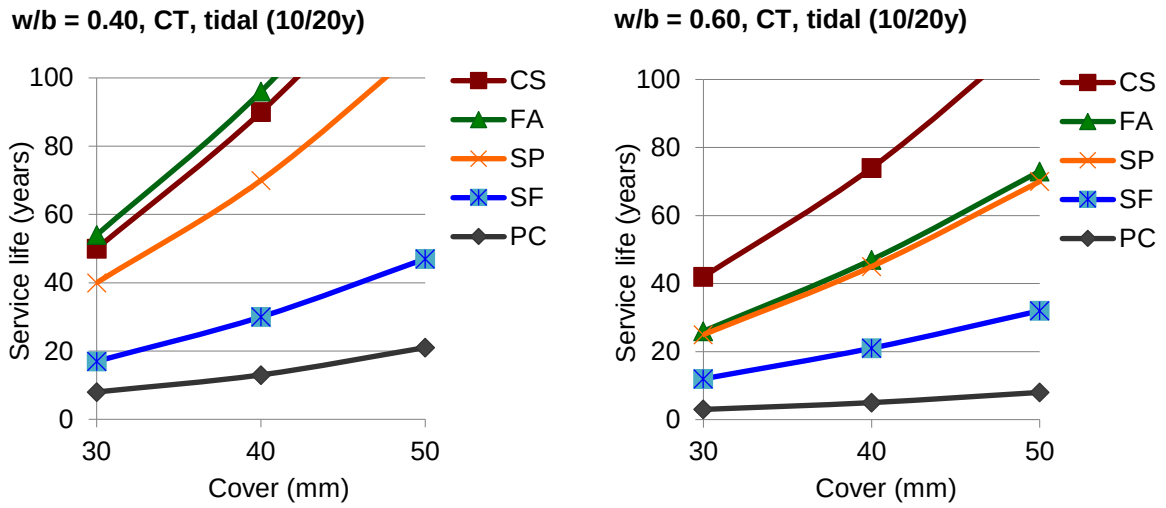

Figure 5.32: Predicted service life versus binder type, CT, tidal exposure, cut-off point: 10 years (PC) or 20 years (blended cements)

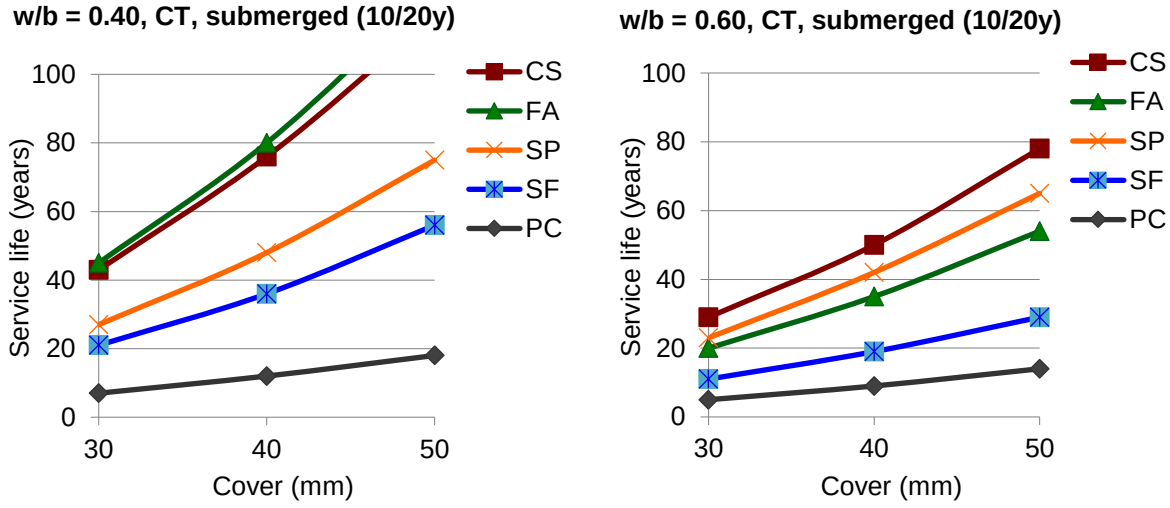

Figure 5.33: Predicted service life versus binder type, CT, submerged exposure, cut-off point: 10 years (PC) or 20 years (blended cements)

5.3.7 Service life duration (Durban)

In order to complete the data presentation for all concretes and exposure conditions investigated, Figures 5.34 to 5.37 show the predicted service life for concretes exposed in Durban, for a 10-year cut-off time. In general, the same trends as already discussed for CT exposure were identified. Differences in chloride ingress and service life prediction between Cape Town and Durban are discussed in Section 5.3.11.

Concrete containing FA and BS in Durban generally has service life predictions of the same order of magnitude, compared to concrete containing FA and CS in Cape Town, with PC concrete performing significantly less favourable in Durban. This trend becomes more apparent when considering a cut-off point of 20 years for the time development of D_a and Cs for the blended cement concretes, as presented in Figures 5.38 to 5.41.

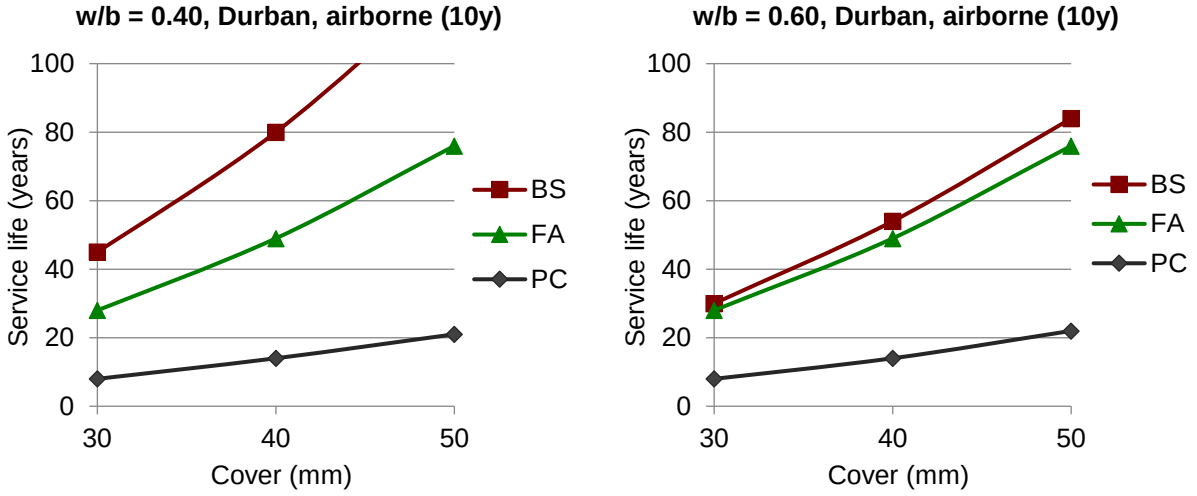

Figure 5.34: Predicted service life versus binder type, Durban airborne, cut-off point: 10y

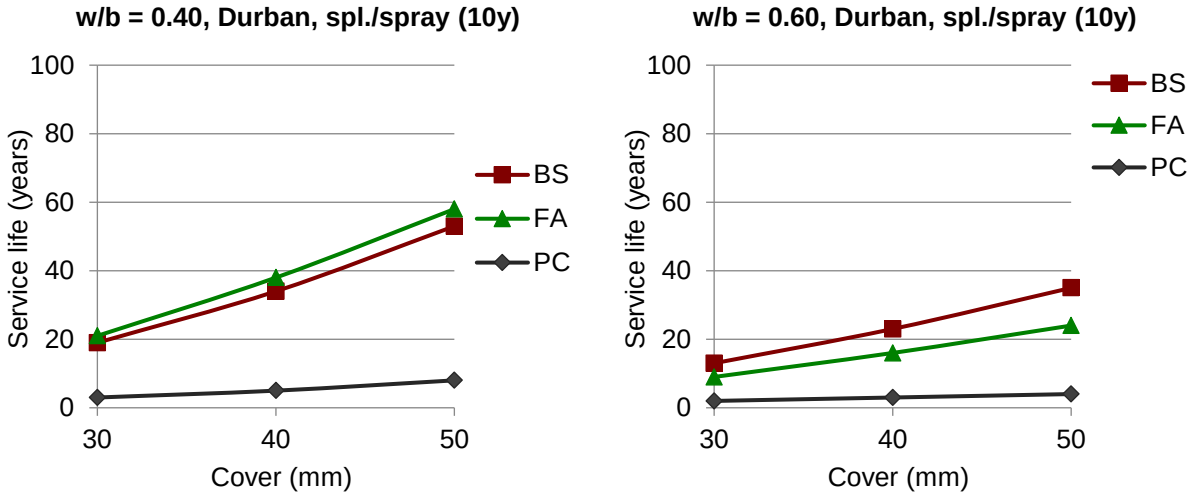

Figure 5.35: Predicted service life versus binder type, Durban splash/spray, cut-off point: 10y

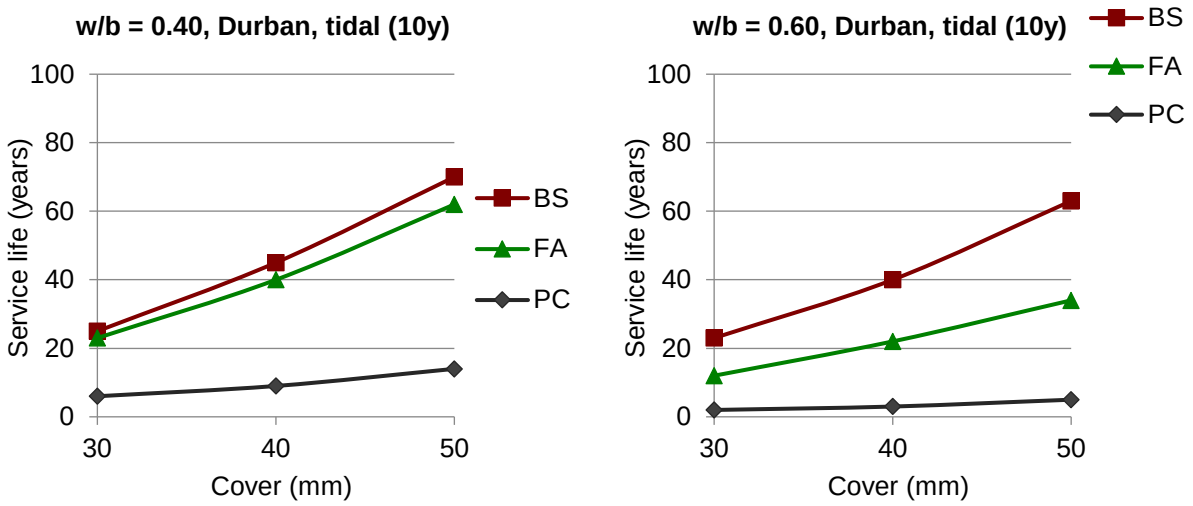

Figure 5.36: Predicted service life versus binder type, Durban tidal, cut-off point: 10y

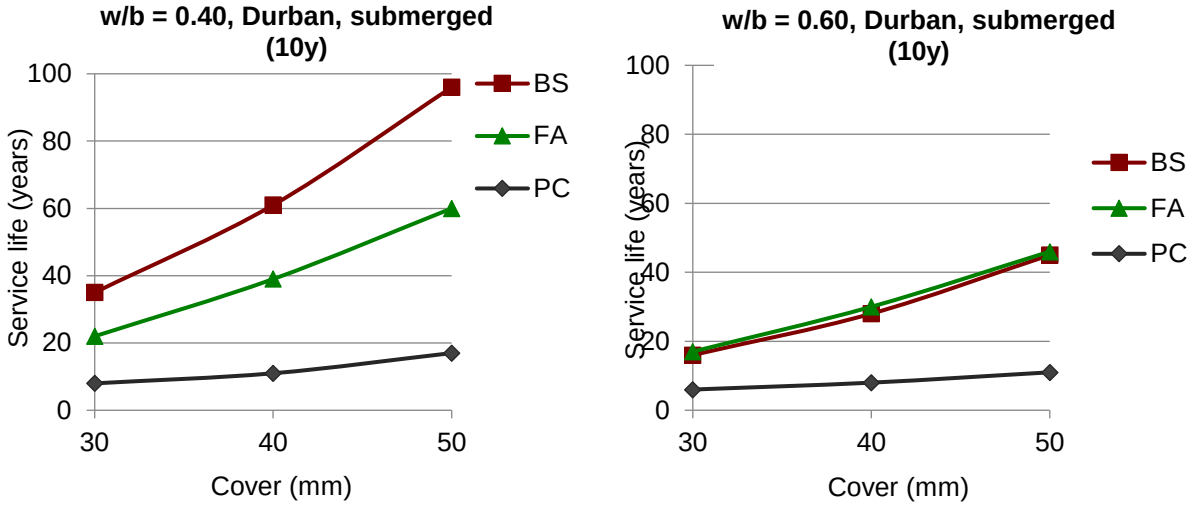

Figure 5.37: Predicted service life versus binder type, Durban submerged, cut-off point: 10y

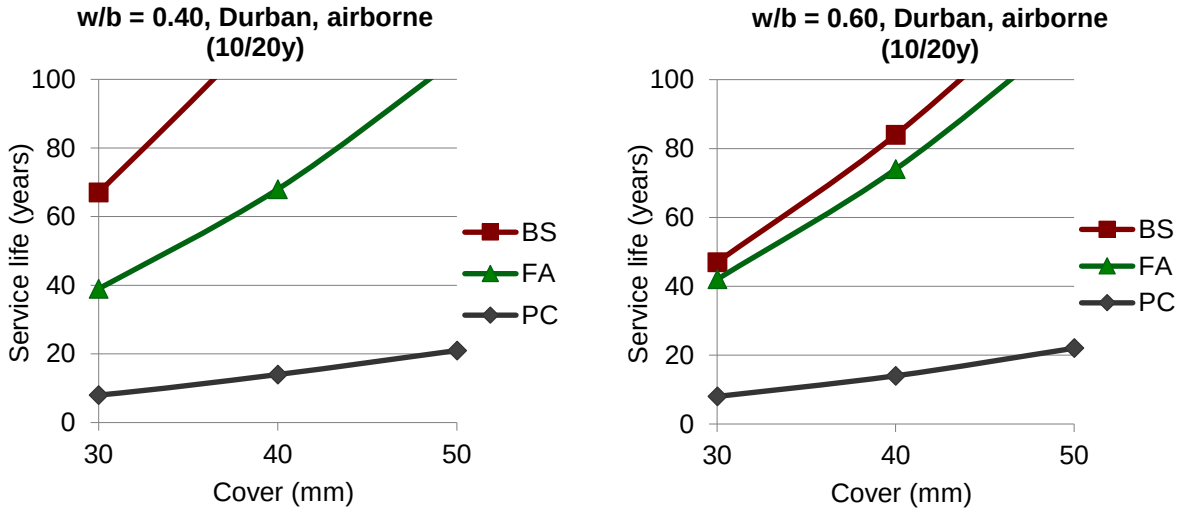

Figure 5.38: Predicted service life versus binder type, Durban airborne, cut-off point: 10/20y

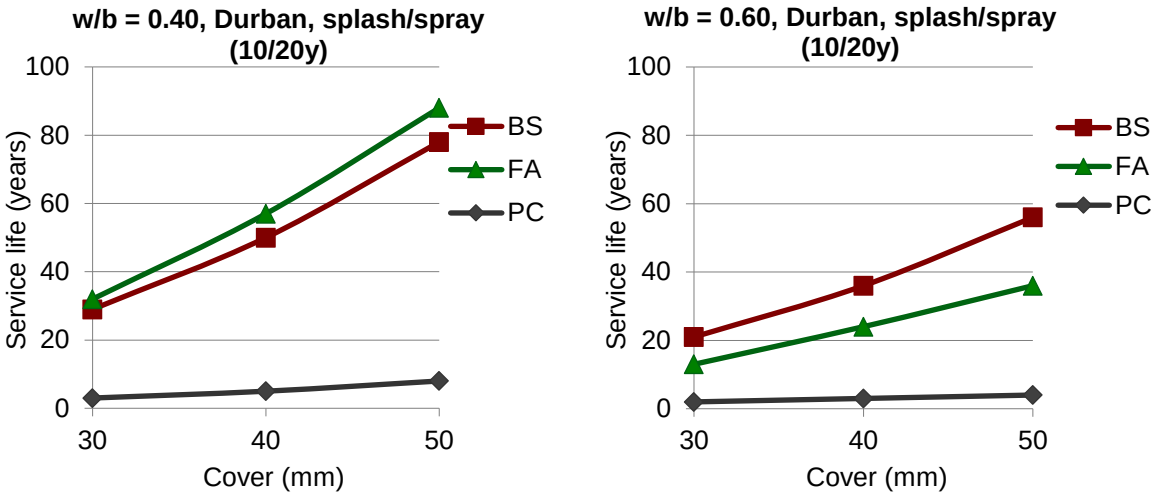

Figure 5.35: Predicted service life versus binder type, Durban splash/spray, cut-off point: 10/20y

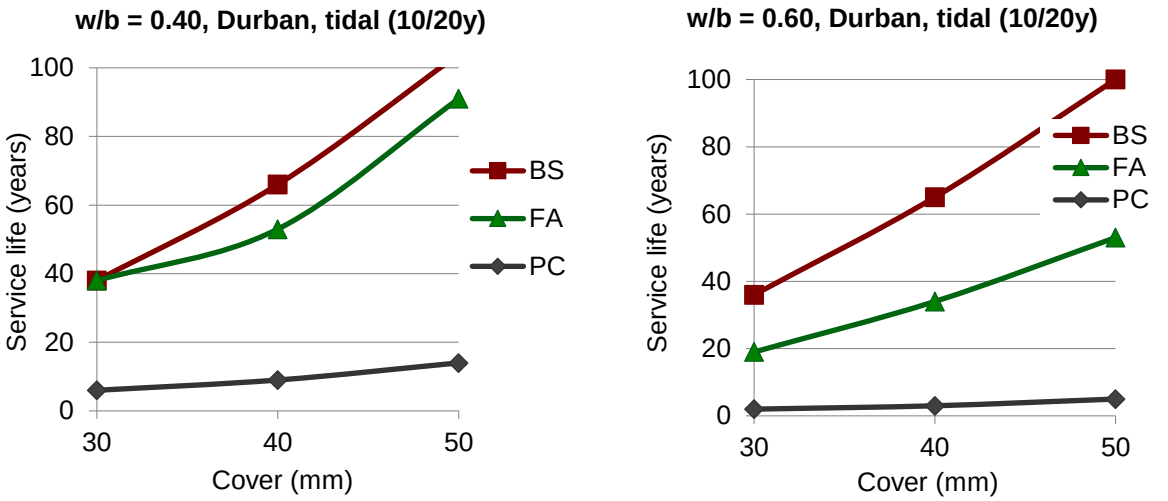

Figure 5.36: Predicted service life versus binder type, Durban tidal, cut-off point: 10/20y

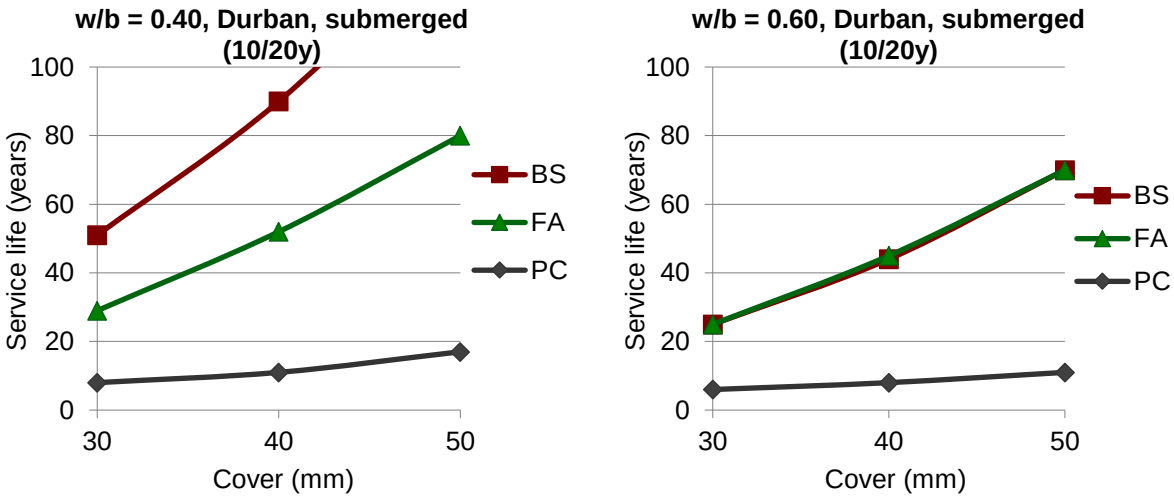

Figure 5.37: Predicted service life versus binder type, Durban submerged, cut-off point: 10/20y

5.3.8 Influence of cover depth

The influence of cover depth on the predicted service life of the various types of concrete in the respective environmental conditions can directly be seen from the graphical representations, for example for CT in Figures 5.26 to 5.29 (Section 5.3.6). In addition to the graphical presentation in previous sections, this section presents a quantification of the influence of cover depth by comparing the service life predicted for cover depths of 30 mm, 40 mm and 50 mm. This is done through the ratios of predicted service life, as shown in Tables 5.1 and 5.2 for concretes with w/b ratio of 0.40 in Cape Town and Durban, respectively. The evaluation of cover versus service life was only carried out for a cut-off point of 10 years for both PC and blended cement concretes. In general, the significance of cover depth on the service life was not affected by binder type or environmental exposure condition, which is indicated by the very similar results across all parameter combinations. Similarly, the ratios were nearly identical for Cape Town and Durban. Increasing the cover depth from 30 mm to 40 mm and from 40 mm to 50 mm results in an average increase in service life of about 80% and 50%, respectively. An increase in cover depth from 30 mm to 50 mm increases the service life duration by about 170%.

Table 5.1: Influence of cover depth on the predicted service life, CT exposure, w/b = 0.4. “Percentage of SL (50 mm)” refers to the percentage-value of the service life (in years) at a certain cover depth (here: 40 or 30 mm) compared to the service life achieved at a cover of 50 mm.

Binder	Exposure zone	Ratio SL(x mm) / SL(y mm)			Percentage of SL (50 mm)	
		50/40	40/30	50/30	40 mm	30 mm
PC	Air	1,6	1,8	2,8	64	36
	Splash	1,5	2,0	3,0	67	33
	Tidal	1,6	1,6	2,6	62	38
	Submerged	1,5	1,7	2,6	67	39
CS	Air	1,4	1,6	2,2	73	45
	Splash	1,5	2,0	3,0	67	33
	Tidal	1,6	1,7	2,7	63	38
	Submerged	1,6	1,8	2,8	64	36
FA	Air	1,6	1,8	2,7	64	37
	Splash	1,6	1,8	2,8	64	36
	Tidal	1,6	1,8	2,8	64	36
	Submerged	1,6	1,8	2,8	64	36
SP	Air	1,6	1,8	2,8	64	36
	Splash	1,6	1,8	2,8	64	36
	Tidal	1,6	1,8	2,8	64	36
	Submerged	1,5	1,8	2,7	65	37
SF	Air	1,6	1,8	2,8	64	36
	Splash	1,6	1,7	2,7	64	37
	Tidal	1,5	1,8	2,7	65	36
	Submerged	1,6	1,8	2,8	64	36
	Average	**1,5**	**1,8**	**2,7**	**65**	**37**

Table 5.2: Influence of cover depth on the predicted service life, Durban exposure, w/b = 0.4

Binder	Exposure zone	Ratio SL(x mm) / SL(y mm)			Percentage of SL(50 mm)	
		50/40	40/30	50/30	40 mm	30 mm
PC	Air	1,5	1,8	2,6	67	38
	Splash	1,6	1,7	2,7	63	38
	Tidal	1,6	1,5	2,3	64	43
	Submerged	1,5	1,4	2,1	65	47
CS	Air	1,6	1,8	2,8	64	36
	Splash	1,6	1,8	2,8	64	36
	Tidal	1,6	1,8	2,8	64	36
	Submerged	1,6	1,7	2,7	64	36
FA	Air	1,6	1,8	2,7	64	37
	Splash	1,5	1,8	2,8	66	36
	Tidal	1,6	1,7	2,7	65	37
	Submerged	1,5	1,8	2,7	65	37
	Average	**1,6**	**1,7**	**2,6**	**64**	**38**

5.3.9 Influence of w/b ratio

The w/b ratio influences the microstructure and penetrability of concrete and is therefore generally considered one of the most relevant mix design parameters in relation to the expected durability performance. In the experimental research, two w/b ratios were used, i.e. w/b = 0.4 and w/b = 0.6. The influence of w/b ratio on chloride ingress was evaluated by calculating the ratio between the predicted service life duration of concrete with a w/b ratio of 0.4 and that of concrete with a w/b ratio of 0.6. This is considered to give a useful practical indication for the relevance of w/b ratio in the design of durable concrete structures in the marine environment. This evaluation of w/b ratio versus service life was only carried out for a cut-off point of 10 years for both PC and blended cement concretes.

Tables 5.1 and 5.2 show the outcome of the modelling for samples exposed in Cape Town and Durban, respectively. For Cape Town exposure, the average ratio of the predicted service life between concretes with w/b ratios of 0.4 and 0.6 ranges between 1.4 and 2.2, with individual values ranging from 1.2 to 3.0. For samples exposed in Durban, the scatter of average values ranged from 1.6 to 1.8. In general, cover depth and exposure condition had no significant influence on the ratios. Similarly, no consistent relationship between binder type and the influence of w/b ratio on chloride ingress was found in terms of these ratios. Remarkably, for each exposure environment, the average ratio across all cover depths for a particular binder type was close to identical. The overall average ratio, across all scenarios investigated is about 1.8.

PC concrete had the highest ratio in both Cape Town and Durban environments, indicating that the w/b ratio has a comparatively higher influence on the service life, compared to concrete containing blended cements.

Table 5.3: Influence of w/b ratio on the predicted service life, CT exposure

Binder	Exposure zone	Service life ratio between w/b = 0.4 and w/b = 0.6 (SL40 / SL60)				
		Cover depth			Average	Average each binder
		50	40	30		
PC	Air	2,0	1,8	1,6	1,8	2,2
	Splash	3,0	3,0	3,0	3,0	
	Tidal	2,6	2,6	2,7	2,6	
	Submerged	1,3	1,3	1,4	1,3	
CS	Air	1,7	1,7	1,8	1,7	1,6
	Splash	2,0	2,0	2,0	2,0	
	Tidal	1,2	1,2	1,2	1,2	
	Submerged	1,6	1,5	1,5	1,5	
FA	Air	1,4	1,5	1,4	1,4	2,0
	Splash	2,2	2,2	2,3	2,2	
	Tidal	2,1	2,1	2,1	2,1	
	Submerged	2,4	2,4	2,4	2,4	
SP	Air	1,4	1,4	1,4	1,4	1,4
	Splash	1,3	1,4	1,3	1,3	
	Tidal	1,7	1,6	1,6	1,6	
	Submerged	1,2	1,2	1,2	1,2	
SF	Air	1,3	1,3	1,3	1,3	1,5
	Splash	1,4	1,4	1,1	1,3	
	Tidal	1,5	1,5	1,4	1,5	
	Submerged	2,1	1,9	1,9	2,0	
	Average	1,78	1,76	1,73	**1,8**	

Table 5.4: Influence of w/b ratio on the predicted service life, Durban exposure

Binder	Exposure zone	Service life ratio between w/b = 0.4 and w/b = 0.6 (SL40 / SL60)				
		Cover depth			Average	Average each binder
		50	40	30		
PC	Air	1,0	1,0	1,0	1,0	1,8
	Splash	2,0	1,7	1,5	1,7	
	Tidal	2,8	3,0	3,0	2,9	
	Submerged	1,5	1,4	1,3	1,4	
BS	Air	1,5	1,5	1,5	1,5	1,6
	Splash	1,5	1,5	1,5	1,5	
	Tidal	1,1	1,1	1,1	1,1	
	Submerged	2,1	2,2	2,2	2,2	
FA	Air	1,0	1,0	1,0	1,0	1,6
	Splash	2,4	2,4	2,3	2,4	
	Tidal	1,8	1,8	1,9	1,9	
	Submerged	1,3	1,3	1,3	1,3	
	Average	1,67	1,65	1,63	**1,7**	

5.3.10 Influence of marine exposure zones

The results of the predicted service life durations in relation to the exposure zone are shown in Figures 5.38 to 5.40. As with the other parameter comparisons, this evaluation was only carried out for a cut-off point of 10 years for both PC and blended cement concretes.

In general, the influence of marine exposure zone on chloride ingress was found to be less pronounced than expected, especially for PC concrete. For all samples exposed in Cape Town, no clear trend could be established, except that the splash/spray zone consistently resulted in the shortest predicted service life duration. For all other exposure conditions, similar service life durations were found, and no clear trend emerged. Similarly, the splash/spray zone also resulted in the shortest service life predictions for samples exposed in Durban. However, samples exposed to airborne chlorides in Durban generally showed an appreciably longer service life, compared to the other exposure zones.

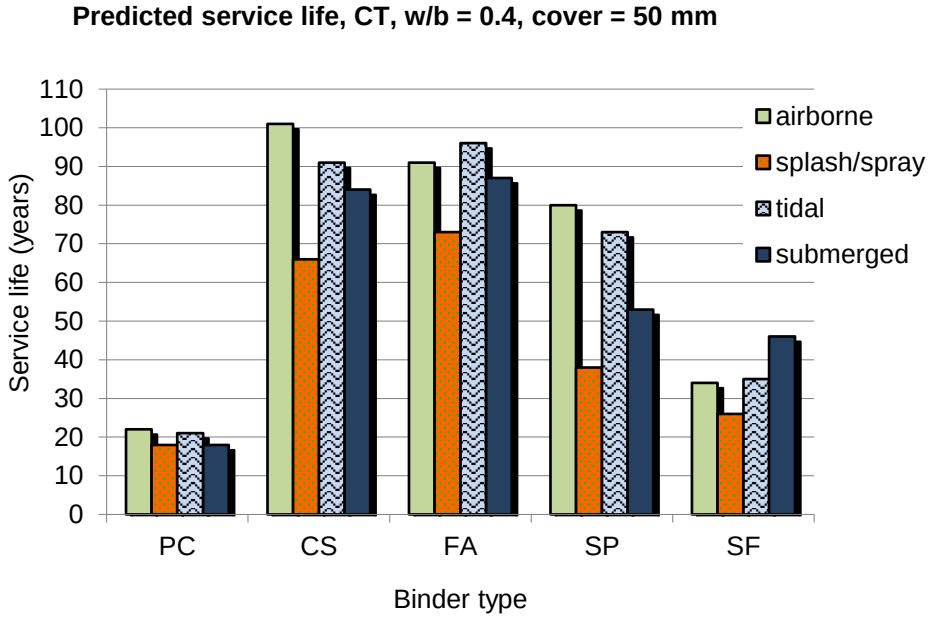

Figure 5.38: Predicted service life, CT, w/b =0.4, cover = 50mm

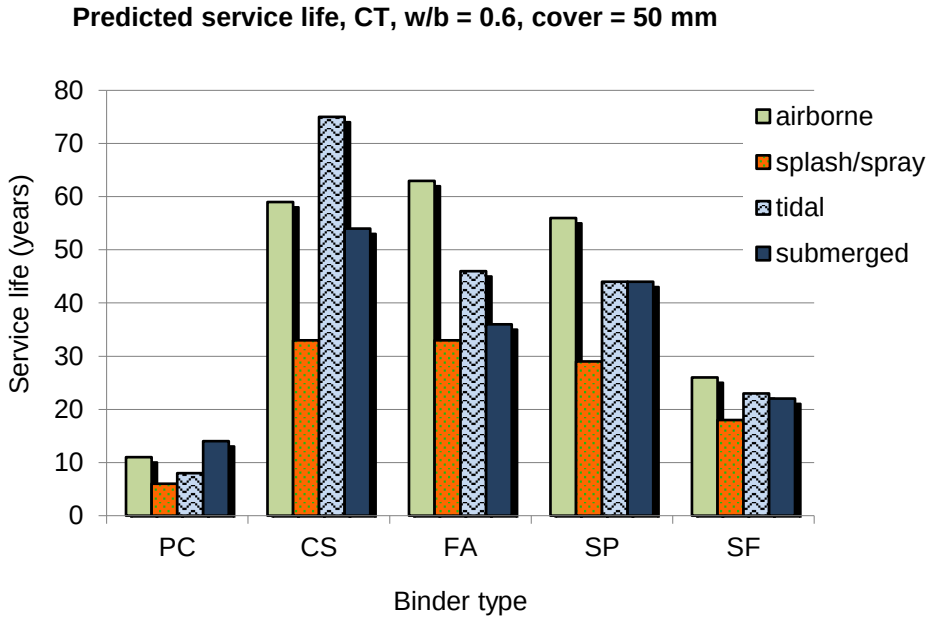

Figure 5.39: Predicted service life, CT, w/b =0.6, cover = 50mm

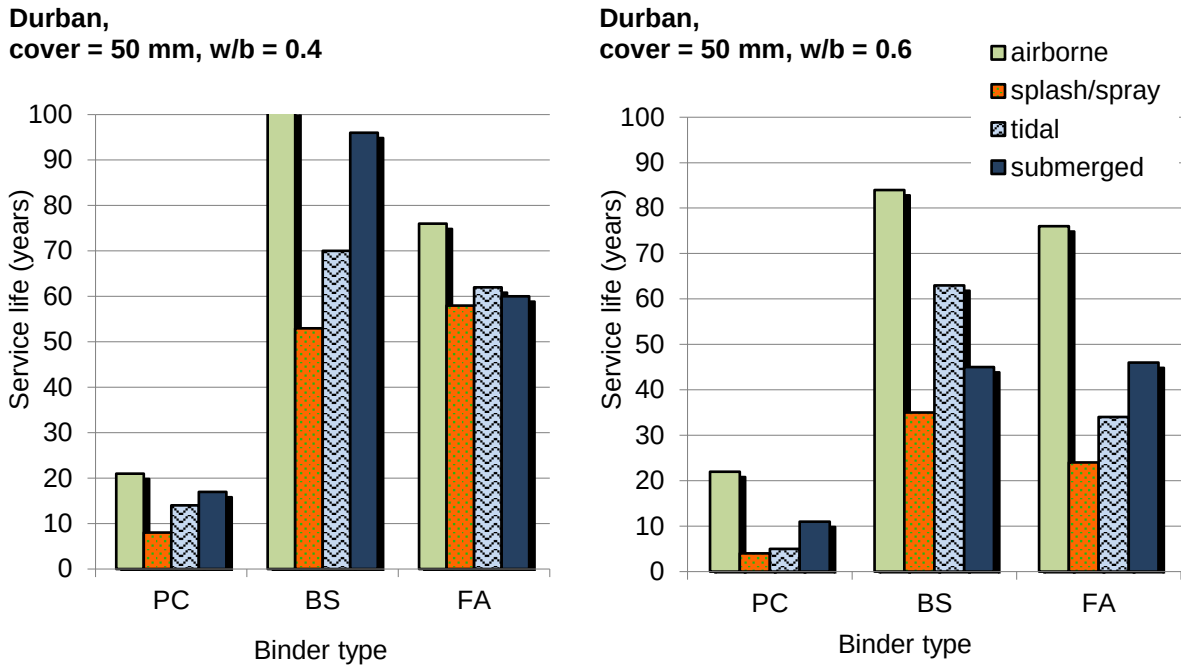

Figure 5.40: Predicted service life, Durban, w/b =0.4 (left) and 0.6 (right), cover = 50 mm

Considering the general trend obtained from all results, air-borne exposure resulted in similar service life durations, as the tidal and submerged zones. Consequently, with regard to chloride ingress, there appears to be little justification to place air-borne exposure into a less severe exposure category, compared to the tidal zone. However, it needs to be stressed that in this research, air-borne exposure was very close to the ocean, as discussed in Chapter 3. The severity of the air-borne exposure zone is expected to largely depend on various influencing factors, including distance from the ocean, wind, general weather conditions, mist, wave activity, and spray water. These factors were not investigated in detail in this research. However, with regard to these factors, one possible explanation why the air-borne samples in Durban had more favourable performance compared to the other exposure zones, while air-borne exposure in Cape Town resulted in very similar chloride ingress compared to other zones, is that Cape Town is characterized by stronger wave action and stronger winds, compared to Durban. This has probably resulted in more direct exposure to chlorides in the Cape Town air-borne exposure site, compared to the Durban exposure site.

Concrete exposed to the splash/spray zone generally showed the lowest service life duration, indicating that this is the most severe environmental exposure class for initiation.

The exposure classes found in the Eurocode (EN 206) distinguish between 3 marine exposure classes: XS1 (air-borne), XS2 (submerged) and XS3 (tidal/splash). With regard to chloride ingress, the results obtained in this research show that the European exposure classes are not directly applicable to South African conditions. A distinction should be made between splash/spray and tidal exposure. In addition, air-borne (close to the ocean) and tidal exposure should be considered equally aggressive with regard to chloride ingress. Air-borne exposure should further be refined with regards to the influencing factors mentioned above (distance from the ocean, wind conditions, wave activity, etc.).

5.3.11 Service life prediction for Cape Town versus Durban

The different chloride ingress behaviour observed in Cape Town and Durban is shown in Figures 5.41 and 5.42, for concretes containing 100% PC and 30%/70% FA/PC. As with the other parameter comparisons, this evaluation was only carried out for a cut-off point of 10 years for both PC and blended cement concretes.

Considering the predicted chloride profiles after 50 years of exposure, the values in Cape Town and Durban are generally in the same order of magnitude. However, in all cases, chloride ingress in Durban is higher, compared to Cape Town. The main reason for this is probably related to the higher temperatures in Durban.

The influence of the exposure location can best be quantified in relation to the predicted service life duration, considering that relatively small differences in time-dependent chloride profiles can result in significantly different times to corrosion-initiation (defined as reaching the chloride threshold at the depth of the reinforcement). As summarized in Table 5.5, exposure to Cape Town marine conditions resulted in predicted service life durations that were 40% longer, compared to Durban, when averaged for all samples tested. The calculated difference in predicted service life duration was not dependent on the concrete cover used in the modelling.

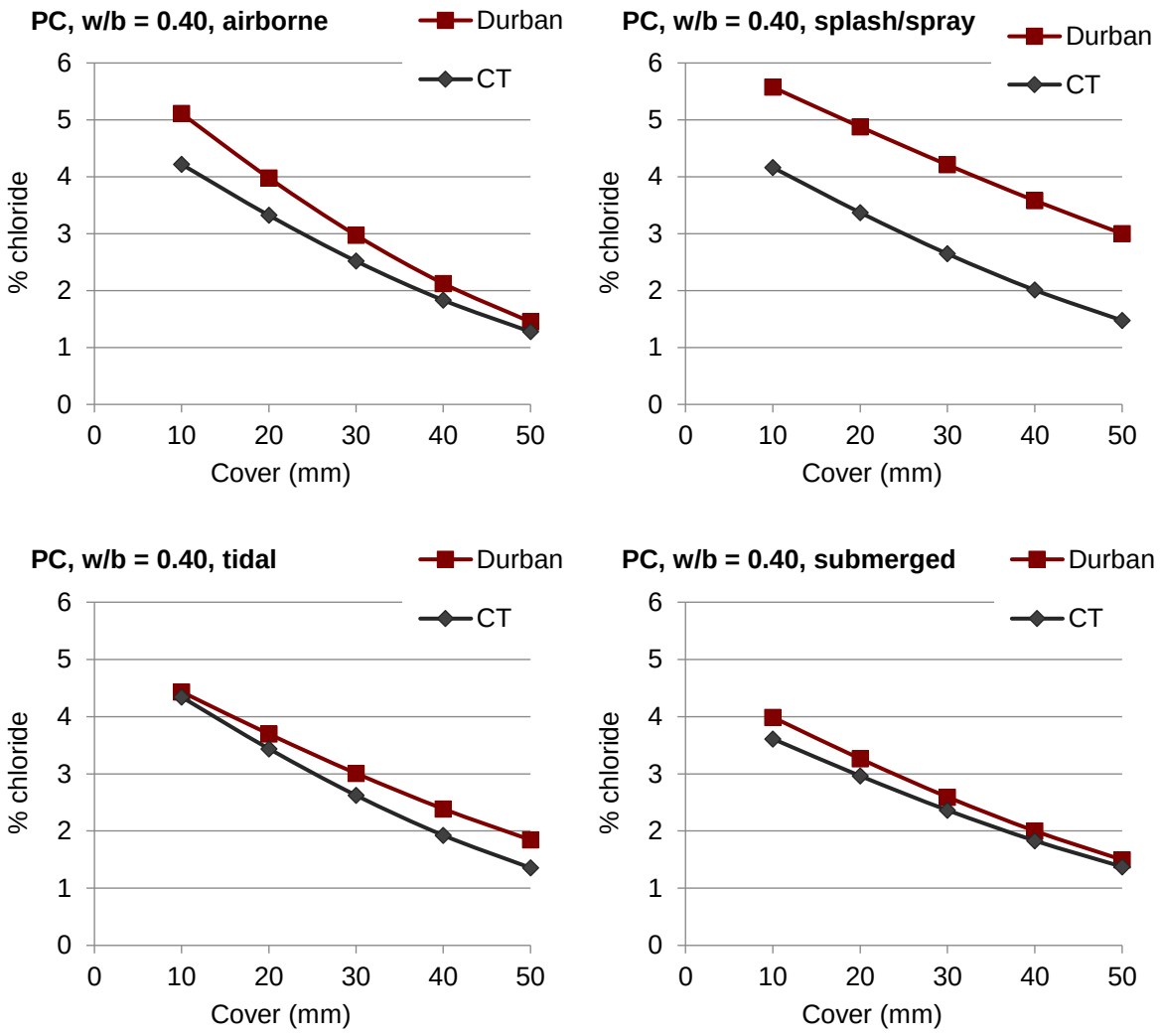

Figure 5.41: 50-year chloride profiles, CT versus Durban, PC concrete, w/b = 0.4

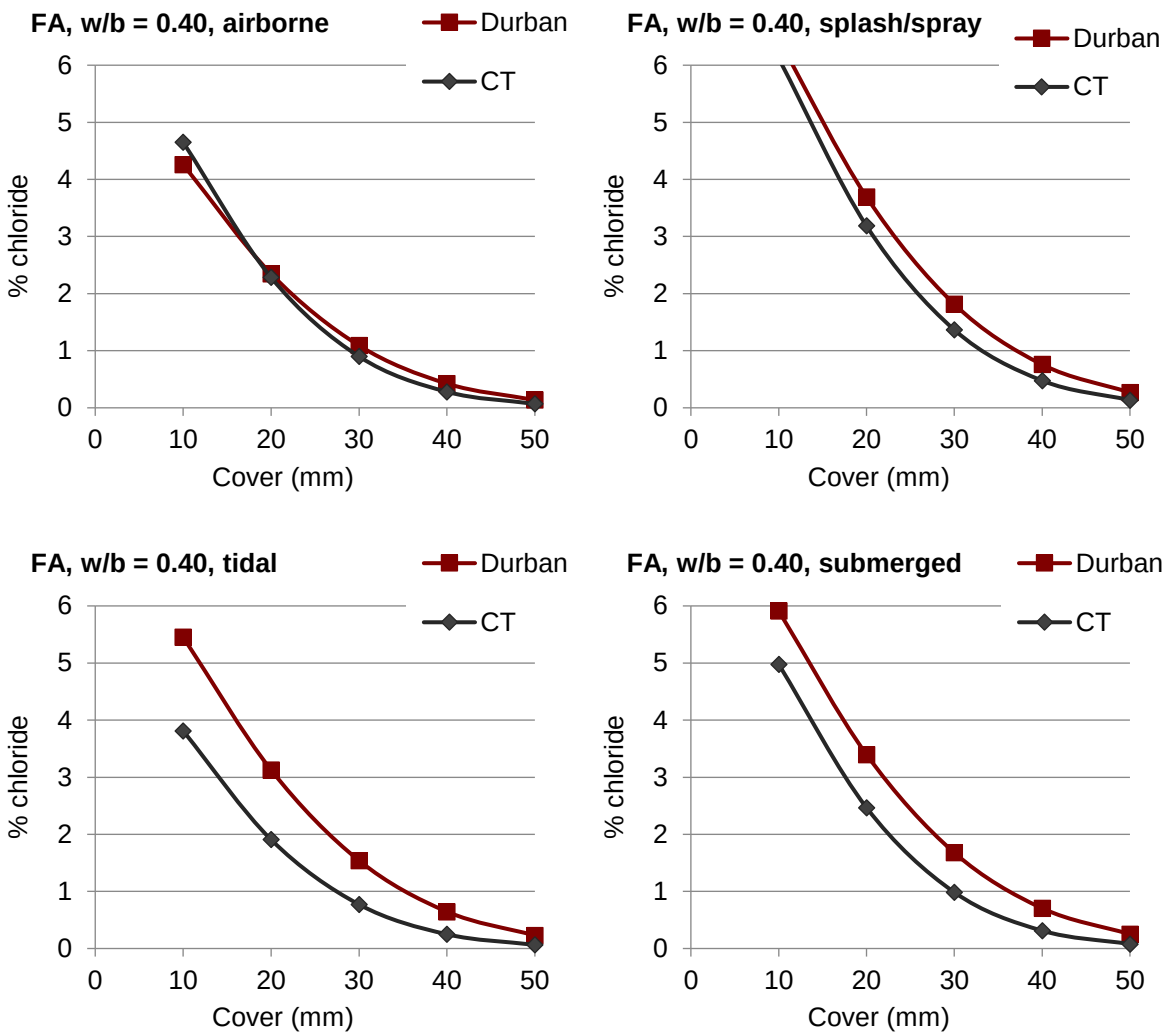

Figure 5.42: 50-year chloride profiles, CT versus Durban, FA concrete, w/b = 0.4

Table 5.5: Comparison of predicted service life in CT and Durban, w/b = 0.4

Binder	Exposure zone	Service life ratio between CT and Durban, w/b = 0.4				
		Cover depth			Average	Average each binder
		50	40	30		
PC 40	Air	1,0	1,0	1,0	1,0	1,1 (1,4)[1]
	Splash	2,3	2,4	2,0	2,2	
	Tidal	1,5	1,4	1,3	1,4	
	Submerged	1,1	1,1	0,9	1,0	
FA 40	Air	1,2	1,2	1,2	1,2	1,4
	Splash	1,3	1,2	1,3	1,3	
	Tidal	1,5	1,6	1,5	1,5	
	Submerged	1,5	1,4	1,4	1,4	

[1] The value in the bracket (1,4) includes the ratio for splash zone, which is considered an outlier

Higher chloride ingress in Durban was most significant for PC concrete in the splash/spray zone, where a significantly different service life was predicted for the two locations. However, the same was not observed for FA concrete or the other exposure conditions. This again indicates that overall, the exposure condition has a less significant influence on the service life of PC concrete, compared to concrete containing blended cements. The same was observed for the various exposure zones, as discussed in Section 5.3.6.

5.3.12 Influence of cut-off point for blended cement concretes

As discussed in previous sections, the modelling of chloride ingress requires the definition of a cut-off point for the time-development of D_a and C_s. Based on long-term chloride ingress obtained on real structures, a cut-off point of 10 years appears appropriate and conservative for concrete containing PC only. For concrete containing blended cements, a cut-off point of 10 years results in an overly conservative prediction for chloride ingress. Blended cement concretes were therefore evaluated with cut-off points of both 10 and 20 years and the results compared in previous sections. This comparison is further quantified in Table 5.6, which summarizes the ratios between the service life predicted for the two scenarios, for all binder combinations and exposure conditions, both w/b ratios, and cover depths of 30, 40 and 50 mm.

Overall, independent of the various parameters (binder type, w/b ratio, exposure condition, cover depth), a cut off-point of 20 years results in approximately 40-50% higher predicted service life duration, compared to a cut-off point of 10 years. This highlights the importance of determining suitable and realistic assumptions for the long-term chloride ingress characteristics. In the scope of this research, it could not be established with certainty, whether a cut-off point of 10 or 20 years is more appropriate for blended cement concretes. However, the use of a cut-off point of 10 years results in overly conservative service life predictions for blended cement concrete, which does not correspond to the general experience in South Africa, that blended cement concretes significantly increase the service life of reinforced concrete structures exposed to the marine environment. A cut-off point of 20 years therefore appears to be more appropriate for blended cement concretes, compared to 10 years. Further refinement of the cut-off point should be done in future research.

Table 5.6: Blended cement concretes, predicted service life (SL) for cut-off points of 20 years versus 10 years (expressed as a ratio SL(20y) / SL(10y))

Cape Town

Binder	Exposure	Cover (mm)		
		50	40	30
CS 40	Air	1.43	1.42	1.41
	Splash	1.53	1.55	1.54
	Tidal	1.53	1.55	1.52
	Submerged	1.39	1.41	1.43
CS 60	Air	1.44	1.42	1.48
	Splash	1.55	1.57	1.50
	Tidal	1.53	1.54	1.56
	Submerged	1.44	1.43	1.45
FA 40	Air	1.43	1.41	1.39
	Splash	1.53	1.53	1.52
	Tidal	1.56	1.55	1.54
	Submerged	1.44	1.43	1.45
FA 60	Air	1.44	1.45	1.43
	Splash	1.58	1.57	1.58
	Tidal	1.59	1.57	1.53
	Submerged	1.50	1.52	1.54
SP 40	Air	1.44	1.44	1.45
	Splash	1.58	1.52	1.50
	Tidal	1.51	1.52	1.54
	Submerged	1.42	1.41	1.42
SP 60	Air	1.43	1.42	1.38
	Splash	1.52	1.56	1.45
	Tidal	1.59	1.61	1.56
	Submerged	1.48	1.50	1.44
SF 40	Air	1.21	1.18	1.25
	Splash	1.35	1.29	1.44
	Tidal	1.34	1.30	1.31
	Submerged	1.22	1.24	1.24
SF 60	Air	1.23	1.24	1.33
	Splash	1.39	1.33	1.13
	Tidal	1.39	1.40	1.33
	Submerged	1.32	1.27	1.22
	average	**1.45**	**1.44**	**1.43**
	STDV	**0.10**	**0.11**	**0.11**

Durban

Binder	Exposure	Cover (mm)		
		50	40	30
BS 40	Air	1.48	1.50	1.49
	Splash	1.47	1.47	1.53
	Tidal	1.49	1.47	1.52
	Submerged	1.47	1.48	1.46
BS 60	Air	1.55	1.56	1.57
	Splash	1.60	1.57	1.62
	Tidal	1.59	1.63	1.57
	Submerged	1.56	1.57	1.56
FA 40	Air	1.39	1.39	1.39
	Splash	1.52	1.50	1.52
	Tidal	1.47	1.33	1.65
	Submerged	1.33	1.33	1.32
FA 60	Air	1.51	1.51	1.50
	Splash	1.50	1.50	1.44
	Tidal	1.56	1.55	1.58
	Submerged	1.52	1.50	1.47
	average	**1.50**	**1.49**	**1.51**
	STDV	**0.07**	**0.08**	**0.08**

5.4 Chapter summary

5.4.1 General

In Chapter 5, long-term chloride ingress was modelled based on the medium-term test results discussed in Chapter 4. The predicted 50-year chloride profiles for samples exposed in Cape Town were compared to long-term data obtained from real structures, which was used to determine suitable cut-off times for the time-development of diffusion coefficients and chloride surface concentrations. The influence of the selected cut-off times on the predicted service life durations was quantified, highlighting the importance of selecting realistic values for the time development of D_a and C_s.

With the establishment of a 10-year period (cut-off point) for the time-development of D_a and C_s, the influence of various test parameters on the expected service life duration was investigated, including binder type, w/b ratio, cover depth and exposure conditions. In addition, a cut-off point of 20 years was used to model chloride ingress and predict service life for concretes made with blended cements.

5.4.2 Selection of cut-off dates for D_a and C_s

D_a and C_s are inter-dependent parameters and cannot be modelled in isolation from each other. Therefore, the cut-off date needs to be the same for D_a and C_s. The three different scenarios presented in Section 5.2.1 result in very different predictions for long-term chloride ingress, indicating a significant influence on cut-off date. The determination of a cut-off date for the variation of D_a and C_s values with time is therefore a key aspect in long-term modelling of chloride ingress into concrete. The comparison of the predicted profiles and long-term chloride ingress profiles in real structures situated on the west coast of South Africa and Namibia, as discussed in Chapter 4 indicates that the 50/10/10 scenario is the most realistic for PC concrete as it results in the expected order of magnitude for chloride ingress, especially in the case for the splash/spray zone, which is generally of most concern with regard to reinforcement corrosion.

For concrete with blended cements, very low chloride concentrations are predicted using the 50/50/50 scenario and therefore seem unrealistic. In contrast, the 50/10/10 scenario yields chloride concentrations that are relatively high. From the three scenarios investigated, 50/20/20 appears closest to what is expected from concrete made with modern binary binder blends. However, no long-term experimental data is available to justify selecting the 20/20 option in the modelling of long-term chloride ingress in blended cement concrete. Further research on long-term chloride ingress into concretes with blended cements is required to define the most suitable cut-off date. Until such research becomes available, it appears justified to conservatively select the same cut-off date for concretes containing PC but to exercise judgement before making a trial selection.

The comparison of the predicted long-term chloride ingress and associated service life duration based on a cut-off point of either 10 or 20 years for concretes with blended cement clearly indicates the relevance in selecting appropriate values. The predicted service life for a cut-off point of 20 years was about 40-50% longer, compared to a cut-off point of 10 years. This is due to the influence of time on the m-values that describe the long-term development of the chloride

diffusion coefficient. Selecting a later cut-off point results in a significantly reduced apparent chloride diffusion coefficient and hence lower predicted long-term chloride concentrations.

5.4.3 Influence of binder type on chloride ingress

PC concrete is found to consistently have the lowest chloride surface concentrations but generally higher chloride concentrations at depths exceeding about 20 to 30 mm, compared to all other concrete types. PC concrete was also found to have lower chloride surface concentrations but higher chloride diffusion coefficients, compared to concrete containing supplementary cementitious materials. Consequently, predicted chloride concentrations at around 10 mm depth are very similar across concretes made with different binders. The differing performance resulting from various binder types is mostly evident in the chloride profiles deeper inside the concrete, which is also the region that is of most practical concern, for limiting reinforcement corrosion.

The predicted long-term chloride profiles for concretes made with FA, slag (CS, BS) and SP are generally fairly similar, however with FA and slag performing generally better than SP concrete. Compared to these binder types, concrete made with SF has significantly higher predicted chloride concentrations, although still notably lower than concrete containing PC only. Overall, the longest predicted service life duration relates to concrete containing either FA or CS (in Cape Town) and FA or BS (in Durban).

5.4.4 Influence of cover depth on service life

The cover depth is conceptually one of the easiest parameters to control in the design of RC structures, but practically it is often poorly controlled. The relationship between cover depth and predicted service life follows an exponential trend. Compared to a cover depth of 30 mm, cover depths of 40 mm and 50 mm result in an increase in predicted service life duration of 50% and 170%, respectively, averaged over all concretes investigated. The relevance of concrete cover on the predicted service life duration was not dependent on the environmental exposure condition, highlighting that cover always has to be considered as one of the most important design parameters, for structures exposed to marine environments.

5.4.5 Influence of w/b ratio on chloride ingress

The w/b ratio is also a very important parameter for concrete mix design. Concretes with lower w/b ratio are typically related to a longer service life duration, which often determines the design of suitable concrete mixes for marine exposure. On average, for all concretes tested in this research, a decrease in w/b ratio from 0.6 to 0.4 resulted in an increase in service life duration of 80%. Notably, this is the same percentage achieved by increasing the cover depth from 40 mm to 50 mm.

5.4.6 Influence of marine exposure zone on chloride ingress

The different exposure zones had a lesser effect on chloride ingress than expected. In general, airborne, tidal and submerged exposure zones resulted in similar chloride profiles and predicted service life durations. For the prediction of chloride ingress in the design of concrete structures, it seems to be unjustified to distinguish between these exposure conditions. In contrast, the splash/spray zone generally resulted in significantly shorter predicted service life durations, i.e., higher chloride ingress, compared to all other exposure zones. Consequently, the splash/spray

zone should be considered the most severe marine exposure zone with regards to chloride ingress into concrete.

5.4.7 Influence of marine exposure site and temperature on chloride ingress

In this research, test specimens were exposed to two different site conditions, i.e., various exposure zones in Durban and Cape Town. Notably, the ambient air temperatures and the temperatures of the ocean are very different in these two locations (see Chapter 3: average ambient air temperatures of 18 – 35^{o}C and 7 – 27^{o}C, respectively; and average ocean temperatures of 18 – 25^{o}C and 12 -15^{o}C, respectively, for Durban and Cape Town).

Concrete samples exposed to Durban had significantly higher chloride ingress, compared to Cape Town. As a consequence, the predicted service life durations in Cape Town were about 40% greater than in Durban, when averaged across all samples tested. This clearly shows that ambient temperatures of the air and the ocean need to be considered in the prediction of chloride ingress into concrete.

It is widely accepted that an increase in temperature accelerates chloride diffusion into concrete, which is related to an increase in molecular speed and a decrease in physical chloride binding. The literature reports various studies on these phenomena (Touil et al., 2017, Lindvall, A, 2006), in which the influence of different (constant) temperatures on chloride ingress was established in the laboratory and the observed effects typically modelled based on the Arrhenius law using the concept of activation energy. It is anticipated that the application of the Arrhenius law in the modelling of chloride ingress into concrete exposed to sites with seasonally varying temperatures can be exploited, to provide additional scientific background to the phenomena observed. This, however, was not within the scope of this research.

6.Summary, conclusions, and recommendations

6.1 Research strategy and outcome

The purpose of this research was to determine service life prediction and performance-based design of reinforced concrete structures in the South African marine environment, aiming in particular at identifying and quantifying the influences of time, binder type, w/b ratio and environmental exposure conditions on chloride ingress and related material parameters. The research included a detailed literature review and extensive experimental and site work. Concrete specimens were produced with various binder types commonly used in the Western Cape and Kwazulu Natal Provinces in South Africa and subjected to marine conditions in the respective locations. The basic binder type was plain Portland cement (PC) with blends of Fly Ash (FA), ground granulated blastfurnace slag (BS), and ground granulated Corex slag (CS). Two water/binder ratios were used, 0.40 and 0.60, representing high and normal strength concrete respectively. Specimens were exposed to different marine conditions in the marine harbours of Cape Town and Durban. The purpose of selecting these two exposure sites was to determine chloride ingress as a function of macro-environmental conditions relevant to South Africa, as Cape Town is exposed to the cold Atlantic Ocean, whereas the Durban harbour is situated in the warmer Indian Ocean. At each site, samples were exposed to the four marine zones commonly used to design concrete structures for durability in South Africa, namely submerged, tidal, splash/spray and airborne exposure zones. In addition, specimens produced from all concrete mixes were exposed to chloride ingress by immersion in a chloride solution in a controlled laboratory environment. The experimental programme resulted in a total of 76 different parameter combinations.

Chloride ingress was measured at approximately 6-month intervals for a period of roughly 4 years, using a potentiometric titration method to determine depth-dependent chloride profiles. The chloride profiles were interpreted using regression analysis based on Fick's laws of diffusion in order to determine time-dependent apparent diffusion coefficients (D_a) and chloride surface concentrations (C_S).

The experimental results yielded information on the influences of binder type and exposure conditions on time-dependent chloride ingress into concrete. The time-dependency was determined through the quantification of the "m" and "n" factors that are used to describe, how the values for D_a and C_S change over time respectively. For the modelling of long-term chloride ingress, it was argued that the two model input parameters, i.e. C_S and D_a are inter-related and dependent on each other. As a consequence, the same cut-off point in time was defined for both parameters, i.e. the same age at which the two parameters are taken to no longer undergo further change. To find realistic cut-off dates, two different scenarios were modelled for all concrete mixes, i.e. cut-off dates of 10 and 20 years. For these two cut-off points, chloride profiles for an age of 50 years were predicted. This was done using Fick's laws of diffusion to extrapolate long-term chloride ingress. The model outputs were compared to long-term chloride ingress data from actual concrete structures along the west coast of Southern Africa. It was concluded that a cut-off date of 10 years is reasonably realistic for concrete made with plain Portland cement. However, for concretes made with blended cements, a cut-off point of 10 years was considered to result in unrealistically conservative predictions for long-term chloride ingress and a cut-off point of 20 years is proposed as a more realistic assumption for such binders.

Predicted long-term chloride profiles were then used to model the service life of reinforced concrete structures, in relation to the various experimental parameters used in the research. Using the commonly used assumption that the end of the reinforcement corrosion initiation period corresponds to the service life of reinforced concrete (RC) structures, the service life duration was modelled as the time needed to reach a threshold value of 0.4% by mass of binder at the depth of the steel reinforcement. This allowed to quantitatively investigate the combined influences of binder type, w/b ratio, exposure condition and cover depth on the expected service life duration of RC structures in South African marine environments. Based on this approach, this research allows making practical recommendations on service life prediction and design of RC structures in South African coastal regions, and substantially enhancing the information available to designers.

This research also aimed at establishing a correlation between laboratory-based testing of chloride ingress and chloride ingress occurring under real site conditions. This was achieved primarily by comparing chloride ingress in submerged conditions on site to chloride ingress observed in standard bulk diffusion experiments. Based on these comparisons, it was determined that the laboratory-based bulk diffusion test gives realistic indications of time-dependent chloride ingress, as well as the influence of the various test parameters investigated, i.e. binder type, w/b ratio and time. This is considered a useful practical outcome of this research, as it helps to correlate laboratory data to actual field performance. Further, it can assist with regularly updating performance-based service life design models for RC structures in marine environments.

The limitations of this research are that chloride ingress was only measured over a period of approximately 4 years, based on which long-term predictions had to be made depending on certain model assumptions, that diffusion was the only transport mechanism considered in the modelling of chloride ingress, and that the influence of cracking on chloride ingress was not considered. Further research will therefore be needed to update service life models for RC structures in these regards.

Following the discussions presented in Chapters 4 and 5, specific conclusions are provided in the following sections, referring to the various factors influencing long-term chloride ingress and associated service life modelling for RC structures exposed to South African marine environments.

6.2 Factors influencing chloride diffusion coefficients and surface concentrations

The time-dependent chloride profiles that were obtained on samples exposed to the various environments were analysed to obtain the two main input parameters used in the modelling of chloride diffusion into concrete, i.e. chloride surface concentrations and the apparent diffusion coefficients, in relation to the various experimental variables. These variables included binder type, w/b ratio, and exposure condition. With regards to exposure conditions, both macro-exposure (i.e. geographical location) and the four standard design exposure zones, which include submerged, tidal, splash/spray and airborne exposure, were investigated.

The test results indicate that within a specific macro-environment, i.e. for a certain geographical location, the specific marine exposure zone may influence the apparent diffusion coefficient. In Cape Town, lower diffusion coefficients were obtained for samples in the airborne and submerged zones, compared to the tidal and splash/spray zones. The Durban exposure sites,

however, did not show the same trend and no consistent relationship could be established between diffusion coefficients and exposure zones.

The influence of the various exposure zones on chloride ingress was more pronounced in the zone-dependent chloride surface concentrations. In this regard, the highest C_s values occur in the splash/spray zone, followed by the tidal, submerged and airborne zones.

The macro-environment has a noticeable influence on chloride ingress. Samples exposed to the Indian Ocean in Durban can be expected to have both higher diffusion coefficients and higher chloride surface concentrations, compared to samples exposed to the Atlantic Ocean in Cape Town, especially in the exposure zones related to regular wetting and drying cycles, i.e. splash/spray and tidal zones. In chloride ingress modelling and durability design of RC structures, the geographical location therefore needs to be considered.

As expected, the binder type and w/b ratio have a significant effect on chloride ingress into concrete, which is mostly evident in their influence on diffusion coefficients. Concrete made with plain Portland cement has substantially higher apparent diffusion coefficients, compared to concrete made with blended cements. For blended cements, concrete containing blast furnace slag was found to have the lowest diffusion coefficient, followed by concretes containing fly ash and Corex slag.

Compared to concrete with a w/b of 0.40, a w/b of 0.60 resulted in predicted D_a values (at 20 years of age) that were about 70% higher (on average, across all samples tested). In this comparison, the binder type had no apparent influence on how much “better” a concrete with lower water/binder ratio performed, indicating that the influence of the w/b ratio is independent of the binder type.

The chloride surface concentration is lowest in concrete containing plain Portland cement, which is a result of the higher chloride binding capacity of blended cements. Notably, the C_S values for blended cement concretes appear to generally be independent of the specific binder type used in the mix. This is believed to be related to similar levels of C3A phases in the binders used, in addition to other effects related to the general alteration of the concrete pore structure obtained through the use of supplementary cementitious materials.

For blended cement concrete, the w/b ratio has a marked influence on chloride surface concentrations. In this research, chloride surface concentrations for concrete containing fly ash and slag were consistently about 20-30% higher in concrete with a w/b of 0.60, compared to concrete with a w/b ratio of 0.40. This indicates that the w/b ratio may need consideration when environmental exposure is quantified in terms of chloride surface concentrations.

The trends discussed above are useful for the modelling of chloride ingress into concrete. However, in isolation, diffusion coefficients and chloride surface concentrations offer limited information on chloride ingress. To evaluate the influence of the various parameters on actual chloride ingress, the values for D_a and C_S need to be used in combination, as model input parameters using Fick’s laws of diffusion. This is covered in the sections below.

6.3 Time-dependency of chloride diffusion coefficients and surface concentrations

The apparent diffusion coefficient reduces with time, which in the literature is commonly stated as a result of the densification of the cement paste matrix due to continuous hydration of the cement. The time-dependency of the D_a value is expressed through the m-value, which is used

as an input parameter in the diffusion model. Notably, the experimental results of this research indicate that the m-value is a basic material property related to the binder type but independent of w/b ratio or exposure conditions. Across all exposure sites, concrete containing plain Portland cement was found to have an average m-value of 0.31 (with a STDV of 0,03). This indicates a relatively small change in D_a over time, compared to blended binder types. The time-dependency of the diffusion coefficient of concrete containing slag (BS or CS) or fly ash can be modelled with an m-value of 0.8, while concrete made with silica fume was found to have an m-value of 0.6.

The chloride surface concentration increases with time, which is indicated by the n-value. Contrary to the time-development of the apparent diffusion coefficients, no clear relationship was found between n-value and binder type. Independent of the experimental variables, most n-values ranged between 0.4 and 0.6, with an average value of 0.47.

For practical applications, and in absence of contrary experimental evidence, an n-value of 0.5 can be used in the modelling of long-term chloride ingress. m-values are binder type-dependent, as quantified above.

6.4 Modelling long-term chloride ingress into concrete

The time-dependency of the apparent diffusion coefficient and chloride surface concentration is considered through the m- and n-values, respectively. However, as argued in previous chapters, it is unrealistic to assume that diffusion coefficients continue to decrease throughout the entire life of a structure. Similarly, chloride surface concentrations can be expected to eventually reach a maximum value, after which they stay constant. The literature does not contain a consistent approach with regard to suitable “cut-off” times for the time development of D_a and C_S. Consequently, this research analysed this aspect in considerable detail.

The long-term chloride ingress modelling done in this research was based on regression analysis of time-dependent measured chloride profiles. The regression analysis, which yielded values for D_a and C_S as model input parameters, defines the chloride surface concentration as a function of the diffusion coefficient and vice versa. This highlights the necessity to define the same cut-off times for apparent diffusion coefficients and chloride surface concentrations, for a self-consistent calculation.

In future research, realistic cut-off dates for South African concretes and exposure conditions could be established with long-term experimental data based on regular measurements of diffusion coefficients and chloride surface concentrations, in relation to various experimental parameters. However, such data does not exist at present.

In this research, long-term (50 year) chloride ingress was predicted for all concretes investigated, using 2 different scenarios, i.e. cut-off dates of 10 and 20 years. The predicted values were used in a service life model based on reinforcement corrosion initiation, assuming a chloride threshold of 0.4% by mass of cement at various cover depths (30, 40, and 50 mm). For concretes with blended cements, a cut-off time of 20 years resulted in a predicted service life that was 40-50% longer, compared to the service life modelled with a cut-off time of 10 years, independent of cover depth and binder type. This underlines the high importance of defining realistic cut-off dates in service life predictions for RC structures in marine

environments, which is an aspect that has been given very little recognition in the existing literature.

To determine which cut-off time is most realistic for local conditions, the predicted 50-year chloride profiles were compared with existing data on long-term chloride ingress into concrete structures along the west coast of Southern Africa. The existing data was obtained on structures containing Portland cement as a sole binder. Based on the comparison, a cut-off date of 10 years was found to be realistic for Portland cement concrete and should be applied in chloride ingress modelling.

For blended cements, no local long-term data is available to determine the most realistic cut-off time for D_a and C_S values. However, a cut-off time of 10 years resulted in prediction of unrealistically high long-term chloride concentrations in concrete with blended cements. In contrast, a cut-off time of 20 years resulted in magnitudes of chloride concentrations that appear to be reasonable.

For the verification of appropriate cut-off points, the lack of experimental data for long-term chloride ingress in concrete structures made with blended cements and exposed to real marine environments are problematic. The determination of suitable cut-off times depending on binder type therefore needs further research. In the interim, based on the modelling done in this research, cut-off times of 10 and 20 years are considered appropriate for plain PC concrete and blended cement concretes, respectively.

6.5 Marine exposure zones

For the durability design of concrete structures, Codes and Standards present exposure categories for marine environments. Typically, the tidal and splash/spray zones are grouped together and considered the most aggressive category, followed by submerged and airborne exposure.

The results obtained in this research confirm that exposure zones influence chloride ingress mainly through their influence on chloride surface concentrations, while a clear relationship between chloride diffusion coefficients and exposure zones could not be established. With regard to chloride surface concentrations, the highest values were generally measured in the splash/spray zone, followed by tidal, submerged and airborne exposure. However, when considering the combined influences of time-dependent diffusion coefficients and surface concentrations in the modelling of long-term chloride ingress, the relevance of specific exposure zones is less pronounced. Based on the results obtained in this research, it appears that in relation to chloride ingress, the splash/spray zone is clearly the most aggressive exposure condition, whereas the tidal, submerged and airborne exposure zones can be grouped together.

Further sub-dividing airborne exposure based on the prevailing conditions, i.e. distance from the ocean, elevation, wind direction, wave activity, climate, etc., is necessary but was not included in this research.

The geographical location also needs to be considered when defining the aggressiveness of the marine exposure conditions. Samples exposed to the Indian Ocean in Durban had consistently higher diffusion coefficients, higher chloride surface concentrations, and shorter predicted service life durations, compared to samples exposed to the Atlantic Ocean in Cape

Town. A direct comparison of concretes containing fly ash (which was used in identical mix compositions in Durban and Cape Town, and which generally results in suitable durability properties for marine exposure) indicates that the service life of structures made with the same concrete would be about 40% longer in Cape Town, compared to Durban, which is substantial and which can be assigned to the influence of ambient air and ocean temperatures on the rate of chloride ingress.

6.6 Chloride ingress versus binder type

When evaluating the influence of binder type on chloride ingress, all relevant factors need to be considered, including diffusion coefficients, chloride surface concentrations, and the time-dependency of these two parameters. To look at how the binder type affects an isolated factor from this list is not informative for chloride ingress assessment.

As discussed above, concrete made with plain Portland cement was shown to have higher diffusion coefficients, lower chloride surface concentrations, and lower m-values, compared to blended cements. In addition, a cut-off time of 10 years is proposed, as opposed to 20 years for blended cements. The overall result, established through the modelling of long-term chloride ingress, is that concrete made with plain Portland cement has lower chloride surface concentrations but significantly higher chloride ingress at depths exceeding about 20 mm, compared to concrete containing blended cements. The predicted service life durations for PC concrete are very low (typically between around 5 – 20 years at 50 mm cover depth, depending on exposure condition and w/b ratio), confirming that plain PC concrete is unsuitable for marine exposure conditions.

Concrete containing fly ash, GGBS and GGCS generally perform comparably with regards to the predicted long-term chloride ingress, indicating that all 3 binder types (at the investigated cement replacement ratios) are suitable for marine concrete structures. Overall, concrete made with SP was outperformed by concrete containing conventional fly ash. In most cases, this was related to significantly lower values for the predicted service life; while in fewer cases, SP concrete had predicted service life durations that were only slightly lower than that of concrete containing FA. Furthermore, the use of silica fume results in lower chloride ingress, compared to plain PC concrete (which resulted in approximately twice as long predicted service life durations in SF concrete, compared to PC concrete) but is far less effective than the use of the other cement extenders investigated in this research.

6.7 Chloride ingress versus w/b ratio

As discussed above, the w/b ratio has a large influence on the apparent diffusion coefficient, a w/b ratio of 0.60 yielding a D_a (20-years) that is on average 70% higher than the D_a of a concrete with w/b = 0.40. Similarly, the w/b ratio has a noteworthy influence on chloride surface concentrations in concrete with blended cements, values for a w/b of 0.60 being about 30% higher than those for a w/b of 0.40. For PC concrete, the influence of w/b ratio on C_s values was less pronounced. Interestingly, the w/b ratio has no apparent influence on the time-dependency (m- and n-values) of the diffusion coefficient and chloride surface concentration, indicating that the change in chloride ingress parameters over time is a function of the pore solution chemistry

(which is primarily related to the binder type) but not the pore structure (which is a function of the w/b ratio).

The combined influence of the w/b on the above parameters becomes visible when the predicted long-term chloride ingress is considered. For all concretes tested in this research, a decrease in w/b ratio from 0.60 to 0.40 resulted in an average increase in service life duration of 80%.

6.8 Influence of cover depth on service life

The cover depth has a significant influence on the predicted service life duration, irrespective of binder type, w/b ratio or exposure condition. Changing the cover from 50 to 40 mm or 50 to 30 mm results in a reduction in the predicted service life of about 35% and 63% respectively on average for all samples tested.

6.9 Bulk-diffusion testing versus chloride ingress on site

The bulk-diffusion test is a common test method for investigating chloride ingress into concrete under laboratory conditions. In countless past research projects, the test has been shown to yield useful results with regard to the influence of various experimental parameters on chloride diffusion. However, the literature does not discuss how bulk diffusion results obtained in the laboratory relate to chloride ingress under specific environmental exposure conditions on site. In this research, results obtained with the bulk-diffusion test were compared with chloride ingress in submerged conditions on site. This direct comparison was done because in both of these environments, the concrete is in constant contact with water. Notably, it was established that the bulk-diffusion test confirmed all trends and results obtained from real site exposure, including time-dependency of chloride ingress (n and m-values) and influence of binder type.

The results of the bulk-diffusion test can be used to establish chloride diffusion coefficients, chloride surface concentration, and n- and m-values, which are characteristic of those expected for concrete exposed to submerged conditions on site. The test can therefore be used to predict long-term chloride ingress in real structures.

6.10 Practical considerations and implications

The durability of concrete structures in the marine environment is dependent on various parameters, which need to be considered in design, service life prediction and quality control procedures. This research has revealed useful information for an improvement of engineering practice.

The influence of binder type, w/b ratio and cover depth on the service life of concrete structures in marine environments was quantified. This can assist in making informed design choices for concrete mix parameters and cover depth, under consideration of the prevailing environmental exposure conditions.

For the modelling of long-term chloride ingress, a sound and realistic approach for the application of m- and n-values was developed and suitable cut-off times for the time-dependency of D_a and C_s were established. An improved methodology based on the application

of Ficks laws of diffusion in combination with realistic assumptions for the time-development of chloride ingress parameters in relation to mix composition and environmental exposure for service life modelling has thus been established. This research further provides a sound basis for service life design based on laboratory-based bulk-diffusion testing, which could result in a major improvement of performance-based design procedures.

For the design of concrete structures, the definition of marine exposure categories needs to be reconsidered. With regards to chloride ingress, the splash/spray zone is the most aggressive exposure condition, while all other conditions (air-borne, tidal, and submerged) can be grouped into one single category. In this approach, further sub-division of the air-borne exposure is required, as discussed above.

For structures exposed to South African coastal environments, the specific location needs to be considered, acknowledging that exposure to the Indian Ocean is more aggressive that exposure to the Atlantic Ocean. Durability specifications need to be updated in this regard.

6.11 Main conclusions

Based on the discussions in previous sections, the following main conclusions are drawn from this research:

- Long-term chloride ingress into concrete structures can be based on bulk-diffusion results obtained in the laboratory. These results relate closely to chloride ingress in submerged conditions on site and allow determination of representative chloride surface concentrations, bulk diffusion coefficients, n-values, and m-values.
- For the long-term modelling of chloride ingress using Fick's laws of diffusion, the following m-values are applicable, independent of the environmental exposure zone or w/b ratio:
    - 0.3 for PC concrete
    - 0.6 for concrete containing silica fume at 10% replacement
    - 0.8 for concrete containing slag (BS or CS) at 50% replacement
    - 0.8 for concrete containing fly ash or SP at 30% replacement
- For the modelling of time-dependent chloride surface concentrations, n-values of 0.50 are applicable, independent of binder type, environmental exposure or w/b ratio.
- Chloride diffusion coefficients and chloride surface concentrations are time-dependent variables. The same "cut-off age" needs to be applied for the time-dependency of both parameters. For blended cement concrete, a cut-off age of 20 years appears appropriate. For PC concrete, a cut-off age of 10 years is proposed.
- The existing exposure categories for concrete durability in South African marine environments need to be reconsidered. The splash/spray zone is the most aggressive exposure with regards to chloride ingress. The remaining 3 categories, i.e. tidal, submerged and air-borne (in close proximity to the ocean) can be grouped together into one single category. The exposure categories need to further distinguish between the Atlantic and Indian Oceans, indicating the higher aggressivity of the environmental exposure in warmer climates.

- With regards to chloride ingress, concrete containing slag (BS or CS) or fly ash can be considered to have very similar performance.
- The influence of w/b ratio on chloride ingress is independent of the binder type. Changing the w/b from 0.60 to 0.40 increases the service life duration by about 80%.
- The influence of cover depth on the service life duration is independent of concrete mix parameters and environmental exposure. Changing the cover from 50 mm to 40 or 30 mm reduces the service life duration by roughly 35 and 65%, respectively.

6.12 Recommendations

6.12.1 Revision of marine exposure classifications

This research has shown that the commonly defined marine exposure classes do not result in a realistic assessment of the environmental aggressiveness. The tidal exposure, which is commonly assumed to be as severe as the splash/spray zone, was found not to result in higher chloride ingress compared to the submerged and air-borne zone. Contrarily, concrete exposed to air-borne chlorides (near the ocean) was found to have similar chloride ingress as concrete directly exposed to salt water in the tidal zone.

For the modelling of chloride ingress, and also for prescriptive and performance-based durability design of RC structures, it is therefore recommended to simplify existing exposure categories into two classes:

- Most severe: splash/spray zone
- Severe: tidal, submerged and airborne zone (close to the ocean)

Further research is needed to characterize airborne exposure with regards to specific site conditions (distance from the ocean, elevation, wind direction, wave activity, climate, etc.).

Furthermore, in South African engineering practice, the geographical location should be considered in the design of RC structures for durability. Locations exposed to the Indian Ocean should be considered more aggressive, compared to sites along the Atlantic Ocean.

6.12.2 Suitable binder types for concrete in marine exposure

This research has shown that chloride ingress into concrete is highly dependent on binder type. For the provision of durable concrete structures in South African marine environments, suitable binder types are those that include slag (CS or BS) or fly ash at the common replacement ratios of 50% for slag or 30% for fly ash. These should be preferred in all situations where durability is an important design parameter for marine structures.

Concrete containing plain Portland cement should not be used in marine environments, including areas with exposure to air-borne chlorides.

Blended cements based on silica fume and Superpozz should not be recommended in marine environments, as their performance with regard to chloride ingress is not as effective as commonly assumed.

6.12.3 Cover depth specifications

Considering the strong influence of cover depth on the service life of RC structures, a minimum cover of 50 mm should be specified for all structures along the coast in South Africa, including structures exposed to airborne chlorides.

6.12.4 Performance testing of concrete design mixes

For unconventional concrete types, or concretes with new binder combinations, performance testing should be done to characterize the concrete for its chloride ingress characteristics. The bulk diffusion test should be used to obtain the information necessary for service life prediction and durability specification.

6.12.5 Future research

The following aspects could not be investigated within the scope of this research and are proposed for future projects:

- The service life prediction done in this research needs to be extended with probabilistic modelling.
- The relationship between the Bulk diffusion and Chloride Conductivity Index tests should be investigated in detail. This will allow to better relate the CCI test to chloride ingress expected on site, through the results obtained in this research. The results of such further studies are expected top assist in refining the South African performance-based durability design approach, which makes use of durability indexes to predict the service life of RC structures and perform associated quality control.
- Long-term chloride ingress on site should be verified with long-term site data.
- The actual reasons for the time-dependency of D_a and C_s need to be established, so that long-term prediction of chloride ingress can be improved.
- Chloride ingress into concrete should be related to the chemical composition of the cementitious binder type.
- Characteristic chloride thresholds values should be determined for concrete made with the various binder types used in this research.
- Chloride binding should explicitly be considered in the modelling of chloride ingress.
- The influence of varying seasonal temperatures on chloride ingress in real structures should be investigated and incorporated in service life prediction models.
- The influence of the water salinity on chloride ingress should be investigated and practical engineering models developed to account for this in service life design.
- Environmental zones for airborne exposure should be further investigated to define aggressive versus non-aggressive airborne exposure conditions.
- Service life prediction models should be updated using the knowledge obtained in this research with factors influencing reinforcement corrosion propagation.
- Results obtained with the service life model developed in this research should be compared to existing models, such as Life 365.

References

Addis, B. and Owens, G. (2001). Fulton's Concrete Technology. Eighth Edition**.** Cement and Concrete institute, South Africa.

Alexander, M. G. et al. (1999). Concrete durability index testing manual, Research Monogram No.1, Department of Civil Engineering, University of Cape Town.

Alonso, C., Castellote, M., Andrade, C. (2002). Chloride threshold dependence of pitting potential of reinforcements. ElectrochimicaActa 47. pp 3469–3481.

Alonso, C. et al. (2000). Chloride threshold values to depassivate reinforcing bars embedded in a standardized OPC mortar. Cement and Concrete Research 30. pp1047–1055.

Amey, S. L. et al. (1998). Predicting the service life of concrete marine structures: an environmental methodology. ACI Structures Journal 95 (2). pp 205-214.

Andrade, C., Diez, J. M. and Alonso, C. (1997). Mathematical Modelling of a concrete surface 'skin effect' on diffusion in chloride contaminated media. Adv. Cem. Based Materials 6 (2). pp 39-44.

Andrade, C., Page, C. L. (1986). Pore solution chemistry and corrosion in hydrated cement systems containing chloride salts: a study of cation specific effects. British Corrosion Journal 21. pp49-53.

Angst, U. and Vennesland, O. (2009). Critical Chloride content in reinforced concrete. State of the art. Concrete Repair, Rehabilitation and Retrofitting II. South Africa.

Angst, U., Elsener, B., Larsen, C. and Vennesland, O. (2008). Critical chloride content in reinforced concrete – A review. Cement and Concrete Research 39. pp. 1122-1138.

ACI Committee 201(1991). Guide to durable concrete. ACI Materials Journal 88 (5).

Ann, K. Y. and Song, H. (2007). Chloride threshold level for corrosion of steel in concrete. Corrosion Science Vol. 49 (11). pp 4113-4133.

Arorap, P. et al. (1997). Corrosion initiation time of steel reinforcement in a chloride environment – A one dimensional solution. Corrosion Science 39(4). pp 739-759.

Arya, C., Buenfeld, N. R., and Newman, J. B. (1987). Assessment of simple methods of determining free chloride ion content of cement pastes. Cement and Concrete Research 17. pp 907-18.

Arya, C. and Xu, Y. (1995). Effect of Cement Type on Chloride Binding and Corrosion of Steel in Concrete. Cement and Concrete Research, Vol. 25, No. 4, pp. 893-902.

Arya, C., Buenfeld, N. R., Newman, J. B. (1990). Factors influencing chloride binding in concrete, Cement and Concrete Research 20. pp 291-300

ASTM Special Technical Publication 818 (1983). Corrosion of metals in association with concrete.

ASTM C1202-94. (1994). Standard Test Method for Electrical Indication of Concrete's Ability to resist Chloride. Annual Book of ASTM Standards V 04.02. ASTM, Philadelphia. pp. 620-625

ASTM C1556-04 (2011), Standard Test Method for Determining the Apparent Chloride Diffusion Coefficient of Cementitious Mixtures by Bulk Diffusion, Book of Standards Volume: 04.02. ASTM, Philadelphia, 7 pp.

ASTM C1543 ASTM C1543 - 10a Standard Test Method for Determining the Penetration of Chloride Ion into Concrete by Ponding. Book of Standards Volume: 04.02. ASTM, Philadelphia, 3 pp. (Withdrawn 2019).

Ballim, Y., Alexander, M. G. and Beushausen, H. (2009). Durability of concrete. Fulton's concrete technology (9). South Africa.

Bamforth, P. B. (1999). The derivation of input data for modelling chloride ingress from eight-year UK coastal exposure trials. Magazine of Concrete Research 51 (2). pp 87-96.

Beeby, A. W. (1993). Design for life. Concrete 2000 - Economic and durable concrete through excellence, Vol 1. E & F N Spon. pp.37-50.

Bentur, A., Diamond, S. and Berke, N. S. (1997). Steel Corrosion in Concrete, Chapman and Hall London.

Bentz, D. P., Clifton, J. R. and Snyder, K.A. (1996). Predicting service life of chloride-exposed steel-reinforced concrete. Concrete International. pp 42-47.

Bentz, D. P., Garboczi, E. J. and Lagergren, E. S. (1996). Multi-scale Microstructural modelling of Concrete Diffusivity: Identification of Significant variables. Cement, Concrete and Aggregates.

Berkely, K. G. C and Pathmanaban, S. (1990). Cathodic protection of reinforcement steel in concrete. London: Butterworths& Co. Ltd.

Breit, W. (1998). Critical chloride content—investigations of steel in alkaline chloride solutions. Materials and Corrosion, 49. pp 539–550.

Birin-Yauri, U.A. and Glasser, F.P. (1998) Frieldel's Salt, Ca2Al(OH)6(Cl,OH).2H2O: It's Solid Solutions and Their Role in Chloride Binding. Cement and Concrete Research, Vol. 28. pp 1713 - 1723.

Boddy, A., Bentz, E., Thomas, M. D. A. and Hooton, R. D. (1999). Overview and sensitivity study of a multi-mechanistic chloride transport model. Cement and Concrete Research 29 (6). pp 827-837.

Broomfield, J. P. (1996). Corrosion of Steel in Concrete, Understanding, Investigation and Repair, Chapman and Hall London.

Broomfield, J. P. (1997). Rebar corrosion – What do we know for sure. Proceedings International Conference on Repair of concrete structures – From Theory to Practice in a Marine Environment, Svolvær. pp 35-47.

Byfors, K. (1990). Chloride-initiated reinforcement corrosion- chloride binding. Swedish Cement and Concrete Research Institute. CBI Report 1:90. Stockholm.

Byfors, K. (1986). Chloride Binding in Cement Paste, Nordic Concrete Research, Vol. 5. pp 27-38.

Cady, P. D., and Weyers, R. E. (1983). Chloride penetration and the deterioration of concrete bridge decks. Cement, Concrete and Aggregates, 5(2). pp 81-87.

Cahyadi, J. H., and Uomoto, T. (1993). Influence of environmental relative humidity on carbonation of concrete (mathematical modelling). Durabilty of building materials and components 6. E & FN Spon. pp 1142-51.

Castellote, M. et al. (2002). Accelerated simultaneous determination of the chloride depassivation threshold and of the non-stationary diffusion coefficient values. Corrosion Science 44. pp 2409–2424.

Chalee, W. and Jaturapitakkul, C. (2009). Effects of W/B ratios and fly ash fineness on chloride diffusion coefficient of concrete in marine environment. Materials and Structures, vol. 42. pp 505 – 514.

Choi, Y. S.,Kim, J. G. and Lee, K. M. (2006). Corrosion behaviour of steel bar embedded in fly Ash Concrete. Corrosion Science 48(7). pp 1733-45.

Costa, A. and Appleton, J. (1999). Chloride penetration into concrete in marine environment-Part II: prediction of long-term chloride penetration. Materials and Structures 32(5). pp 354-359.

Crank, J. (1975). The mathematics of diffusion, 2nd edition. The Clarendon Pres. Oxford, UK.

Delagrave, A., Marchand, J., Ollivier, J. P., Julien, S. and Hazrati, K. (1997). Chloride Binding Capacity of Various Hydrated Cement Paste Systems. Advanced Cement Based Materials, Vol. 6. pp 28-35.

Dhir, R.K.; El-Mohr, M.A.K.; and Dyer, T.D. (1996). Chloride binding in GGBS concrete. Cement and Concrete Research, Vol. 26. pp 1767 - 1773.

Dhir, R.K, and Jones, M.R. (1999). Development of chloride-resisting concrete using fly ash. Fuel 78. pp 137–142.

DuraCrete. (1999). Probabilistic Methods for Durability Design, Document BE95- 1347/R0, The European Union – BriteEuRam III. Gouda.

DuraCrete. (1997). Design Framework. Document BE95-1347/R1, The European Union – BriteEuRam III. Gouda.

DuraCrete. (2001). General Guidelines for Durability Design and Redesign. Document BE95-1347/R15. The European Union – BriteEuRam III. Gouda.

DuraCrete. (2001) Statistical quantification of the variables in the Limit State Functions. Document BE95-1347/R9. The European Union – BriteEuRam III. Gouda.

Elsener, B. and Böhni, H. (1986). Corrosion of steel in mortar studied by impedance measurements. Electrochemical Methods in Corrosion Research (ed. M. Duprat), Materials Science Forum 8. pp 363–372.

EN 1991-1 (2002). Eurocode 1 : Basis of design and actions on structures - Part 1: Basis of design. CEN (European Committee for Standardization). Brussels.

FIB (2006). Model Code for Service Life Design. FIB Bulletin 34. pp 110.

Ferreira, R. M. (2004). Probability-based Durability Analysis of Concrete Structures in Marine Environments. PhD Thesis. University of Minho. Guimarães.

Ferreira, R. M., Jalali, S. and Gjorv, O. E. (2004). Software for probability-based durability analysis of concrete structures. Concrete under severe conditions: environment and loading. CONSEC' 04, Korea.

Gardner, T. J. (2006). Chloride transport through concrete and implications for rapid chloride testing, MSc. Thesis. University of Cape Town. South Africa.

Glanville, J., Neville, A. (1997). Prediction of Concrete Durability. E&FN SPON, London. pp 97.

Glanville, J and Neville, A. (2000). Prediction of concrete durability. Proceedings of STATS 21stAniversary Conference. E&FN Spon. London UK. pp 185.

Glass, G.K., Reddy, B. and Buenfeld, N. R. (2000). The participation of bound chloride in passive film breakdown on steel in concrete. Corrosion Science 42. pp 2013-2021.

Glass, G.K., Wang, Y. and Buenfeld, N.R. (1996). An Investigation of Experimental Methods used to determine free and total chloride contents**.** Cement and Concrete Research, Vol. 26, No 9. pp 1433 – 1449.

Glass, G.K. and Buenfeld, N.R. (1995). The Determination of Chloride Binding Relationships. Chloride Penetration into Concrete. Proceedings of the RILEM INT Workshop, France. RILEM Publications. France.

Glass, G.K., Hassanein, N.M. and Buenfeld, N.R. (1997). Neural Network Modelling of Chloride Binding. Magazine of Concrete Research, Vol. 49. pp 323 - 335.

Glass, G.K, Stevenson, G.M. and Buenfeld, N.R. (1998). Chloride – binding isotherms from the diffusion cell test. Cement and Concrete Research, Vol. 28, No. 7.

Gonzalez, J. and Jalali, S. (2004). Development of Negative Pore Water Pressure During Cement Hydration.

Gouda, V. K. (19700. Corrosion and corrosion inhibition of reinforcing steel immersed in alkaline solutions. British Corrosion Journal 5. pp 198-203.

Gouda, V.K. and Halaka, W.Y (1970). Corrosion and corrosion inhibition of reinforcing steel Embedded in concrete. British Corrosion Journal 5. pp 204–208.

Gulikers, J., Castellote, M., Andrade, C., Kropp, Setzer, M., Stevenson, C.E. (2006). Round-Robin test on methods for determining chloride transport parameters in concrete, Materials and Structures/Materiaux et Constructions, 39(294), pp. 955–990.

Gulikers, J., Luping, T. (2007). On the mathematics of time-dependent apparent chloride diffusion coefficient in concrete, Cement and Concrete Research, 37(4), pp. 589–595

Hansson, C. M. and Sorenson, B. (1990). The Threshold Concentration of Chloride in Concrete for the Initiation of Corrosion. Corrosion rates of Steel in Concrete, ASTM SP 1065, 99.3-16.

Hansson, C. M. and Sorensen, B. (1990). 'The threshold concentration of chloride in concrete for the initiation of reinforcement corrosion' in Berke, N. S., Chaker, V. and Whiting, D (ed(s).). Corrosion rates of steel in concrete. ASTM STP 1065. pp 3-16.

Hausmann, D. A. (1967). Steel corrosion in concrete. How does it occur? Materials Protection 6. pp 19-23.

HETEK 53 (1996). Chloride penetration into concrete. State of the Art. Transport processes, corrosion initiation, test methods and prediction models. Report No. 53.

Holden, W. R., Page, C. L., and Short, N. R. (1983). 'The influence of Chlorides and Sulphates on Durability' in Crane, A. P. (ed). Corrosion of reinforcement in Concrete Construction. Ellis, Horwood. Chichester. pp. 143-15.

Hope, B. B., and Alan, Ip K. C. (1987). Chloride corrosion threshold in concrete. ACI Materials Journal, 1987: 84. pp 306-14.

Ho, D. W. S. and Lewis, R. K. (1987). Carbonation of concrete and its prediction. Cement, Concrete Research 1987; 17. pp 489-504.

Hong, K. and Hooton, R. D. (1999). Effects of cyclic chloride exposure on penetration of concrete cover. Cement and Concrete Research, vol. 29. pp. 1379 – 1386.

Jaegermann, C. (1990). Effect of w/c ratio and curing on chloride penetration into concrete exposed to Mediterranean sea climate. ACI Materials Journal 1990; 87 (4). pp 333-9.

Jensen, O.M., Korzen, M.S.H., Jakobsen, H.J. and Skibsted, J. (2000). Influence of cement constitution and temperature on chloride binding in cement paste. Advances in Cement Research, Vol. 12, No. 2. pp. 57 – 64.

Justnes, H. (1998). A review of chloride binding in cementitious systems, Nordic Concrete Research, Publication No. 21. 1/98. Nordic Concrete Federation. Norsk Betongforening. Oslo. pp. 48–63.

Kassir, M. K. and Ghosn, M. (2002). Chloride-induced corrosion of reinforced concrete bridge decks. Cement and Concrete Research 32 (1). pp 139-143.

Kayyali, O. A. and Haque, M. N. (1995). The Cl−/OH−ratio in chloride-contaminated concrete - a most important criterion. Magazine of Concrete Research 47. pp 235–242.

Khan, M. I. (2010). Nanostructure and microstructure of cement concrete incorporating multi-cementitious composites. Transport Research Rec: J Transp Res Brd 2141. pp 21-7.

Kim, J. et al. (2016). Chloride ingress into marine exposed concrete: A comparison of empirical and physically based model. Cement and Concrete Composites 72. pp 133-145.

Kobayashi, K and Suttoh, K. (1991). Oxygen diffusivity of various cementitious materials. Cement Concrete Research, 21. pp 273-84.

Krop, J. and Hilsdorf, H. K. (1995), 'Performance criteria for concrete durability' in Krop, J. and Hilsdorf, H. K. (ed(s)). Rilem Report 12. E&FN Spon. London.

Lambert, P., Page, C. L. and Short, N. R. (1985). Pore Solution Chemistry of the Hydrated System Tricalcium Silicate/Sodium Chloride/Water. Cement and Concrete research, Vol. 15. pp 675-680.

Lambert, P. et al. (1991). Investigations of reinforcement corrosion 2. Electrochemical monitoring of steel in chloride-contaminated concrete. Materials and Structures 24. pp 351–358.

Larsson, J (1995). The enrichment of chloride in expressed concrete pore solution submerged in saline solution. Proceedings of the Nordic Seminar on Field studies of chloride-initiated reinforcement corrosion in concrete. Lund University of Technology, Report TVBM-3064. pp 171-176.

Lee, N. P. and Chisholm, D. M. (2005). Durability of Reinforced Concrete Structures under Marine Exposure. Environmental Actions and Response – Reinforced Concrete Structures exposed in Road and Marine Environments. Publication P-01:3. Chalmers University of Technology. pp 320.

Li, K. et al. (2008). Concepts and requirements of durability design for concrete structures: An extensive review of CCES01. Materials and Structures, 41(4). pp 717-731.

Lindvall, A. (2007). Chloride ingress data from field and laboratory exposure- Influence of salinity and temperature. Cement and Concrete Composites 29. pp 88-93.

Locke, C.E. and Siman, A. (1980). Electrochemistry of reinforcing steel in salt-contaminated concrete' in D.E.Tonini and J.M. Gaidis (ed(s)). Corrosion of Reinforcing Steel in Concrete. ASTM STP 713.

Luo, R., Cai, Y., Wang, C. and Huang, X. (2003). Study of chloride binding and diffusion in GGBS concrete. Cement and Concrete Research, Vol. 33. pp 1 – 7.

Lu, X., Li, C. and Zhang, H. (2002). Relationship between the free and total chloride diffusivity in concrete. Cement and Concrete Research 32(2). pp. 323-6

Maage, M., Helland, S. and Carlsen, J. E. (2003). Chloride penetration into concrete with lightweight aggregates. BriteEuRam Report BE96-3942/R3.

Maage, M., Helland, S, Poulsen, E., Vennrsland, O. and Carlsen, J. E. (1996). Service life prediction of existing concrete structures exposed to marine environment. ACI Materials Journal 93 (6). pp 602-608.

Mangat, P. S. and Molloy, B. T. (1994). Prediction of long term chloride concentration concrete. Materials and Structures 27 (6). pp 338-346.

Mackechnie, J.R., Alexander, M.G. and Jaufeerally, H. (2003). Structural and Durability Properties of Concrete Made with Corex Slag. Research Monograph No. 6. The University of Cape Town and the University of the Witwatersrand. South Africa.

Mackechnie, J.R. and Alexander, M.G. (2000). Rapid Chloride Test Comparisons. Concrete International, Vol. 22, No 5.

Mackechnie, J.R. and Alexander, M.G. (2000). Practical Considerations for Rapid Chloride Conductivity Testing. Proceedings of the 2nd International RILEM Workshop on Testing and Modelling the Chloride Ingress into Concrete. Paris, France.

Maheswaran, T. and Sanjayan, J. G. (2004). A semi-closed-form solution for chloride diffusion in concrete with time-varying parameter. Magazine of Concrete Research, 56, No.6. pp 359-366.

Mackechnie, J. R. (1997). Predictions of reinforced concrete durability in the marine environment. Doctoral Research Monograph. Department of Civil Engineering, University of Cape Town. South Africa.

Manera, M. et al. (2008). Chloride threshold for rebar corrosion in concrete with addition of silica fume. Corrosion Science 50(2). pp 554–560.

Mangat, P. S. and Molloy, B. T. (1994). Prediction of long-term chloride concentration in concrete. Materials and Structures 27. pp 338-346.

Mangat, P.S and Molloy, B.T. (1994). Predicting of long-term chloride concentration in concrete. Materials and Structures, Vol. 27. pp 338-346.

Mangat, P.S. and Molloy, B.T. (2000). Chloride binding in concrete containing PFA, GGBS or silica fume under sea water exposure. Magazine of Concrete Research. Volume 47 Issue 171, June 1995, pp. 129-141

Manera, M., Vennesland, O. and Bertolini, L. (2008). Chloride threshold for rebar corrosion in concrete with addition of silica fume. Corrosion Science 50(2). pp. 554-60.

Markeset, G. and Kioumarsi, M. (2017). Need for further development in service life modelling of concrete structures in chloride environment. Procedia Engineering 171. pp 549-556.

Markeset, G. and Skjolsvold, O. (2011). Time dependent chloride diffusion coefficient- field studies of concrete exposed to marine environment in Norway. Service life design for infrastructure, RILEM publication. pp 83-90

Martin-Perez, B., Pantazopoulou, S. J. and Thomas, M. D. A. (1998). Finite element modelling of corrosion in highway structures. Second International Conference on Concrete Under Severe Conditions, CONSEC' 98. Tromso, Norway.

Maslehuddin, M. (1981). Optimization of concrete mix design for durability in the Eastern province of Saudi Arabia. MSc Thesis, Department of Civil Engineering, King Fahd University of Pertoleum and Minerals. Dhahran.

Meijers, S. J. H. (2005). Computational results of a model for chloride ingress in concrete including convection, drying-wetting cycles and carbonation. Materials and Structures 38 (276). pp 145-154.

Midgley, H.G and Illston, J. M. (1984). The Penetration of Chlorides into Hardened Cement Pastes. Cement and Concrete Research, Vol. 14, No. 4. pp. 546-558.

Morris, W., Vico, A and Vazquez, M. (2004). Chloride induced corrosion of reinforcing steel evaluated by concrete resistivity measurements, Electrochimica Acta 49. pp 4447-4453.

Mozer, J. D. et al. (1985). Corrosion of reinforcing bars in concrete. Journal Am ConcrInst, pp 909-31.

Munch-Petersen, C. (2001). Demolish, construct or repair – the optimal strategy. Presented at Dansk Brodag Mars 2001. Taastrup.

Nagataki, S., Otsuki, N., Tiong-Huan, W and Nakashita, K. (1995). Condensation of Chloride Ion in Hardened Cement Matrix Materials and on Embedded Steel Bars. ACI Materials Journal, Vol. 90, No. 4. pp. 323 – 332.

Neville, A. M. (1995). Chloride Attack of Reinforced Concrete: an Overview. Materials and Structures, Vol. 28. pp 63 – 70.

Ngala, V.T., Page, C.L., Parrott, L.J and Yu, S.W. (1995). Diffusion in cementitious materials: II. Further investigations of chloride and oxygen diffusion in well cured OPC and OPC/30% PFA pastes. Cement and Concrete Research, Vol. 25, No 4. pp. 819 – 826.

Nguyen, T. Q., Baroghel-Bouny, V. and Dangla, P. (2006). Prediction of chloride ingress into saturated concrete on the basis of a multi-species model by numerical calculations. Composite Concrete 2006; 3 (6). pp 401-22.

Nokken, M., Boddy, A., Hooton, R. D. and Thomas, M. D. A. (2006). Time dependent diffusion in concrete-three laboratory studies. Cement and Concrete Research 36 (2006). pp 200-207.

Oh, B. H, Jang, S. Y and Shin, Y. S. (2003). Experimental investigation of the threshold chloride concentration for corrosion initiation in reinforced concrete structures. Magazine of Concrete Research 55. pp 117–124.

Oh, B. H and Jang, S. Y. (2007). Effects of material and environmental parameters on chloride penetration profiles in concrete structures. Cement and Concrete Research, Vol. 37. pp. 47-53.

Page, C. L. (1975). Mechanism of corrosion protection in reinforced concrete marine structures. Nature 258. pp 514-515.

Page, C.L. and Vennesland, Ø. (1982). Pore Solution Composition and Chloride Binding Capacity of Silica Fume Cement Pastes. SINTEF Report STF65 A82025. SINTEF, Norway.

Page, C. L., Lambert, P. and Vassie, P. R. W. (1991). Investigations of reinforcement corrosion 1, The electrolyte phase in chloride-contaminated concrete. Materials and Structures, Vol. 24, No. 142. pp. 243-252.

Papadakis, V. G. (2000). Effect of supplementary cementing materials on concrete resistance against carbonation and chloride ingress. Cement and Concrete Research 30. pp 291-299.

Pang, L. and Li, Q. (2016). Service life prediction of RC structures in marine environments using long term chloride ingress data: Comparison between exposure trials and real structure surveys. Construction and Building Materials 113. pp 979-987.

Pack, S. W. et al. (2010). Prediction of time dependent chloride transport in concrete structures exposed to a marine environment. Cement and Concrete Research 40 (2). pp 301-312.

Petcherdchoo, A. (2013). Time dependent models of apparent diffusion coefficient and surface chloride for chloride transport in Fly ash concrete. Concrete Construction Building Materials 38 (January). pp 497-507.

Pettersson, K. (1995). Chloride threshold value and the corrosion rate in reinforced concrete. Proc. of the Nordic Seminar. Lund. pp. 257-266.

Poupard, O., Ait-Mokhtar, A. and Dumargue, P. (2004). Corrosion by chlorides in reinforced concrete: determination of chloride concentration threshold by impedance spectroscopy. Cement and Concrete Research 34. pp 991-1000.

Trapin, J. P., Renaudin, G., Elkaim, E. and Francois, M. (2002). Structural Transition of Friedel's Salt Studied by Synchrotron Powder Diffraction. Cement and Concrete Research, Vol. 32. pp 513-519.

Rasheeduzzafar. (1992). Influence of cement composition on concrete durability. ACI Materials Journal 89 (6). pp 574-86.

Rasheeduzzafar, Al-Gahtani, A. S. and Al-Saadoun, S. S. (1989). Influence of construction practises on concrete durability. ACI Materials Journal 86 (6). pp 566-75.

Rasheeduzzafar, Dakhil, F. D., Bader, M. A. and Khan, M. M. (1990). Performance of Corrosion Resisting Steels in Chloride Bearing Concrete. ACT Materials Journal, Vol. 89, No. 5. pp. 439-448.

Richartz, W. (1969). Die Bindung von Chlorid bei der Zementerhärtung. Zement-Kalk-Gips 10. pp 447–456.

Riding, K. A. et al. (2013). Apparent diffusivity model for concrete containing supplementary cementitious materials. ACI Materials Journal 110(6). pp 705-714.

Roberts, M. H. (1962). Effect of calcium on the durability of pretensioned wire in prestressed concrete. Magazine of Concrete Research, Vol. 14, No. 42. pp. 143-154.

Saetta, A., Scotta, R. and Vitaliani, R. (1993). Analysis of chloride diffusion into partially saturated concrete. ACI Materials Journal, Vol. 90 (5). pp 441-451.

Sandberg, P. and Larrson, J. (1993). Chloride Binding in Cement Pastes in Equillibrium with Synthetic Pore Solutions. Chloride Penetration into Concrete Structures. Nordic Miniseminar, Gotenberg. pp 98-107.

Sandberg, P. (1996). Critical evaluation of factors affecting chloride-initiated reinforcement corrosion in concrete. Report TVBM-7088. Division of Building Materials, Lund Institute of Technology. Sweden. pp.24-25.

Schiessl, P. and Lay, S. (2005). 'Influence of concrete composition' in: H. Bohni (ed). Corrosion in Reinforced Concrete Structures. Woodhead Publishing Limited, Cambridge. pp 91-134.

Schiessl, P. (1998). 'Report of RILEM Technical Committee 60- CSC' in Schiessl, P (ed). Corrosion of Steel in Concrete. Chapman & Hall, London.

Schiessl, P and Breit, W. (1996). Local repair measures at concrete structures damaged by reinforcement corrosion-aspects of durability. Proceedings 4th Int. Symposium Corrosion of Reinforcement in Concrete Construction. The Royal Society of Chemistry, Cambridge. pp. 525–534.

Schiessl, P and Raupach, M. (1990). Influence of concrete composition and microclimate on the critical chloride content in concrete. Proceedings 3rd Int. Symposium Corrosion of Reinforcement in Concrete. Wishaw, UK.

Shi, X. et al. (2012). Durability of steel reinforced concrete in chloride environments: An overview. Construction and Building Materials 30. pp 125-138.

Skjolsvold, O. (2009). Chloride diffusion into concrete. Evaluation of the ageing effect based on results from field studies. COIN Project Report 11.

Song, W., Lee, C. and Ann, K. Y. (2008). Factors influencing chloride transport in concrete structures exposed to marine environments. Cement and Concrete Composites 30. pp 113 - 121

Soroka, I. (1993). Concrete in Hot Environments**.** E & FN Spon, UK.

Stanish, K. and Thomas, M. D. A. (2003). The use of bulk diffusion tests to establish time-dependent concrete chloride diffusion coefficients. Cement and Concrete Research 33 (1). pp 55-62.

Stratfull, R.F. et al. (1975). Corrosion testing of bridge decks. Transportation Research Record 539. pp 50–59.

Streicher, P. E. and Alexander, M. G., A (1995). Chloride Conduction Test for Concrete. Cement and Concrete Research, Vol. 25, No. 6. pp 1284-1294.

Tadayon, M. H., Shekarchi, M. and Tadayon, M. (2016). Long-term field study of chloride ingress in concretes containing pozzolans exposed to severe marine tidal zone. Construction and Building Materials 123. pp 611-616.

Takewaka, K and Mastumoto, S. (1988). Quality and Cover Thickness of Concrete Based on the Estimation of Chloride Penetration in Marine Environments. ACI SP 109-17, American Concrete Institute. pp 381-400.

Tamimi, A. K., Abdalla, J. A. and Sakka, Z. I. (2008). Prediction of long term chloride diffusion of concrete in harsh environments. Construction and Building Materials 22. pp 829 – 836.

Tang, L. and Nilsson, L. O. (1992). Chloride diffusivity in high strength concrete at different ages. Nordic Concrete Research (11). pp 162-171.

Tang, L. (1996). Chloride Transport in concrete: Measurement and prediction. PhD dissertation, Chalmers University of Technology, Goteborg, Sweden.

Tang, L and Nilsson, L. O. (1993). Chloride binding capacity and binding isotherms of OPC pastes and mortars. Cement and Concrete Research, 23. pp 247-253.

Tang, L. and Nilsson, L. O. (1999). Modelling of chloride penetration into concrete tracing 5 years field exposure. MRS 1999 Fall Meeting, Symposium GG: Transport Properties and Microstructure of Cement based Systems.

Tang, L. and Gulikers, J. (2007). On the mathematics of time-dependent apparent chloride diffusion coefficient in concrete. Cement and Concrete Research, 37[4]. pp 589-595.

Thomas, M. D. A. and Bamforth, P.B. (1999). Modelling chloride diffusion in concrete- effect of fly ash and slag. Cement and Concrete Composites 29. pp 487-495.

Thomas, M. D. A., Pantazopoulou, S. J. and Martin-Perez, B.(1995). Service Life Modelling of Reinforced Concrete Structures Exposed to Chlorides-A Literature Review. Ministry of Transportation, Ontario, University of Toronto

M. Thomas. (1996). Chloride threshold in marine concrete. Cement and Concrete Research 26. pp 513–519.

Thomas M. D. A., Matthews, J. D. and Haynes, C. A. (1990). Chloride diffusion and reinforcement corrosion in marine exposed concrete containing pulverized-fuel ash. Proceedings 3rd International Symposium: Corrosion of Reinforcement in Concrete. Wishaw, UK. pp. 198–212.

Thomas, M. D. A. and Bentz, E. C. (2000). Life 365, Computer Program for Predicting the Service Life and Life Cycle Costs of Reinforced Concrete Exposed to Chlorides. American Concrete Institute, Detroit, USA.

Thomas, M. D. A and Matthews, J. D. (2004). Performance of PFA concrete in a marine environment: 10 year results. Cement and Concrete Composites, Vol. 26. pp 5 – 20.

Trejo, D. and Pillai, R.G. (2003). Accelerated chloride threshold testing: Part I-ASTM A 615 and A 706 reinforcement. Materials Journal 100(6). pp 519–527.

Tritthart, J. (1989). Chloride binding in cement. II.: The influence of the hydroxide concentration in the pore solution of hardened cement paste on chloride binding. Cement and Concrete Research 19. pp 683-691.

Tuutti, K. (1982). Corrosion of steel in concrete. Swedish Cement and Concrete Research Institute (CBI). Stockholm.

Tuutti, K. (1993). Effect of cement type and different additions on service life. Proceedings International Conference, Concrete 2000. UK. pp 1285-1295.

Uhlig, H. H. (1983). Corrosion and corrosion control. New York, USA.

(1975). US Bureau of Reclamation. Concrete Manual. Denver. USA.

Vassie, P (1984). Reinforcement corrosion and the durability of concrete bridges. Proceedings of the Institution of Civil Engineers Part 1 (76). pp 713–723.

Venu, K., Balakrishnan, K. and Rajagopalan, K. S. (1965). A potentiokinetic polarization study of the behaviour of steel in NaOH-NaCl system. Corrosion Science 5. pp 59-69.

Weyers, R. E. (1998). Service life model for concrete structures exposed to chloride laden environments. ACT Materials Journal 95 (4). pp 445-454.

Wu, L., Li, W. and Yu, X. (2017). Time-dependent chloride penetration in concrete in marine environments. Construction and Building Materials 152. pp 406-413.

Yang, C. C. and Cho, S. W. (2003). An electrochemical method for accelerated chloride migration test of diffusion coefficient in cement-based materials. Materials PhysChem 81(1). pp. 116-25.

Yu, Z. and Ye, G. (2013). New perspective of service life prediction of fly ash concrete. Construction and Building Materials 48(11). pp 764-771.

Yu, Z. W. et al. (2015). Accelerated simulation of chloride ingress into concrete under drying-wetting alternation condition chloride environment. Construction and Building Materials 93. pp 205-213.

Zhao, J. et al. (2020). Investigation on effect of time dependent surface chloride concentration on apparent average chloride diffusion coefficient in concrete. 4th International RILEM conference on Microstructure Related Durability of cementitious Composites. pp 640-648.

Appendix A: Chloride ingress data

A1: Cape Town, w/b = 0.40, PC, submerged

Values shown are an average of three individual specimens.

0.4 PC submerged

mean depth (mm)	% Cl by mass of cement					
	1 year	1.5 years	2 years	2.5 years	3 years	3.5 years
1	0,810	0,950	1,270	1,600	1,740	1,950
3,5	1,010	1,250	1,510	1,850	1,920	2,080
7,5	0,750	0,850	1,120	1,350	1,490	1,600
12,5	0,210	0,340	0,520	0,780	0,920	1,070
17,5	0,140	0,200	0,310	0,450	0,560	0,700
22,5	0,100	0,150	0,150	0,290	0,300	0,410
27,5	0,070	0,090	0,100	0,180	0,190	0,180
35	0,02	0,03	0,080	0,100	0,130	0,160
45	0,16	0,4				
55	0,19	0,38				

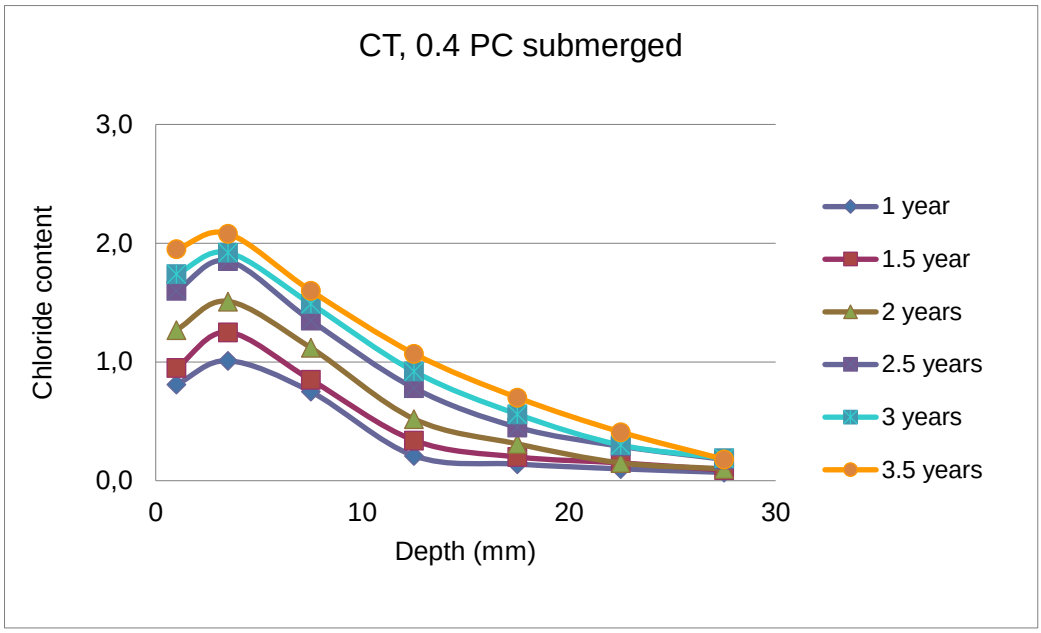

A2: Cape Town, w/b = 0.60, PC, submerged

Values shown are an average of three individual specimens.

0.6 PC submerged

mean depth (mm)	% Cl by mass of cement					
	1 year	1.5 years	2 years	2.5 years	3 years	3.5 years
1	0,940	1,050	1,380	1,810	1,900	2,050
3,5	1,340	1,580	1,950	2,140	2,250	2,420
7,5	0,970	1,160	1,550	1,720	1,830	2,080
12,5	0,500	0,750	1,060	1,230	1,300	1,590
17,5	0,260	0,440	0,650	0,820	0,920	1,120
22,5	0,100	0,250	0,390	0,450	0,490	0,650
27,5	0,090	0,100	0,180	0,280	0,300	0,350
35	0,080	0,060	0,080			
45	0,08	0,07				
55	0,93	0,03				

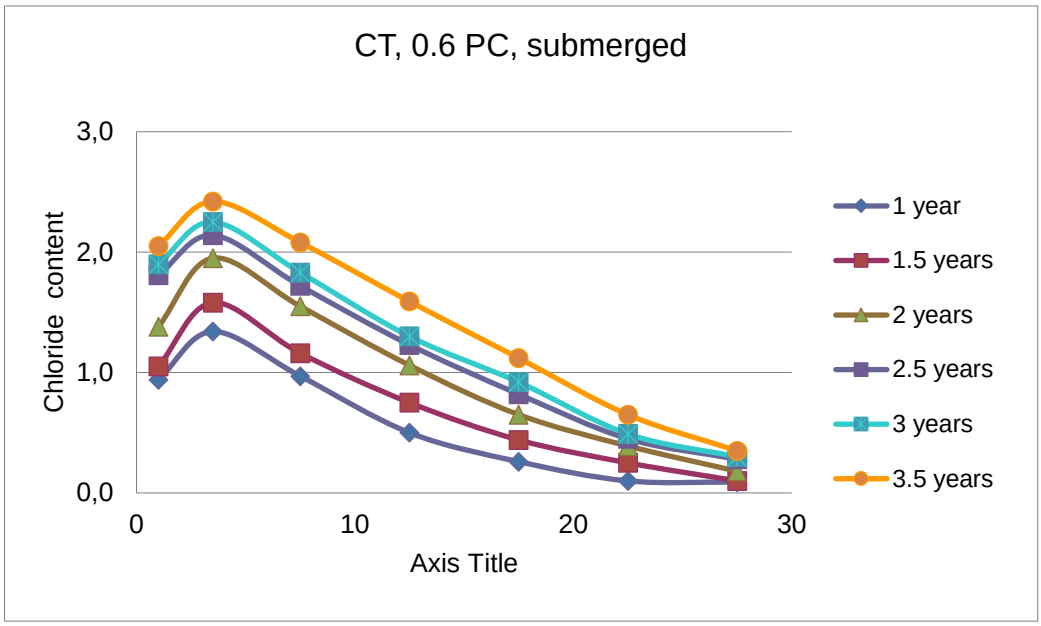

A3: Cape Town, w/b = 0.40, CS, submerged

Values shown are an average of three individual specimens.

0.4 CS subm.

mean depth (mm)	% Cl by mass of cement					
	1 year	1.5 years	2 years	2.5 years	3 years	3.5 years
1	0,720	1,250	1,800	1,950	2,350	2,820
3,5	1,350	1,740	2,130	2,400	2,700	3,020
7,5	0,580	0,720	0,860	1,060	1,200	1,380
12,5	0,160	0,180	0,230	0,420	0,510	0,620
17,5	0,080	0,090	0,140	0,210	0,200	0,250
22,5	0,030	0,100	0,090	0,120	0,100	0,150
27,5			0,060		0,090	0,150

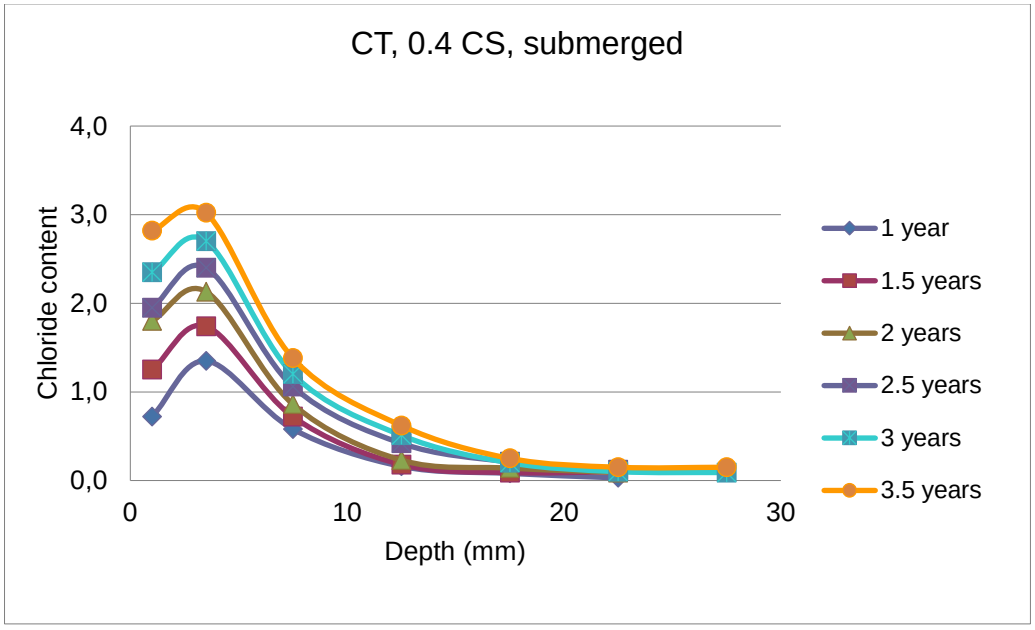

A4: Cape Town, w/b = 0.60, CS, submerged

Values shown are an average of three individual specimens.

0.6 CS subm.

mean depth (mm)	% Cl by mass of cement					
	1 year	1.5 years	2 years	2.5 years	3 years	3.5 years
1	0,810	2,140	2,210	2,550	2,840	3,420
3,5	1,936	2,240	2,460	2,820	3,240	3,570
7,5	0,950	1,350	1,480	1,820	1,950	2,480
12,5	0,390	0,430	0,550	0,620	0,630	0,850
17,5	0,090	0,090	0,100	0,150	0,200	0,160
22,5	0,020	0,100	0,050	0,100	0,230	0,090

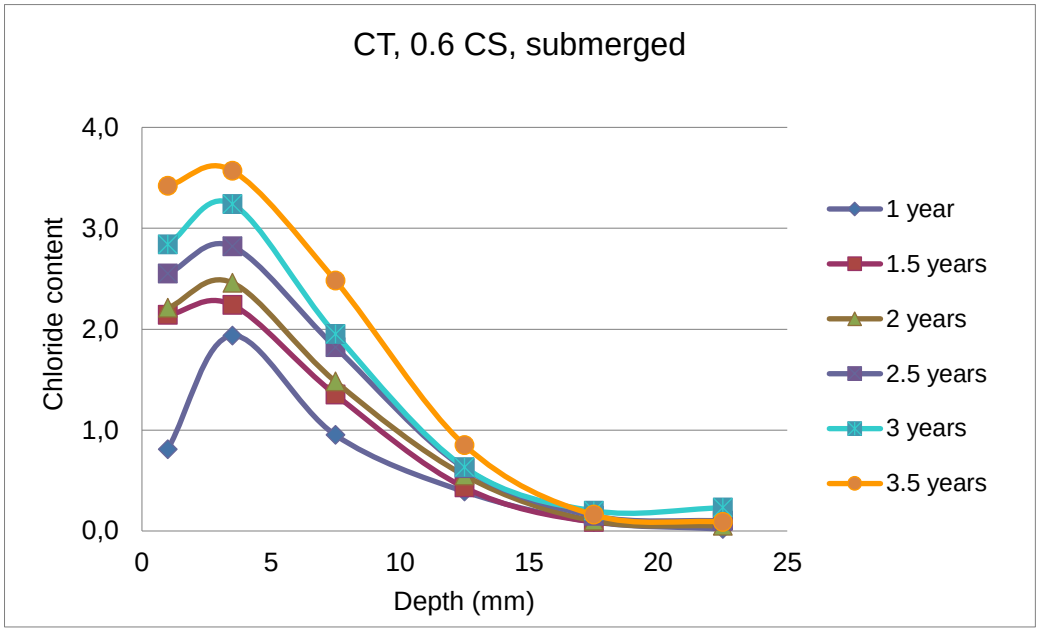

A5: Cape Town, w/b = 0.40, FA, submerged

Values shown are an average of three individual specimens.

0.4 FA submerged

mean depth (mm)	% Cl by mass of cement					
	1 year	1.5 years	2 years	2.5 years	3 years	3.5 years
1	1,450	1,380	1,15	1,88	2,400	2,650
3,5	1,240	1,550	1,96	2,19	2,720	3,200
7,5	0,540	0,700	0,84	1,11	1,320	1,560
12,5	0,080	0,100	0,28	0,43	0,400	0,500
17,5	0,060	0,050	0,06	0,10	0,140	0,110
22,5	0,050	0,250	0,05	0,25	0,090	0,100
27,5	0,100			0,13	0,07	

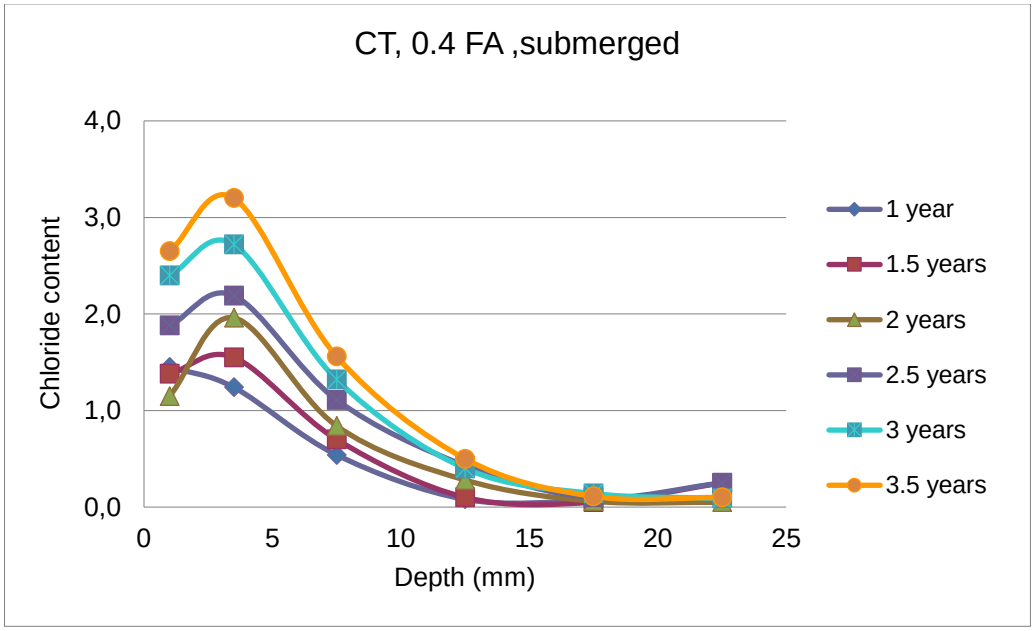

A6: Cape Town, w/b = 0.60, FA, submerged

Values shown are an average of three individual specimens.

0.6 FA submerged

mean depth (mm)	% Cl by mass of cement					
	1 year	1.5 years	2 years	2.5 years	3 years	3.5 years
1	1,730	2,100	2,620	2,900	3,120	2,860
3,5	1,860	2,560	2,600	2,980	3,200	3,450
7,5	1,080	1,550	1,650	1,920	2,050	2,500
12,5	0,360	0,400	0,720	0,840	0,980	0,980
17,5	0,180	0,100	0,250	0,300	0,350	0,290
22,5	0,170	0,090	0,080	0,150	0,100	0,090
27,5	0,17	0,05				

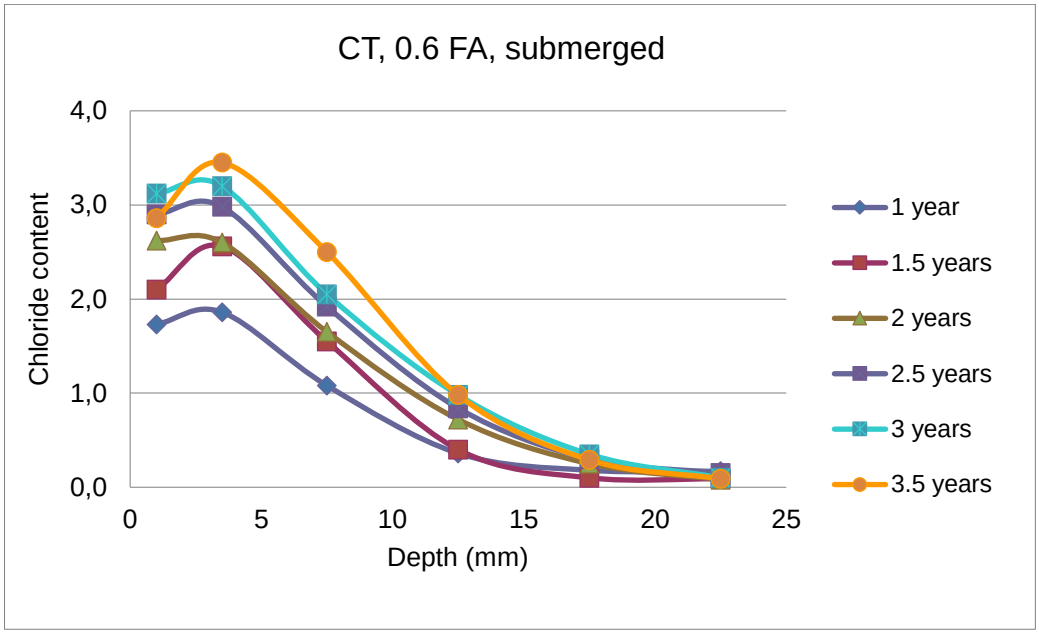

A7: Cape Town, w/b = 0.40, SP, submerged

Values shown are an average of three individual specimens.

0.4 SP submerged

mean depth (mm)	% Cl by mass of cement					
	1 year	1.5 years	2 years	2.5 years	3 years	3.5 years
1	1,180	1,900	1,310	2,160	2,490	3,120
3,5	1,570	1,910	2,210	2,390	2,950	3,450
7,5	0,810	1,100	1,350	1,500	1,700	1,870
12,5	0,120	0,270	0,400	0,510	0,600	0,750
17,5	0,070	0,040	0,200	0,230	0,260	0,240
22,5	0,090	0,040	0,130	0,130	0,120	0,160
27,5	0,15	0,120	0,090	0,14	0,25	0,14

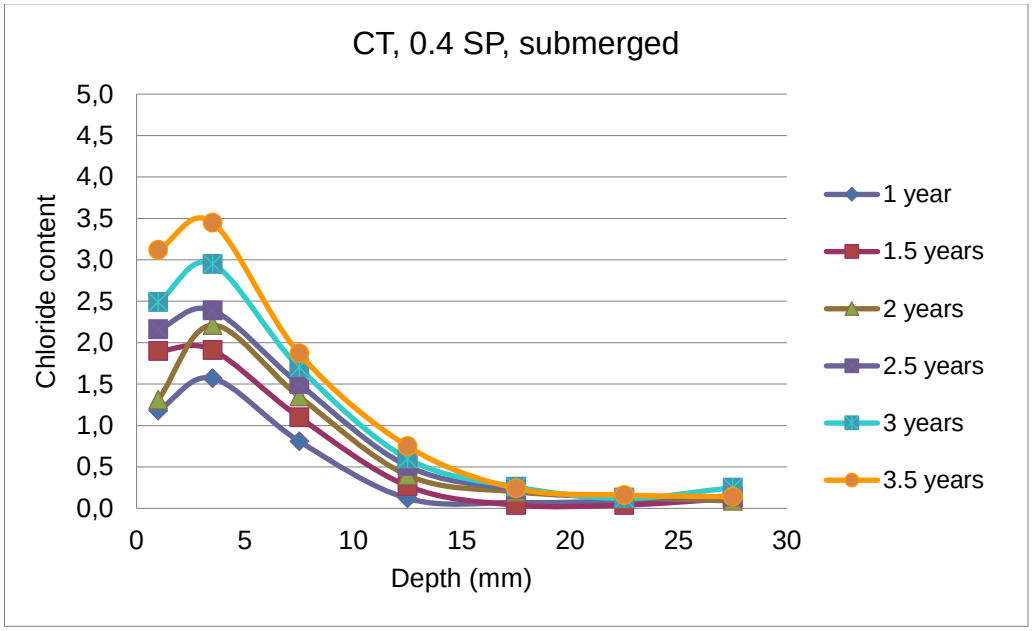

A8: Cape Town, w/b = 0.60, SP, submerged

Values shown are an average of three individual specimens.

0.6 SP submerged

mean depth (mm)	% Cl by mass of cement					
	1 year	1.5 years	2 years	2.5 years	3 years	3.5 years
1	1,960	1,510	2,520	3,200	3,610	3,520
3,5	2,100	3,000	3,100	3,340	3,600	3,910
7,5	1,260	1,700	1,940	2,300	2,510	2,680
12,5	0,420	0,860	0,970	1,140	1,290	1,230
17,5	0,150	0,300	0,410	0,440	0,570	0,550
22,5	0,090	0,150	0,300	0,250	0,300	0,330
27,5	0,23	0,18	0,160	0,300	0,250	0,310

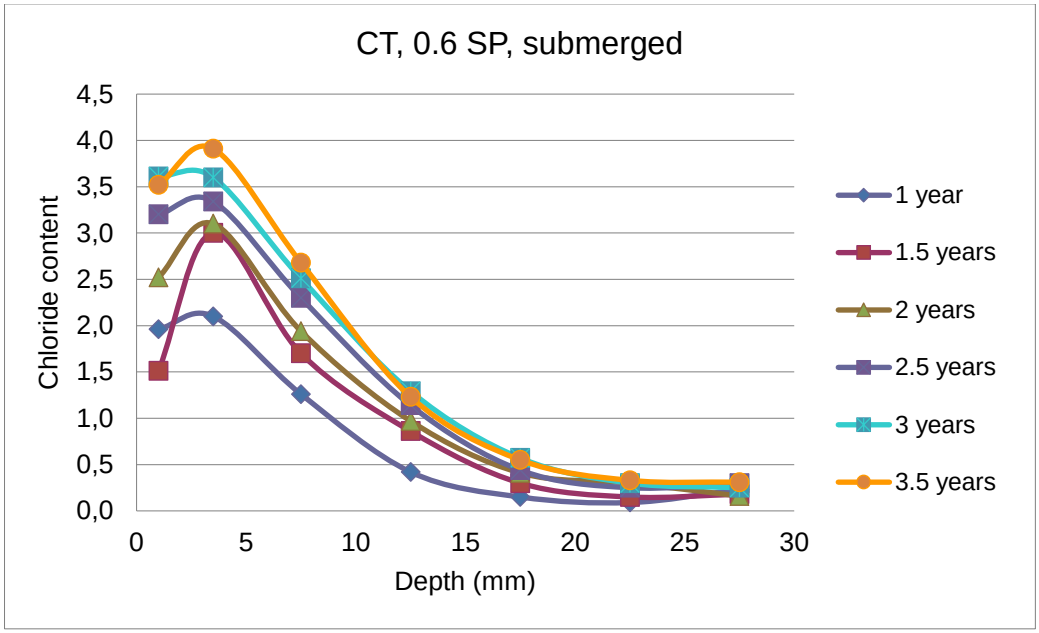

A9: Cape Town, w/b = 0.40, SF, submerged

Values shown are an average of three individual specimens.

0.4 SF submerged

mean depth (mm)	% Cl by mass of cement					
	1 year	1.5 years	2 years	2.5 years	3 years	3.5 years
1	1,310	1,400	2,280	1,500	2,290	2,850
3,5	1,510	1,970	2,250	2,420	2,490	2,860
7,5	0,880	1,070	1,330	1,520	1,740	1,950
12,5	0,270	0,350	0,420	0,700	0,760	0,980
17,5	0,090	0,110	0,090	0,310	0,250	0,430
22,5	0,100	0,090	0,100	0,180	0,100	0,140
27,5	0,040	0,100		0,120		0,090
35	0,04					

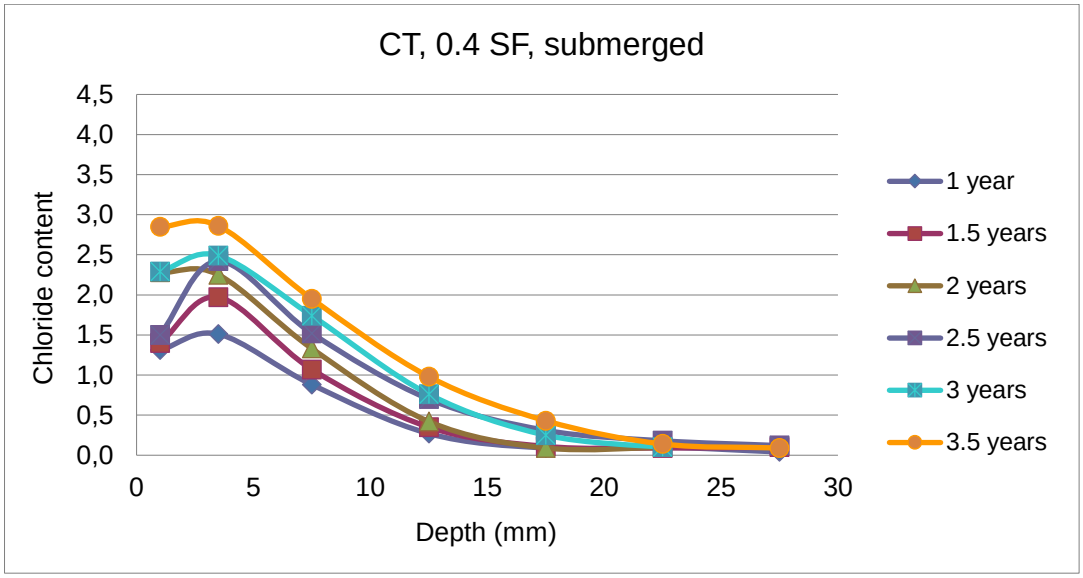

A10: Cape Town, w/b = 0.60, SF, submerged

Values shown are an average of three individual specimens.

0.6 SF submerged

mean depth (mm)	% Cl by mass of cement					
	1 year	1.5 years	2 years	2.5 years	3 years	3.5 years
1	1,680	2,300	2,950	3,200	3,350	3,200
3,5	2,300	2,600	3,150	3,300	3,500	3,790
7,5	1,400	1,650	2,020	2,390	2,670	2,920
12,5	0,670	0,900	1,030	1,350	1,500	1,750
17,5	0,230	0,440	0,600	0,590	0,710	0,890
22,5	0,090	0,190	0,380	0,200	0,230	0,430
27,5	0,090	0,050	0,230		0,100	0,120
35	0,56	0,05				
45	0,55	0,09				
55	0,41	0,03				

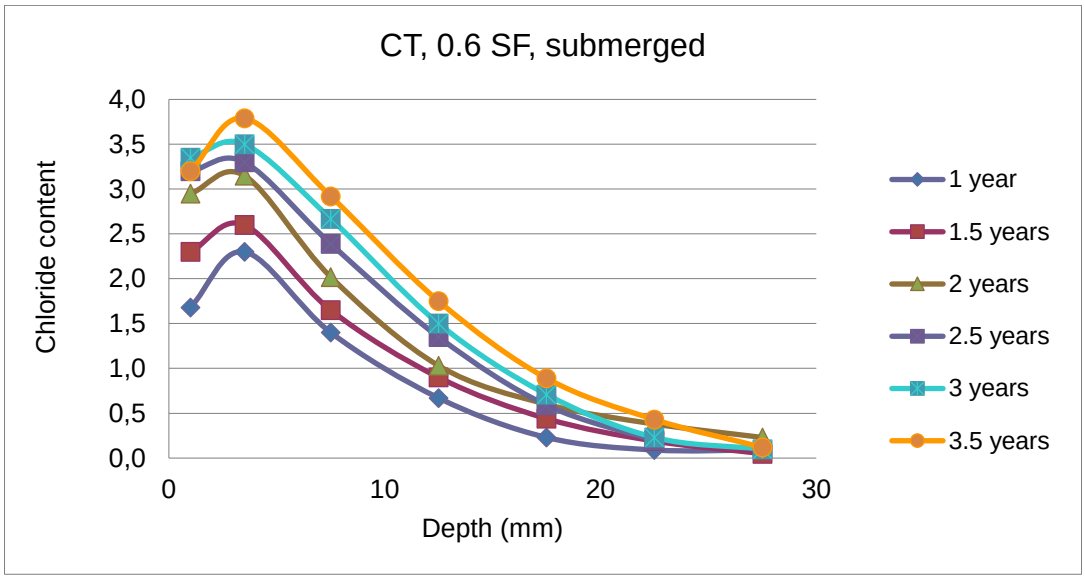

A11: Cape Town, w/b = 0.40, PC, tidal

Values shown are an average of three individual specimens.

0.4 PC tidal

mean depth (mm)	% Cl by mass of cement					
	1 year	1.5 years	2 years	2.5 years	3 years	3.5 years
1	1,140	1,150	1,580	2,120	1,800	2,550
3,5	1,140	1,420	1,900	2,340	2,550	2,700
7,5	0,710	1,160	1,450	1,750	1,850	2,040
12,5	0,320	0,430	0,780	1,050	1,200	1,320
17,5	0,120	0,100	0,350	0,590	0,650	0,800
22,5	0,060	0,040	0,120	0,220	0,330	0,420
27,5	0,020	0,130		0,090	0,120	0,230
35	0,05					

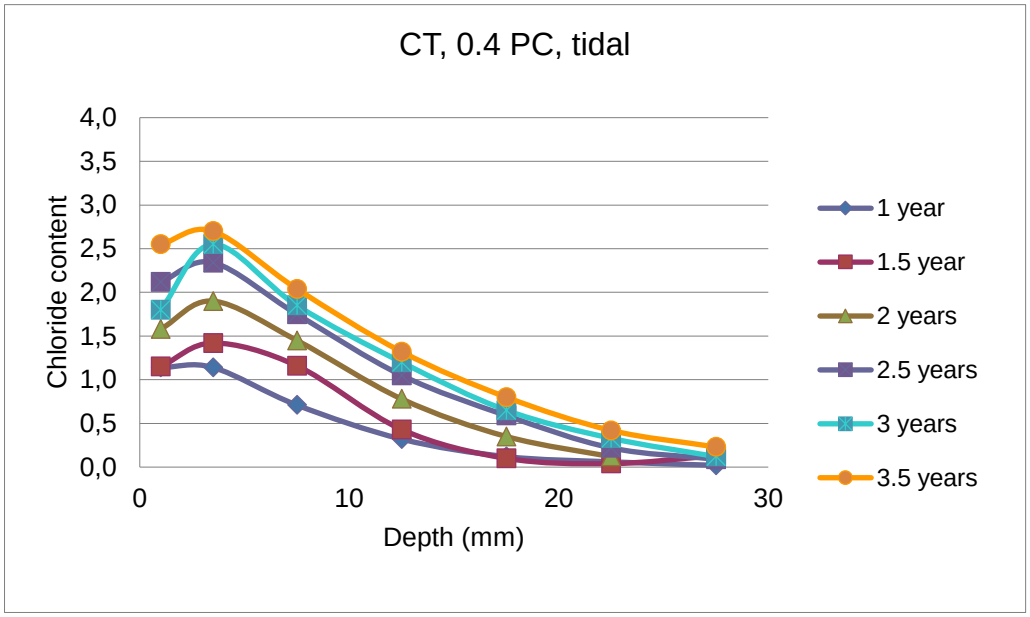

A12: Cape Town, w/b = 0.60, PC, tidal

Values shown are an average of three individual specimens.

0.6 PC tidal

mean depth (mm)	% Cl by mass of cement					
	1 year	1.5 years	2 years	2.5 years	3 years	3.5 years
1	0,780	1,740	2,180	1,920	2,560	3,100
3,5	1,470	1,850	2,250	2,380	2,800	3,000
7,5	1,200	1,330	1,670	1,990	2,340	2,620
12,5	0,710	0,890	1,150	1,420	1,700	2,060
17,5	0,350	0,510	0,780	0,940	1,110	1,440
22,5	0,200	0,300	0,540	0,650	0,700	0,930
27,5	0,090	0,160	0,350	0,400	0,440	0,500
35	0,05	0,13				

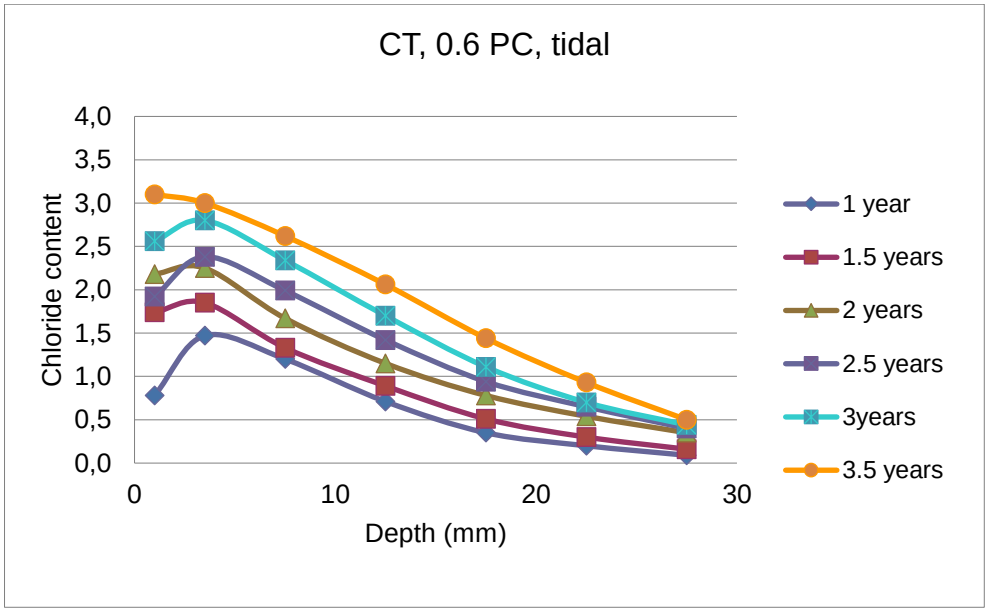

A13: Cape Town, w/b = 0.40, CS, tidal

Values shown are an average of three individual specimens.

0.4 CS tidal

mean depth (mm)	% Cl by mass of cement					
	1 year	1.5 years	2 years	2.5 years	3 years	3.5 years
1	1,470	1,780	2,750	2,78	2,960	3,720
3,5	1,620	2,330	2,600	2,82	3,450	4,200
7,5	0,650	1,180	1,200	1,4	1,560	1,800
12,5	0,120	0,280	0,300	0,52	0,700	0,640
17,5	0,090	0,100	0,160	0,25	0,320	0,280
22,5	0,080	0,170	0,100	0,14	0,180	0,200
27,5		0,030				0,230
35		0,05				

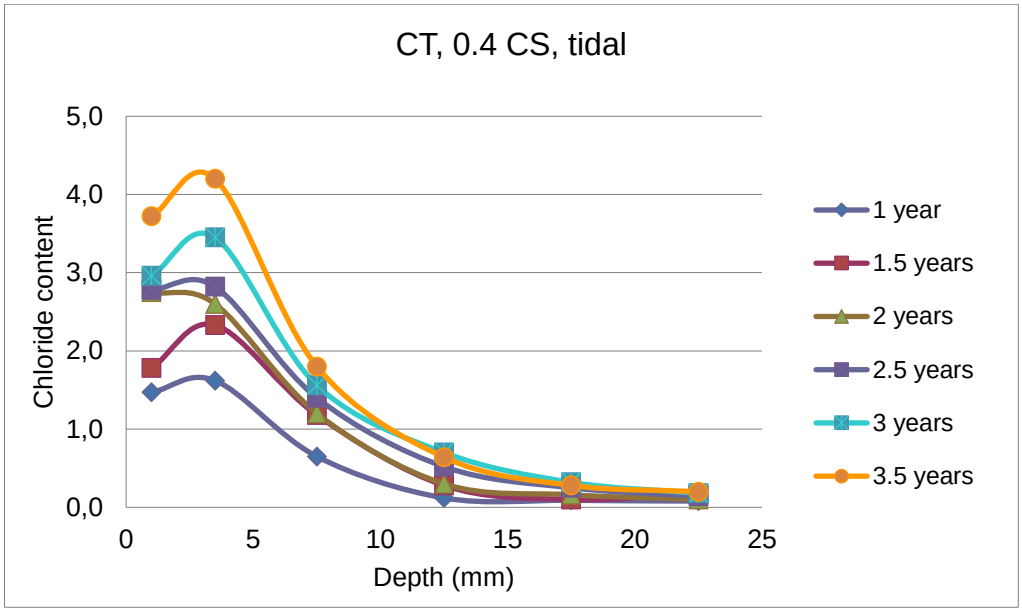

A14: Cape Town, w/b = 0.60, CS, tidal

Values shown are an average of three individual specimens.

0.6 CS tidal

mean depth (mm)	% Cl by mass of cement					
	1 year	1.5 years	2 years	2.5 years	3 years	3.5 years
1	0,860	2,100	2,870	2,950	3,160	4,000
3,5	2,340	2,350	2,910	3,400	4,060	4,150
7,5	1,420	1,440	1,880	2,100	2,240	2,650
12,5	0,450	0,400	0,720	0,950	1,090	1,200
17,5	0,140	0,150	0,210	0,270	0,300	0,420
22,5	0,280	0,100	0,090	0,160	0,170	0,200
27,5	0,03	0,18	0,03		0,18	

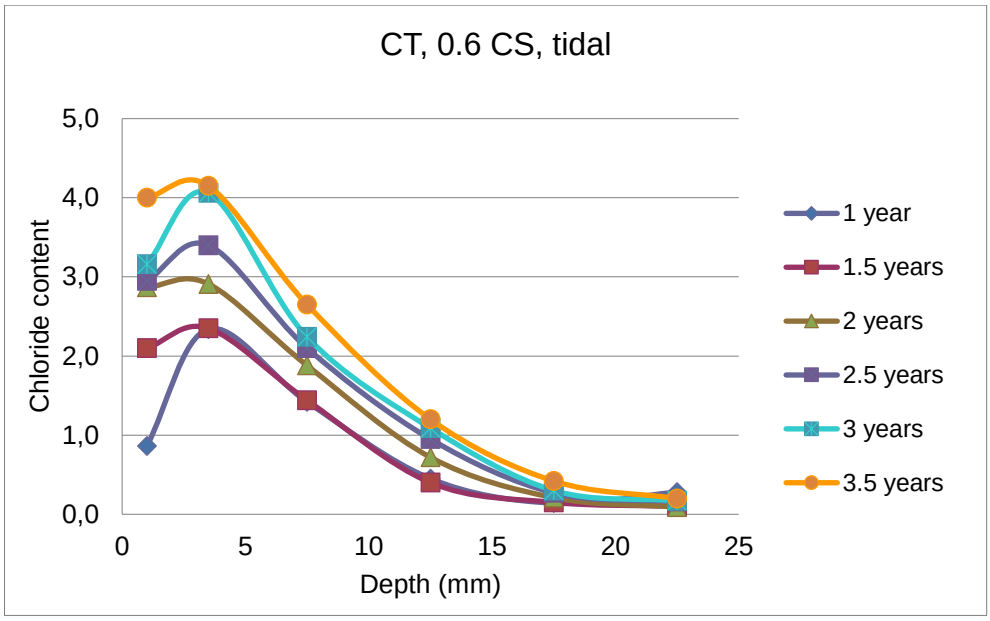

A15: Cape Town, w/b = 0.40, FA, tidal

Values shown are an average of three individual specimens.

0.4 FA tidal

mean depth (mm)	% Cl by mass of cement					
	1 year	1.5 years	2 years	2.5 years	3 years	3.5 years
1	1,310	2,190	2,220	2,490	2,190	3,150
3,5	1,690	2,010	2,310	2,650	3,310	3,680
7,5	0,810	1,030	1,250	1,520	1,760	2,080
12,5	0,230	0,330	0,300	0,660	0,630	0,750
17,5	0,070	0,140	0,160	0,200	0,140	0,200
22,5	0,030	0,130	0,100	0,170	0,130	0,150
27,5	0,10	0,14	0,09		0,14	0,090
35	0,00	0,14			0,14	0,09
45	0,04	0,13			0,13	
55	0,54	0,11			0,11	

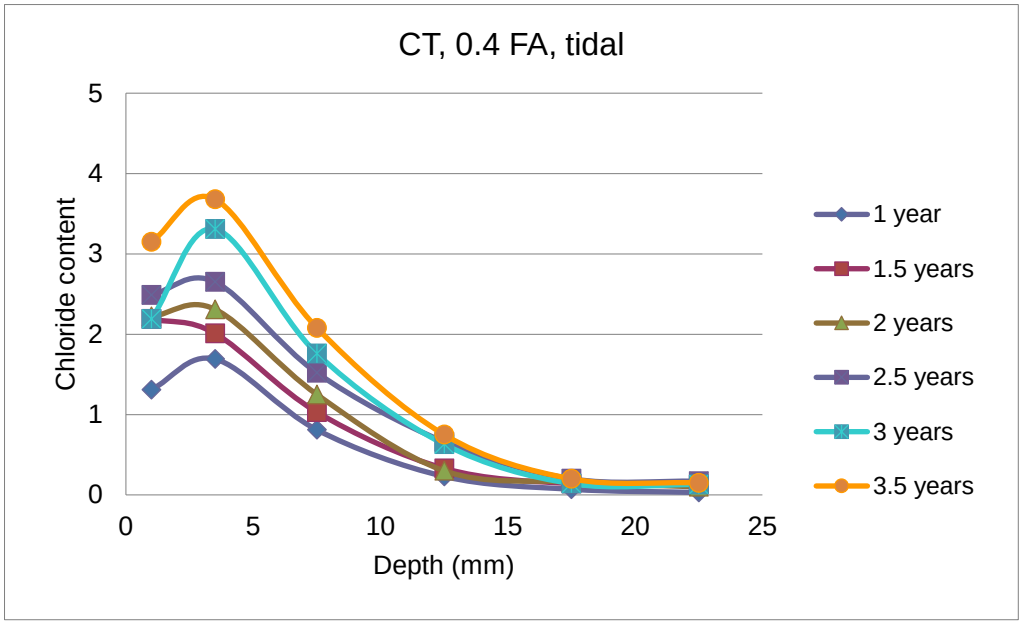

A16: Cape Town, w/b = 0.60, FA, tidal

Values shown are an average of three individual specimens.

0.6 FA tidal

mean depth (mm)	% Cl by mass of cement					
	1 year	1.5 years	2 years	2.5 years	3 years	3.5 years
1	1,960	0,920	2,980	2,850	3,610	3,650
3,5	2,020	2,700	3,010	3,320	3,560	3,800
7,5	1,370	1,750	2,100	2,350	2,430	2,780
12,5	0,520	0,680	0,950	1,120	1,190	1,340
17,5	0,200	0,200	0,320	0,340	0,370	0,550
22,5	0,130	0,180	0,200	0,190	0,200	0,210
27,5	0,080	0,200				
35		0,050				
45		0,20				
55		0,34				

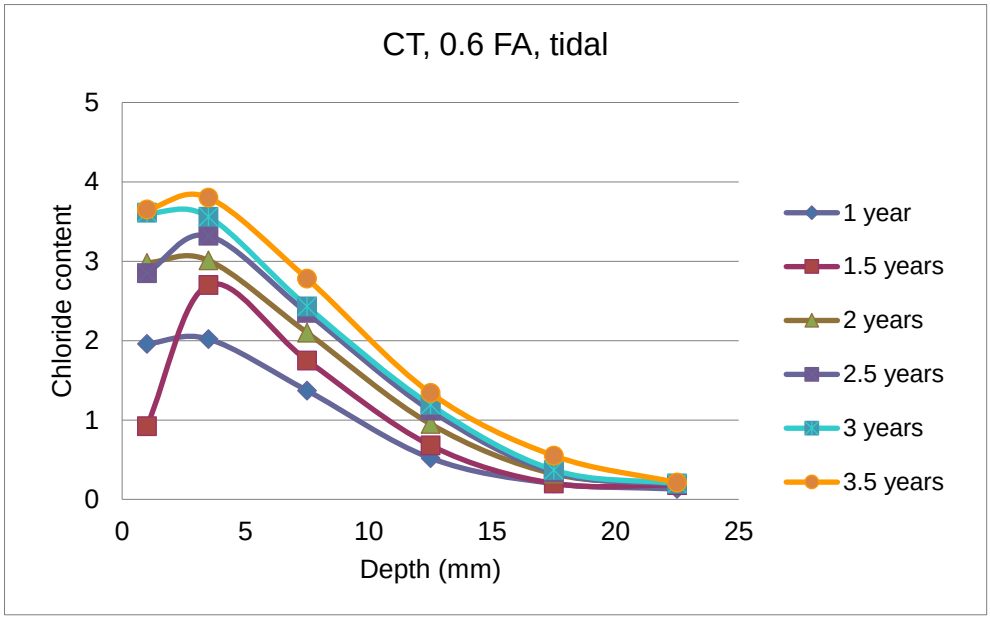

A17: Cape Town, w/b = 0.40, SP, tidal

Values shown are an average of three individual specimens.

0.4 SP tidal

mean depth (mm)	% Cl by mass of cement					
	1 year	1.5 years	2 years	2.5 years	3 years	3.5 years
1	1,160	1,240	2,150	2,640	2,650	3,150
3,5	1,760	2,090	2,440	2,850	3,220	3,650
7,5	0,930	1,230	1,450	1,600	1,880	2,090
12,5	0,300	0,380	0,560	0,700	0,820	0,920
17,5	0,100	0,150	0,150	0,250	0,260	0,350
22,5	0,030	0,120	0,080	0,120	0,100	0,180
27,5	0,020	0,130	0,090		0,25	
35	0,03	0,12				
45	0,28	0,12				
55	0,28	0,03				

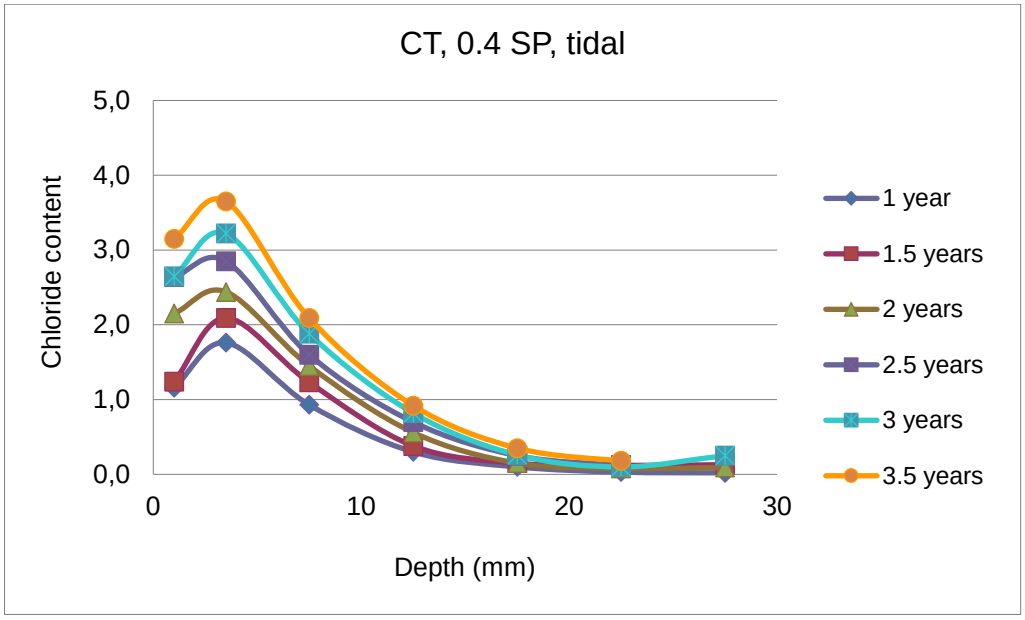

A18: Cape Town, w/b = 0.60, SP, tidal

Values shown are an average of three individual specimens.

0.6 SP tidal

mean depth (mm)	% Cl by mass of cement					
	1 year	1.5 years	2 years	2.5 years	3 years	3.5 years
1	1,640	2,050	2,800	3,150	3,820	3,650
3,5	2,550	3,170	3,120	3,350	3,960	4,470
7,5	1,680	1,960	2,220	2,400	2,740	2,850
12,5	0,820	0,960	1,090	1,220	1,400	1,570
17,5	0,300	0,360	0,400	0,550	0,710	0,740
22,5	0,050	0,220	0,260	0,290	0,400	0,360
27,5	0,04	0,220			0,250	
35	0,16	0,19				
45	0,57	0,37				
55	0,62	0,28				

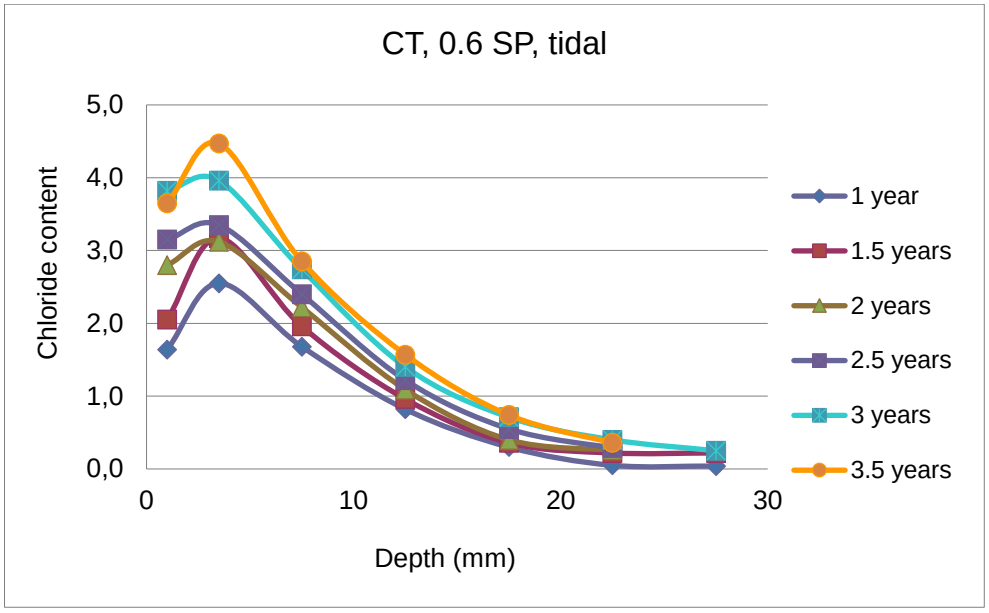

A19: Cape Town, w/b = 0.40, SF, tidal

Values shown are an average of three individual specimens.

0.4 SF tidal

mean depth (mm)	% Cl by mass of cement					
	1 year	1.5 years	2 years	2.5 years	3 years	3.5 years
1	1,380	1,770	1,740	2,000	2,330	2,700
3,5	1,720	2,040	2,400	2,310	2,600	3,150
7,5	0,980	1,310	1,550	1,550	1,900	2,250
12,5	0,400	0,660	0,700	0,740	0,950	1,210
17,5	0,080	0,260	0,300	0,300	0,460	0,620
22,5	0,020	0,040	0,090	0,190	0,300	0,350
27,5	0,03	0,03		0,10		
35	0,03	0,36				
45	0,05	0,53				
55	0,04	0,37				

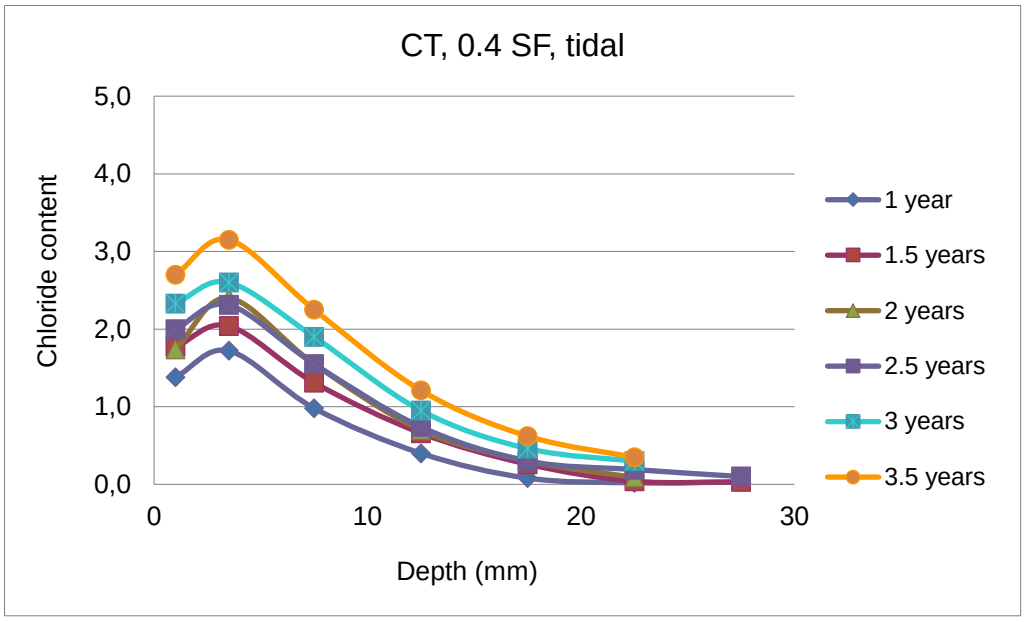

A20: Cape Town, w/b = 0.60, SF, tidal

Values shown are an average of three individual specimens.

0.6 SF tidal

mean depth (mm)	% Cl by mass of cement					
	1 year	1.5 years	2 years	2.5 years	3 years	3.5 years
1	1,810	1,050	2,800	2,120	3,120	3,500
3,5	2,650	2,950	3,360	3,600	3,950	4,220
7,5	1,760	1,920	2,210	2,470	2,960	3,250
12,5	0,900	1,160	1,280	1,370	1,800	2,180
17,5	0,430	0,670	0,750	0,660	0,950	1,210
22,5	0,180	0,370	0,460	0,340	0,510	0,600
27,5	0,100	0,250	0,100	0,180	0,300	0,220
35	0,29					
45	0,63					
55	0,38	0,25				

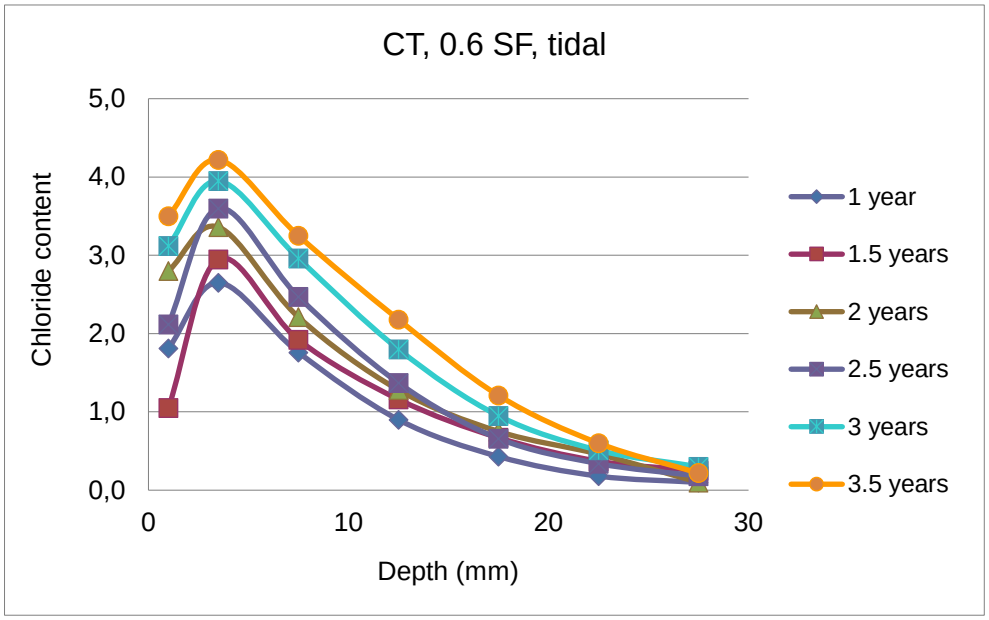

A21: Cape Town, w/b = 0.40, PC, splash/spray

Values shown are an average of three individual specimens.

0.4 PC splash spray

mean depth (mm)	% Cl by mass of cement					
	1 year	1.5 years	2 years	2.5 years	3 years	3.5 years
1	1,110	1,520	1,600	2,520	2,600	2,800
3,5	1,700	1,950	2,230	2,600	2,580	2,790
7,5	1,090	1,450	1,700	1,890	2,200	2,350
12,5	0,590	0,920	1,070	1,240	1,470	1,650
17,5	0,300	0,550	0,560	0,720	0,910	1,040
22,5	0,150	0,260	0,250	0,380	0,520	0,600
27,5	0,100	0,140	0,120	0,170	0,180	0,240
35	0,03	0,25				
45	0,02	0,17				
55	0,07	0,04				

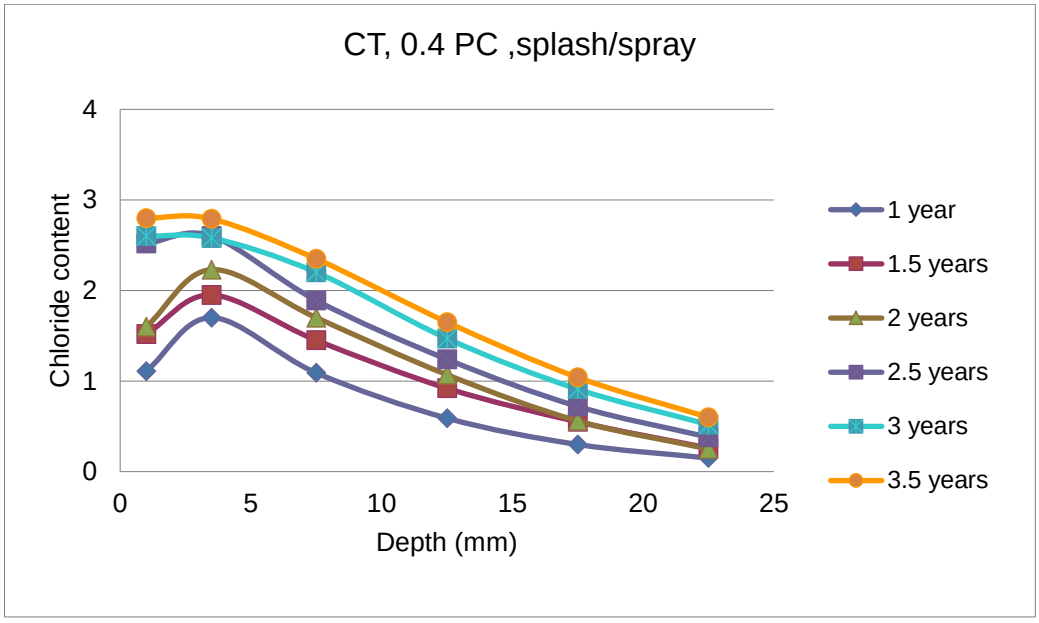

A22: Cape Town, w/b = 0.60, PC, splash/spray

Values shown are an average of three individual specimens.

0.6 PC splash spray

mean depth (mm)	% Cl by mass of cement					
	1 year	1.5 years	2 years	2.5 years	3 years	3.5 years
1	1,310	1,270	2,150	2,920	2,800	3,100
3,5	1,910	2,000	2,430	2,810	3,200	3,420
7,5	1,450	1,500	1,950	2,300	2,650	2,990
12,5	0,985	1,080	1,370	1,580	1,960	2,400
17,5	0,620	0,750	1,010	1,130	1,400	1,850
22,5	0,350	0,510	0,630	0,750	0,950	1,340
27,5	0,230	0,380	0,400	0,610	0,580	0,790
35	0,100	0,190				
45	0,14	0,19				
55	0,04	0,23				

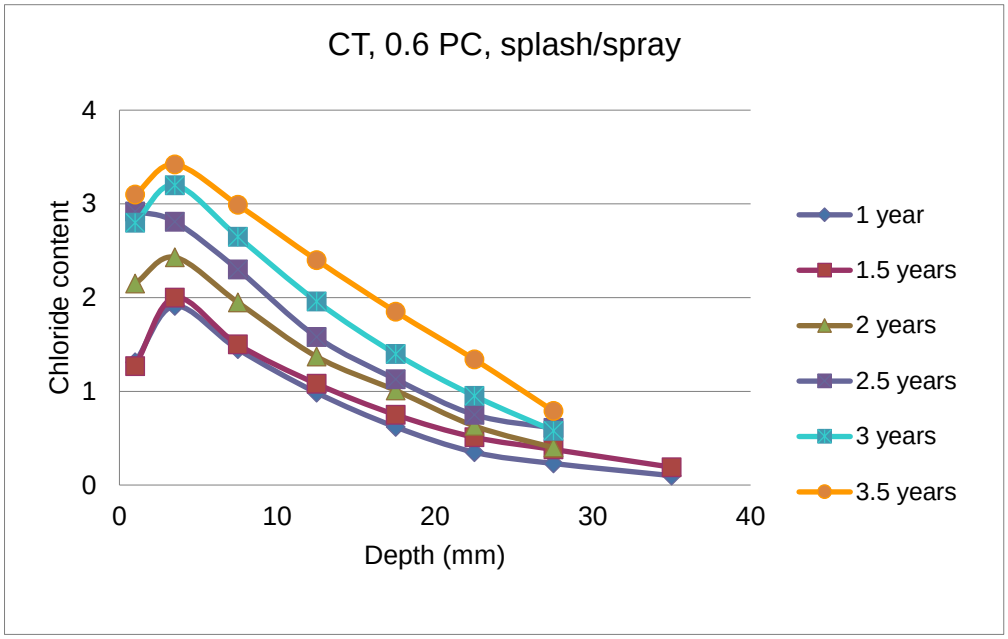

A23: Cape Town, w/b = 0.40, CS, splash/spray

Values shown are an average of three individual specimens.

0.4 CS splash spray

mean depth (mm)	% Cl by mass of cement					
	1 year	1.5 years	2 years	2.5 years	3 years	3.5 years
1	1,470	1,380	2,810	3,200	3,700	3,400
3,5	1,970	2,540	2,950	3,340	3,660	4,250
7,5	0,870	1,400	1,680	1,950	2,180	2,450
12,5	0,160	0,490	0,520	0,750	0,940	0,870
17,5	0,120	0,140	0,200	0,280	0,350	0,390
22,5	0,130	0,120	0,150	0,180	0,220	0,200
27,5	0,13	0,11	0,090	0,120	0,200	0,220
35	0,13	0,12				
45	0,25	0,13				
55	0,23	0,14				

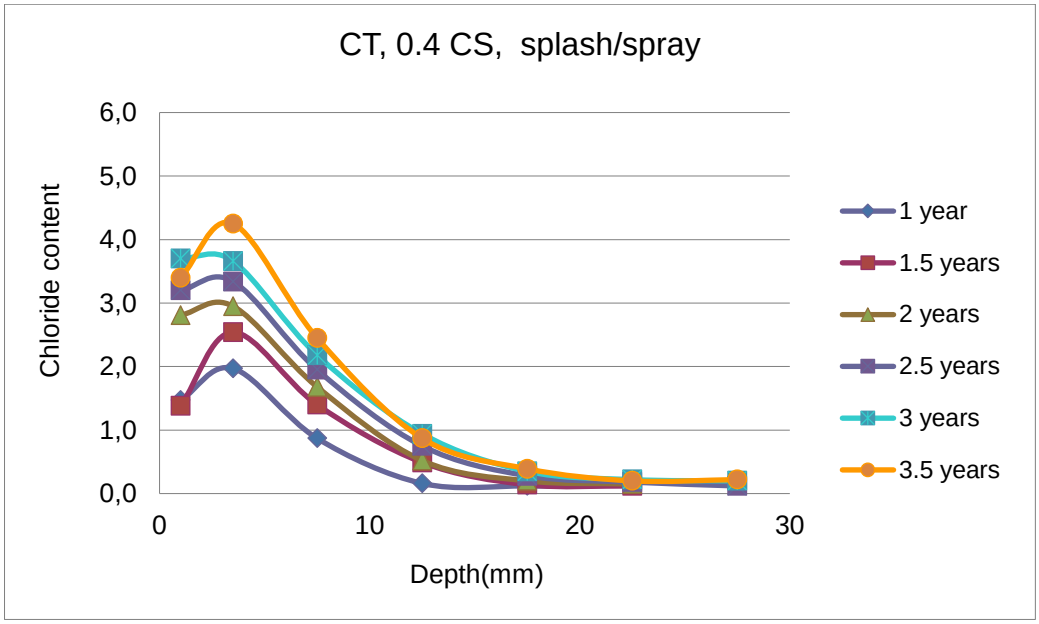

A24: Cape Town, w/b = 0.60, CS, splash/spray

Values shown are an average of three individual specimens.

0.6 CS splash spray

mean depth (mm)	% Cl by mass of cement					
	1 year	1.5 years	2 years	2.5 years	3 years	3.5 years
1	2,870	3,550	3,500	4,000	4,590	4,520
3,5	2,680	3,422	3,690	4,020	4,450	4,940
7,5	1,800	1,950	2,400	2,800	3,050	3,270
12,5	0,820	0,890	1,050	1,320	1,600	1,840
17,5	0,350	0,280	0,370	0,450	0,610	0,800
22,5	0,100	0,190	0,250	0,290	0,350	0,380
27,5	0,04	0,200	0,210	0,200		
35	0,05	0,04				
45	0,05	0,23				
55	0,1	0,23				

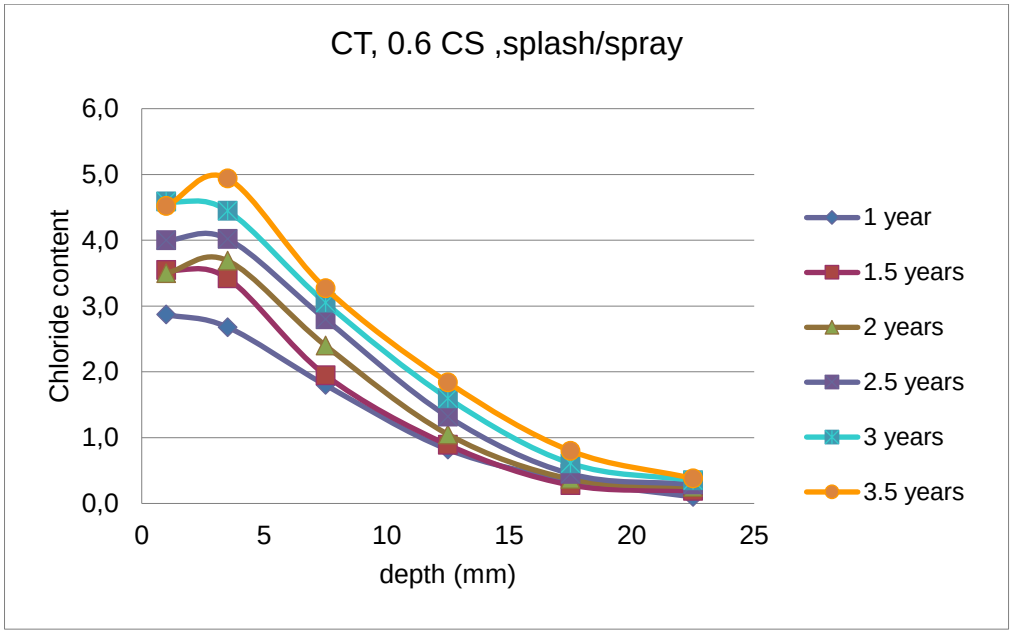

A25: Cape Town, w/b = 0.40, FA, splash/spray

Values shown are an average of three individual specimens.

0.4 FA splash spray

mean depth (mm)	% Cl by mass of cement					
	1 year	1.5 years	2 years	2.5 years	3 years	3.5 years
1	2,190	2,360	3,100	3,050	3,680	3,710
3,5	2,230	2,650	3,100	3,480	3,700	4,350
7,5	1,100	1,470	1,770	2,010	2,310	2,470
12,5	0,410	0,520	0,650	0,830	0,980	1,010
17,5	0,120	0,230	0,180	0,300	0,400	0,400
22,5	0,100	0,130	0,100	0,140	0,200	0,260
27,5	0,09	0,13				
35	0,09	0,12				
45	0,23	0,13				
55	0,22	0,14				

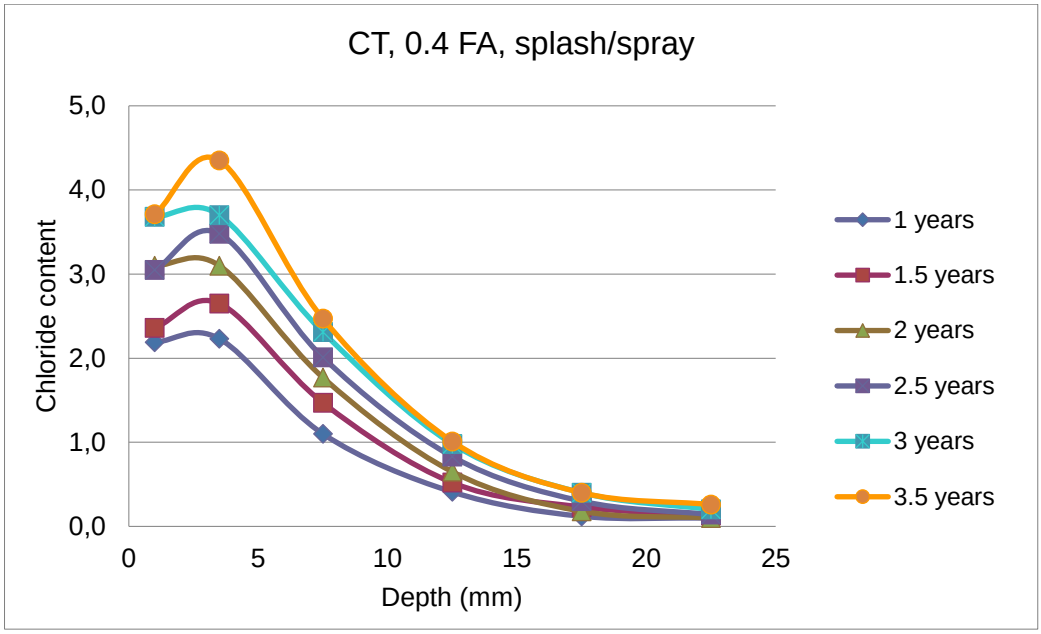

A26: Cape Town, w/b = 0.60, FA, splash/spray

Values shown are an average of three individual specimens.

0.6 FA splash spray

mean depth (mm)	% Cl by mass of cement					
	1 year	1.5 years	2 years	2.5 years	3 years	3.5 years
1	2,020	2,460	3,520	3,400	3,920	4,500
3,5	2,290	2,850	3,410	3,800	4,050	4,420
7,5	1,550	1,930	2,350	2,620	2,700	3,080
12,5	0,740	0,820	1,140	1,250	1,420	1,850
17,5	0,280	0,250	0,450	0,520	0,560	0,920
22,5	0,150	0,180	0,150	0,240	0,180	0,400
27,5	0,050	0,210				
35	0,05	0,21				
45	0,05	0,2				
55	0,21	0,27				

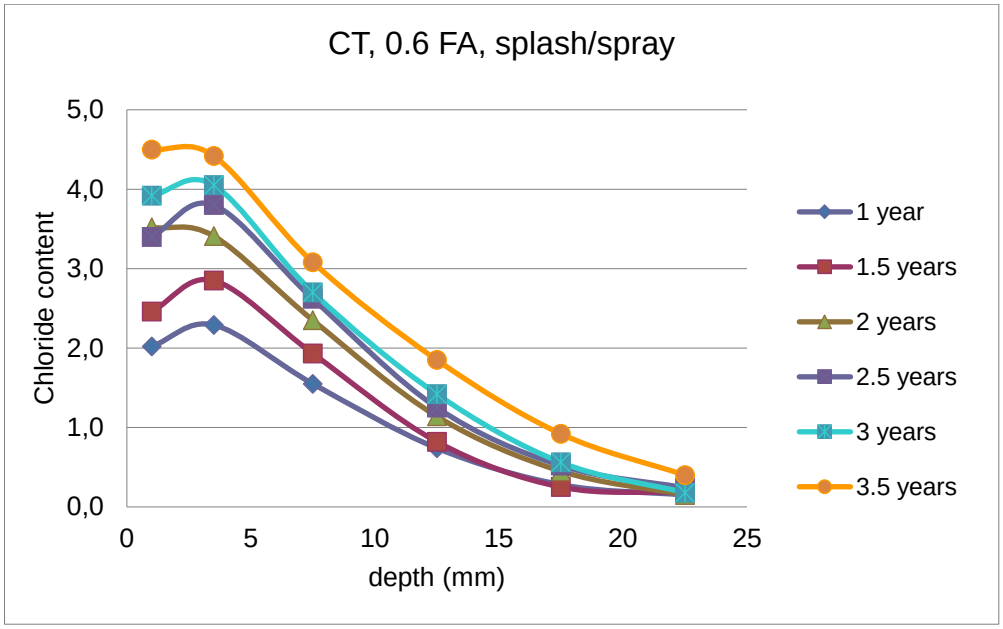

A27: Cape Town, w/b = 0.40, SP, splash/spray

Values shown are an average of three individual specimens.

0.4 SP splash spray

mean depth (mm)	% Cl by mass of cement					
	1 year	1.5 years	2 years	2.5 years	3 years	3.5 years
1	1,950	1,900	2,430	2,850	3,000	3,100
3,5	2,090	2,510	2,660	2,980	3,320	3,720
7,5	1,220	1,510	1,740	1,810	2,150	2,360
12,5	0,440	0,570	0,700	0,920	0,990	1,000
17,5	0,200	0,180	0,280	0,450	0,400	0,420
22,5	0,110	0,100	0,100	0,130	0,150	0,200
27,5	0,12	0,130				
35	0,12	0,13				
45	0,13	0,17				
55	0,24	0,17				

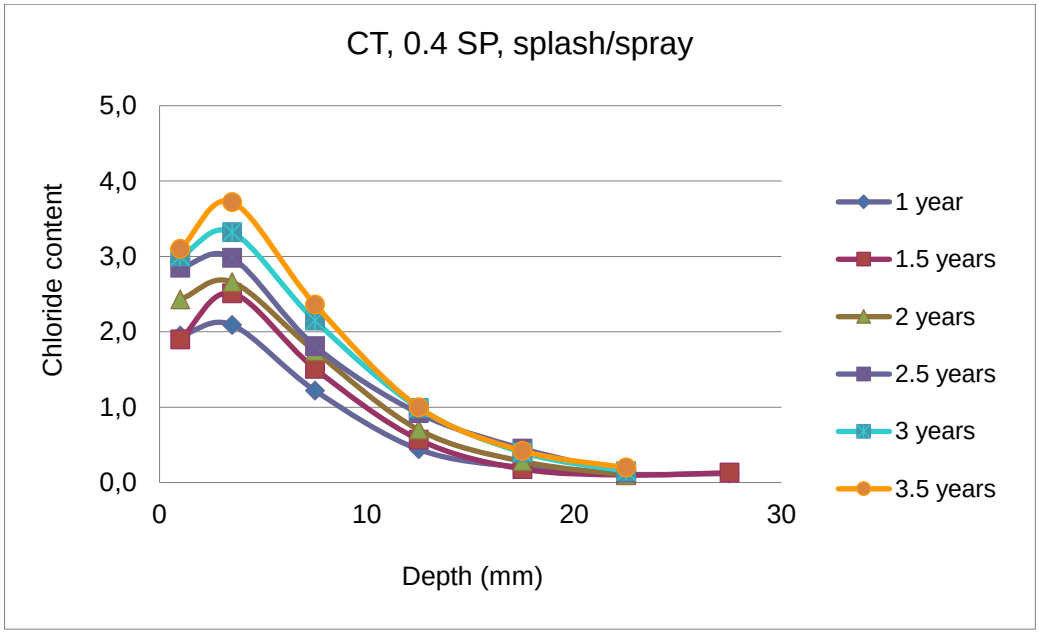

A28: Cape Town, w/b = 0.60, SP, splash/spray

Values shown are an average of three individual specimens.

0.6 SP splash spray

mean depth (mm)	% Cl by mass of cement					
	1 year	1.5 years	2 years	2.5 years	3 years	3.5 years
1	1,910	2,050	3,560	3,000	4,150	4,700
3,5	2,730	3,440	3,600	3,860	4,200	4,650
7,5	1,710	2,300	2,450	2,610	2,790	3,200
12,5	0,750	1,190	1,310	1,290	1,550	1,750
17,5	0,260	0,480	0,500	0,600	0,720	0,810
22,5	0,030	0,180	0,150	0,240	0,300	0,250
27,5	0,040	0,200				
35	0,19	0,21				
45	0,39	0,21				
55	0,41	0,24				

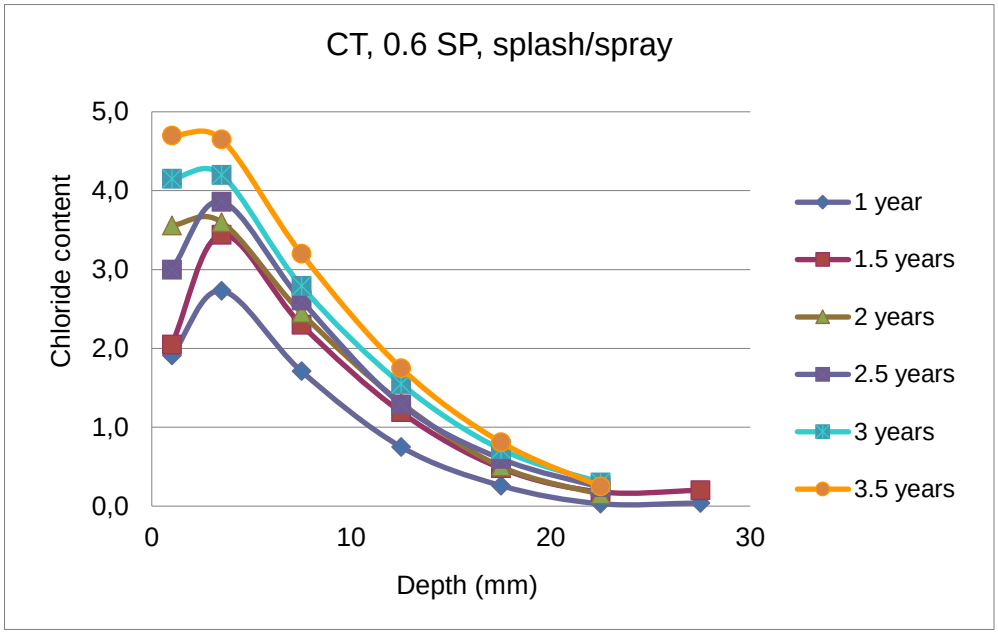

A29: Cape Town, w/b = 0.40, SF, splash/spray

Values shown are an average of three individual specimens.

0.4 SF splash spray

mean depth (mm)	% Cl by mass of cement					
	1 year	1.5 years	2 years	2.5 years	3 years	3.5 years
1	1,310	1,440	2,000	1,900	2,830	3,500
3,5	1,800	2,200	2,520	2,920	3,380	3,800
7,5	1,190	1,450	1,710	1,970	2,280	2,510
12,5	0,520	0,690	0,870	1,200	1,300	1,500
17,5	0,130	0,300	0,380	0,700	0,750	0,900
22,5	0,130	0,150	0,200	0,320	0,390	0,460
27,5	0,040	0,19	0,120	0,100	0,150	0,200
35	0,03	0,13				
45	0,05	0,14				
55	0,04	0,16				

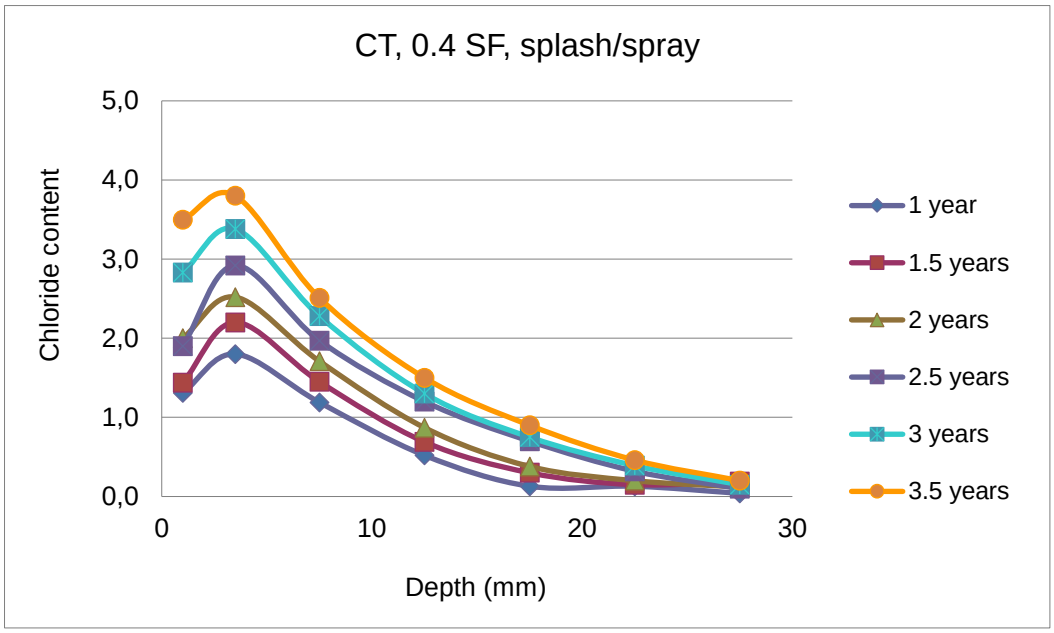

A30: Cape Town, w/b = 0.60, SF, splash/spray

Values shown are an average of three individual specimens.

0.6 SF splash spray

mean depth (mm)	% Cl by mass of cement					
	1 year	1.5 years	2 years	2.5 years	3 years	3.5 years
1	2,000	2,500	2,800	3,560	3,000	3,400
3,5	2,760	2,720	3,330	3,600	3,850	4,300
7,5	1,870	2,050	2,420	2,760	2,950	3,420
12,5	1,050	1,240	1,450	1,750	1,900	2,360
17,5	0,590	0,780	0,910	1,050	1,250	1,460
22,5	0,300	0,450	0,650	0,600	0,820	0,870
27,5	0,140	0,290	0,350	0,390	0,450	0,560
35	0,15	0,200				
45	0,16	0,05				
55	0,15	0,2				

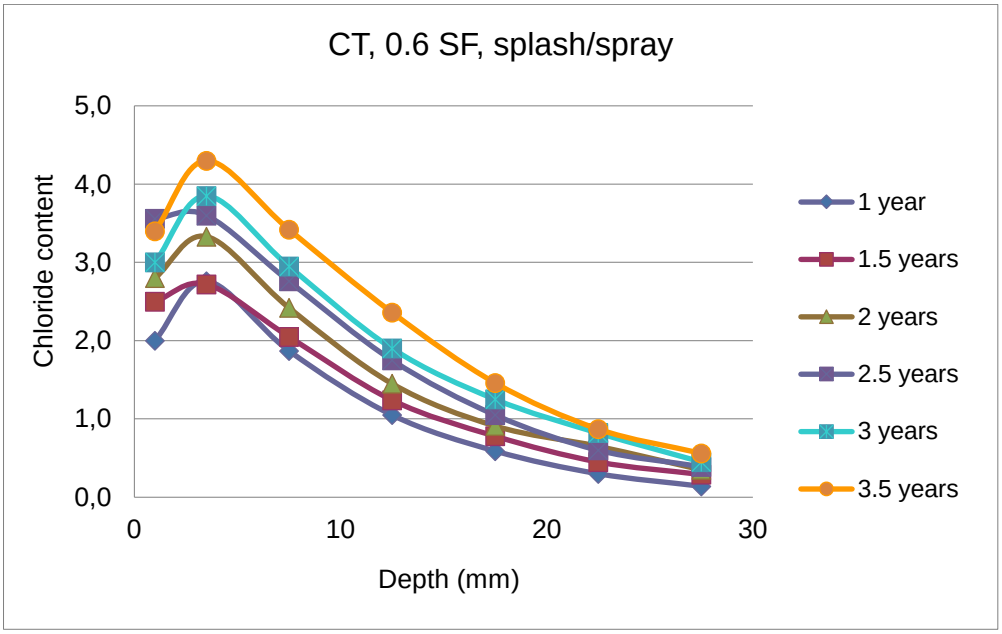

A31: Cape Town, w/b = 0.40, PC, airborne

Values shown are an average of three individual specimens.

0.4 PC airborne

mean depth (mm)	% Cl by mass of cement					
	1 year	1.5 years	2 years	2.5 years	3 years	3.5 years
1	0,500	0,660	1,340	0,930	1,600	1,900
3,5	0,750	1,150	1,400	1,780	1,740	1,920
7,5	0,390	0,710	0,850	1,170	1,310	1,400
12,5	0,150	0,280	0,400	0,560	0,700	0,880
17,5	0,060	0,160	0,180	0,300	0,350	0,470
22,5	0,010	0,100	0,100	0,160	0,200	0,210
27,5	0,15	0,090	0,100	0,090	0,090	0,100
35	0,24	1,15				
45	0,44	0,97				
55	0,57	0,71				

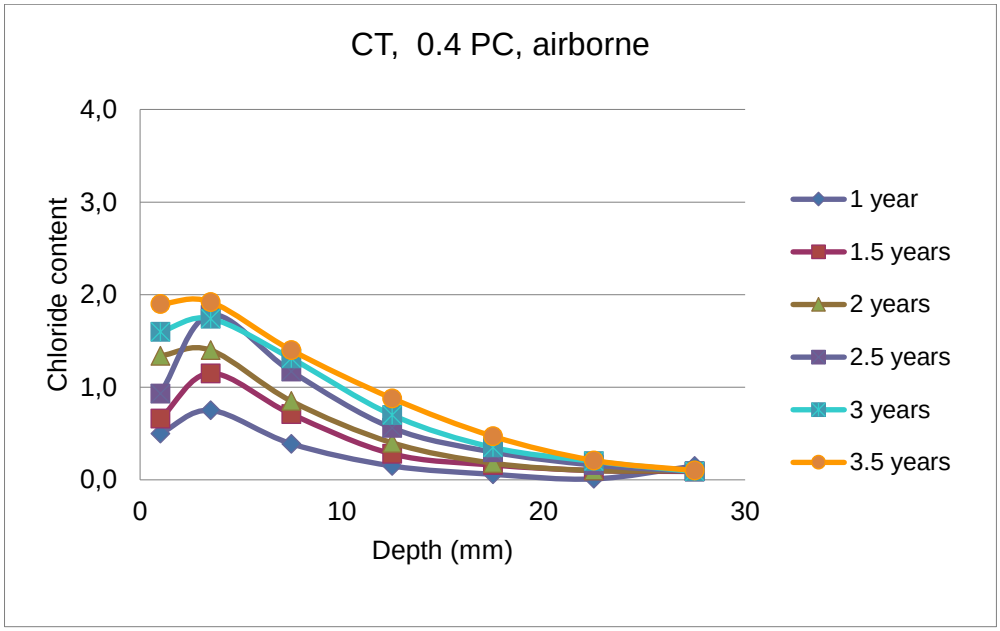

A32: Cape Town, w/b = 0.60, PC, airborne

Values shown are an average of three individual specimens.

0.6 PC airborne

mean depth (mm)	% Cl by mass of cement					
	1 year	1.5 years	2 years	2.5 years	3 years	3.5 years
1	0,960	1,280	1,320	1,800	2,300	2,100
3,5	1,330	1,400	1,810	2,070	2,200	2,400
7,5	0,890	1,020	1,300	1,610	1,750	1,920
12,5	0,450	0,610	0,880	1,070	1,210	1,450
17,5	0,210	0,290	0,500	0,620	0,800	0,960
22,5	0,090	0,150	0,230	0,300	0,420	0,600
27,5	0,010	0,060	0,100	0,150	0,100	0,200
35				0,06		

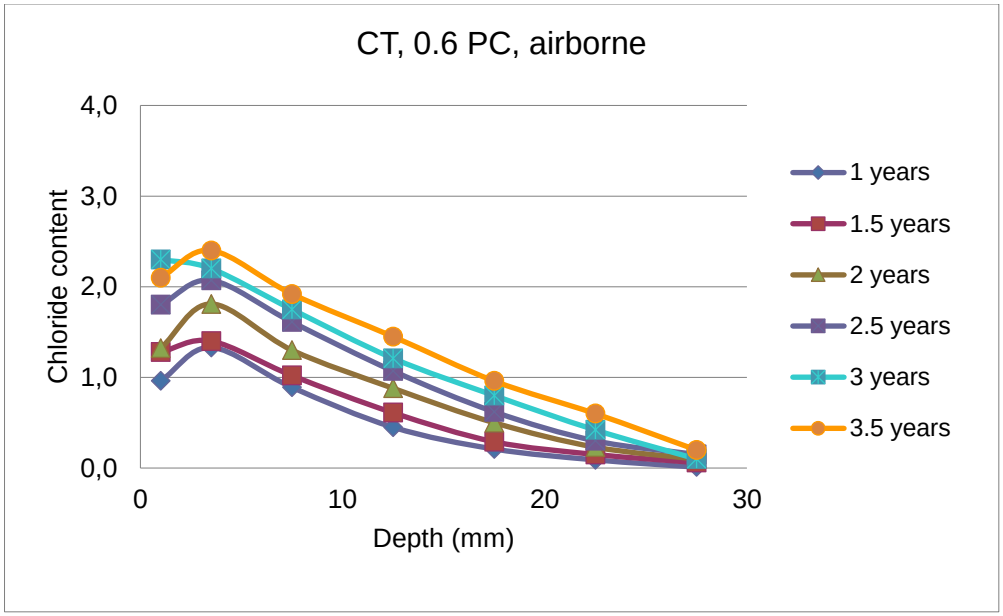

A33: Cape Town, w/b = 0.40, CS, airborne

Values shown are an average of three individual specimens.

0.4 CS airborne

mean depth (mm)	% Cl by mass of cement					
	1 year	1.5 years	2 years	2.5 years	3 years	3.5 years
1	1,050	1,520	1,900	1,510	2,700	2,500
3,5	1,210	1,740	1,960	2,290	2,790	2,950
7,5	0,450	0,590	0,970	0,990	1,050	1,330
12,5	0,100	0,130	0,170	0,300	0,310	0,350
17,5	0,050	0,080	0,100	0,090	0,120	0,120
22,5	0,010	0,080	0,060	0,100	0,100	0,110
27,5		0,14	0,17	0,08	0,09	0,1
35		0,12		0,05		

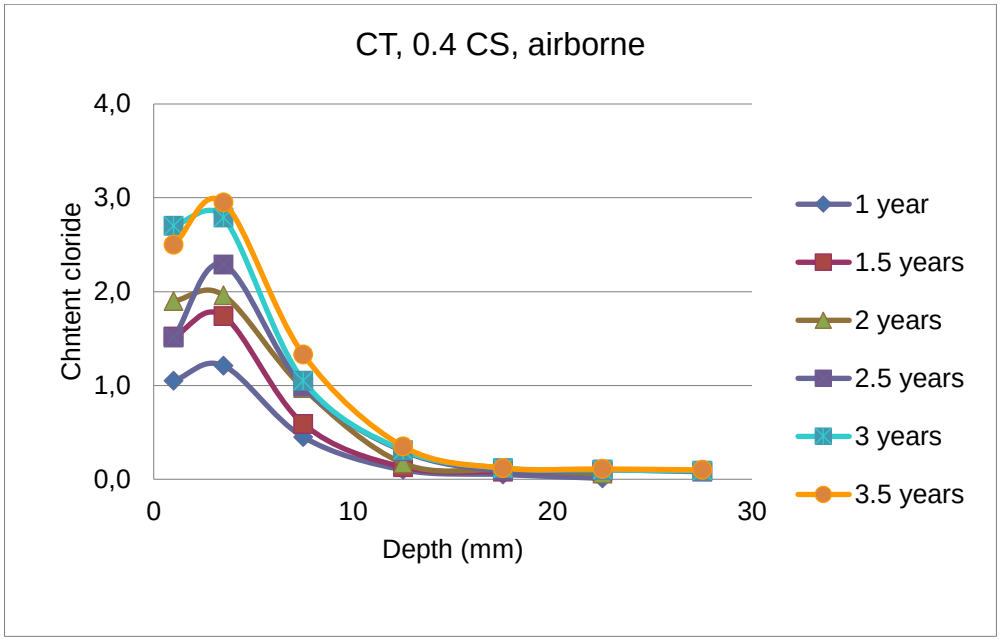

A34: Cape Town, w/b = 0.60, CS, airborne

Values shown are an average of three individual specimens.

0.6 CS airborne

mean depth (mm)	% Cl by mass of cement					
	1 year	1.5 years	2 years	2.5 years	3 years	3.5 years
1	1,500	1,970	2,300	2,200	2,400	3,160
3,5	1,800	1,950	2,310	2,670	3,120	3,300
7,5	0,850	1,170	1,340	1,550	1,720	2,100
12,5	0,280	0,270	0,400	0,460	0,490	0,740
17,5	0,100	0,090	0,100	0,090	0,100	0,180
22,5	0,030	0,020	0,050	0,040	0,080	0,090
27,5	0,020	0,020				

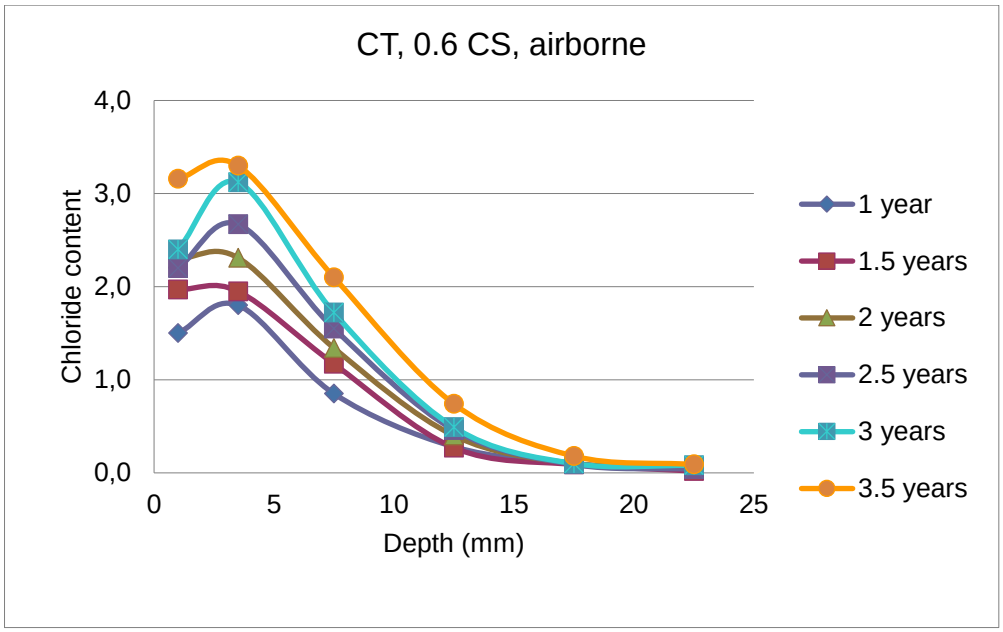

A35: Cape Town, w/b = 0.40, FA, airborne

Values shown are an average of three individual specimens.

0.4 FA airborne

mean depth (mm)	% Cl by mass of cement					
	1 year	1.5 years	2 years	2.5 years	3 years	3.5 years
1	1,030	1,300	1,350	1,600	2,250	1,460
3,5	1,100	1,530	1,820	1,900	2,400	2,670
7,5	0,420	0,550	0,700	0,860	1,010	1,210
12,5	0,090	0,100	0,220	0,300	0,250	0,370
17,5	0,050	0,100	0,150	0,100	0,120	0,150
22,5	0,050	0,040	0,200	0,090	0,100	0,100
27,5			0,19	0,13	0,09	0,080
35			0,21	0,13		0,22
45			0,15	0,14		0,15
55			0,23	0,14		0,09

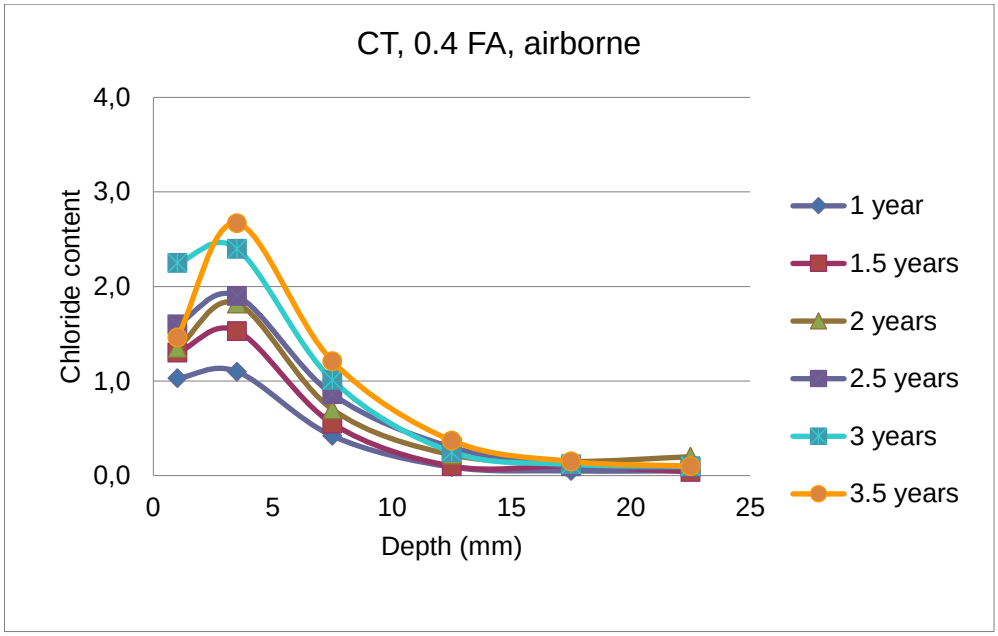

A36: Cape Town, w/b = 0.60, FA, airborne

Values shown are an average of three individual specimens.

0.6 FA airborne

mean depth (mm)	% Cl by mass of cement					
	1 year	1.5 years	2 years	2.5 years	3 years	3.5 years
1	1,510	1,810	2,400	1,740	3,000	2,740
3,5	1,590	1,880	2,350	2,700	3,150	3,300
7,5	0,710	1,090	1,230	1,520	1,600	1,840
12,5	0,200	0,410	0,500	0,590	0,650	0,750
17,5	0,100	0,200	0,140	0,220	0,240	0,300
22,5	0,100	0,090	0,080	0,120	0,110	0,130
27,5	0,26					0,38
35	0,51					0,45
45	0,61					0,46
55				0,04		0,04

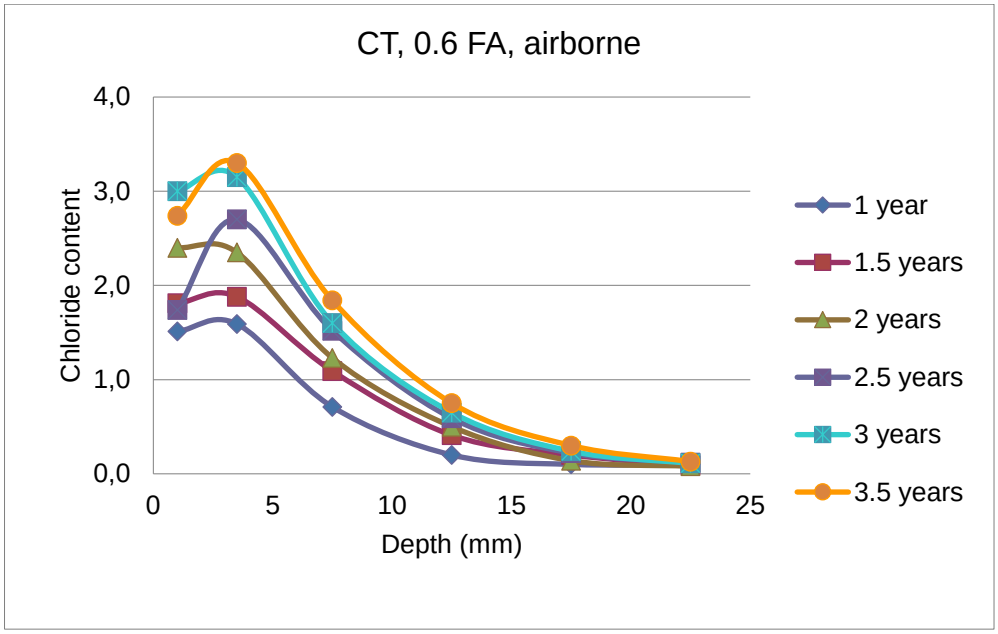

A37: Cape Town, w/b = 0.40, SP, airborne

Values shown are an average of three individual specimens.

0.4 SP airborne

mean depth (mm)	% Cl by mass of cement					
	1 year	1.5 years	2 years	2.5 years	3 years	3.5 years
1	1,300	1,730	2,150	2,290	2,100	2,460
3,5	1,320	1,850	2,100	2,280	2,650	2,920
7,5	0,600	0,780	1,210	1,380	1,350	1,490
12,5	0,050	0,150	0,290	0,330	0,350	0,400
17,5	0,020	0,100	0,140	0,190	0,100	0,060
22,5	0,100	0,080	0,100	0,100	0,050	0,090
27,5			0,06	0,14		0,030
35			0,09	0,13		0,03
45			0,07	0,1		0,92
55			0,16	0,32		0,38

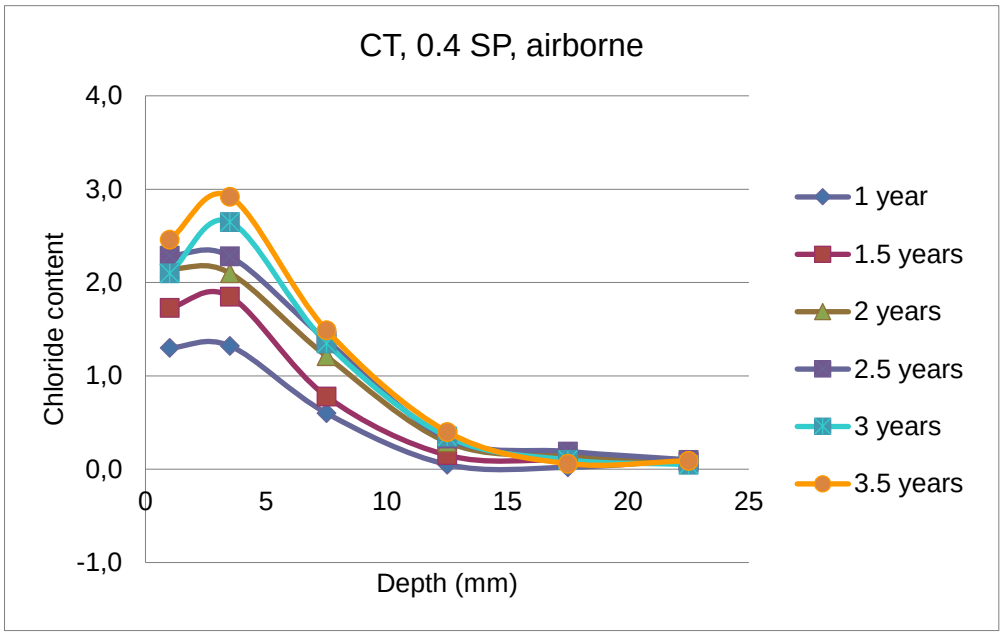

A38: Cape Town, w/b = 0.60, SP, airborne

Values shown are an average of three individual specimens.

0.6 SP airborne

mean depth (mm)	% Cl by mass of cement					
	1 year	1.5 years	2 years	2.5 years	3 years	3.5 years
1	2,150	2,500	2,500	2,710	2,870	3,200
3,5	1,930	2,750	2,750	2,930	3,300	3,620
7,5	0,930	1,250	1,450	1,530	1,840	2,070
12,5	0,300	0,350	0,450	0,590	0,700	0,760
17,5	0,090	0,070	0,200	0,200	0,240	0,240
22,5	0,050	0,210	0,210	0,070	0,120	0,150
27,5		0,2		0,2	0,100	0,19
35		0,21		0,21	0,18	0,22
45		0,07		0,07	0,2	0,18
55		0,39		0,39	0,2	0,06

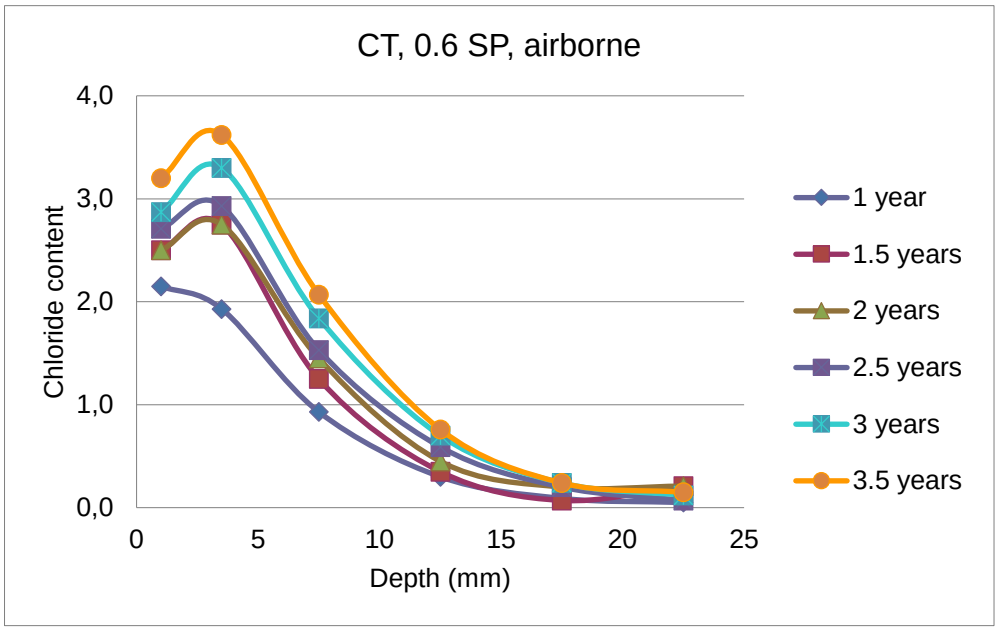

A39: Cape Town, w/b = 0.40, SF, airborne

Values shown are an average of three individual specimens.

0.4 SF airborne

mean depth (mm)	% Cl by mass of cement					
	1 year	1.5 years	2 years	2.5 years	3 years	3.5 years
1	1,080	1,540	2,100	1,610	1,450	3,000
3,5	1,400	1,680	2,050	2,130	2,370	2,870
7,5	0,670	0,780	1,120	1,370	1,510	1,620
12,5	0,200	0,320	0,400	0,610	0,700	0,720
17,5	0,090	0,100	0,200	0,200	0,230	0,280
22,5	0,070	0,050	0,090	0,090	0,100	0,100
27,5	0,05			0,070	0,040	0,100
35	0,13			0,06	0,12	
45	0,14			0,09	0,12	
55	0,13			0,07	0,04	

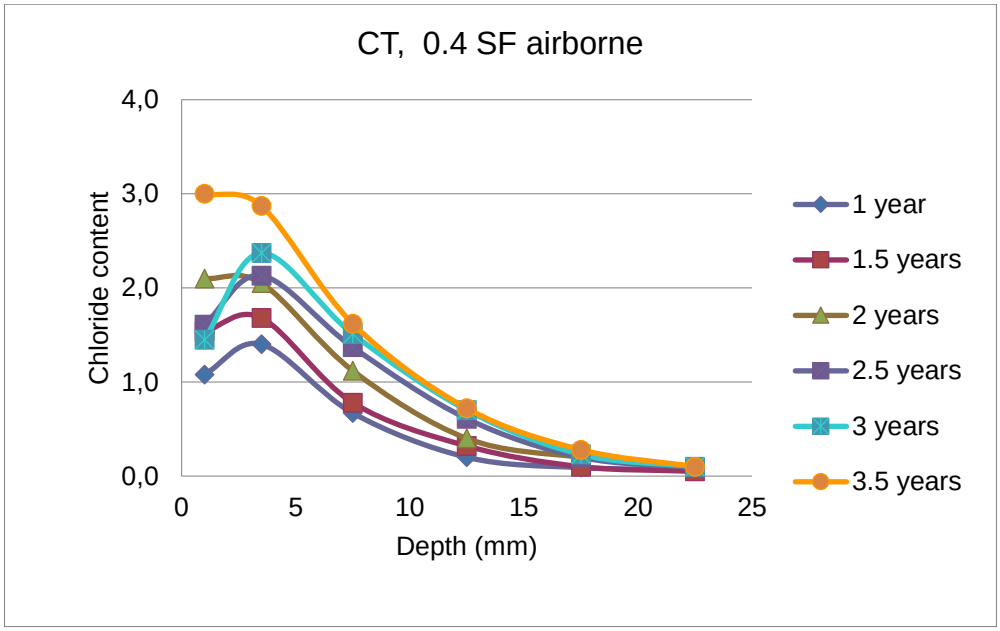

A40: Cape Town, w/b = 0.60, SF, airborne

Values shown are an average of three individual specimens.

0.6 SF airborne

mean depth (mm)	% Cl by mass of cement					
	1 year	1.5 years	2 years	2.5 years	3 years	3.5 years
1	0,940	2,450	2,060	2,100	3,130	3,050
3,5	2,040	2,650	2,920	2,750	3,050	3,300
7,5	1,350	1,580	1,820	1,690	2,160	2,520
12,5	0,570	0,700	0,940	0,810	1,250	1,460
17,5	0,260	0,400	0,510	0,300	0,610	0,840
22,5	0,150	0,280	0,350	0,160	0,300	0,400
27,5	0,24		0,200	0,150		
35	0,24		0,18	0,28		
45	0,3		0,06	0,35		
55	0,2		0,87	0,17		

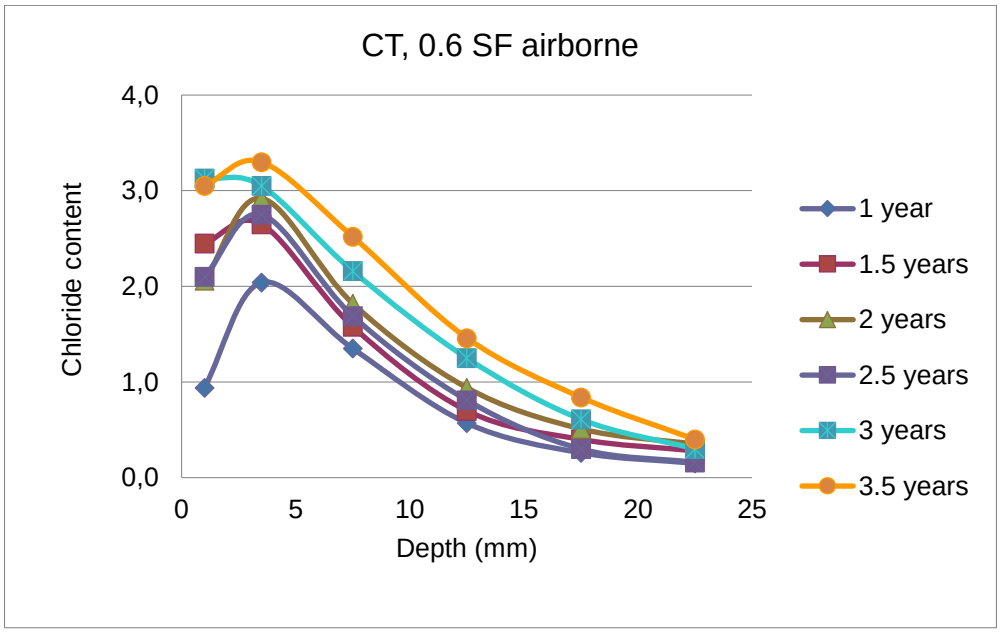

A41: Durban, w/b = 0.40, PC, submerged

Values shown are an average of three individual specimens.

0.4 PC, submerged

mean depth (mm)	% Cl by mass of cement					
	1 year	1.5 years	2 years	2.5 years	3 years	3.5 years
1	1,280	1,470	1,850	2,150	2,110	2,370
3,5	1,250	1,550	1,890	2,130	2,210	2,470
7,5	0,860	1,110	1,330	1,580	1,980	2,080
12,5	0,340	0,500	0,790	1,020	1,510	1,390
17,5	0,120	0,300	0,430	0,540	1,030	0,790
22,5	0,050	0,140	0,200	0,220	0,630	0,400
27,5	0,050	0,090	0,090	0,100	0,400	0,230
35	0,1	0,11	0,03	0,15	0,03	0,21
45		0,09	0,03	0,09	0,03	0,27
55		0,09	0,04	0,25	0,03	0,07

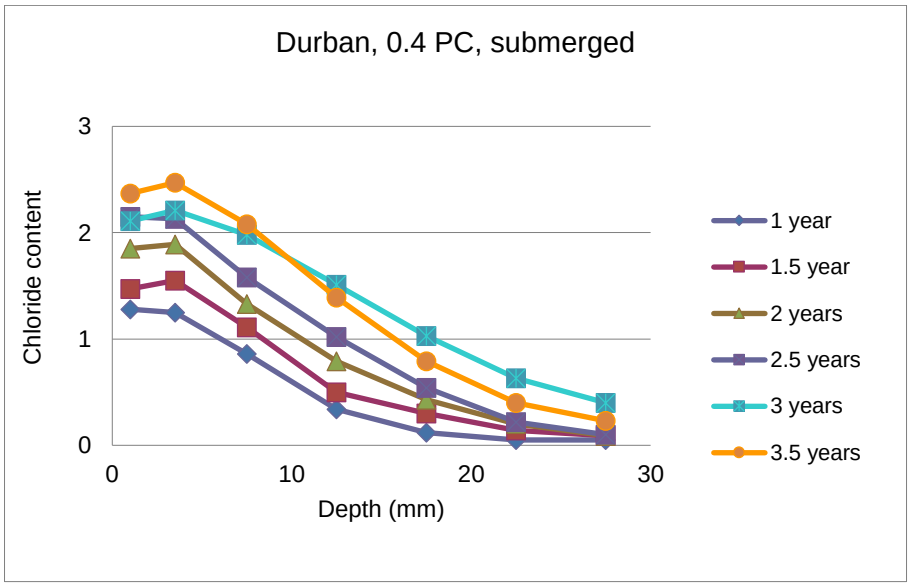

A42: Durban, w/b = 0.60, PC, submerged

Values shown are an average of three individual specimens.

0.6 PC, submerged

mean depth (mm)	% Cl by mass of cement					
	1 year	1.5 years	2 years	2.5 years	3 years	3.5 years
1	1,090	1,400	1,680	1,700	1,690	2,120
3,5	1,400	1,650	2,090	2,140	2,350	2,540
7,5	1,110	1,480	1,700	1,830	1,970	2,110
12,5	0,620	1,080	1,250	1,430	1,550	1,760
17,5	0,250	0,750	0,850	1,070	0,970	1,330
22,5	0,100	0,520	0,450	0,810	0,620	1,090
27,5	0,100	0,25	0,23	0,460	0,210	0,900
35	0,28	0,23	0,2	0,35	0,05	0,48
45	0,32	0,3	0,2	0,31	0,14	0,31
55	0,34	0,34	0,13	0,37	0,06	0,32

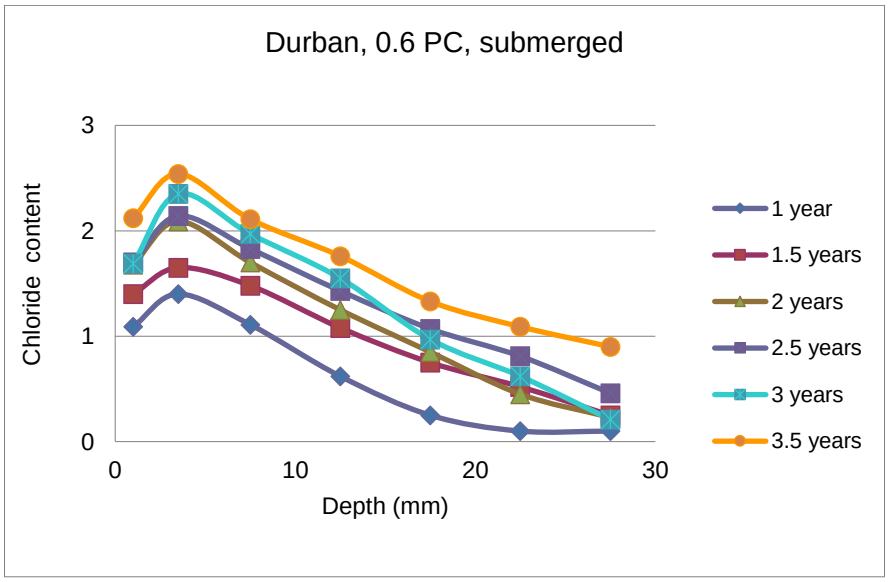

A43: Durban, w/b = 0.40, BS submerged

Values shown are an average of three individual specimens.

0.4 BS, subm.

mean depth (mm)	% Cl by mass of cement					
	1 year	1.5 years	2 years	2.5 years	3 years	3.5 years
1	1,400	1,600	2,000	sample lost		
3,5	1,500	1,800	2,180			
7,5	0,630	0,740	0,920			
12,5	0,150	0,230	0,360			
17,5	0,050	0,100	0,100			
22,5	0,020	0,030	0,050			
27,5	0,03	0,12	0,03			
35	0,03	0,02	0,09			
45	0,03	0,3	0,05			
55	0,23	0,14	0,03			

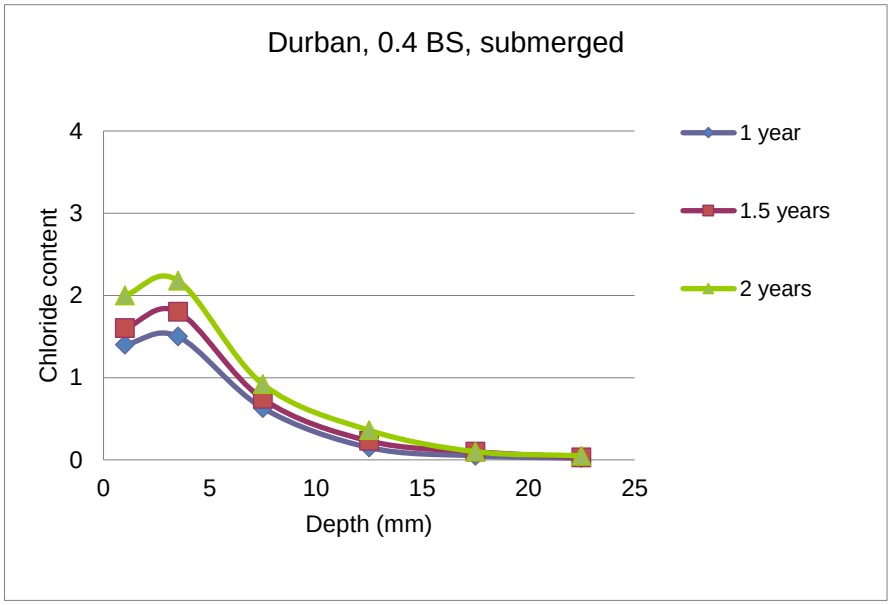

A44: Durban, w/b = 0.60, BS, submerged

Values shown are an average of three individual specimens.

0.6 BS subm.

mean depth (mm)	% Cl by mass of cement					
	1 year	1.5 years	2 years	2.5 years	3 years	3.5 years
1	1,110	2,080	1,890	2,540	2,720	3,200
3,5	2,200	2,380	2,560	2,960	3,320	3,950
7,5	1,390	1,620	1,720	2,110	2,530	2,720
12,5	0,320	0,490	0,570	0,610	1,240	0,960
17,5	0,050	0,050	0,030	0,220	0,460	0,200
22,5	0,050	0,060	0,030	0,130	0,270	0,130
27,5	0,05	0,07	0,05		0,04	0,09
35	0,06	0,06	0,03		0,05	0,09
45	0,06	0,09	0,36		0,22	0,08
55	0,06	0,55	0,05		0,04	0,07

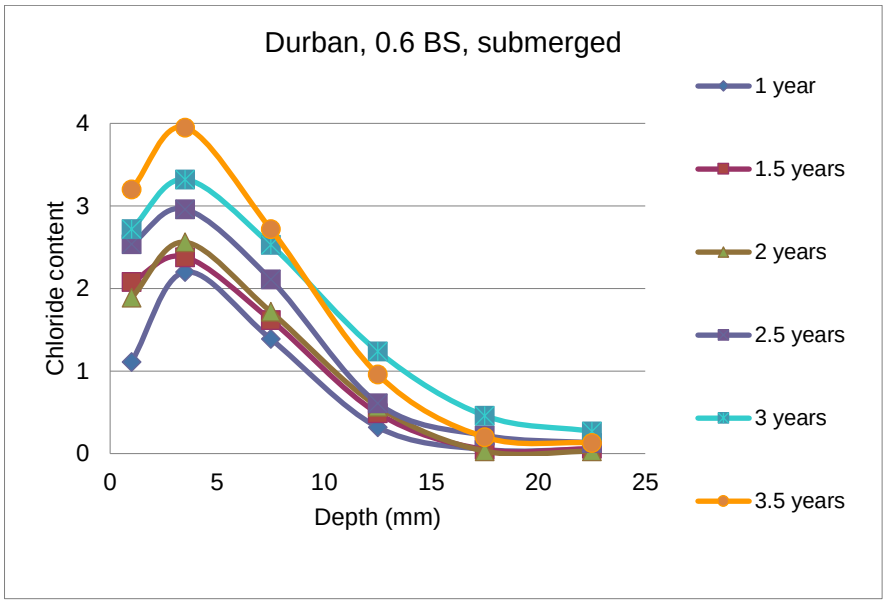

A45: Durban, w/b = 0.40, FA, submerged

Values shown are an average of three individual specimens.

0.4 FA subm.

mean depth (mm)	% Cl by mass of cement					
	1 year	1.5 years	2 years	2.5 years	3 years	3.5 years
1	1,88	2,03	2,200	2,250	2,410	2,700
3,5	1,68	1,85	2,350	2,500	2,790	3,200
7,5	0,38	0,68	1,100	1,330	1,500	1,800
12,5	0,08	0,08	0,260	0,450	0,480	0,440
17,5	0,08	0,08	0,020	0,150	0,170	0,100
22,5	0,08	0,08	0,020	0,140	0,160	0,210
27,5	0,08	0,07	0,02	0,14	0,04	0,10
35	0,09	0,08	0,02	0,14	0,17	0,23
45	0,05	0,07	0,09	0,16	0,06	0,16
55	0,15	0,08	0,04	0,18	0,22	0,14

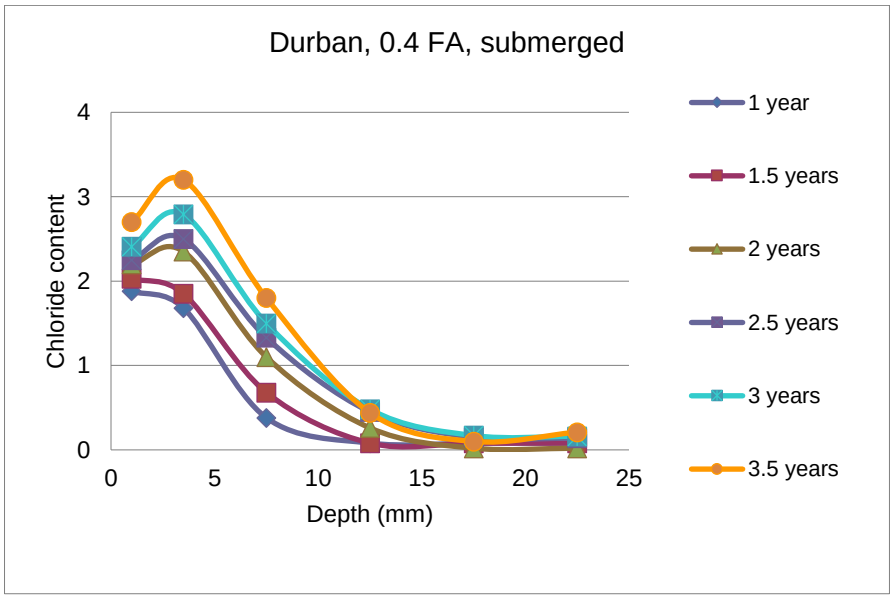

A46: Durban, w/b = 0.60, FA, submerged

Values shown are an average of three individual specimens.

0.6 FA submerged

mean depth (mm)	% Cl by mass of cement					
	1 year	1.5 years	2 years	2.5 years	3 years	3.5 years
1	1,800	2,170	2,250	2,900	2,650	3,290
3,5	2,090	2,690	2,870	3,060	2,950	3,620
7,5	1,320	1,630	2,180	2,420	2,520	2,650
12,5	0,370	0,540	0,700	1,160	1,310	1,060
17,5	0,150	0,030	0,140	0,450	0,550	0,320
22,5	0,140	0,030	0,120	0,080	0,240	0,180
27,5	0,13	0,04	0,12	0,08	0,22	0,140
35	0,14	0,02	0,22	0,08	0,25	0,58
45	0,29	0,37	0,67	0,17	0,05	0,11
55	0,94	0,16	0,55	0,18	0,59	1,06

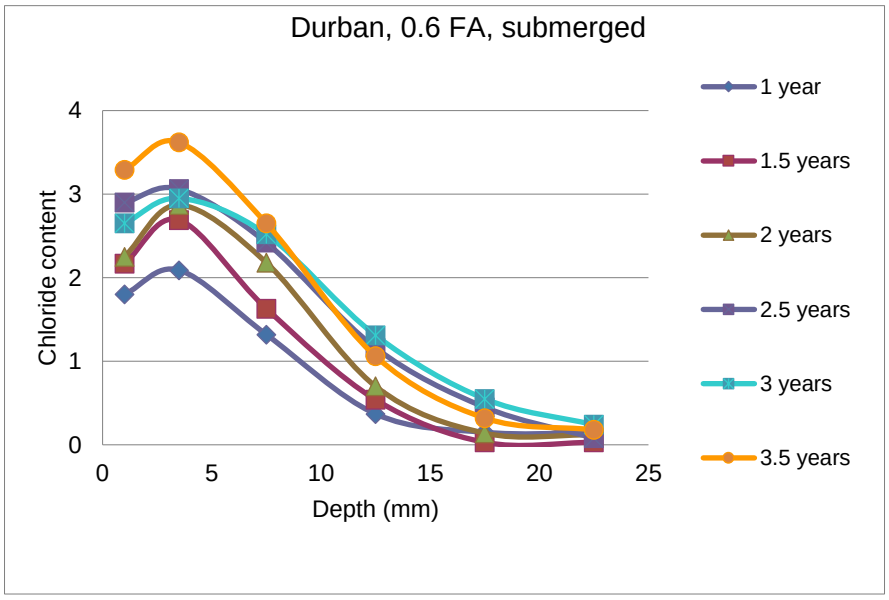

A47: Durban, w/b = 0.40, PC, tidal

Values shown are an average of three individual specimens.

0.4 PC, tidal

mean depth (mm)	% Cl by mass of cement					
	1 year	1.5 years	2 years	2.5 years	3 years	3.5 years
1	1,470	1,780	2,000	2,200	2,230	3,120
3,5	1,620	2,000	2,310	2,510	2,580	3,050
7,5	1,290	1,430	1,740	1,980	2,110	2,480
12,5	0,780	0,960	1,120	1,550	1,570	1,950
17,5	0,340	0,470	0,540	0,960	1,040	1,340
22,5	0,150	0,100	0,160	0,570	0,490	0,980
27,5	0,090	0,080	0,030	0,150	0,350	0,700
35	0,08	0,08	0,08	0,04	0,04	0,21
45	0,08	0,1	0,04	0,14	0,15	0,17
55	0,11	0,1	1,87	0,19	0,05	0,18

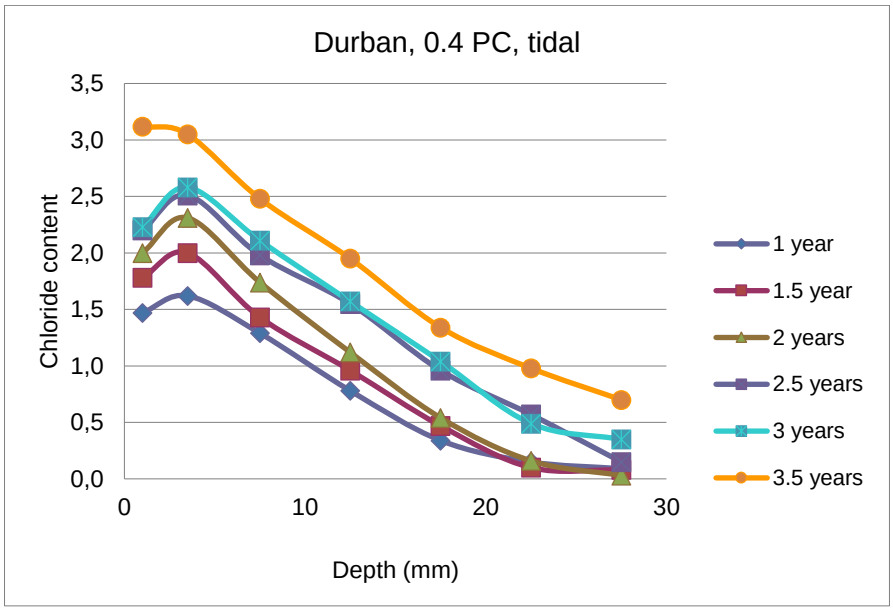

A48: Durban, w/b = 0.60, PC, tidal

Values shown are an average of three individual specimens.

0.6 PC tidal

mean depth (mm)	% Cl by mass of cement					
	1 year	1.5 years	2 years	2.5 years	3 years	3.5 years
1	1,76	1,81	1,850	2,150	2,900	2,820
3,5	1,85	1,94	2,400	2,560	3,240	3,400
7,5	1,48	1,67	2,190	2,150	2,780	2,850
12,5	1,06	1,36	1,600	1,780	2,280	2,290
17,5	0,72	0,85	1,170	1,270	1,720	1,840
22,5	0,38	0,51	0,860	0,980	1,340	1,420
27,5	0,23	0,31	0,470	0,770	0,930	1,150
35	0,23	0,24	0,260	0,26	0,27	0,800
45	0,29	0,26	0,31	0,37	0,4	0,16
55	0,34	0,29	0,27	0,38	0,06	0,24

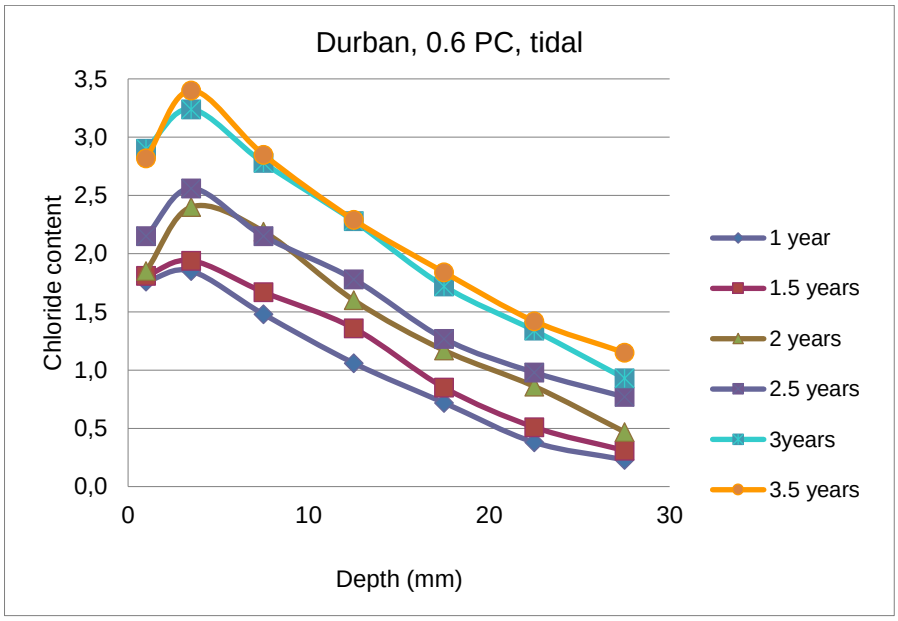

A49: Durban, w/b = 0.40, BS tidal

Values shown are an average of three individual specimens.

0.4 BS, tidal

mean depth (mm)	% Cl by mass of cement					
	1 year	1.5 years	2 years	2.5 years	3 years	3.5 years
1	1,580	2,3	2,650	2,7	3,100	4,100
3,5	1,680	2,55	2,800	2,95	3,600	4,360
7,5	0,750	1,27	1,350	1,57	2,130	2,500
12,5	0,090	0,44	0,350	0,1	0,410	0,550
17,5	0,090	0,13	0,100	0,04	0,140	0,250
22,5	0,050	0,03	0,050	0,04	0,160	0,090
27,5	0,050	0,12	0,10	0,04	0,150	0,050
35	0,01	0,12	0,09	0,04	0,14	0,16
45	0,1	0,12		0,02	0,13	0,04
55	0,19	0,13		0	0,16	0,03

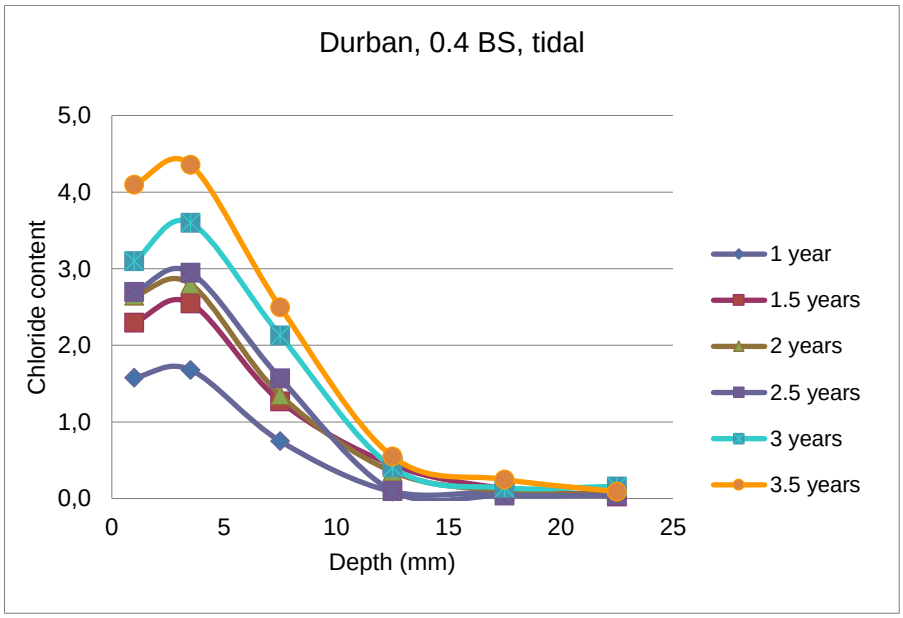

A50: Durban, w/b = 0.60, BS, tidal

Values shown are an average of three individual specimens.

0.6 BS tidal

mean depth (mm)	% Cl by mass of cement					
	1 year	1.5 years	2 years	2.5 years	3 years	3.5 years
1	1,980	3,730	2,960	2,950	2,990	3,620
3,5	3,200	3,390	3,530	3,700	4,290	4,580
7,5	1,980	2,680	2,700	3,020	3,380	3,450
12,5	0,730	0,850	0,980	1,310	1,740	1,310
17,5	0,090	0,090	0,100	0,220	0,450	0,490
22,5	0,050	0,090	0,060	0,100	0,300	0,200
27,5	0,04	0,09	0,05	0,07	0,25	0,080
35	0,33	0,07	0,04	0,06	0,1	0,08
45	0,22	0,1	0,05	0,54	0,03	0,09
55	0,12	0,49	0,05	0,48	0,03	0,08

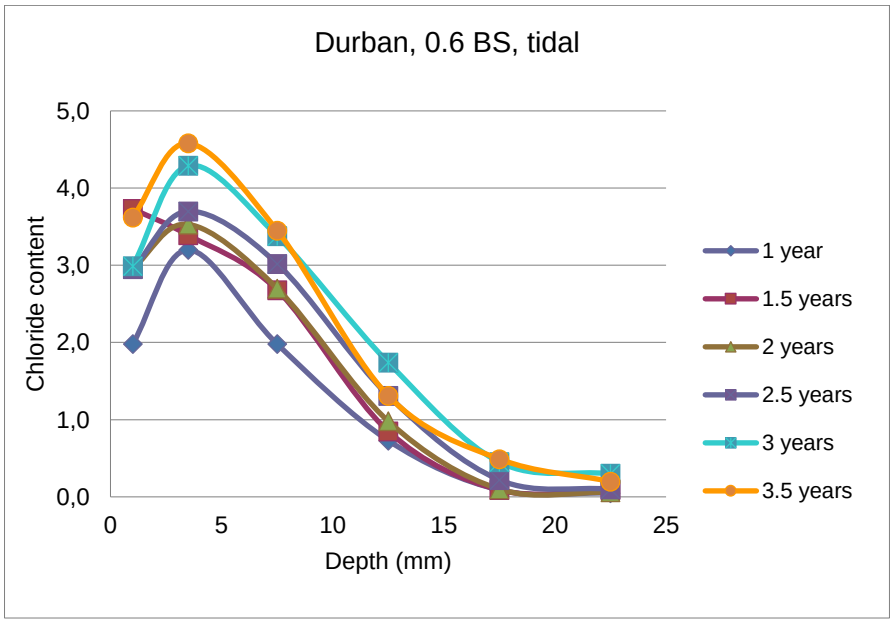

A51: Durban, w/b = 0.40, FA, tidal

Values shown are an average of three individual specimens.

0.4 FA tidal

mean depth (mm)	% Cl by mass of cement					
	1 year	1.5 years	2 years	2.5 years	3 years	3.5 years
1	1,850	1,890	2,200	2,380	2,600	2,690
3,5	1,960	2,150	2,400	2,600	3,340	3,600
7,5	0,850	1,050	1,550	1,740	2,000	2,230
12,5	0,340	0,300	0,400	0,480	0,550	0,740
17,5	0,160	0,090	0,020	0,090	0,160	0,240
22,5	0,140	0,090	0,030	0,030	0,150	0,120
27,5	0,11	0,09	0,03	0,03	0,18	0,07
35	0,13	0,09	0,03	0,03	0,14	0,08
45	0,14	0,10	0,04	0,04	0,16	0,05
55	0,04	0,31	0,07	0,07	0,04	0,23

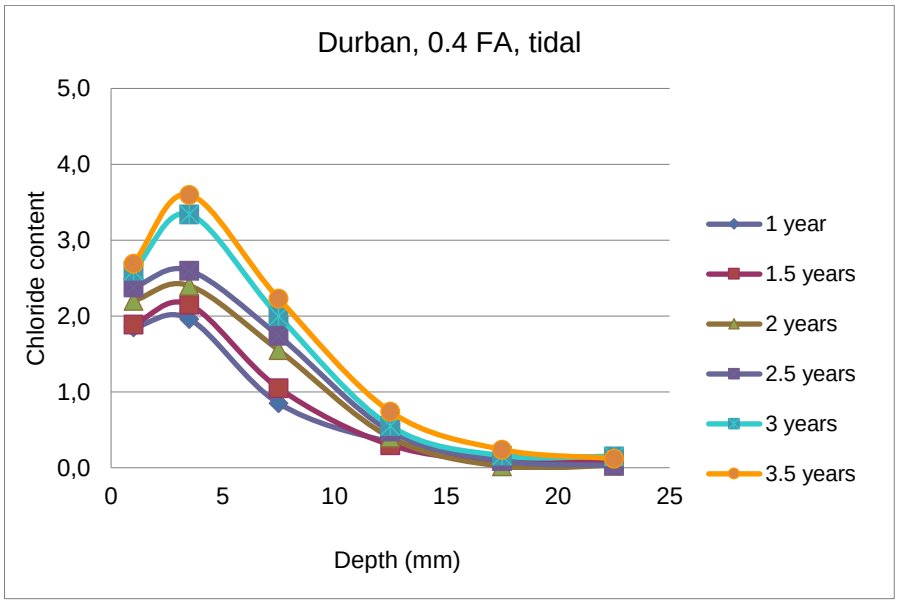

A52: Durban, w/b = 0.60, FA, tidal

Values shown are an average of three individual specimens.

0.6 FA tidal

mean depth (mm)	% Cl by mass of cement					
	1 year	1.5 years	2 years	2.5 years	3 years	3.5 years
1	1,730	2,610	3,140	2,920	3,260	3,480
3,5	2,800	3,030	3,460	3,530	3,750	4,100
7,5	1,980	2,090	2,350	2,510	2,450	2,750
12,5	0,750	0,850	1,010	1,150	1,150	1,550
17,5	0,260	0,300	0,400	0,510	0,600	0,800
22,5	0,110	0,150	0,100	0,180	0,330	0,250
27,5	0,11	0,120	0,02	0,18	0,220	0,61
35	0,12	0,13	0,02	0,18	0,23	0,67
45	0,48	0,45	0,02	0,20	0,22	0,83
55		0,74	0,04	0,19	0,28	1,00

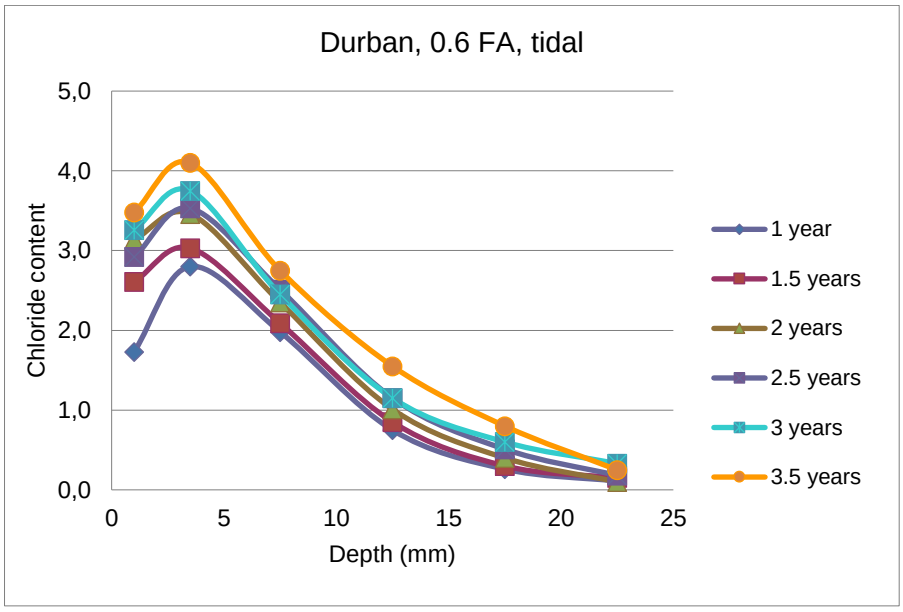

A53: Durban, w/b = 0.40, PC, splash/spray

Values shown are an average of three individual specimens.

0.4 PC, splash/spray

mean depth (mm)	% Cl by mass of cement					
	1 year	1.5 years	2 years	2.5 years	3 years	3.5 years
1	1,810	2,210	2,410	2,600	2,720	3,480
3,5	1,800	2,130	2,540	2,750	2,850	3,540
7,5	1,420	1,800	2,190	2,300	2,430	2,950
12,5	0,850	1,310	1,530	1,750	1,790	2,060
17,5	0,460	0,720	0,950	1,050	1,180	1,420
22,5	0,230	0,290	0,530	0,450	0,600	0,740
27,5	0,09	0,150	0,220	0,300	0,400	0,550
35	0,08	0,07	0,03	0,13	0,16	0,08
45	0,1	0,09	0,04	0,15	0,06	0,05
55	0,09	0,11	0,03	0,16	0,04	0,05

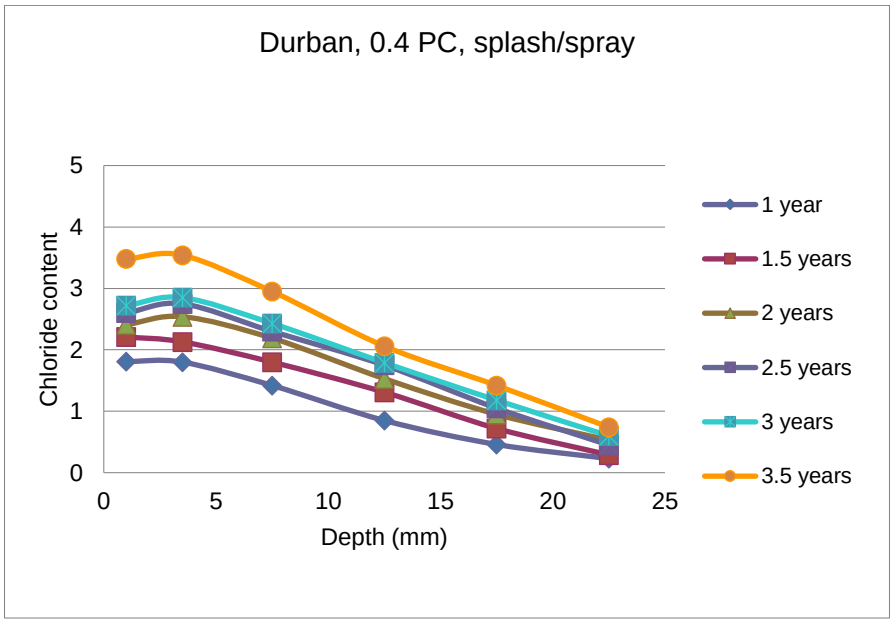

A54: Durban, w/b = 0.60, PC, splash/spray

Values shown are an average of three individual specimens.

0.6 PC, splash/spray

mean depth (mm)	% Cl by mass of cement					
	1 year	1.5 years	2 years	2.5 years	3 years	3.5 years
1	1,890	2,000	2,660	3,21	3,680	3,700
3,5	2,040	2,350	2,780	3,59	3,800	4,000
7,5	1,640	2,170	2,680	3,1	3,550	3,700
12,5	1,200	1,550	2,020	2,36	2,770	3,160
17,5	0,820	1,030	1,410	1,57	1,960	2,350
22,5	0,420	0,680	0,850	1	1,150	1,700
27,5	0,250	0,450	0,510	0,57	0,540	1,100
35	0,150	0,370	0,210	0,34	0,13	0,32
45	0,13	0,18	0,16	0,31	0,08	0,12
55	0,17	0,15	0,18	0,21	0,27	0,09

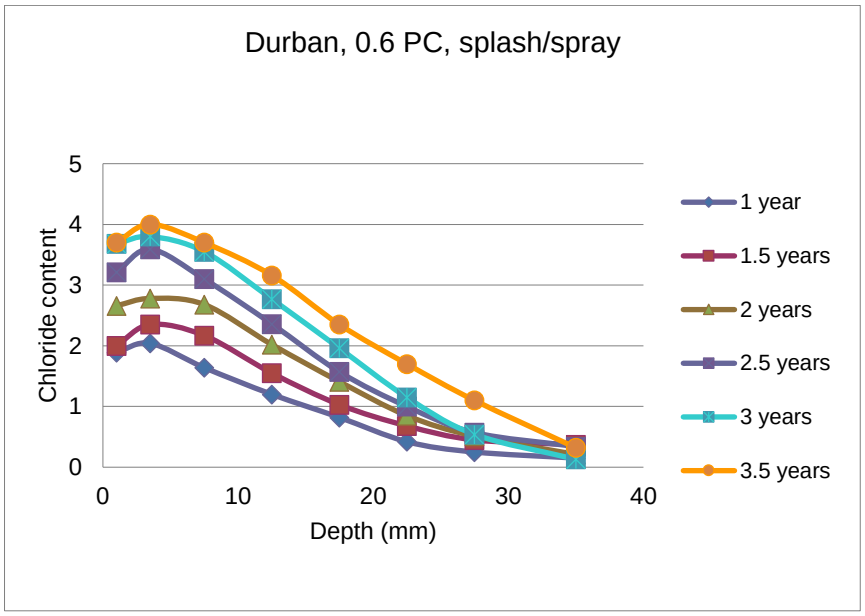

A55: Durban, w/b = 0.40, BS, splash/spray

Values shown are an average of three individual specimens.

0.4 BS, splash/spray

mean depth (mm)	% Cl by mass of cement					
	1 year	1.5 years	2 years	2.5 years	3 years	3.5 years
1	1,850	2,800	3,050	Sample lost		
3,5	2,000	3,050	3,180			
7,5	1,010	1,940	1,810			
12,5	0,250	0,460	0,450			
17,5	0,050	0,100	0,120			
22,5	0,050	0,040	0,090			
27,5						
35						
45						
55						

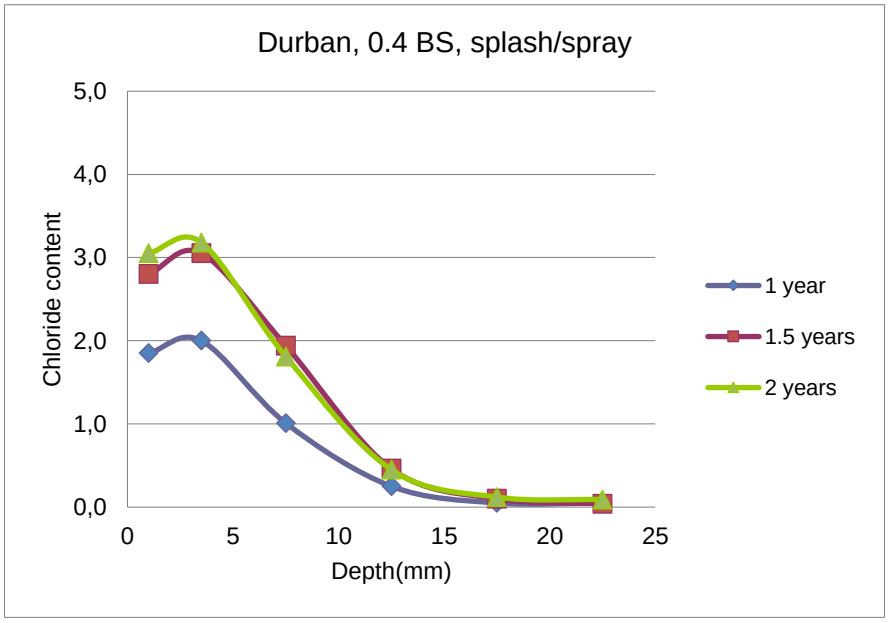

A56: Durban, w/b = 0.60, BS, splash/spray

Values shown are an average of three individual specimens.

0.6 BS, splash/spray

mean depth (mm)	% Cl by mass of cement					
	1 year	1.5 years	2 years	2.5 years	3 years	3.5 years
1	2,310	2,780	3,3	2,48	4,2	4,400
3,5	2,700	3,080	3,85	3,47	4,47	4,670
7,5	2,180	2,350	3,41	3,63	4,04	4,360
12,5	0,880	1,150	1,09	1,52	1,56	1,970
17,5	0,070	0,330	0,12	0,08	0,33	0,400
22,5	0,070	0,050	0,09	0,09	0,29	0,090
27,5	0,07	0,030	0,12	0,29	0,04	0,08
35	0,08	0,05	0,09	0,1	0,05	0,09
45	0,07	0,04		0,32	0,25	0,08
55	0,07	0,04		0,16	0,05	0,07

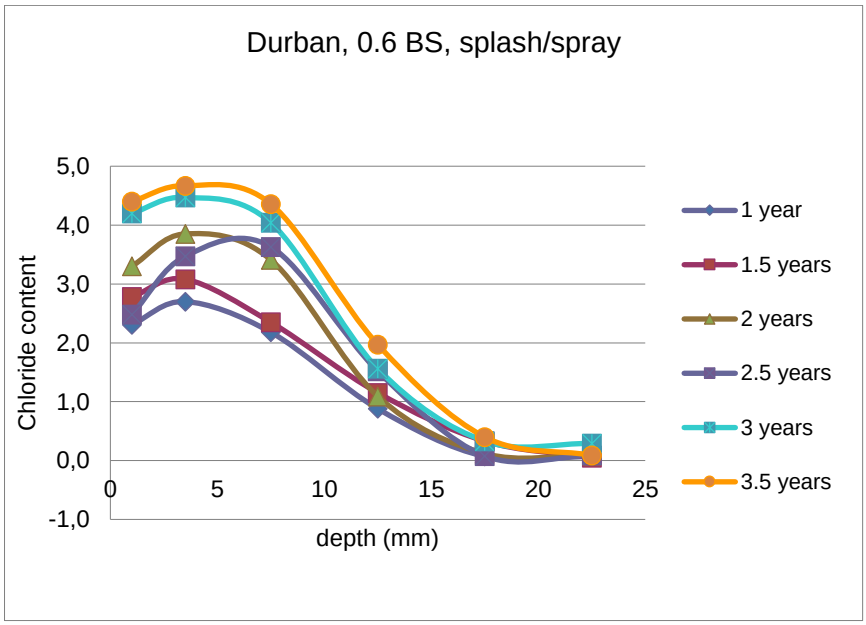

A57: Durban, w/b = 0.40, FA, splash/spray

Values shown are an average of three individual specimens.

0.4 FA, splash/spray

mean depth (mm)	% Cl by mass of cement					
	1 year	1.5 years	2 years	2.5 years	3 years	3.5 years
1	2,510	2,270	2,990	2,850	3,610	3,84
3,5	2,460	2,460	3,070	3,060	3,850	4,54
7,5	1,180	1,400	1,710	1,640	2,500	2,94
12,5	0,250	0,420	0,410	0,680	0,670	0,59
17,5	0,160	0,150	0,090	0,210	0,150	0,17
22,5	0,140	0,080	0,080	0,010	0,150	0,2
27,5	0,13	0,07	0,08	0,010	0,14	0,15
35	0,13	0,07	0,08	0,02	0,16	0,16
45	0,13	0,07	0,07	0,02	0,14	0,21
55	0,2	0,08	0,08	0,1	0,15	0,23

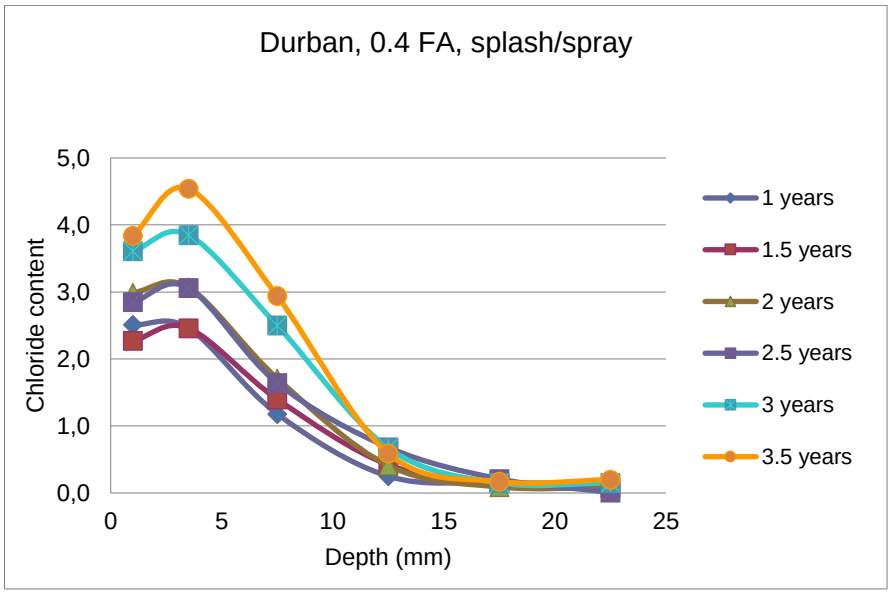

A58: Durban, w/b = 0.60, FA, splash/spray

Values shown are an average of three individual specimens.

0.6 FA, splash/spray

mean depth (mm)	% Cl by mass of cement					
	1 year	1.5 years	2 years	2.5 years	3 years	3.5 years
1	2,100	2,240	3,440	3,240	2,930	3,490
3,5	2,710	2,960	3,830	3,980	4,370	4,560
7,5	1,750	2,250	2,650	2,850	4,070	3,300
12,5	0,820	1,020	1,450	1,470	1,850	2,030
17,5	0,350	0,230	0,610	0,400	0,640	0,820
22,5	0,120	0,130	0,120	0,250	0,210	0,250
27,5	0,110	0,120	0,12	0,200	0,22	0,200
35	0,12	0,12	0,11	0,22	0,23	0,36
45	1,56	0,13	0,12	0,26	0,04	0,7
55		0,04	0,12	0,22	0,61	0,11

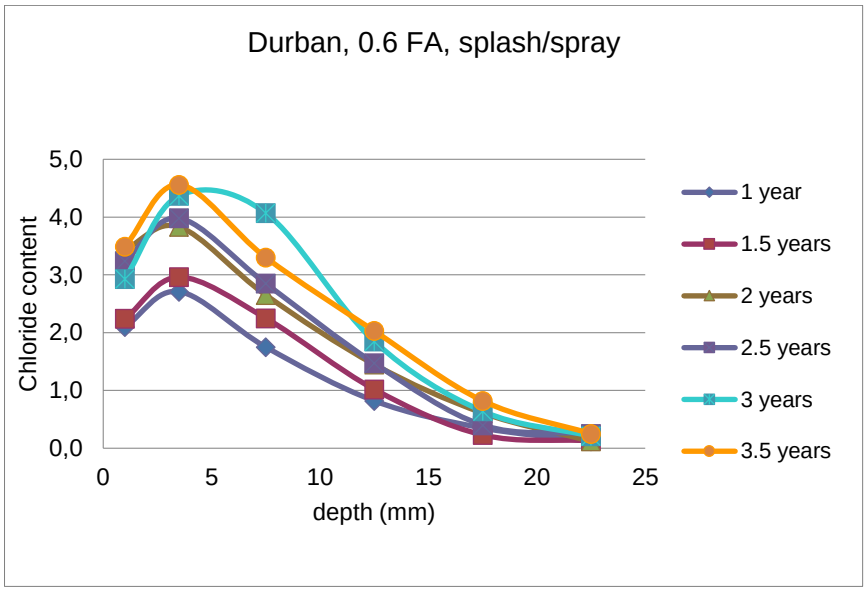

A59: Durban, w/b = 0.40, PC, airborne

Values shown are an average of three individual specimens.

0.4 PC, airborne

mean depth (mm)	% Cl by mass of cement					
	1 year	1.5 years	2 years	2.5 years	3 years	3.5 years
1	1,040	1,020	1,520	1,850	1,750	1,950
3,5	1,150	1,150	1,840	2,050	2,230	2,500
7,5	0,620	0,850	1,050	1,540	1,680	2,020
12,5	0,200	0,330	0,540	0,770	0,850	1,220
17,5	0,090	0,100	0,150	0,300	0,400	0,610
22,5	0,080	0,070	0,060	0,090	0,100	0,260
27,5	0,08	0,07	0,010	0,050	0,050	0,100
35	0,06		0,01			
45	0,05		0,02			
55	0,05					

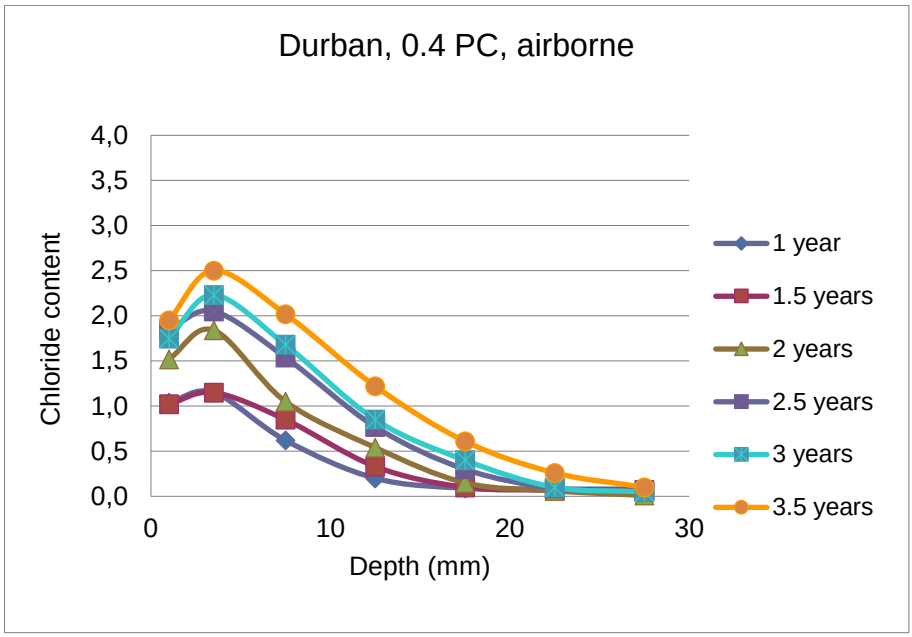

A60: Durban, w/b = 0.60, PC, airborne

Values shown are an average of three individual specimens.

0.6 PC, airborne

mean depth (mm)	% Cl by mass of cement					
	1 year	1.5 years	2 years	2.5 years	3 years	3.5 years
1	1,100	1,200	1,100			
3,5	1,300	1,450	1,670			
7,5	0,930	1,080	1,380			
12,5	0,510	0,700	0,860			
17,5	0,220	0,400	0,550			
22,5	0,090	0,200	0,280			
27,5	0,080	0,110	0,100			
35	0,01	0,09	0,090			
45	0,01					
55						

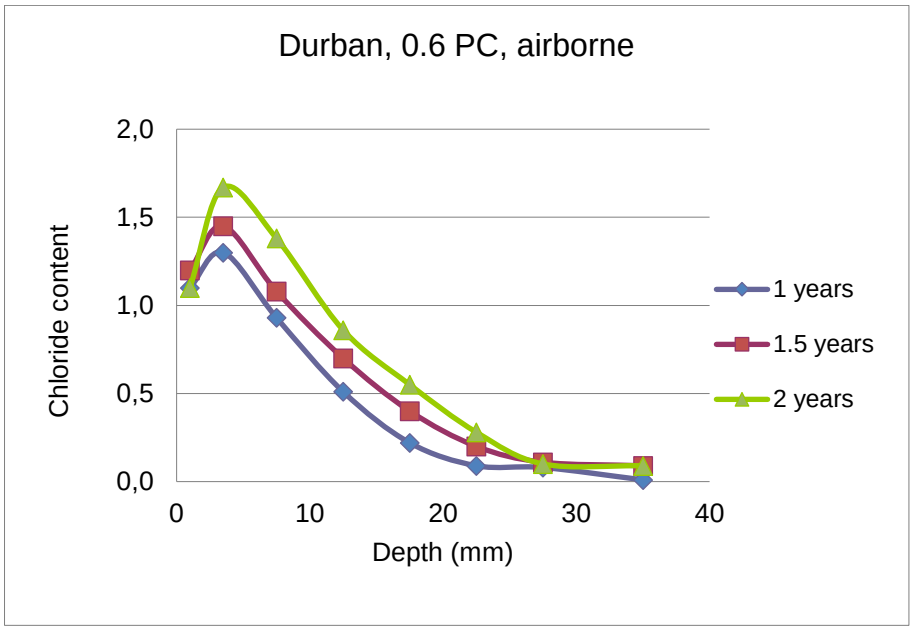

A61: Durban, w/b = 0.40, BS, airborne

Values shown are an average of three individual specimens.

0.4 BS, airborne

mean depth (mm)	% Cl by mass of cement					
	1 year	1.5 years	2 years	2.5 years	3 years	3.5 years
1	1,000	1,250	1,420			
3,5	1,200	1,590	1,800			
7,5	0,400	0,540	0,700			
12,5	0,120	0,100	0,180			
17,5	0,020	0,050	0,090			
22,5	0,020	0,020	0,050			
27,5						
35						
45						
55						

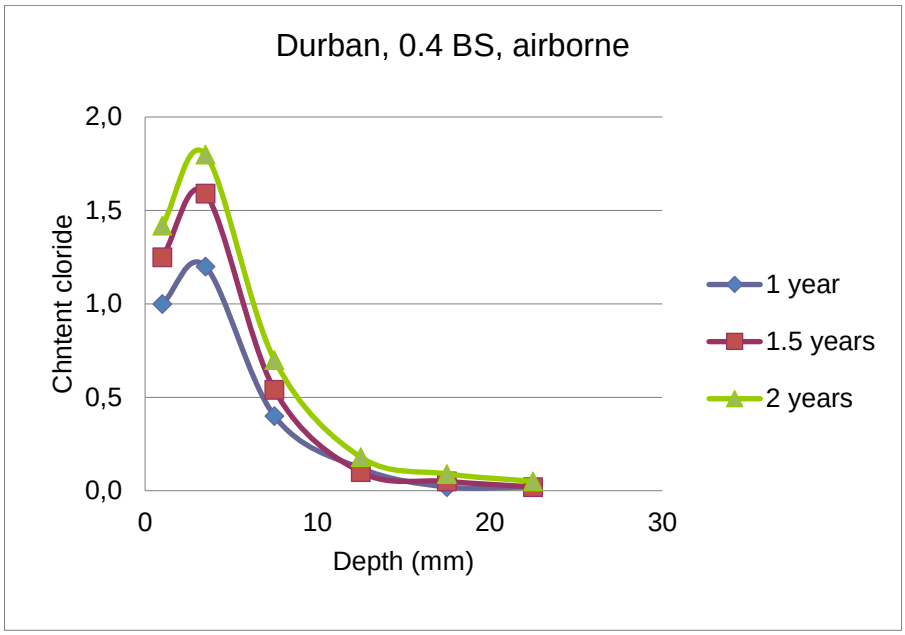

A62: Durban, w/b = 0.60, BS, airborne

Values shown are an average of three individual specimens.

0.6 BS, airborne

mean depth (mm)	% Cl by mass of cement					
	1 year	1.5 years	2 years	2.5 years	3 years	3.5 years
1	0,950	1,800	1,920			
3,5	1,830	2,080	2,450			
7,5	0,930	1,340	1,490			
12,5	0,360	0,380	0,540			
17,5	0,120	0,090	0,090			
22,5	0,100	0,020	0,050			
27,5	0,020	0,020				
35						
45						
55						

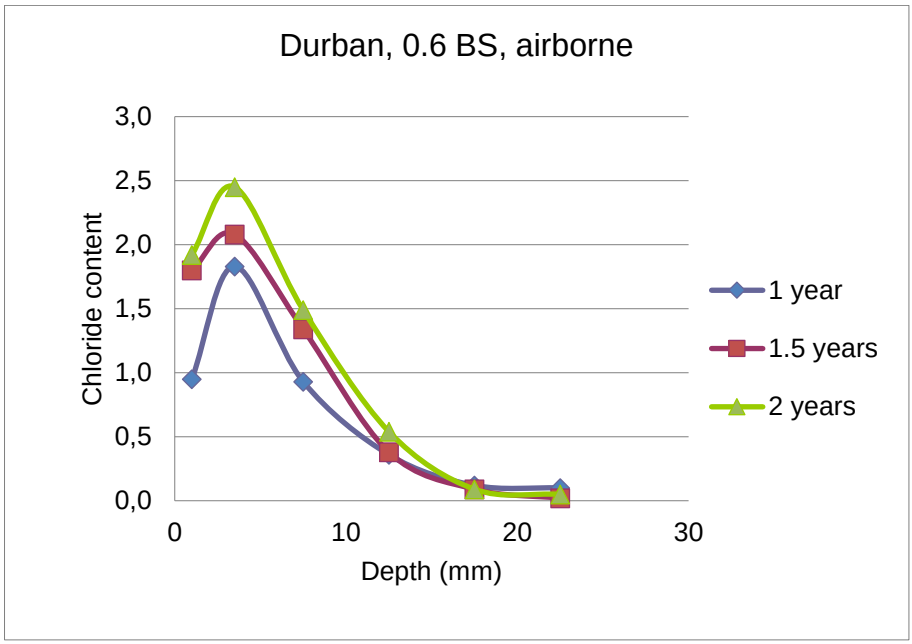

A63: Durban, w/b = 0.40, FA, airborne

Values shown are an average of three individual specimens.

0.4 FA, airborne

mean depth (mm)	% Cl by mass of cement					
	1 year	1.5 years	2 years	2.5 years	3 years	3.5 years
1	1,240	1,350	1,500	1,640	1,850	1,930
3,5	1,280	1,380	1,970	2,250	2,250	2,350
7,5	0,540	0,630	0,750	0,920	1,270	1,460
12,5	0,150	0,160	0,330	0,190	0,400	0,380
17,5	0,040	0,020	0,040	0,020	0,060	0,050
22,5	0,040	0,020	0,020	0,010	0,050	0,040
27,5				0,010		0,020

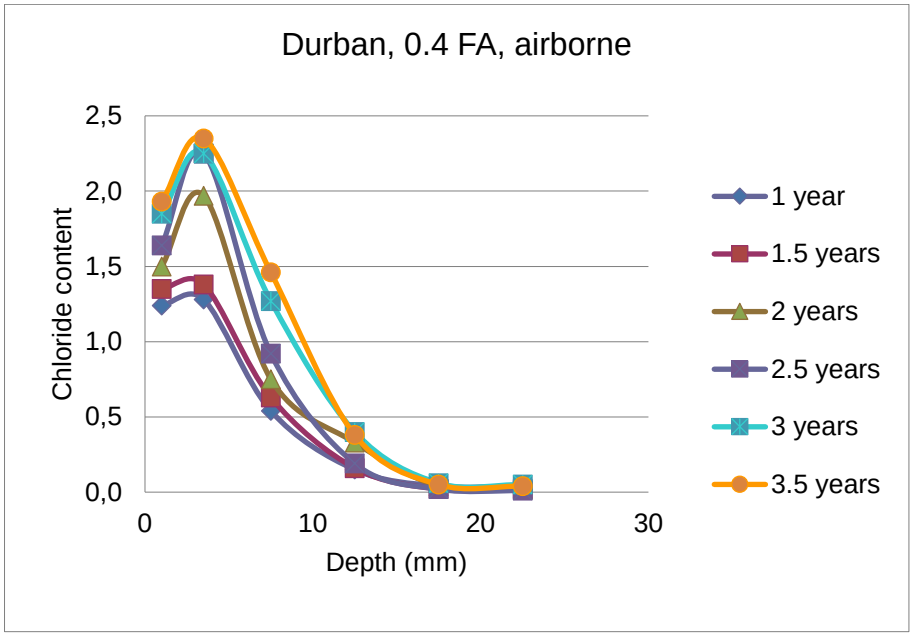

A64: Durban, w/b = 0.60, FA, airborne

Values shown are an average of three individual specimens.

0.6 FA, airborne

mean depth (mm)	% Cl by mass of cement					
	1 year	1.5 years	2 years	2.5 years	3 years	3.5 years
1	1,300	1,600	1,750	2,130	2,330	2,700
3,5	1,750	1,950	2,450	2,450	2,810	3,490
7,5	0,760	0,910	1,160	1,860	1,950	2,130
12,5	0,290	0,350	0,380	0,730	1,080	0,880
17,5	0,100	0,040	0,090	0,100	0,250	0,100
22,5	0,050	0,020	0,050	0,050	0,050	0,090

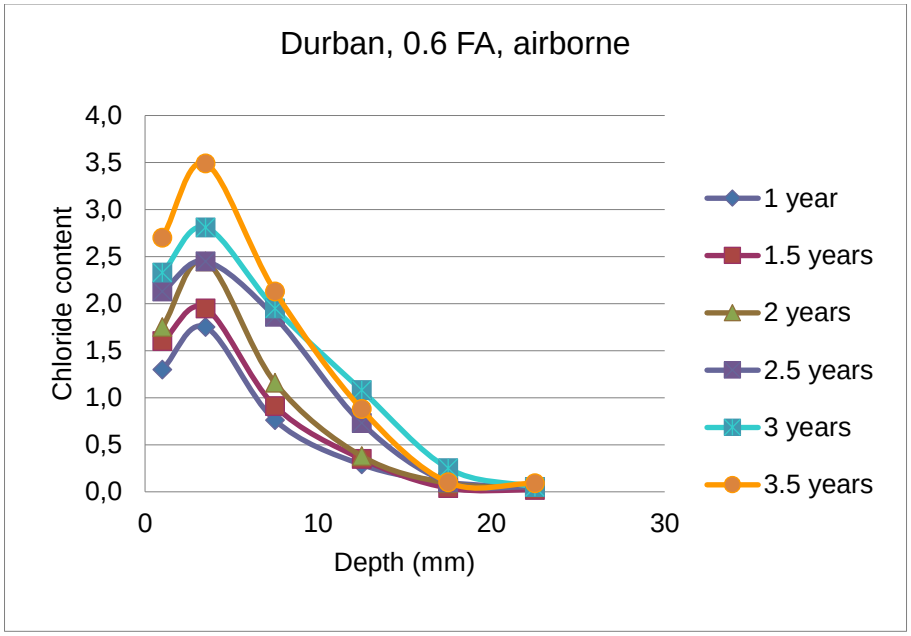

A65: Laboratory (Bulk Diffusion), w/b = 0.40, PC

0.4 PC

mean depth (mm)	% Cl by mass of cement											
	1 year		1.5 years		2 years		2.5 years		3 years		3.5 years	
spec.:	1	2	1	2	1	2	1	2	1	2	1	2
1	0,880	1,080	1,480	1,600	2,370	2,310	2,170	2,400	2,190	2,400	3,230	3,500
3,5	1,050	1,220	1,570	1,550	2,290	2,150	2,530	2,630	2,650	3,270	3,580	3,740
7,5	0,630	0,670	0,870	1,000	1,660	1,550	1,840	1,920	1,970	2,510	2,600	2,730
12,5	0,280	0,290	0,460	0,400	0,890	0,940	1,010	1,270	1,120	1,830	1,850	1,900
17,5	0,100	0,120	0,170	0,190	0,400	0,440	0,490	0,600	0,560	0,970	1,010	1,200
22,5	0,050	0,050	0,080	0,100	0,180	0,260	0,280	0,350	0,270	0,540	0,580	0,570
27,5										0,280		

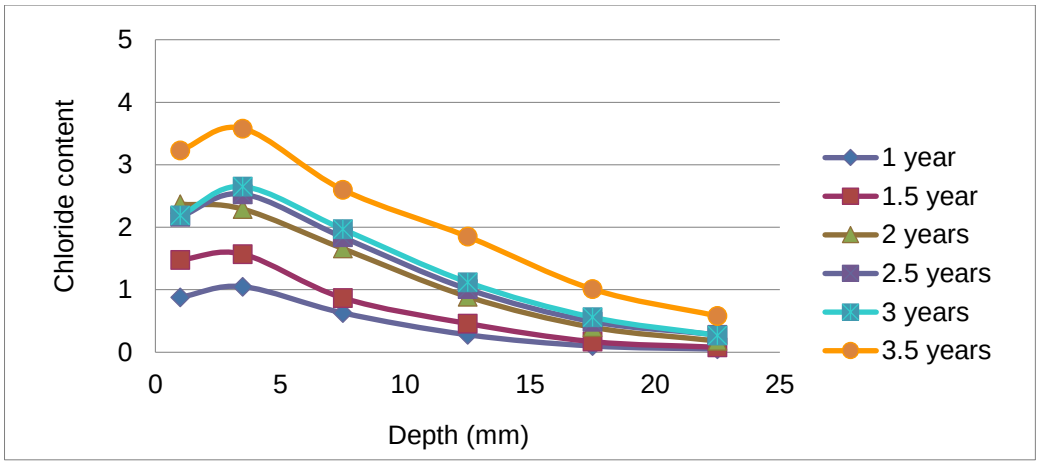

A66: Laboratory (Bulk Diffusion), w/b = 0.60, PC

0.6 PC

mean depth (mm)	% Cl by mass of cement											
	1 year		1.5 years		2 years		2.5 years		3 years		3.5 years	
spec.:	1	2	1	2	1	2	1	2	1	2	1	2
1	2,530	2,560	2,120	2,300	2,960	3,230	3,270	3,700	3,950	4,080	4,230	3,980
3,5	2,210	1,980	2,440	2,420	3,100	3,420	3,770	3,910	4,060	4,180	4,410	4,360
7,5	1,520	1,550	1,880	1,950	2,530	2,710	3,100	3,290	3,450	3,620	3,850	3,900
12,5	0,920	1,010	1,130	1,200	1,700	1,850	2,150	2,200	2,440	2,510	2,830	2,910
17,5	0,460	0,580	0,690	0,680	0,930	1,100	1,310	1,380	1,540	1,700	1,880	2,000
22,5	0,210	0,250	0,320	0,350	0,400	0,600	0,670	0,700	0,800	0,900	0,920	1,100
27,5	0,130	0,100	0,090	0,120		0,350						

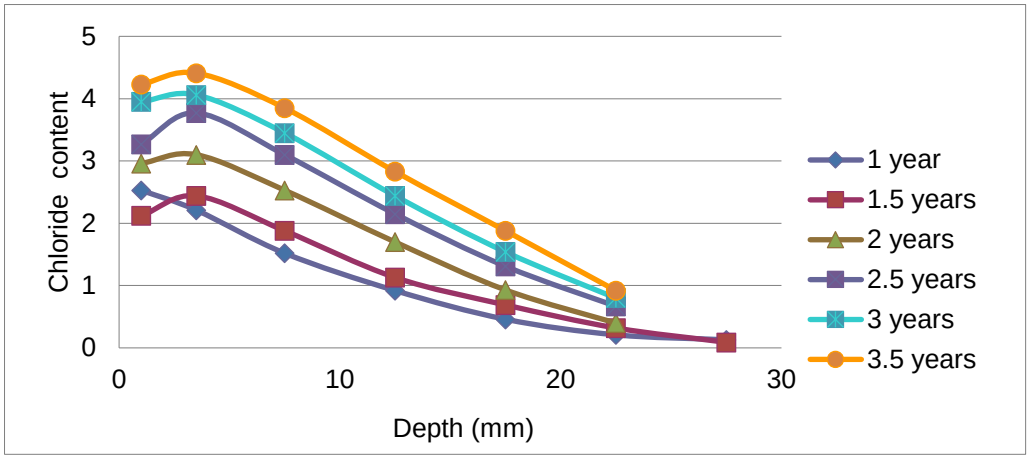

A67: Laboratory (Bulk Diffusion), w/b = 0.40, BS

0.4 BS

mean depth (mm)	% Cl by mass of cement											
	1 year		1.5 years		2 years		2.5 years		3 years		3.5 years	
spec.:	1	2	1	2	1	2	1	2	1	2	1	2
1	1,540	1,220	1,710	1,840	2,100	1,950	2,500	2,920	3,000	3,200	3,600	3,500
3,5	1,780	1,680	2,060	2,080	2,560	2,670	3,110	3,050	3,440	3,400	3,750	3,770
7,5	0,640	0,560	0,770	0,710	1,010	1,020	1,260	1,180	1,300	1,350	1,500	1,570
12,5	0,130	0,160	0,330	0,290	0,360	0,400	0,450	0,430	0,490	0,520	0,610	0,660
17,5	0,080	0,090	0,130	0,140	0,150	0,180	0,200	0,200	0,230	0,240	0,220	0,250
22,5	0,030	0,020	0,080	0,050	0,060	0,080	0,080	0,050	0,090	0,080	0,100	0,090

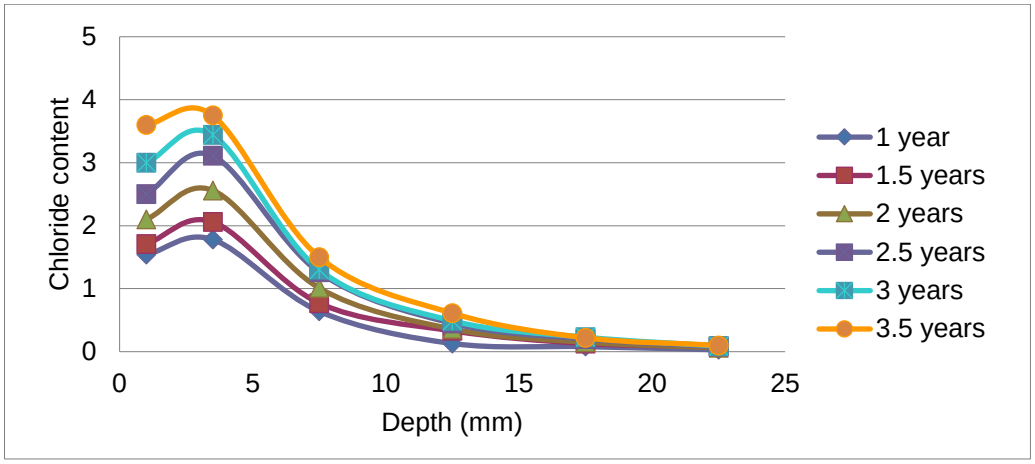

A68: Laboratory (Bulk Diffusion), w/b = 0.60, BS

0.6 BS

mean depth (mm)	% Cl by mass of cement											
	1 year		1.5 years		2 years		2.5 years		3 years		3.5 years	
spec.:	1	2	1	2	1	2	1	2	1	2	1	2
1	1,850	2,640	3,080	2,950	4,130	3,000	3,150	3,400	4,230	4,000	4,210	4,600
3,5	2,290	2,900	3,250	3,100	3,450	3,230	3,550	3,630	4,400	4,390	4,750	4,910
7,5	1,250	1,460	1,650	1,570	1,930	1,700	2,120	2,170	2,400	2,270	2,580	2,670
12,5	0,420	0,600	0,690	0,670	0,880	0,820	0,720	0,960	1,210	1,100	1,290	1,290
17,5	0,090	0,070	0,160	0,190	0,300	0,230	0,310	0,360	0,430	0,490	0,520	0,520
22,5	0,040	0,040	0,090	0,080	0,090	0,070	0,080	0,090	0,100	0,090	0,080	0,090

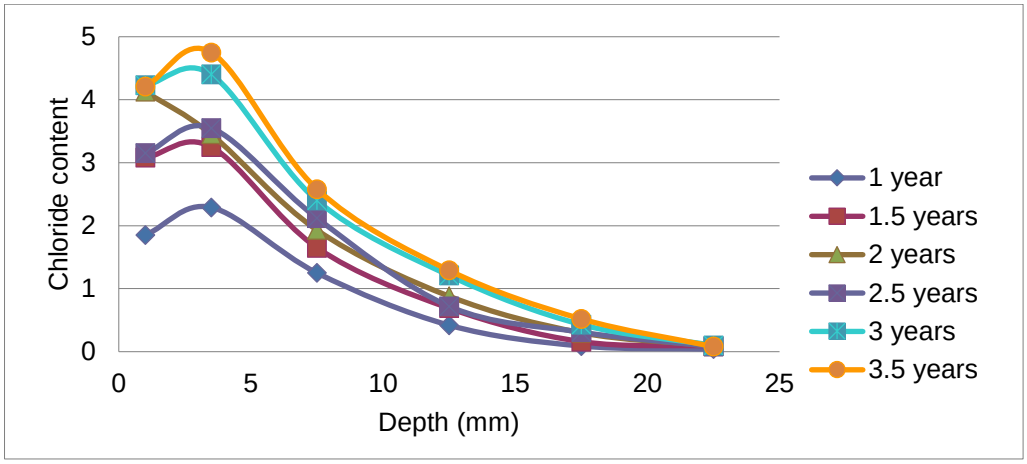

A69: Laboratory (Bulk Diffusion), w/b = 0.40, CS

0.4 CS

mean depth (mm)	% Cl by mass of cement											
	1 year		1.5 years		2 years		2.5 years		3 years		3.5 years	
spec.:	1	2	1	2	1	2	1	2	1	2	1	2
1	1,210	1,500	2,210	1,500	2,120	2,500	3,200	2,840	3,100	3,000	3,500	3,720
3,5	1,460	1,760	2,450	2,390	2,700	2,870	3,240	3,200	3,590	3,660	4,280	4,250
7,5	0,510	0,660	0,750	0,900	1,130	0,960	1,240	1,310	1,540	1,500	1,570	1,690
12,5	0,140	0,170	0,330	0,310	0,400	0,450	0,550	0,540	0,700	0,650	0,670	0,720
17,5	0,070	0,100	0,170	0,120	0,180	0,200	0,240	0,180	0,280	0,300	0,310	0,330
22,5	0,040	0,060	0,080	0,080	0,040	0,080	0,100	0,090	0,100	0,120	0,090	0,080

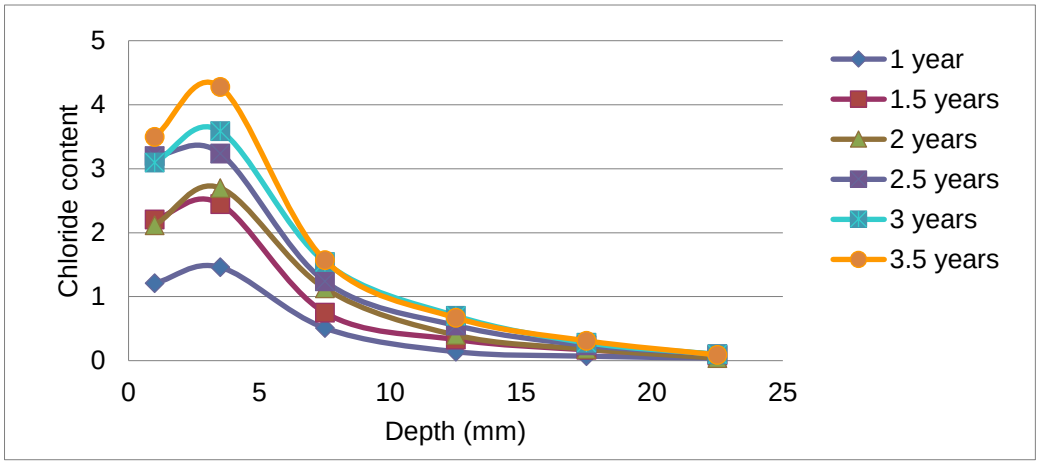

A70: Laboratory (Bulk Diffusion), w/b = 0.60, CS

0.6 CS

mean depth (mm)	% Cl by mass of cement											
	1 year		1.5 years		2 years		2.5 years		3 years		3.5 years	
spec.:	1	2	1	2	1	2	1	2	1	2	1	2
1	1,620	1,960	2,100	2,240	2,800	3,000	3,530	3,120	3,950	4,090	4,100	4,400
3,5	1,980	2,100	2,450	2,510	3,090	3,200	3,990	3,840	4,140	4,460	4,700	4,780
7,5	0,940	1,180	1,450	1,500	1,880	1,890	2,340	2,370	2,500	2,610	2,790	2,850
12,5	0,360	0,430	0,550	0,530	0,730	0,690	0,920	0,970	1,000	1,180	1,200	1,260
17,5	0,120	0,150	0,180	0,190	0,220	0,330	0,460	0,450	0,560	0,500	0,550	0,570
22,5	0,060	0,070	0,100	0,090	0,100	0,090	0,110	0,120	0,150	0,100	0,110	0,090

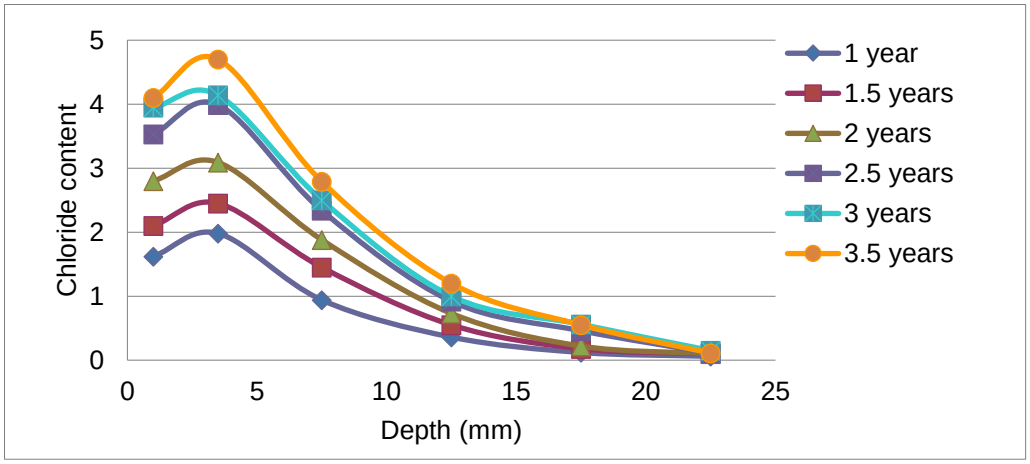

A71: Laboratory (Bulk Diffusion), w/b = 0.40, FA

0.4 FA

mean depth (mm)	% Cl by mass of cement											
	1 year		1.5 years		2 years		2.5 years		3 years		3.5 years	
spec.:	1	2	1	2	1	2	1	2	1	2	1	2
1	1,000	1,200	1,310	1,360	1,950	2,500	2,610	2,740	3,050	3,100	3,550	3,400
3,5	1,320	1,390	1,720	1,800	2,400	2,780	3,080	3,100	3,420	3,500	3,800	3,860
7,5	0,580	0,420	0,850	0,750	1,190	1,250	1,340	1,440	1,640	1,570	1,680	1,700
12,5	0,110	0,290	0,410	0,290	0,340	0,530	0,600	0,610	0,720	0,710	0,780	0,750
17,5	0,050	0,200	0,210	0,200	0,220	0,250	0,270	0,290	0,310	0,340	0,320	0,350
22,5	0,040	0,110	0,120	0,100	0,120	0,170	0,160	0,150	0,160	0,170	0,160	0,170

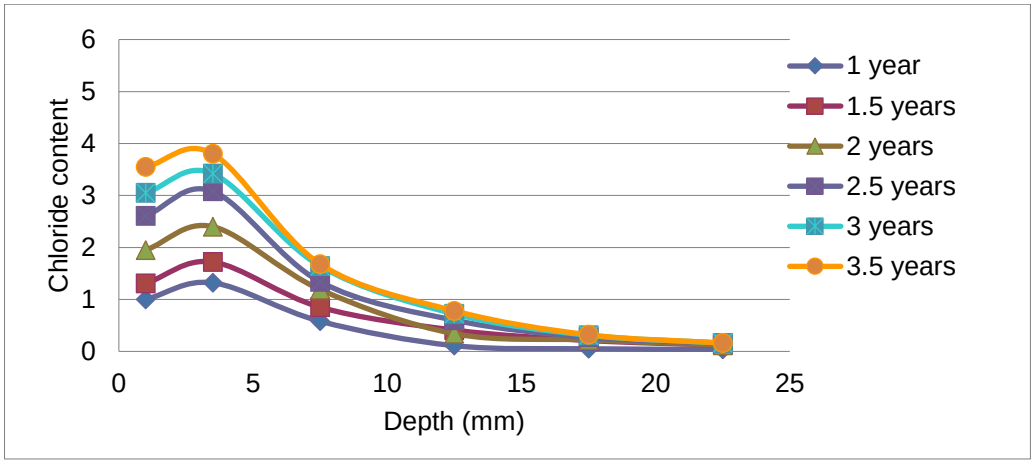

A72: Laboratory (Bulk Diffusion), w/b = 0.60, FA

0.6 FA

mean depth (mm)	% Cl by mass of cement											
	1 year		1.5 years		2 years		2.5 years		3 years		3.5 years	
spec.:	1	2	1	2	1	2	1	2	1	2	1	2
1	2,200	2,650	3,200	3,130	3,420	3,640	4,000	3,850	4,500	4,630	4,900	5,100
3,5	2,910	3,060	3,610	3,530	3,850	3,950	4,260	4,250	4,800	4,980	5,100	5,200
7,5	1,430	1,570	1,980	1,850	2,150	2,260	2,340	2,370	2,580	2,790	3,130	3,280
12,5	0,770	0,610	0,880	0,850	0,990	1,080	1,160	1,170	1,430	1,390	1,490	1,680
17,5	0,420	0,240	0,360	0,350	0,350	0,380	0,570	0,480	0,680	0,610	0,690	0,750
22,5	0,240	0,170	0,130	0,100	0,150	0,160	0,180	0,190	0,230	0,250	0,270	0,250

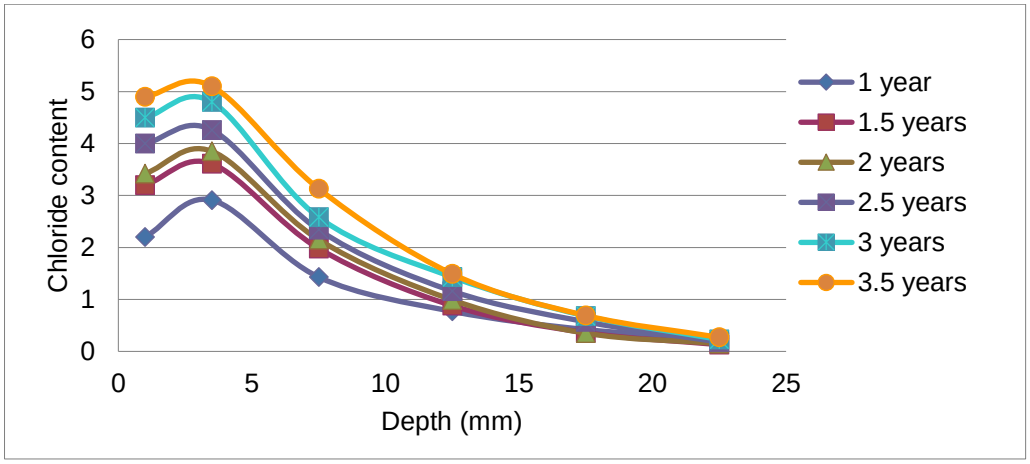

A73: Laboratory (Bulk Diffusion), w/b = 0.40, SP

0.4 SP

mean depth (mm)	% Cl by mass of cement											
	1 year		1.5 years		2 years		2.5 years		3 years		3.5 years	
spec.:	1	2	1	2	1	2	1	2	1	2	1	2
1	1,150	1,480	1,500	1,730	2,100	2,330	2,500	2,650	3,000	2,600	3,000	3,120
3,5	1,700	1,720	1,860	1,950	2,490	2,650	2,900	2,820	3,110	3,190	3,450	3,620
7,5	0,850	0,850	1,010	1,150	1,350	1,400	1,560	1,540	1,800	1,870	1,960	1,960
12,5	0,170	0,180	0,380	0,390	0,480	0,560	0,670	0,750	0,870	0,800	0,840	0,770
17,5	0,090	0,090	0,130	0,140	0,190	0,210	0,280	0,250	0,280	0,260	0,250	0,240
22,5	0,070	0,030	0,070	0,090	0,100	0,120	0,100	0,110	0,120	0,090	0,110	0,090

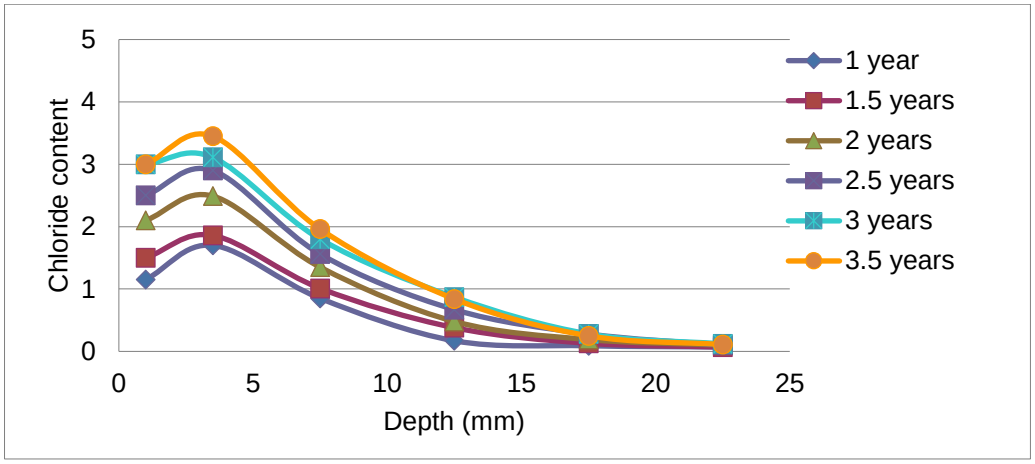

A74: Laboratory (Bulk Diffusion), w/b = 0.60, SP

0.6 SP

mean depth (mm)	% Cl by mass of cement											
	1 year		1.5 years		2 years		2.5 years		3 years		3.5 years	
spec.:	1	2	1	2	1	2	1	2	1	2	1	2
1	2,100	2,100	2,550	2,900	3,180	3,110	3,200	3,000	3,510	3,400	4,050	4,280
3,5	2,500	2,450	3,050	3,180	3,300	3,410	3,560	3,500	3,750	3,840	4,220	4,510
7,5	1,600	1,700	1,730	2,030	2,140	2,100	2,400	2,310	2,540	2,620	2,800	3,090
12,5	0,710	0,680	0,820	0,830	1,230	1,200	1,390	1,280	1,450	1,560	1,580	1,550
17,5	0,280	0,280	0,350	0,430	0,520	0,450	0,680	0,550	0,720	0,680	0,800	0,700
22,5	0,100	0,100	0,130	0,150	0,180	0,200	0,190	0,150	0,210	0,220	0,200	0,180

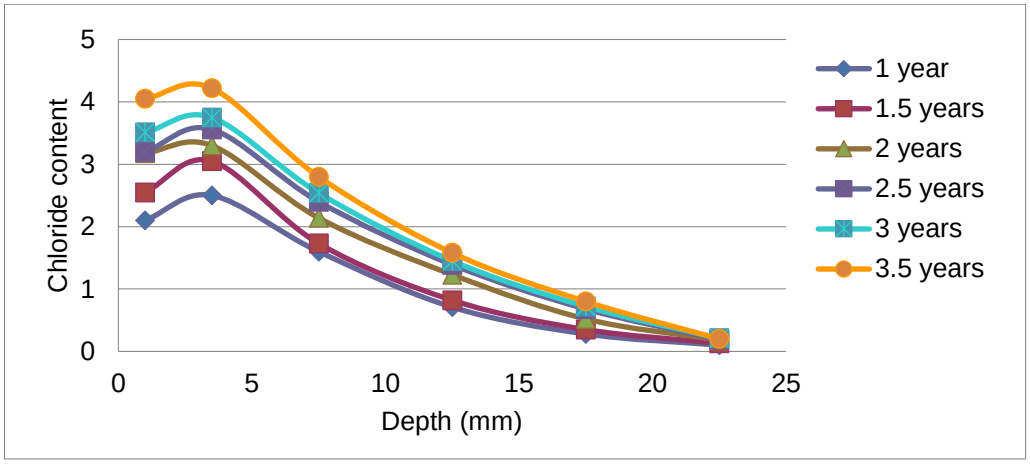

A75: Laboratory (Bulk Diffusion), w/b = 0.40, SF

0.4 SF

mean depth (mm)	% Cl by mass of cement											
	1 year		1.5 years		2 years		2.5 years		3 years		3.5 years	
spec.:	1	2	1	2	1	2	1	2	1	2	1	2
1	1,420	1,240	1,580	1,920	2,130	2,230	2,320	2,050	2,100	2,320	2,560	2,900
3,5	1,600	1,440	1,960	2,050	2,220	2,300	2,500	2,450	2,640	2,710	2,830	3,100
7,5	0,790	0,850	1,100	1,190	1,250	1,290	1,600	1,500	1,790	1,800	2,100	2,230
12,5	0,290	0,230	0,320	0,330	0,460	0,550	0,590	0,500	0,670	0,750	0,950	1,080
17,5	0,100	0,090	0,120	0,140	0,200	0,190	0,290	0,240	0,340	0,300	0,510	0,540
22,5	0,080	0,070	0,090	0,080	0,100	0,080	0,140	0,100	0,110	0,090	0,120	0,100

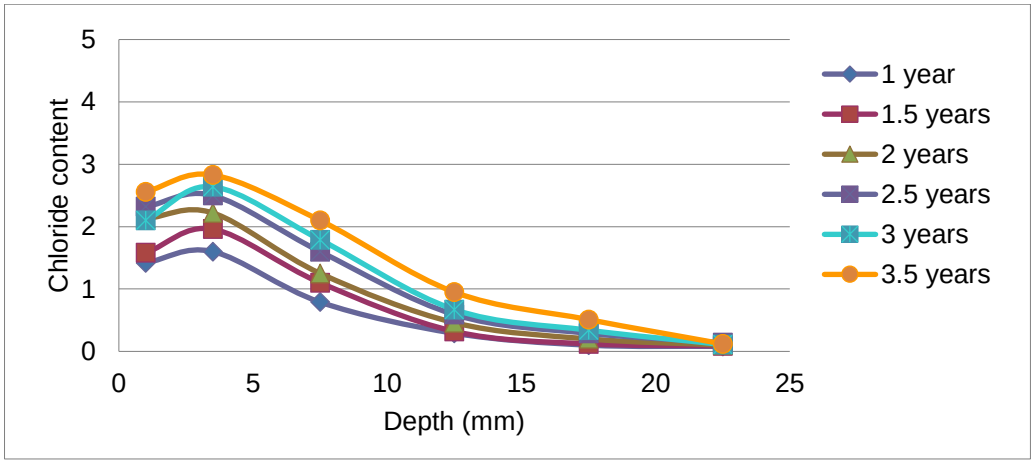

A76: Laboratory (Bulk Diffusion), w/b = 0.60, SF

0.6 SF

mean depth (mm)	% Cl by mass of cement											
	1 year		1.5 years		2 years		2.5 years		3 years		3.5 years	
spec.:	1	2	1	2	1	2	1	2	1	2	1	2
1	1,890	2,050	2,130	2,300	2,630	2,500	3,100	2,900	3,050	3,120	3,810	4,020
3,5	2,130	2,400	2,450	2,650	2,900	2,820	3,290	3,180	3,540	3,450	3,830	4,020
7,5	1,290	1,600	1,640	1,890	2,140	1,990	2,500	2,430	2,760	2,790	3,100	3,150
12,5	0,580	0,750	0,820	1,040	1,200	1,300	1,410	1,450	1,650	1,700	1,870	1,930
17,5	0,260	0,340	0,400	0,410	0,560	0,480	0,620	0,530	0,750	0,690	0,920	0,990
22,5	0,100	0,100	0,150	0,220	0,240	0,200	0,210	0,220	0,250	0,210	0,380	0,530